Freshwater in Coupled Human-Natural Systems in Bangladesh

By

Chelsea Nicole Peters, M.S.

Dissertation

Submitted to the Faculty of the

Graduate School of Vanderbilt University

in partial fulfillment of the requirements

for the degree of

DOCTOR OF PHILOSOPHY

in

Civil and Environmental Engineering

August 10, 2018

Nashville, Tennessee

Approved:

George M. Hornberger, Ph.D.

Hiba Baroud, Ph.D.

David J. Furbish, Ph.D.

John Ayers, Ph.D.

Ralf Bennartz, Ph.D.

For the girls who must walk to fetch water each and every day.

ACKNOWLEDGMENTS

This work is a collaboration, and would surely have been impossible without the support and guidance of so many inspirational people. It is impossible not to start by thanking my tireless and always-brilliant adviser, George Hornberger. You were the reason I started this journey at Vanderbilt, and most definitely the reason for my ability to finish it. I will always be grateful for the many life chats, philosophical and intellectual discussions, and, of course, the constant guidance you offered in all of my academic endeavors.

I also would like to thank my terrific committee members–Hiba, Ralf, John, and David. The opportunity to collaborate with each of you was the greatest gift I have received through out my entire schooling. It has been an honor to absorb from your wisdom and intelligence. You have encouraged my curiosity and always reminded me that the important part of research is not to stop questioning.

A majority of my success is due the many colleagues and friends that have accompanied me in this adventure over the past few year. I surely would have lost my sanity without the many intramural softball games, ballet sculpt chats, office breaks, evenings at Kaybob's, and CEE Council and GSC committee meetings. A special thank you goes out to Tyler, Erin, Emily, Elizabeth, T., and my right-hand man, Chris. To all my other graduate student friends– you are brilliant, genuine, and forever dear to me. Thank you.

And finally, this work would not have been possible without the constant support of my family. You encourage me to purse my hopes and dreams, yet always welcome me back home again. I would especially like to thank my mother for enduring my incessant growing pains and being absolutely indispensable in the creation of *Farzana's Journey*.

This research was supported by the Office of Naval Research grant No. N00014–11–1–0683 and by the National Science Foundation Graduate Fellowship under Grant No. 1445197.

TABLE OF CONTENTS

LIST OF TABLES

LIST OF FIGURES

LIST OF ACRONYMS

GBM Ganges-Brahmaputra-Meghna

GW-SW groundwater-surface water

EMI electromagnetic induction

bgl below ground level

CTD conductivity, temperature, and depth diver

EC electrical conductivity

MCDA multicriteria decision analysis

RWH rainwater harvesting

PSF pond sand filter

MAR managed aquifer recharge

TW tubewell

NGO non-governmental organization

MAVT multiple attribute value theory

AHP analytic hierarchy process

ELECTRE ELimination and Choice Translating Reality

NSF National Science Foundation

ISEE Vanderbilt Integrated Social, Environmental and Engineering

SDG sustainable development goals

CHAPTER 1

INTRODUCTION

1.1 Background and Objectives

Freshwater links coupled human and natural systems. Freshwater is necessary for sustaining a healthy human-natural system, yet its availability is a function of both human and natural controls. Water resources are equally dependent on society's demand, management, and anthropological alterations as they are controlled by climate, geomorphology, hydrology, and geochemistry (*Liu et al.*, 2007). The coevolution of human-natural systems is especially important in a country like Bangladesh, where people must continually adapt to too much and too little water.

Bangladesh encompasses an area of 143,998 km^2 with a population of 160 million people (*FAO*, 2014), making its population density five times greater than any other mega-country (*Streatfield and Karar*, 2008). This is a challenging backdrop for a society with a predominantly poor rural population whose livelihood relies heavily on water-intensive agriculture (*Bangladesh Bureau of Statistics*, 2015a). Increasing poverty, growing population, and competition for resources–especially the right amount of water at the right time–develops a human-natural system that is particularly complex and unstable. To better understand (and potentially improve) the coevolution of this joint system, we need to first understand the water resources paradox–flooding, shortage, and lack of a plan.

Bangladesh receives massive volumes of water both from transboundary rivers and from monsoon rains (averaging 2.3 m annually) (*Alamgir et al.*, 2015). The largest sedimentary basin in the world, the floodplains of the Ganges-Brahmaputra-Meghna (GBM) river basin cover 80% of the country (*Morgan and McIntire*, 1959; *Shamsudduha et al.*, 2011; *Brouwer et al.*, 2007) and form the third largest freshwater outlet in the world (*Chowdhury and Ward*,

Figure 1.1: Location of poldered region in southwest Bangladesh.

2004a). The combination of high river discharge and the magnitude and pattern of precipitation has created one of the most fertile regions of the world, but the copious amount of freshwater also causes the regular floods that devastate the region. The flood vulnerability of the country is immense and increasing with projected climate change. While enhanced greenhouse gases may increase monsoon precipitation, changes in hydrological landscape in Bangladesh may also increase greenhouse gases.[1] This coupled water (and climate) sys-

[1]See Appendix A for additional work on the relationship between Bangladesh methane emission and inundation.

tem can create a cyclical cascade of instabilities and, therefore, exacerbate the flooding problem in these vulnerable regions.

Meanwhile drinking water shortages also continue to be one of the Bangladesh's most challenging problems (*Gain et al.*, 2012). Obstacles arise in resource availability due to seasonal variability in rainfall, improper allocation to the community, and difficult access to groundwater. Limited capacity for storage during the wet season leaves depleted water resources for use during the dry season, when irrigation and drinking water is most needed. Additionally, quality limitations occur when water resources are contaminated or improperly treated. This trade-off between water quantity and quality is inescapable, especially in coastal regions.

The coastal lowlands are particularly susceptible to water resource issues–where densely populated communities are faced with the challenges of sea-level rise, saline and arsenic-laced groundwaters, microbiological contamination of surface waters, a growing population, and poor water resource infrastructure and governance. Here, water development has primarily targeted embankments for flood control and storm-surge. In the 1960s and 1970s, much of the tidal mangrove forest of the lower delta region was converted to polders, or embanked islands (Fig. 1.1) (*Auerbach et al.*, 2015). An unintended consequence of these embankment projects has been a gradual reduction in elevation of the polder and fertility of the soil due to the prevention of natural siltation associated with flooding. Now living on extremely vulnerable landscapes, the locals must adapt to the long dry season by using multiple sources to meet drinking water needs.

Locals often rely on a mix of untreated surface and groundwater drinking water sources. A combination of contamination, failing infrastructure, and difficult access seem to subdue the success of each option. The lack of functioning infrastructure is often attributed to top-down supply-driven planning, which ignores what users want and will maintain in this remote region (*Cai et al.*, 2004; *Starkl et al.*, 2013). To achieve sustainable solutions, underdeveloped, rural regions need transparent and participative water resource planning

(*Starkl et al.*, 2013). We must (1) better understand the local context–both hydrologically and socially–and then (2) equip the local communities with the knowledge and means to better manage their water resources as they see fit.

Based on this dynamic environment, this dissertation investigates the freshwater resources in the coastal region of Bangladesh. Although we consider the interesting effects of flooding country-wide[2], the majority of this research investigates hydrological, decision-making, and educational (and subsequent adaptation) factors associated with drinking water shortages on a polder in southwestern Bangladesh. We combine physical and social modeling, field-based research, and community outreach to better understand the environmental complexity and people's adaptation to water systems in the region. The research objectives are as follows:

Objective 1: Assess localized groundwater-surface water interactions while searching for potable groundwater resources.

Objective 2: Explore the regional physical and social factors that influence drinking water sources and their likely success.

Objective 3: Demonstrate collaborative science research communication with local non-science communities through a story about water, land, and people.

1.2 Research Overview

In Chapter 2, we attempt to locate pockets of freshwater amidst brackish groundwater in remote villages in Bangladesh. This work explores inferences about local groundwater-surface water interactions in the poldered region of coastal Bangladesh. We conclude that active exchange of freshwater may be limited. Localized regions of recharge may be possible but small-scale heterogeneity in delta formation likely caused groundwater salinity variation. Without adequate ground truthing of groundwater quality, the ability to deduce

[2] See Appendix A.

the exact location of freshwater pockets may be restricted so other drinking water sources should be pursued.

The objective of Chapter 3 is to explore the various technical, economic, social, and environmental factors that influence the most frequent drinking water sources and management schemes in southern Bangladesh. Using multicriteria decision analysis, we assess the probable success of drinking water supplies and prioritize the sources that are most likely to succeed in the future. We consider differences among stakeholder preferences and multicriteria decision analysis methods to investigate the influences of prioritization and methodological process. This work demonstrates the multifaceted approach that will be needed to resolve water management problems, while also showing that rainwater harvesting is often the most effective, high quality source of drinking water in coastal Bangladesh.

Academics are encouraged to integrate their environmental research with education and societal outreach, but the methods of doing so can be transient and insubstantial. In Chapter 4 we use a children's book to create a sustainable relationship with vulnerable communities in Bangladesh. We demonstrate the coupling of the natural environment and human adaptation through the journey of a girl fetching water. Written, illustrated, and freely distributed in the Bengali-language, the book is a place-based tool to disseminate our understanding of the coupled human-natural system back to the rural Bangladesh communities, as well as to teach others about the water, land, and people of Bangladesh.

Chapter 5 synthesizes findings from this dissertation, discusses the broader impacts of this work, and offers an outlook on other water links between coupled natural-human systems in Bangladesh and other developing nations.

CHAPTER 2

A SEARCH FOR FRESHWATER IN THE SALINE AQUIFER OF COASTAL BANGLADESH

2.1 Introduction

Low-lying coastal deltas encompass dense populations due to their relative abundance of natural resources. Deltas are vital centers of agriculture, commerce, transportation, and development, but also dynamic natural landscapes that are becoming increasingly vulnerable to environmental change. The juxtaposition of intense development and resource exploitation alongside the increasing frequency of natural hazards (e.g. erosion, seawater intrusion, subsidence, flooding, sea level rise, etc.) make these regions especially fragile. These increasing physical and social pressures already are substantially impacting water resources. Degradation of water quality (*Paerl et al.*, 2014; *Sá et al.*, 2015; *Seitzinger and Phillips*, 2017), flooding (*Neumann et al.*, 2015a; *Wyncoll et al.*, 2016; *Bilskie et al.*, 2014; *Ali*, 1996), rising sea levels and salt water intrusion (*Carson et al.*, 2016; *Klassen and Allen*, 2017; *Werner and Simmons*, 2009; *Khublaryan et al.*, 2008), loss of wetlands (*Davidson*, 2014; *Nicholls*, 2004), land subsidence (*Schmidt*, 2015; *Wang et al.*, 2012; *Jelgersma*, 1996), changes in recharge (*Appleyard*, 1995; *Priyantha Ranjan et al.*, 2006; *Lambrakis and Kallergis*, 2001), shifts in stream flow and runoff due to regulation (*Wilson et al.*, 2017; *Richter et al.*, 1998; *Gain and Giupponi*, 2014), increased water use (*Erban et al.*, 2014; *Bui et al.*, 2012; *Vandenbohede et al.*, 2009), and changes in climatic patterns and storm strengths (*Ali*, 1996; *Neumann et al.*, 2015b) are a few hydrological changes being noticed around the globe.

Lying at the intersection of oceanic and riverine environments, coastal fresh groundwater is often the most highly valued resource, providing for more than one billion people living in coastal regions (*Post*, 2005; *Small and Nicholls*, 2003; *Oude Essink et al.*, 2010; *Ferguson and Gleeson*, 2012). Although relatively protected compared to surface water resources, coastal aquifers are susceptible to degradation from groundwater extraction, saltwater intrusion, and contamination (*Worland et al.*, 2015; *Tran et al.*, 2012). Small perturbations to the deltaic system may result in significant aquifer salinization and contamination (*Tasich*, 2013; *Nicholls and Cazenave*, 2010). As deltas evolve and water availability stress intensifies, it is critical for researchers and communities to assess groundwater resources and the evolution of aquifer quality on a local scale.

The Ganges-Brahmaputra-Meghna (GBM) delta in Bangladesh is one of the most drastic examples of coastal delta vulnerability (*Warrick et al.*, 1996; *Ali*, 1996; *Gain et al.*, 2014; *Wassmann et al.*, 2004). The hydrological impact of climate change on GBM basin is expected to be stronger than that of other basins as it is subject to the combined effect of (1) glacier and snow melt (*Immerzeel*, 2008; *Immerzeel et al.*, 2009), (2) extreme shifts in monsoon rainfall with increases in rainfall during the wet season but drier winter seasons (*Chowdhury and Ward*, 2004b; *Mirza et al.*, 1998; *Turner and Annamalai*, 2012), (3) relatively fast economic development and demand (*Jahangir Alam et al.*, 2012; *Mallick and Vogt*, 2014), and (4) little water buffering storage capacity over the entire basin (*Gain et al.*, 2012, 2014; *Mondal et al.*, 2010). At large, the delta is home to two-fifths of the developing world's population living below the poverty line (*Biswas*, 2008). Inhabitants in the low-lying regions, which are considered most at risk from climate change impacts, may experience a net increase in poverty of approximately 15% by 2030 (*Hertel et al.*, 2010; *Hijioka et al.*, 2014).

In the coastal zone alone, 170 million Bangladeshi inhabitants depend on water-intensive livelihoods, such as aquaculture, fishing, and rice production (*Rahman and Salehin*, 2013; *Michael and Voss*, 2009; *Benneyworth et al.*, 2016; *Worland et al.*, 2015). Here, the people face an interesting interplay of environment, human adaptation, and coevolution. The landscape is characterized by agricultural islands constructed during the 1960s and 1970s

(*Rahman and Salehin*, 2013; *Michael and Voss*, 2009). Modeled after the Dutch polders, these small islands are protected from tidal and storm-surge inundation by constructed earthen embankments that wrap around the exterior of each island (*Auerbach et al.*, 2015).

Although the region has immense natural water resources, drinking water resources on the polders vary in availability, quality, and susceptibility to hazards. This ubiquitous water stress has prompted significant research efforts related to water quality and potable drinking water supply. According to *Benneyworth et al.* (2016), polder residents use multiple drinking water sources throughout the year. Without adequate water storage and infrastructure, rainwater resources dwindle during the long dry season. Surface water reservoirs are stagnant and susceptible to microbiological contamination. In cases where these reservoirs are connected to the tidal network, the water becomes increasingly salty through the dry season. Groundwater use on the polders is far less than the national average, due to cost of well implementation, higher than average arsenic concentrations, and, most importantly, high salinity (*Benneyworth et al.*, 2016). Although some families own household tubewells, the wells are more often community tubewells that pump from the shallow Holocene aquifer. Typically, the water is unfiltered, and the usage is suspected to be a function of perceived water quality, taste, smell, and proximity (*Shumaker*, 2017; *Benneyworth et al.*, 2016).

A study by *Benneyworth et al.* (2016) noted that all local groundwater tubewells exceeded the Bangladesh guidelines for specific conductivity (despite few residents perceiving their water as having a 'bad' or 'salty' taste). But *Ayers et al.* (2016) discussed unpredictable groundwater salinity variations in the region, suggesting that some wells are fresher than the World Health Organization guidelines (*World Health Organization*, 2011). The cause and location of these fresher regions are unknown, and studies have speculated to the possibility that groundwater-surface water (GW-SW) interactions play a role. Although seasonal monsoonal recharge would be expected, the shallow subsurface consists of deposits of clay varying in thickness, overlying the fine sand aquifer (Fig. 2.1) (*Ayers et al.*, 2016; *Ravenscroft*, 2003). *Worland et al.* (2015) suggest that this lateral heterogeneity in polder stratigraphy may allow for regions of meteoric recharge where the clay cap thins. *Wilson et al.* (2017) also present bathymetry and channel stratigraphy data that indicate potential for channel-aquifer connections.

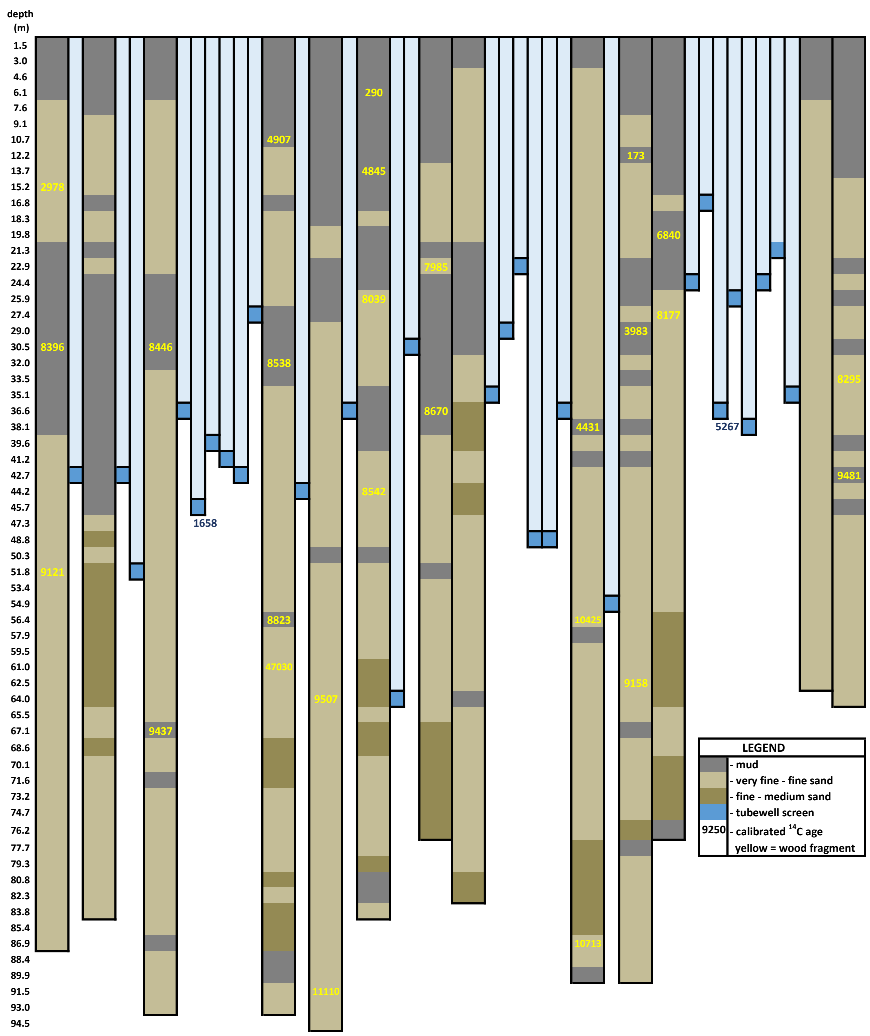

Figure 2.1: Summary of sediment lithology and radiocarbon ages from Polder 32 cores and tubewells with the northernmost on the right. Tan colors designate sand layers and gray marks mud. Numbers are calibrated radiocarbon ages in calendar years before present as recovered from mangrove wood (in yellow) and 14C groundwater ages (in black). Figure adapted from *Ayers et al.* (2016).

Residents may be under utilizing groundwater resources if fresh surface water is exchanging with the shallow aquifer. But is it possible to locate these pockets of fresh groundwater? This study explores what we can infer from local GW-SW interactions on these coastal Bangladesh polders, in an attempt to find an untapped drinking water resource. In doing so, the study (1) assesses the extent of tidal channel and aquifer exchange, (2) explores the possibility of detecting meteoric freshwater recharge through electromagnetic induction (EMI), and (3) evaluates differences in GW-SW interactions between the natural and poldered environment.

2.1.1 Study Region

Bangladesh is the largest sedimentary basin in the world with fluxes from the Himalayan and Indo-Burman mountain ranges through the GBM river system (*Morgan and McIntire*, 1959; *Shamsudduha et al.*, 2011). The surficial geology is characterized by Quaternary deposits surrounded by the Indian Shield to the west, the Shillong Massif and the Himalayas to the north, and the Indo-Burman Mountains to the east (*Morgan and McIntire*, 1959). The massive Holocene floodplains consist of poorly developed, immature silt and clay soils that are underlain by Himalayan derived sediments deposited since the Pliocene (*Alamgir et al.*, 2015; *Ravenscroft et al.*, 2005; *Morgan and McIntire*, 1959). On a national scale, the simplified hydrogeology is represented by two distinct aquifers vertically separated by Pleistocene clays (*MPO*, 1987; *Rahman et al.*, 2011).

In the coastal region, a semiconfined, shallow Holocene aquifer reaches 100 m below ground level (bgl) before the vertical confining unit that separates the two deeper Pleistocene aquifers (*Rahman et al.*, 2011; *Burgess et al.*, 2010). This aquifer primarily consists of fine sands and is overlain by a variably thick mud confining unit (Fig. 2.1). This confining unit, and potentially the Holocene aquifer, are carved by major tidal channels (12 km wide) conveying semi-diurnal tides over 120 km inland of the coast (*Wilson et al.*, 2017). The tidal range varies from 2 m at the coast and amplifies inland to 3 m near Khulna, before decreasing farther inland (*Wilson et al.*, 2017). The polders, and the embankments that surround them, channelize these major rivers and prevent flooding of the intertidal platforms.

This study focuses on one particular polder, Polder 32, located in the Khulna district, Dacope Upazila in southwest Bangladesh, 60 km north of the Bay of Bengal (Fig. 2.2) (*Tasich*, 2013; *Auerbach et al.*, 2015; *Worland et al.*, 2015; *Ayers et al.*, 2016; *Benneyworth et al.*, 2016). This polder is 19.3 km by 7.1 km with a total area of 68.2 km^2 and is home to a population of roughly 40,000 inhabitants (*Ayers et al.*, 2016). Lying at the sharp interface between natural and highly-altered landscapes, Polder 32 was likely part of the mangrove forest before deforestation. Its southern portion borders the protected Sundarbans mangrove forest, separated only by the Bhadra and Shibsha tidal rivers (Fig. 2.2).

Polder 32 embankments were breached during the 2009 cyclone Aila along the Shibsha and Dhaki rivers, leaving the island inundated for upwards of two years. With an average vertical relief of nearly zero across its entirety and only microlevel topographical differences over tens to hundreds of meters, the polder is highly susceptible to similar flooding events in the future (*Auerbach et al.*, 2015). The climate in this region is humid and biseasonal with a dry season from November to May and wet season from June to October (*Chowdhury*, 2010). Polder 32 is estimated to receive between 1500 mm to 2100 mm of rainfall per year (*Nobi and Gupta*, 1997).

2.2 Methods

2.2.1 Meteorological and Tidal Gauges

Rainfall intensity and atmospheric temperature were collected using a Vaisala WXT520 Weather Station connected to a Trimble GPS base station at 22°30′16”N 80°26′09”E (Fig. 2.2). Data were processed in Python. Barometric pressure was collected using a Schlum-

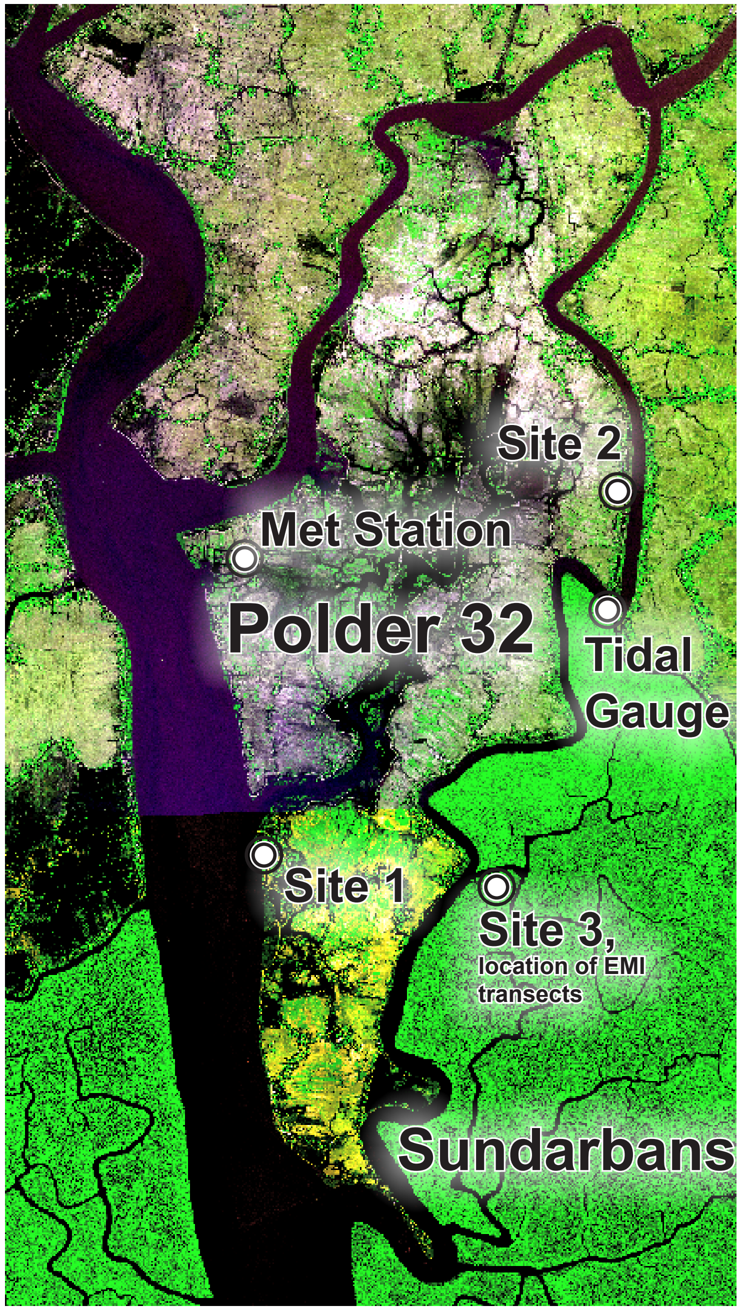

Figure 2.2: Geoeye image of study region including Polder 32 and the Sundarbans, where sites mark piezometer transects, tidal gauge, and meteorological station.

berger Baro Diver.

A Schlumberger CTD Diver was deployed in the tidal channel adjacent to the eastern margin of Polder 32 from May 2014 to June 2016 (Fig.2.2). The deployed gauge collected pressure, temperature, and specific conductivity measurements every 10 minutes.

2.2.2 Piezometers

Three transects–two sites on Polder 32 and one site in the Sundarbans– were installed with monitoring piezometers at different depths and distances from the tidal channel (Fig. 2.2 and Table 2.1). Installation was completed using the traditional Bangladeshi hand flapper method–a reverse circulation percussion drilling method that involves the lifting and dropping of the drill tube with circulation to expel mud pit drilling fluid out the top of the drill pipe during the percussion (*Shuai et al.*, 2017; *Horneman et al.*, 2004). We collected wash samples expelled from the drill pipe either as slurry (sand) or solid plugs (clay) every 1.5 m for visual detection of subtle lithological changes.

Piezometers were installed between 10 and 40 m depth. Each piezometer was constructed from 6.35 cm diameter PVC with a 2.5 m slotted screen on the lower end. The piezometers were equipped with Schlumberger (Specific) Conductivity, Temperature, and Depth Divers (CTD) (measuring every 10 minutes) or HOBOware U20L (measuring pressure and temperature every 30 minutes) pressure transducers from May 2014 to May 2016.

Shallow piezometers were also dug at 2 m depth at Sites 2 and 3. These piezometers were screened above the surface to 2 meters below the surface to capture platform inundation frequency, irrigation patterns, and infiltration patterns. In all cases the shallow piezometers were installed in mud with a sand pack around the screen.

Piezometer pressure transducers were corrected by removing the mean barometric pressure. Specific conductivity measurements from piezometer CTD divers were smoothed with Robust spline smoothing in MATLAB, due to instrument sensitivities from well water sloshing or equipment malfunction. A 36-hr low-pass filter is used to assess trends.

Table 2.1: Site and piezometer details.

Site	Piezo.	Dist.to TC (m)	Depth	Instrument	Interval (min)	Valid Data (mon/yr)
1	A	5	26	CTD	10	5/14-10/14
1	B	145	44	CTD	10	5/14-10/15
2	C	17.5	18	CTD	10	5/14-10/15
2	D	17.5	30	CTD	10	5/14-10/15
2	E	113.5	2	CTD	10	5/14-10/15
2	F	113.5	11	HOBO	30	5/14-10/15
2	G	113.5	30.5	HOBO	30	5/14-10/15
3	H	10.5	2	CTD	10	5/14-10/15
3	I	10.5	38	CTD	10	–
3	J	19	39.5	CTD	10	5/14-10/15
3	K	130	2	HOBO/CTD	30/10	5/14-3/15; 3/15-10/15

In October 2014, falling-head measurements of hydraulic conductivity were made at each piezometer using a solid, 1.25 m long, 3.18 cm diameter slug. Decay of the hydraulic head was monitored with a HOBO pressure transducer at 1 second intervals. The pressure measurements were converted to water level using the barometric compensation tool on the HOBOware software. Water depth is determined from the top of the piezometer, but is referenced from the initial water level. Tests were interpreted using the *Bouwer and Rice* (1976) method as implemented in the USGS Bouwer-Rice Slug Test spreadsheet (*Halford and Kuniansky*, 2002). Although originally designed for unconfined aquifers, the *Bouwer and Rice* (1976) method can be applied to confined aquifers with partially penetrating wells of finite diameter. It is assumed that the well water was displaced instantaneously at t = 0.

2.2.3 Chemical Analysis

The shallow aquifer tubewells and three bounding tidal channels were sampled seasonally using a portable Hydrolab 4a, which measures Eh oxidation-reduction potential in millivolts (mV), pH, temperature in degrees Celsius ($^{\circ}C$), and specific conductivity (SpC) in microsiemens per centimeter ($\mu S/cm$). Wells were purged and water samples were collected following the procedure outlined by *Ayers et al.* (2016). Preserved aqueous samples were analyzed for metal cation concentrations using ICP-OES via EPA Method 6010B.

Analyses of anions were performed on unpreserved samples using an IC (ASTM Method D-4327-03). Analyses of organic and inorganic carbon were completed on unpreserved samples using TOC (ASTM Method D-7573-09).

2.2.4 Electromagnetic Induction

Direct measurement of shallow groundwater salinity variations in coastal environments would require costly wells to locate areas of freshwater recharge. Resistivity and EMI methods can be used to map conductivity contrasts in shallow subsurface pore water and predict salinity between well locations (*Greenwood et al.*, 2006; *Hoefel and Evans*, 2001; *Manheim et al.*, 2004). Following methods described by *Worland et al.* (2015), we conducted a geophysical survey using a Geophex GEM-2 handheld, multi-frequency terrain conductivity meter in multiple transects during May 2014. The GEM-2 was held in a horizontal coplanar position 1 m above the ground surface while walking a transect. GPS points were taken at the start and end of each transect. The instrument recorded transmission frequencies of 6030 Hz, 15030 Hz, 37410 Hz, and 93090 Hz. The EMI output was converted to apparent conductivity using *Aeroquest* software (*Huang and Won*, 2000). Using the University of British Columbia Geophysical Inversion facility (UBC-GIF) EM1DFM inversion program, we constructed 1-D inversion models for the frequency-domain output. Additional details on the method are described in *Worland et al.* (2015).

2.2.5 1-D Tidal Propagation Model

An adaptation of a one-dimensional finite-difference groundwater flow model (*Tasich*, 2013) is employed to analyze the connectivity of the tidal channel and aquifer. Connectivity of a shallow aquifer and a river often is regulated by a layer of channel sediments. We conceptualize this by considering a veneer of sediments acting as a restriction to groundwater-surface water exchange. The model estimates the range of thicknesses and the hydraulic conductivity of the channel clogging layer adjacent to the tidal channel as a function of head variations in the horizontal direction due to tidal river fluctuations. We calibrate the model with tidal propagation data from Polder 32 and the Sundarbans. A tidal river serves as the left boundary conditions fluctuating between a maximum (TR) and minimum (-TR) tidal extent while groundwater flow equations govern at $0 < x < X$. The right boundary condition is a no flow boundary at X. The space between the boundaries is subdivided into n nodes. The tidal channel boundary condition is defined using sinusoids with a period of 12 hours for the solar tidal cycle and 12.42 hours for the lunar tidal cycles, as described by

$$h_{bc} = \sin a_l(2\pi\frac{t}{12.41}) + \sin a_s(2\pi\frac{t}{12}), \tag{2.1}$$

where h_{bc} is the head at the boundary condition, a_l and a_s are the lunar and solar components of the tidal amplitude, respectively, and t is time. Flow within the aquifer is described as

$$\frac{\partial h}{\partial t} = \frac{1}{S}\frac{\partial}{\partial x}(T\frac{\partial h}{\partial x}) + \frac{R_e}{S}, \tag{2.2}$$

where h is groundwater head, t is time, T is transmissivity, S is storativity, x is horizontal space, and R_e is effective surface recharge. Model parameters are outlined in Table 2.2. Transmissivity varies to reflect differences in aquifer and channel characteristics over horizontal space. While varying the channel clogging layer width and transmissivity, we optimized the model by minimizing differences between observed apparent tidal efficiency and model tidal efficiency at each piezometer site. Apparent tidal efficiency is defined as the ratio of well-water amplitude to tidal amplitude at a specific point in the aquifer (*Jacob*, 1940; *Gregg*, 1966; *Fetter*, 2001).

Table 2.2: Finite-difference groundwater model parameters.

Notation	**Parameters**	**Unit**	**Value or Range**
T_A	Aquifer Transmissivity	m^2/hr	10
TR	Channel Transmissivity	m^2/hr	1.22
T_C	Confining Unit Transmissivity	m^2/hr	5.4x10^{-6} to 0.1
S	Storativity		1
RR	Recharge Rate	m/hr	2x10^{-6} to 3x10^{-6}
TR	Tidal Range	m	2 to 4
XC	Channel Clogging Layer Width	m	2.5 to 16

2.3 Results

2.3.1 Meteorological and Tidal Data

The characteristic fortnightly variations in tidal range reflect spring-neap astronomical cycles. Tidal channel CTD captured freshening (35 to 0.5 mS/cm) during wet season and cooling (31 to 20$°C$) during winter months (Fig. 2.3). In 2015, the nearly immediate freshening of the tidal channel occurred in mid July, which is very similar to the freshening shown in *Ayers et al.* (2017). Peak tidal channel temperatures mimic the ambient air temperature, rather than rainfall frequency, and remain approximately 30° from May to August. In 2014, water temperatures drop to the lowest in late October, whereas in 2015 similar temperatures are not reached until mid December. Although site meteorological data is missing for 2014, the channel temperature follows the air temperature patterns in 2015.

Barometric pressure shows clear diurnal signal with amplitudes between 1 and 1.5 cm, so we ignore barometric conditions relative to the tidal forcing.

2.3.2 Shallow Piezometers

Shallow piezometers show similar patterns but more subdued changes in specific conductivity and temperature (Fig. 2.4). Piezometers were serviced in October 2014 and May

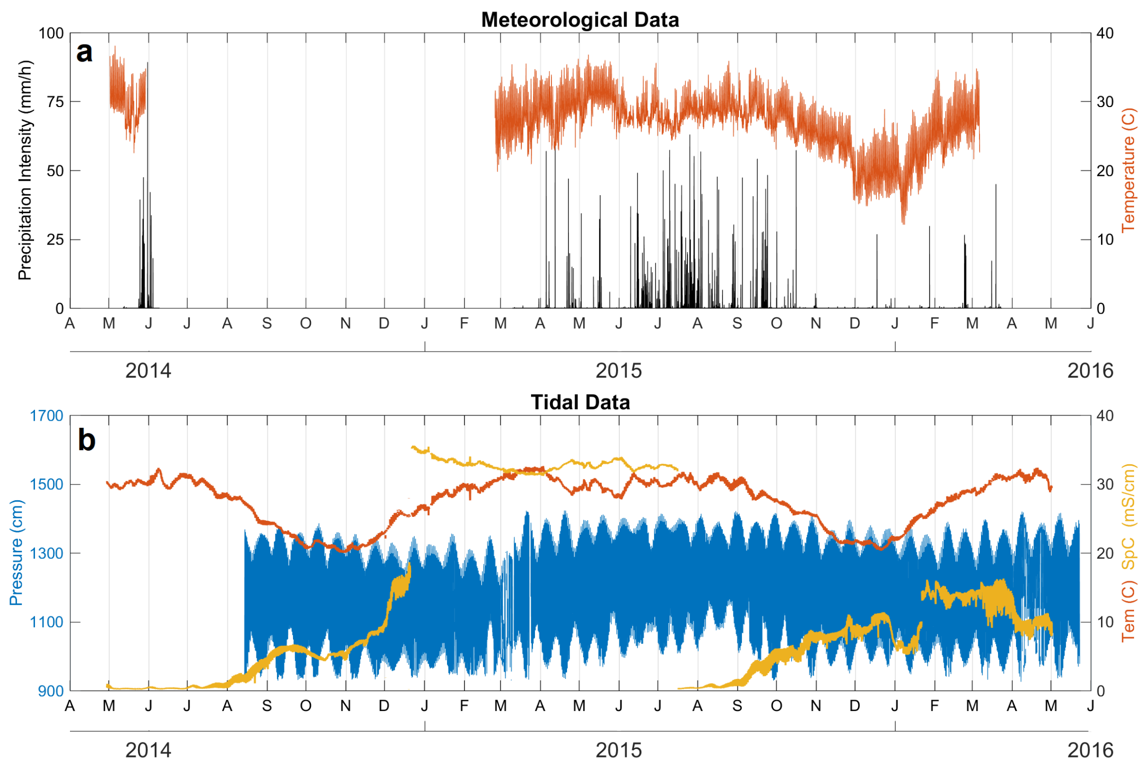

Figure 2.3: Meteorological and tidal data measured between April 2014 and June 2016. Invalid and missing data have been removed.

2015, and differences between the mean depth between service periods are likely due to re-installation errors (i.e. kinking of suspension wire, elevation disturbance around piezometer base, etc.). Although the overall depth of water is skewed and unattainable due to these errors, the pattern of inundation and infiltration is meaningful. Site 3 shows the regular spring and neap flooding of the mangrove platform during high tide, and subsequent draining and infiltration of the platform during ebbing. Site 2 shows a steady inundation level due to the regulated flooding of the paddy field inside the embankment. High pressure periods between August 2014 to November 2014 and October 2015 suggest sluice gate failure, which was confirmed by local residents.

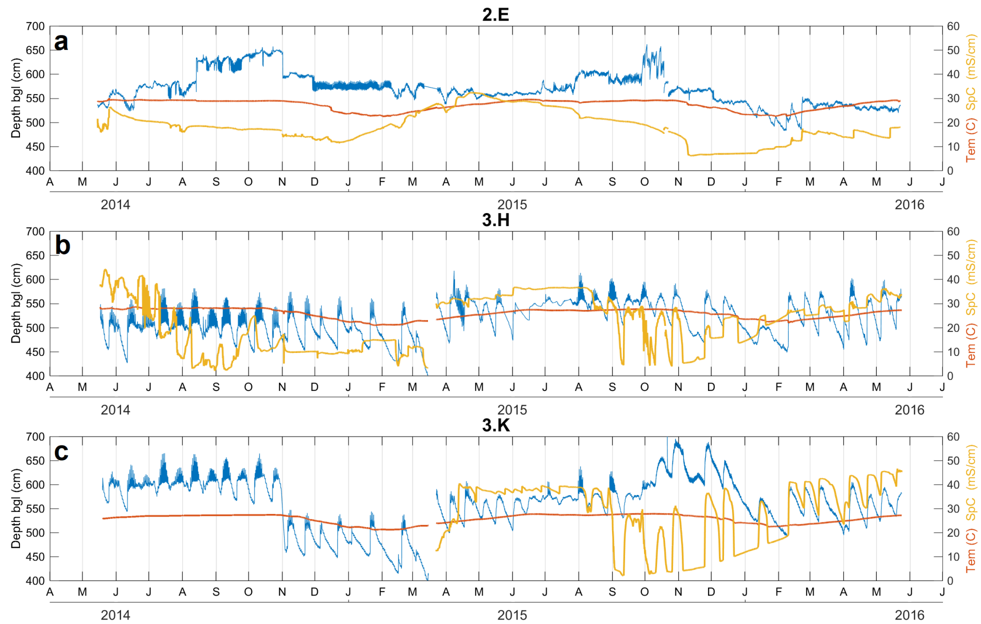

Figure 2.4: Shallow piezometer pressure, temperature, and specific conductivity at Site 2 and 3 between April 2014 and July 2016.

2.3.3 Piezometers

Lithology from piezometer drilling wash samples indicates disparity in clay cap thickness and depth to aquifer, ranging from depths of 10 to 45 m. The D_{50} of the clay cap sediments is an average of 18μm. From the slug tests, hydraulic conductivity beneath the confining unit is on the order of 10^{-3} to $10^{-4} cm/s$ (Table 2.3). These values are typical of medium to fine sands in the Bengal Basin (*Zheng et al.*, 2005).

Table 2.3: Slug test calculations of hydraulic conductivity (K) for Polder 32 and Sundarbans piezometers.

Site	Piezometer	Distance from TC (m)	Depth	K (cm/s)
1	B	145	44	$3.1\text{x}10^{-4}$
2	C	17.5	18	$2.1\text{x}10^{-3}$
2	D	17.5	30	$1.7\text{x}10^{-3}$
2	F	113.5	11	$1.5\text{x}10^{-3}$
3	J	19	39.5	$8.1\text{x}10^{-4}$

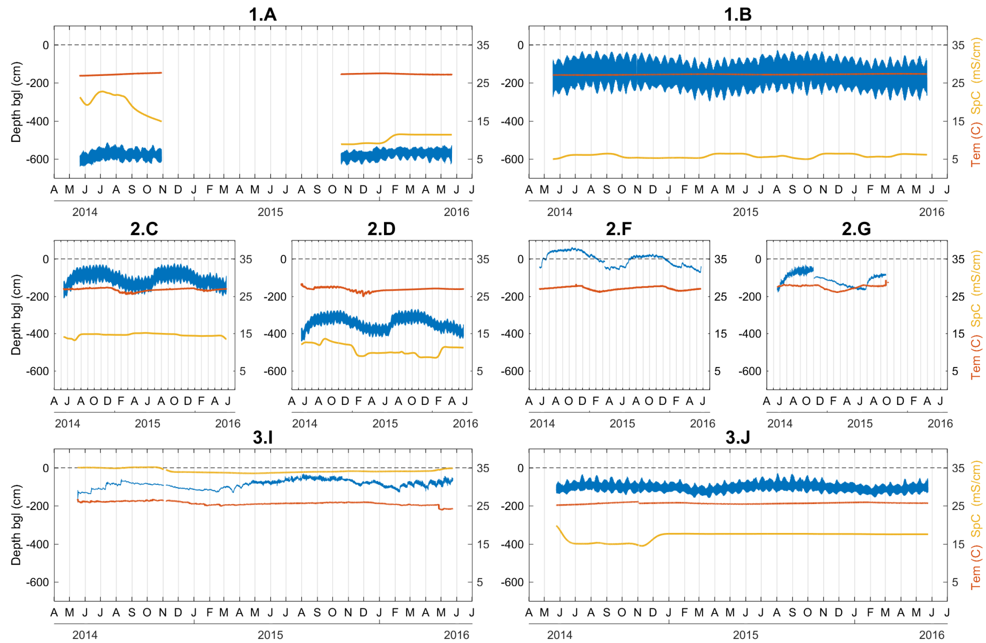

Figure 2.5: Water level (blue), temperature (red), and specific conductivity (orange) measured in piezometers. Invalid and missing data have been removed.

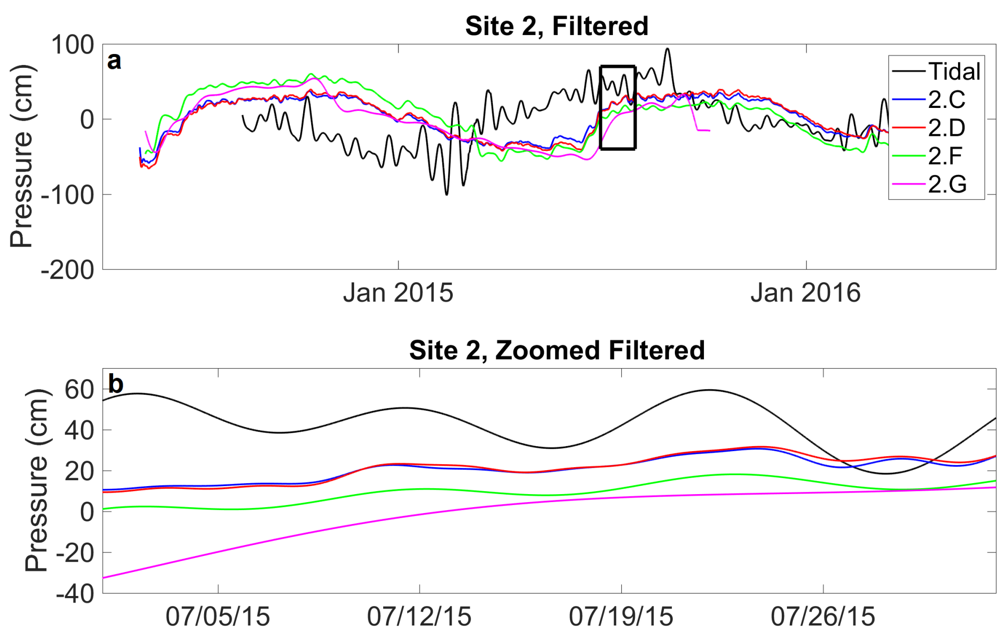

Figure 2.6: Resulting pressure response for Site 2 after using a 36-hr low-pass filter.

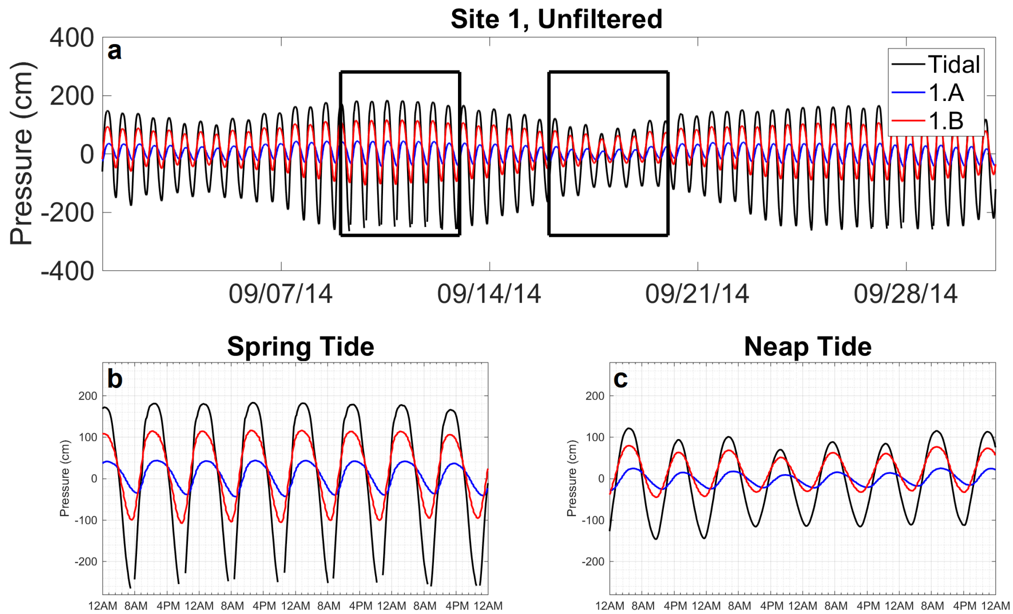

Figure 2.7: Piezometer pressure response at Site 1 during the spring-neap cycle of September 2014. Black box inset are shown in b and c.

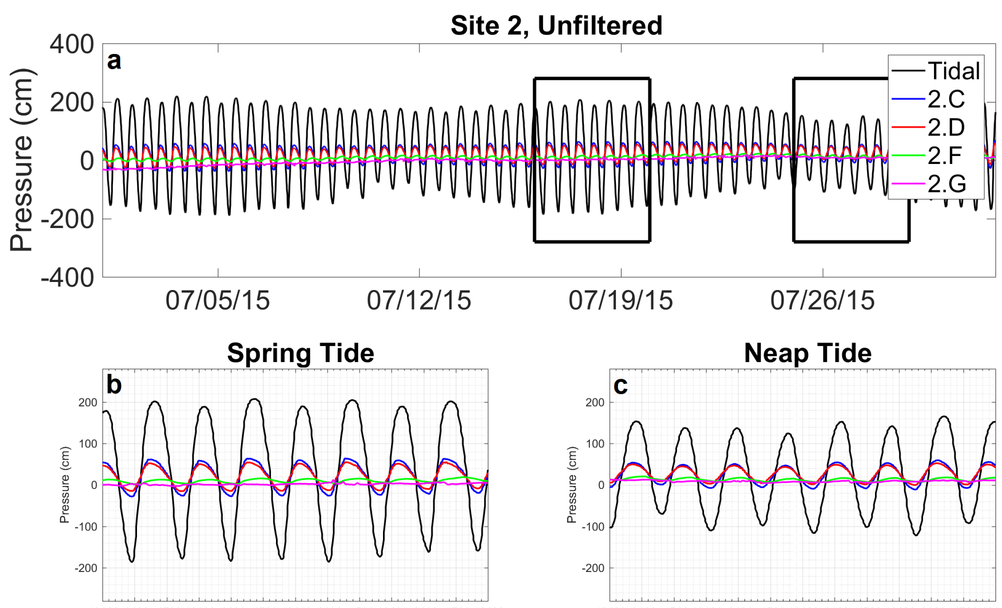

Figure 2.8: Piezometer pressure response at Site 2 during the spring-neap cycle of July 2015. Black box inset are shown in b and c.

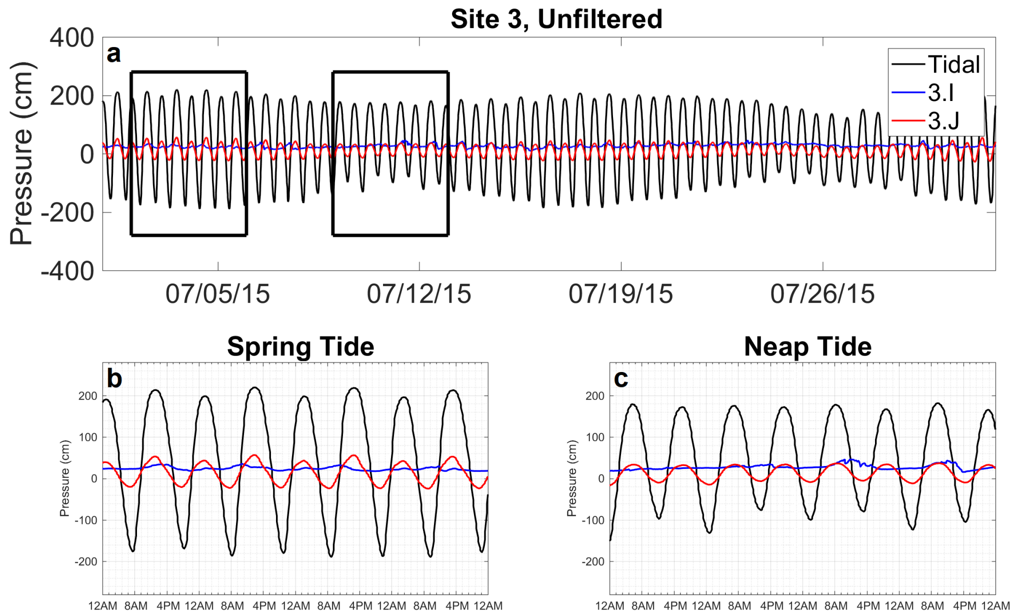

Figure 2.9: Piezometer pressure response at Site 3 during the spring-neap cycle of July 2015. Black box inset are shown in b and c.

Piezometer instruments show varying pressure amplitudes and lags, uncorrelated with screen depth or distance from tidal channel (Fig. 2.5). The piezometer pressure is dominated by the tidal signal and shows only seasonal pressure frequencies when filtered (Fig. 2.6). The pressure sinusoid is asymmetric with an incline steeper than the decline, with similar peak gradients in both spring and neap tides (Figs. 2.7, 2.8, and 2.9). This asymmetry is equivalent to peak attenuation due to floodplain storage. The gradient of the rising limb changes when the incoming high tide breeches the platform, explaining the flatter peaks and the sharper bottoms of the tidal sinusoid.

Site 1 pressure lags are especially confounding. Outside of the embankment, it takes an average of 50 min for the pressure signal to propagate to piezometer A, although the lag is much greater during the neap cycle (Fig. 2.7.c). The piezometer B farther from the channel actually has a negative lag of approximately 9 min (i.e., the groundwater head peaks prior to the tidal channel). The negative lag is especially pronounced during the spring tide (Fig. 2.7.b). At Site 2, piezometers C and D, closest to the tidal channel, have a relatively constant pressure lag of -64 min and -71 min, respectively (Fig. 2.8). The Sundarbans piezometer is synchronized with the tidal signal and only shows a -3 min lag response (Fig. 2.9).

Several piezometers show a 1°C seasonal change in temperature but no trend in specific conductivity (Fig. 2.5). Salinity of groundwater from tubewells is spatially variable and uncorrelated with distance from tidal channel or depth. The average salinity is 10 ppt, which exactly matches *Ayers et al.* (2016) findings. The concentrations of soluble salt components are highly correlated, indicating conservative behavior (Fig. 2.10).

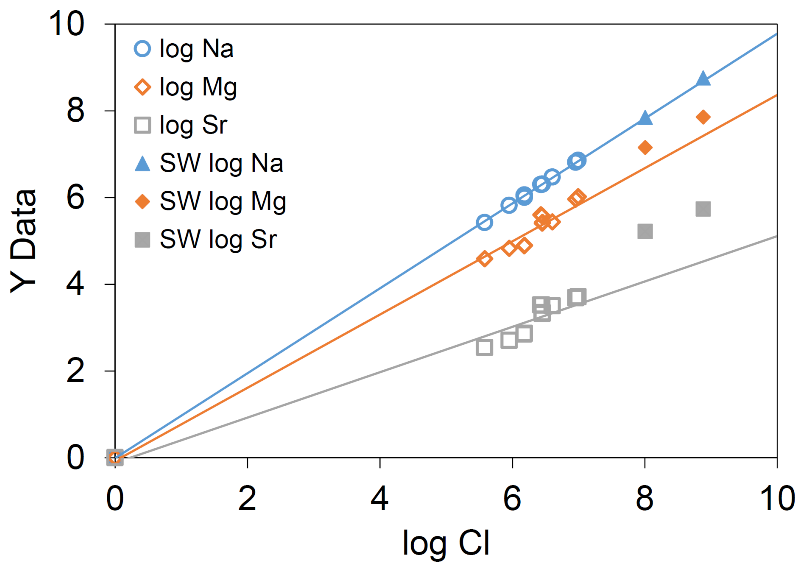

Figure 2.10: Concentration of Cl plotted versus concentrations of conservative elements Na, Mg, and Sr with best-fit linear regression lines. The filled symbols at high Cl concentration come from tidal channel samples. All concentrations are log10 values in mg/L.

2.3.4 Groundwater Model

The groundwater model suggests that a clayey silt channel clogging layer with widths ranging from 2.5 – 10 m between the tidal channel and aquifer may induce the piezometer pressure amplitudes we observe. The model results indicate hydraulic conductivity of the clogging layer between 1x10^{-9} cm/s and 2x10^{-5} cm/s, which are typical of silts and clays (*Fetter*, 2001).

2.3.5 EMI

Highly variable EMI output suggest lateral variation in soil conductivities, which is a function of clay content, water content, and salinity. The four frequencies correspond to varying electrical conductivity (EC), with the highest EC associated with 93090 Hz and the lowest EC associated with 6030 Hz on average (Fig. 2.11). Borehole lithology and salinity readings show relative differences corresponding with EC results. Because of drilling limitations, we were unable to locate areas of surface water recharge for inversion validation.

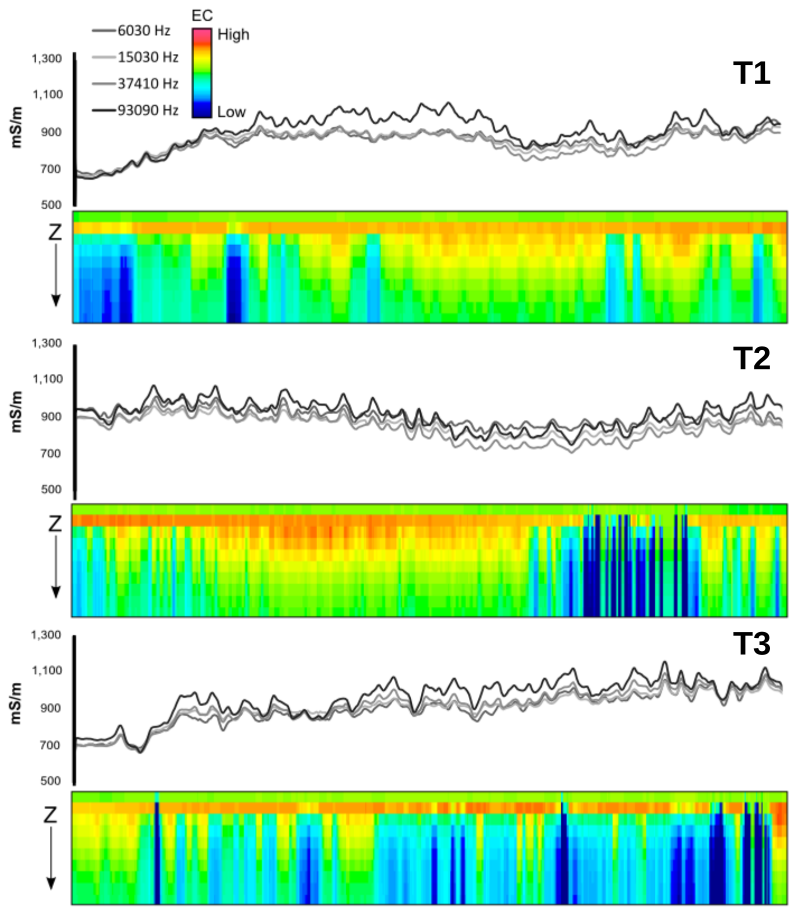

Figure 2.11: The electrical conductivity (EC) results for four frequencies on three different transects. An 10-layer inversion model that goes to an unknown depth Z was built from the inphase and quadrature data. In all transects, a higher EC unit caps a lower EC unit. Location of transects is shown in Fig. 2.2.

2.4 Discussion

Understanding complex GW-SW exchanges in deltaic plains is key to locating potable drinking water in the brackish aquifer system. Surface water resources are susceptible to contamination and flood risks, making groundwater options preferable in these dynamic coastal environments. In the poldered region of southwestern Bangladesh, large tidally-fluctuating rivers and intense periods of monsoonal rains are potential sources of freshwater infiltration through aquifer-tidal channel exchange and meteoric recharge, respectively. *Worland et al.* (2015) suggest extremely small groundwater velocity flows in this region. With localized regions of GW-SW exchange, this setting would allow for the development of pockets of freshwater within brackish aquifer. This study suggests, however, that GW-SW interactions on Polder 32 are likely (1) limited and (2) difficult to identify.

2.4.1 Aquifer-Tidal Exchange

Tidal channel-aquifer exchange is minimal on Polder 32. Piezometers show little variation in aquifer salinity and temperature over time that would correspond to the signal fluctuations in channel water. The thick clay units overlying the shallow aquifer and low permeability of tidal channel banks prevent infiltration. Furthermore, heterogeneity within aquifer sediments further prevent large spatial signatures of any site of aquifer-tidal exchange. This varied stratigraphy (of clay and sand lenses) across Polder 32 is characteristic of many coastal delta formations, and the resulting anisotropy from this lithology may affect the tidal pulse propagation inland (*Trefry and Johnston*, 1998).

Varying pressure attenuation responses within and between Polder 32 piezometer sites demonstrate the complex aquifer connectivity to the channel. Although we were limited to 3 sites with a total of 7 pressure transducer records, we differentiated site specific transmissivity of the shallow aquifer through slug tests and channel clogging layer along banks. We were unable to confirm, however, tidal propagation and attenuation relationships with respect to distance from the channel.

The typical response of water in a well to oceanic tidal loading occurs as a result of three processes: (1) mechanical loading of the aquifer, (2) propagation and attenuation of the pressure wave inland through the aquifer, and (3) flow of groundwater between the aquifer and the borehole (*Ingersoll et al.*, 1954; *Furbish*, 1991; *Carslaw and Jaeger*, 1959). This process assumes that the aquifer is homogeneous, confined, and that the flow of groundwater into the well is horizontal (*Rojstaczer*, 1988; *Furbish*, 1991). The confusing pressure lags we observe are likely due to a combination of (1) errors during tubewell installation, (2) paleochannels or heterogeneous aquifer structures, or (3) the complex tidal prism around Polder 32.

To address the first point, it is necessary to highlight the basic drilling process. During the traditional hand-flapper method, PVC pipes are joined by heating and molding the plastic ends. This relatively secure, albeit loose joint, may have allowed vertical leakage along the outside of well pipes or leakage into the well at union of two pipes. An improper seal is a well-known cause of hydraulic short circuit and may impact the response of the piezometer (*Chesnaux et al.*, 2006).

Peferential flowpaths and connectivity patterns in the shallow aquifer may also influence tidal propagation. Paleochannels correspond to high-permeability zones that may act as preferential pathways and that make transmissivity distribution highly heterogeneous (*Mulligan et al.*, 2007). *Worland et al.* (2015) speculated whether paleochannels are connected beneath the entire polder and their influence on the salinity variations in tubewells. But it is possible that instead of acting as preferred pathways for flow, area of high transmissivity can enhance the pressure propagation inland. (*Xia et al.*, 2012).

Lastly, we acknowledge that it is always preferable to measure river stage fluctuations as close to the groundwater investigation site as possible. Unfortunately the tidal currents on the Shibsha River at Site 1 disable installation of any longterm pressure transducer. For this reason, we used time series data from a river gauge located at Site 3, which is 25 km from Site 1 and 2 km from Site 2, by tidal channel. A lag in the tidal signal would be expected as the tide propagates over the 25 km and additional complex lags can be expected because of the branching tidal channel network. This additional lag time (or negative lag) can be explained by the unique tidal propagation around Polder 32 from the Pasur River in the Northeast and the Shibsha River east of Polder 32 (Rachel Bain and Richard Hale, personal communication).

Alternatively, our field observations of time advance in aquifers fluctuation may be explained by complex interactions of channel-aquifer geometries in response to tidal fluctuation in a confined coastal aquifer with an impermeable outlet capping. *Li et al.* (2007), *Xia et al.* (2007), and *Maas and De Lange* (1987) all propose analytical solutions that describe the head responses of a confined aquifer under a tidal river. For an aquifer with impermeable outlet capping (i.e., negligible aquitard leakage), there may be a negative phase shift of tidal groundwater flow of up to 1.5 hrs for semidiurnal tides (Fig. 2.12) (*Li et al.*, 2007). This implies that the confining unit between the shallow aquifer and the tidal

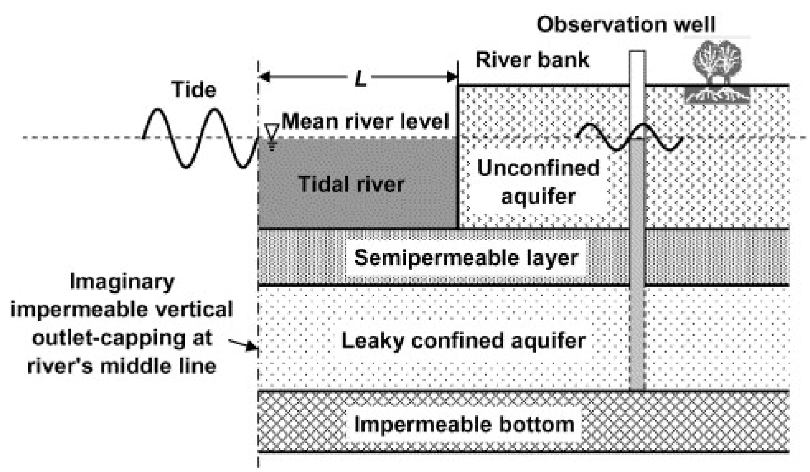

Figure 2.12: Schematic of a confined aquifer extending under a tidal river *Xia et al.* (2007). Copyright 2007 by Elsevier B.V. Reprinted with permission.

channel around Polder 32 has negligible leakage.

Piezometers revealed more about the heterogeneity of the landscape than any potential difference between the polder and natural environments. The variability in hydraulic properties was as high within each site as between Polder 32 and Sundarbans. One difference that plays a role in meteoric recharge is the variation in inundation patterns.

2.4.2 Recharge

The importance of describing the spatial variability of groundwater recharge is especially important in saline environments. If high recharge areas can be identified, successful site selection of tubewells is more likely. This requires fine spatial resolution of recharge rather than regional averages. Traditional techniques of estimating groundwater recharge give varying degrees of spatial resolution, and often are associated with high cost and labor requirements (*Cook et al.*, 1992). To overcome these obstacles, studies now use geophysical techniques to locate areas of groundwater recharge. The soil profile at a given site influences the rate of infiltration, which therefore affects water and salt content. All of these factors–soil properties, wetness, and salinity– influence the electrical conductivity (EC) of the soil, making electromagnetic induction (EMI) a useful detection tool (*Rhoades and Chanduvi*, 1999; *Cook et al.*, 1992; *Davis*, 2007; *McNeill*, 1980; *Topp et al.*, 1993). In complex environments with wet or highly saline soil, however, it is more difficult to delineate causation of high EC measurements with particular subsurface properties (*Davis*, 2007; *Johnston et al.*, 1994; *Doolittle et al.*, 2001).

With our EMI transects, we were able to observe lateral variability in conductivity, which may be attributed to thinning of the confining unit or the presence of fresher water. However, we were unable to locate areas of surface water recharge for validation. Although *Worland et al.* (2015) find similar results, it is possible to conclude that EMI cannot be used in coastal systems (with multiple EC contributors such as clay content, salt, and soil moisture) due to the complexity of the environment. All geophysical techniques should be checked with borehole lithologies and we were unable to satisfy that recommendation in this study.

Studies, including this investigation, point repetitively to variable groundwater salinities in this region (*Ayers et al.*, 2016; *Worland et al.*, 2015; *Bahar and Reza*, 2010). We were unable to explain the regions of freshwater with GW-SW interactions. It is equally possible that the seemingly unpredictable heterogeneity may be due to variation in depositional history instead. The shallow groundwater may be trapped connate porewater laid down with surface sediments at the time of deposition. In the low flow aquifer, the salinity (either fresh river discharge or saline seawater) of that connate porewater would be preserved with very little effects of advection.

2.5 Conclusion

In an attempt to locate fresh, potable groundwater, this study explores GW-SW interactions on coastal Bangladesh polders. Findings suggest heterogeneity in groundwater salinity and shallow subsurface lithology, but limited evidence of exchange with fresh surface water. Direct exchange between the tidal channel and aquifers is negligible at our study sites and the possibility of detecting meteoric freshwater recharge with EMI methods is unlikely. We revealed more about localized heterogeneity in the shallow subsurface than any differences in GW-SW interactions between the natural and poldered environment. Although we were unsuccessful at identifying a reliable method for identifying fresh groundwater resources, the polder residents likely will continue to use the fresher tubewells. Other studies are needed to resolve the complex water resource problems in the poldered region. A multifaceted approach that considers technical and social aspects of water sources, instead of only environmental conditions, may be more effective at overcoming the water insecurity issues of the coastal communities (*Hoque et al.*, 2016).

CHAPTER 3

MULTICRITERIA DECISION ANALYSIS OF FRESHWATER RESOURCE MANAGEMENT IN SOUTHWESTERN BANGLADESH

3.1 Introduction

Inadequate provision of domestic water services to rural areas of developing countries is still a global challenge. The United Nations set Sustainable Development Goals to achieve universal and equitable access to safe and affordable drinking water for all by 2030 (*UN Economic and Social Council*, 2016; *WHO and UNICEF*, 2017), however, this will not be easily attainable. As of 2015, only 55% of the rural populations used safely managed drinking water sourcessources that are accessible on the premises, available when needed, and free from fecal and priority chemical contamination (*WHO and UNICEF*, 2017). The lack of functioning infrastructure is often attributed to top-down supply-driven planning, which ignores the local context (*Cai et al.*, 2004; *Starkl et al.*, 2013). Decision-makers and water resource planners often fail to give attention to what users want and will maintain. To achieve sustainable solutions, underdeveloped, rural regions need transparent, participative, and democratic demand-driven planning (*Starkl et al.*, 2013). Even with thoughtful planning, careful implementation is also necessary to avoid unexpected infrastructure failures. In regions where successful water systems could fail and go undetected, water quality is especially important in order to prevent users from consuming hazardous water (*Starkl et al.*, 2013). These issues can be prevented if decision-makers consider solutions to avoid infrastructure failures and robust plans to provide safe and sustainable water sources.

Decision analysis methods offer an opportunity to support public participation and provide structured, rational, and transparent solutions to complex management problems in water resources and environmental projects (*Belton and Stewart*, 2002; *Cai et al.*, 2004;

Hajkowicz and Collins, 2007; *Chowdhury and Rahman*, 2008; *Mutikanga et al.*, 2011). In particular, multicriteria decision analysis (MCDA) is globally used as a holistic, analytical tool for evaluation of decision options. A variety of MCDA approaches allow decision makers to account explicitly for multiple criteria while ranking, selecting, and/or comparing different alternatives (e.g. products, technologies, policies) (*Kirkwood*, 1997; *Belton and Stewart*, 2002). MCDA approaches generally follow one of three underlying theories: (1) utility function, (2) outranking relation, and (3) sets of decision rules. Unfortunately the selection of the MCDA method can be tricky and is often chosen based on familiarity and affinity with the approach, rather than an assessment of the decision-making situation and goal (*Cinelli et al.*, 2014). Most often, MCDA approaches are used to tease out stakeholder preferences and formalize the decision-making process among participants. Emerging in the 1960s and 1970s, MCDA has been used in a wide array of applications, including water resources and environmental projects (*Stewart and Scott*, 1995; *Cai et al.*, 2004; *Hajkowicz and Collins*, 2007; *Chowdhury and Rahman*, 2008; *Mutikanga et al.*, 2011; *Jha et al.*, 2014; *Scholten et al.*, 2015). These complex projects are seldom guided by a single objective. MCDA may provide the insight to overcome stakeholder bias and institutional hurdles that prevent the longevity of successful water resource projects. To date decision tools have not been implemented for planning for water resources in rural areas of developing countries, and only considered in a few studies (*Chowdhury and Rahman*, 2008; *Calizaya et al.*, 2010).

Drinking water resources in rural, coastal Bangladesh vary in availability, quality, and susceptibility to hazards and other water security risks. Although the country has immense natural water resources, the monsoon climate is the major control on drinking water quantity and quality. With 80% of the rainfall occurring during June to September (*Chowdhury*, 2010; *Abedin et al.*, 2014), locals must adapt to the subsequent dry season (October to May) by using multiple sources to meet drinking water needs. Inadequate water storage infrastructure intensifies water insecurity, often resulting in communities improperly allocating surface water to meet multiple needs–drinking, cooking, bathing, and serving livestock. Microbiological contamination of surface waters occurs due to livestock and human fecal pollution (*Abedin et al.*, 2014; *Benneyworth et al.*, 2016). Salinity from seawater mixing and arsenic contamination from naturally occurring arsenic-laced sediments hinder groundwater resources. Considering the projected climate change and population growth, the vulnerability of Bangladesh water resources inadequacies is likely to intensify (*Huq*, 2001; *McGranahan et al.*, 2007; *World Bank*, 2011; *Jongman et al.*, 2012; *Jiménez Cisneros et al.*, 2014; *Wong et al.*, 2014). In many developing countries, a suitable option for providing adequate safe drinking water can be elusive, with no option free from disadvantages.

The five most frequently used sources (both natural and human engineered) for drinking water across coastal Bangladesh are rainwater harvesting, ponds, pond sand filters, managed aquifer recharge (MAR), and tubewells. A mixture of stakeholdershouseholds, local community members, non-governmental organizations (NGOs), and governmental agencieshave played key roles in promoting, installing, and maintaining these natural and human-engineered water sources, but success of each source has varied as a result of physical and social factors. Although factors may vary on a case-by-case basis, the planning and decision-making process of water source implementation, maintenance, and overall success are not well understood. Often public participation in water resources management is overlooked in developing countries like Bangladesh (*Chowdhury and Rahman*, 2008), giving power to decision-makers outside of the community.

The objective of this paper is to explore the various technical, economic, social, and environmental factors that influence the most frequent drinking water technologies and management schemes in southern Bangladesh. Using MCDA, we assess the probable success of drinking water supply technologies and rank the sources based on their likely success in the future. We consider differences among stakeholder preferences and MCDA methods to investigate the influences of prioritization and process, as well as to ensure robustness of our methods. Although site-specific water quality, treatment actions, and ultimately infrastructure building must be considered in water supply solutions, this study supports the underlying decision-making and is the first step toward the selection of preferred options considering local context.

3.2 Background

3.2.1 Study Area

The coastal region of Bangladesh is predominantly rural. In the 1960s and 1970s, much of the tidal mangrove forest of the lower delta was converted to 56 agricultural islands that now sustain a population of 150 million through paddy farming, fishing and aquaculture (*Rahman and Salehin*, 2013). These large islands, or polders, are protected from tidal and storm-surge inundation by constructed earthen embankments (*Auerbach et al.*, 2015). Significant research has been based on one particular polder, Polder 32, located in the Khulna district, Dacope Upazila in southwest Bangladesh, 60 km north of the Bay of Bengal (Fig. 3.1) (*Tasich*, 2013; *Auerbach et al.*, 2015; *Worland et al.*, 2015; *Ayers et al.*, 2016; *Benneyworth et al.*, 2016). This polder has similar hydrological and geological characteristics of the other 56 polders in the region, however it provides an extreme case study for environmental hazards and community resilience in coastal Bangladesh due to devastation by cyclone Aila in 2009 (*Mehedi et al.*, 2010; *Auerbach et al.*, 2015). The cyclone breached embankments in several locations, leaving a majority of the Polder 32 inundated for two years (*Auerbach et al.*, 2015).

A formerly forested and intertidal system, Polder 32 is bordered by tidal channels that are distributaries of the Ganges River. Its lower half lies adjacent to the protected Sundarbans forest while its upper half is surrounded by other polders. There is no significant local topography for the study area, with an average vertical relief of nearly zero (*Auerbach et al.*, 2015). The shallow hydrogeology of the area consists of a semiconfined, shallow

Figure 3.1: Map of study area showing location of Polder 32.

Holocene sand aquifer (*Rahman et al.*, 2011; *Burgess et al.*, 2010) extending 100 m below ground level that is vertically separated from two deeper Pleistocene aquifers by a variably thick, heterogeneous aquitard. The shallow groundwater is primarily brackish with isolated instances where fresher water can be found.

The region experiences a humid, biseasonal climate with a dry season from November to May and wet season from June to October (*Chowdhury*, 2010; *Rashid*, 1977; *Shahid*, 2010). Polder 32 is estimated to receive between 1500 mm to 2100 mm of rainfall per year (*Nobi and Gupta*, 1997). Tropical cyclones typically form over the Bay of Bengal during the transitional monsoon months of May and November (**?**). The tropical cyclone frequency in the Bay of Bengal has a prominent El Nio-Southern Oscillation cycle of 2 to 5 years during the wet season and transitional monsoon months (**?**). The average temperature ranges from 7 to 13°C during winter and 24 to 31°C during summer, with May being the hottest month (*Shahid*, 2010).

Currently, approximately 44,000 people live on this 19 km by 7 km wide polder (*Benneyworth et al.*, 2016; *Bangladesh Bureau of Statistics*, 2012, 2015b, 2014). Impoverished in comparison to Bangladesh as a whole, 17% of the rural population on Polder 32 has an electricity connection and 35% has access to sanitary toilets (*Benneyworth et al.*, 2016). Most residents live on monthly family incomes of less that Tk. 3,000 (approximately $39 USD) (*Islam et al.*, 2013). Nearly all residents rely on multiple sources for drinking water throughout the year, most of which are surface water sources (*Islam et al.*, 2013). Of these sources, approximately half are maintained by households, rather than by the community or an NGO, and some are not maintained at all (*Benneyworth et al.*, 2016).

3.2.2 Water Sources and Infrastructure

Rainwater harvesting has been used for drinking purposes since people inhabited the coastal region of Bangladesh (*Hussain and Ziauddin*, 1989). In recent years, NGOs and governmental programs have invested in and promoted the installation of several types of household and community-based rainwater harvesting systems (*Ansari et al.*, 2010; *Islam et al.*, 2013). Storage tanks include plastic pitchers and clay jars fed by rooftop runoff, ferrocement storage reservoirs, and plastic tanks. Often the capacity of jars and pitchers is insufficient to last the entire dry season, but the construction cost of larger tanks is prohibitive for lower income families. The rainwater harvesting tanks vary in capacity from 500 to 3,200 liters, costing from Tk. 3000 to 8000 (or approximately \$35 to \$100 USD) (*Ansari et al.*, 2010; *Islam et al.*, 2013). The main advantages of rainwater harvesting include the provision of water at or near the point of consumption, the lack of operation and maintenance problems, and the minimal maintenance costs. Generally harvested rainwater is free of contaminants, but it is at risk of developing coliform bacteria if stored for long periods of time (*Islam et al.*, 2007).

Although the 2009 cyclone and subsequent inundation left many ponds salty, a few scattered freshwater ponds, locally known as ”sweet water ponds,” survive around the Polder 32. These artificially constructed reservoirs are replenished by rainwater during the monsoon season, and often serve a myriad of purposes including cleaning, cooking, water for livestock, and drinking water. These ponds have a significant risk of biological contamination from livestock and salinization during storm inundation (*Alam et al.*, 2006; *Ansari et al.*, 2010). To remediate contamination, the ponds are occasionally associated with pond sand filters, or slow sand filtration systems. In the pond sand filters system, users hand pump pond water to a large tank to allow water percolation through a bed of fine sand, resulting in the removal of pathogens and fine grain sediments. Initially pond sand filters were designed by the Department of Public Health Engineering in 1984, and now NGOs often administer the installation of the filters in areas that face salinity and arsenic problems (*Ansari et al.*, 2010). Although reliant on a pond water source, pond sand filters' requirement for significant construction costs and regular maintenance to replace dirtied sand necessitates a separate designation and is, therefore, assessed as an independent source separate from ponds. The lack of proper maintenance often leads to non-functioning and abandoned pond sand filters.

Managed aquifer recharge (MAR) is a technology to induce recharge to aquifers and increase subsurface water storage. This technology has been implemented since the early 2000s in the coastal Bangladesh (*Bouwer*, 2002). Water is collected from ponds and roofs, passed through a sand filter, and injected into the shallow brackish Holocene aquifer through a ring of infiltration wells. The injected water forms a small (couple meter-wide) stagnant freshwater lens in the dense saline groundwater. The stored water can later be extracted according to demand (*Holländer et al.*, 2009). The underground storage offers significant flood protection during regular cyclonic surges. Each MAR scheme can serve several hundreds of people with 15 liters of water per day during the dry season, but the pumps, filters, and wells must be maintained regularly (**?**). It is possible that the MAR could provide an average recoverable volume of 750 m^3 per year–based on a 0.75 recovery efficiency (**?**). A pilot MAR was installed and maintained by NGOs and academic institutions, but Polder 32 residents became the sole operators of the source in 2016.

The last most common drinking water source on Polder 32 is a shallow tubewells, which pumps from the same shallow Holocene aquifer as described above. Across broader Bangladesh the majority of the rural population uses tubewell water as their primary source, however, in the coastal areas both shallow and deep tubewells are used less often because of high salinity groundwater. Only an estimated 13.6% of residents of Polder 32 report using tubewells as a main drinking water source (*Benneyworth et al.*, 2016). Families may own a household tubewell, but they are more often community wells. Typically the water is unfiltered, and some wells are even marked with red to warn against high arsenic contamination. The use of most tubewell is suspected to be a function of perceived water quality, taste, smell, and proximity (*Shumaker*, 2017).Rainwater harvesting has been used for drinking purposes since people inhabited the coastal region of Bangladesh (*Hussain and Ziauddin*, 1989). In recent years, NGOs and governmental programs have invested in and promoted the installation of several types of household and community-based rainwater harvesting systems (*Ansari et al.*, 2010; *Islam et al.*, 2013). Storage tanks include plastic pitchers and clay jars fed by rooftop runoff, ferrocement storage reservoirs, and plastic tanks. Often the capacity of jars and pitchers is insufficient to last the entire dry season, but the construction cost of larger tanks is prohibitive for lower income families. The rainwater harvesting tanks vary in capacity from 500 to 3,200 liters, costing from Tk. 3000 to 8000 (or approximately $35 to $100 USD) (*Ansari et al.*, 2010; *Islam et al.*, 2013). The main advantages of rainwater harvesting include the provision of water at or near the point of consumption, the lack of operation and maintenance problems, and the minimal maintenance costs. Generally harvested rainwater is free of contaminants, but it is at risk of developing coliform bacteria if stored for long periods of time (*Islam et al.*, 2007).

Although the 2009 cyclone and subsequent inundation left many ponds salty, a few scattered freshwater ponds, locally known as ”sweet water ponds,” survive around the Polder 32. These artificially constructed reservoirs are replenished by rainwater during the monsoon season, and often serve a myriad of purposes including cleaning, cooking, water for livestock, and drinking water. These ponds have a significant risk of biological contamination from livestock and salinization during storm inundation (*Alam et al.*, 2006; *Ansari et al.*, 2010). To remediate contamination, the ponds are occasionally associated with pond sand filters, or slow sand filtration systems. In the pond sand filters system, users hand pump pond water to a large tank to allow water percolation through a bed of fine sand, resulting in the removal of pathogens and fine grain sediments. Initially pond sand filters were designed by the Department of Public Health Engineering in 1984, and now NGOs often administer the installation of the filters in areas that face salinity and arsenic problems (*Ansari et al.*, 2010). Although reliant on a pond water source, pond sand filters' requirement for significant construction costs and regular maintenance to replace dirtied sand necessitates a separate designation and is, therefore, assessed as an independent source separate from ponds. The lack of proper maintenance often leads to non-functioning and abandoned pond sand filters.

Managed aquifer recharge (MAR) is a technology to induce recharge to aquifers and increase subsurface water storage. This technology has been implemented since the early 2000s in the coastal Bangladesh (*Bouwer*, 2002). Water is collected from ponds and roofs, passed through a sand filter, and injected into the shallow brackish Holocene aquifer through a ring of infiltration wells. The injected water forms a small (couple meter-wide) stagnant freshwater lens in the dense saline groundwater. The stored water can later be extracted according to demand (*Holländer et al.*, 2009). The underground storage offers significant flood protection during regular cyclonic surges. Each MAR scheme can serve several hundreds of people with 15 liters of water per day during the dry season, but the pumps, filters, and wells must be maintained regularly (**?**). It is possible that the MAR could provide an average recoverable volume of 750 m^3 per year–based on a 0.75 recovery efficiency (**?**). A pilot MAR was installed and maintained by NGOs and academic institutions, but Polder 32 residents became the sole operators of the source in 2016.

The last most common drinking water source on Polder 32 is a shallow tubewells, which pumps from the same shallow Holocene aquifer as described above. Across broader Bangladesh the majority of the rural population uses tubewell water as their primary source, however, in the coastal areas both shallow and deep tubewells are used less often because of high salinity groundwater. Only an estimated 13.6% of residents of Polder 32 report using tubewells as a main drinking water source (*Benneyworth et al.*, 2016). Families may own a household tubewell, but they are more often community wells. Typically the water is unfiltered, and some wells are even marked with red to warn against high arsenic contamination. The use of most tubewell is suspected to be a function of perceived water quality, taste, smell, and proximity (*Shumaker*, 2017).

3.3 Methods

Decision models allow for an overall ranking and/or utility of alternatives with respect to the achievement of a set of objectives. In multicriteria decision analysis (MCDA), decision makers examine various alternatives and use a weighting scheme to identify an efficient set, or preferred option (*Kirkwood*, 1997). Although objectivity can be limited by imprecise data and personal preferences, MCDA better informs us of the decision-making process and the structure of the objectives (*Figueira et al.*, 2013). The three basic concepts included in a MCDA are the (1) problem or objective of the model, (2) potential actions or alternatives which need to be ranked or scored by the decision maker, and (3) a set of criteria, typically measured in a variety of different units. The MCDA model includes an evaluation matrix $\boldsymbol{X}$ of n_a alternatives and m criteria. The performance score for each alternative i with respect to criteria j is denoted by $x_{i,j}$. The importance of each criterion is denoted in the weights vector $\boldsymbol{W}$ containing m weights, where w_j denotes the weight assigned to the jth criterion (Table 3.1).

In this study, the model objective is to determine the most feasible, or successful, freshwater drinking source in coastal Bangladesh. The alternatives we consider, based on their frequent use, include: managed aquifer recharge (MAR), pond, pond sand filter, rainwater harvesting, and tubewells. Criteria are grouped into four categories: environmental, technical, social, and economic (Fig. 3.2). The criteria were determined from a literature review and from informal conversations with local community members and academic experts in the region. Scores for each criteria ranged from 0 to 100, where 100 represents the best performance. For example, if an alternative scores a high value for the ”failure rate” criterion then the alternative shows good performance in this area. This high score can be interpreted as infrequent failure of the alternative to provide drinking water. See Table S1 in supporting information for raw criteria performance scores and formula.

Four MCDA methods are used for this analysis–including multiple attribute value theory (MAVT), analytic hierarchy process (AHP), ELimination and Choice Translating Reality (ELECTRE) I, and ELECTRE III–to ensure agreement between methods. The weights were determined from the normalized mean of survey results for academic and NGO stakeholders and from semi-structured interviews with local community focus group, as de-

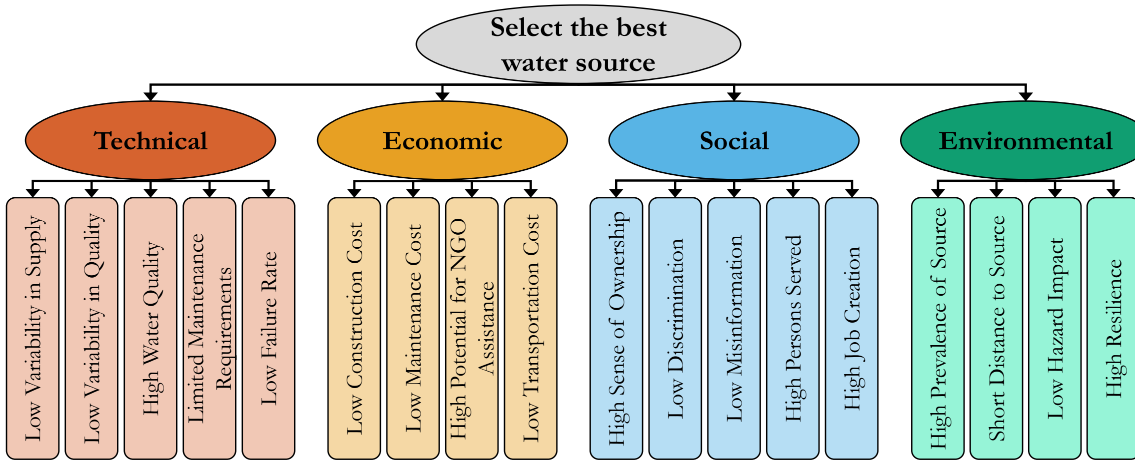

Figure 3.2: Objective and criteria used for the evaluation of drinking water alternatives in the MCDA. The ”best water source” is the drinking water source that is most likely to succeed.

scribed in the data section. Weights for each criteria range between 0 and 1, with 1 designating the greatest importance.

3.3.1 Multiple Attribute Value Theory

MAVT is a commonly applied value function used to represent the performance of the alternatives. The weighted summation method is expressed as

$$u_i = \sum_{j=1}^{m} v_{i,j} w_j. \tag{3.1}$$

In Eq. 3.1, the alternative's total score u_i is a function of the weights w_j and the normalized performance score $v_{i,j}$ for $x_{i,j}$. Variables w_j and $v_{i,j}$ range between 0 and 1 and 0 and 100, respectively. Under this study, the assumption of mutual preferential independence is considered to be appropriate. The preference between two attributes is not impacted by the value of any one of the other attributes. Though criteria may be correlated with one another, no two or more criteria independently have a large impact on the overall ranking of the options (**??**).

Table 3.1: Stakeholder preferences w_j and alternative performance scores $x_{i,j}$ based on 18 criteria j for 5 drinking water alternatives i. Weights range from 0 to 1 with 1 denoting the greatest importance. Scores range from 0 to 100 with 100 being the highest performance.

Weights w_j			Criteria		Alternative Scores $x_{i,j}$				
Academic	**NGO**	**Local**			**RWH**	**Pond**	**PSF**	**MAR**	**TW**
0.88	0.87	0.70	Technical	Variability in Supply	43.9	73.3	86.9	41.7	94.7
0.78	0.73	0.60		Variability in Quality	100	25	75	75	75
0.95	0.93	0.70		Water Quality	97.3	40.3	86.4	64.0	35.9
0.89	0.93	0.80		Maintenance Requirements	75	100	0	0	75
0.80	0.67	0.60		Failure Rate	100	75	50	50	75
0.80	0.73	0.90	Economic	Construction Cost	96.1	59.2	95.4	40.2	79.8
0.82	0.87	1.00		Potential for NGO/Governmental Help	100	25	100	100	25
0.94	0.93	1.00		Maintenance Cost	100	100	97.5	18.8	100
0.74	0.60	0.80		Transportation Costs	100	0	100	100	100
0.80	0.87	0.70	Social	Sense of Ownership	100	75	50	25	75
0.83	0.73	0.60		Discrimination	50	100	75	50	75
0.78	0.67	0.50		Misinformation	75	75	50	0	50
0.85	0.87	0.60		Persons served	0.6	70.8	71.2	30	8.3
0.63	0.60	0.40		Job Creation	0	25	25	25	25
0.82	0.80	0.80	Environmental	Prevelence of Source	93.5	55	35	3.5	61
0.82	0.80	0.80		Distance to Source	87.3	66.5	68.5	0.0	24.1
0.86	0.73	0.50		Hazard Impact	100	0	25	50	100
0.83	0.67	0.50		Resilience	100	25	25	50	100

3.3.2 Analytic Hierarchy Process

AHP is the most widely applied pairwise comparison technique (*Saaty*, 2008). This approach establishes priorities between elements of hierarchies through pairwise comparisons. Criteria are grouped into a hierarchy of elements, which in this case only includes two tiers–criteria category (n=4) and criteria (4≤n≤5 depending on the criteria category). A priority is assigned to each element of the hierarchy by means of pairwise comparisons. The priorities express the importance of one element over the others, and are given on the nine-point Saaty's scale (**??**). See *Saaty* (2008) or **?** for a more detailed explanation of the method. For example, all technical criteria elements are pairwise compared to each other (i.e. variability in supply v.s. variability in quality, variability in supply v.s. water quality, etc.). Then the higher-level technical category is pairwise compared to the other criteria categories (i.e. technical v.s. economic, technical v.s. social, and technical v.s. environmental).

After taking the geometric mean of each element, the criteria priorities are then weighed by the priority of their higher-level criterion categories to obtain a global priority, or weight w_j, for each criteria. This weight is then applied to the alternative scores $v_{i,j}$ as described in *Saaty* (2008). The result of each pairwise comparison is determined from survey responses about the importance of each criterion (see supporting information) and the semi-structured interviews with local focus groups.

3.3.3 ELimination and Choice Translating Reality (ELECTRE) I

ELECTRE was developed in 1966 as one of the earliest multi-criteria evaluation methods developed among outranking methods (*Benayoun et al.*, 1966; *Roy et al.*, 1986; *Roy*, 1991). The objective of this method is to select a desirable alternative from a subset $\boldsymbol{F}$ of alternatives based on two indices, the concordance index and the discordance index. These indices are defined for each pair of alternatives i and i' such that any alternative not included in $\boldsymbol{F}$ is outranked by at least one alternative in $\boldsymbol{F}$. The concordance index $c(i,i')$ measures the strength of the information that supports the hypothesis that i is at least as good as i', while the discordance index $d(i,i')$ measures the strength of evidence against this hypothesis. Given a set A of n alternatives and an ordered pair of alternatives (i,i') in A, evaluated by a set of m criteria $(g1, g2, ..., gm)$, each criterion is given the following attributes: (1) a weight w_j increasing with the relative importance of the criterion g_j, and (2) a veto threshold $v_j(g_j) > 0$. The concordance index $c(i,i')$ is calculated for each ordered pair of alternatives $(i,i') \in n$ using Eq. 3.2 and Eq. 3.3.

$$c(i,i') = \frac{1}{W} \sum_{j:g_j(i)>=g_j(i')} w_j \tag{3.2}$$

$$W = \sum_{j=1}^{m} w_j \tag{3.3}$$

The concordance index takes values between 0 and 1 as a measure of a favorable assertion that i outranks i' such that higher values indicate stronger evidence in support of the claim

(*Shofade*, 2011).

The discordance index uses the veto threshold defined for each criterion. If the score for i' on any one of these criteria is greater than the score of option i on the same criterion, with a value greater than or equal to the v, then the assertion that "i outranks i'" is refuted, Eq. 3.4.

$$d(i,i') = \begin{cases} 1 & \text{if } g_j(i') - g_j(i) > v_j(g_j) \text{ for any } j \\ 0 & \text{otherwise} \end{cases} \tag{3.4}$$

The final outranking relation iSi', also called the credibility matrix, can be defined by Eq. 3.5, where $\hat{c}$ and $\hat{d}$ are arbitrary relatively large and small thresholds, respectively (*Rogers and Bruen*, 1998; **?**). In this study, we use the mean of the concordance and discordance matrices as the thresholds.

$$iSi' iff \begin{cases} c(i,i') >= \hat{c} \\ d(i,i') <= \hat{d} \end{cases} \tag{3.5}$$

3.3.4 ELimination and Choice Translating Reality III

ELECTRE III is a ranking method designed to be less sensitive to inaccuracy, imprecision, and uncertain data. ELECTRE III uses the notion of pseudo criteria. Instead of assuming that any difference in performance corresponds to a difference in preference, indifference and preference thresholds allow for uncertainty criteria performance and subsequently its preference.

$$c_j(i,i') = \begin{cases} 1 & \text{if } g_j(i) + q_j(g_j(i)) >= g_j(i') \\ 0 & \text{if } g_j(i) + p_j(g_j(i)) <= g_j(i') \\ \frac{p_j(g_j(i)) - g_j(i) - g_j(i')}{p_j - q_j} & \text{if } g_j(i') - p_j <= g_j(i) <= g_j(i') - q_j \end{cases} \tag{3.6}$$

In Eq. 3.6, p_j and q_j denote the indifference and preference thresholds, respectively (*Rogers and Bruen*, 1998). Similarly, the discordance matrix is defined in Eq. 3.7.

$$d_j(i,i') = \begin{cases} 1 & \text{if } g_j(i') > g_j(i') + v_j(g_j(i)) \\ 0 & \text{if } g_j(i') <= g_j(i) + p_j(g_j(i)) \\ \text{otherwise} & \frac{g_j(i') - g_j(i) - p_j(g_j(i))}{v_j(g_j(i)) - p_j(g_j(i))} \end{cases} \tag{3.7}$$

The overall outranking relation for ELECTRE III is then defined using the credibility matrix in Eq. 3.8, where $J(i,i')$ is the set of criteria j for which the discordance index is greater that the concordance index. For both ELECTRE I and ELECTRE III, we assume a quantitative value for the overall ranking of the alternatives from the normalized sum of the rows of the credibility matrix.

$$\rho(iSi') = \begin{cases} c(i,i') & \text{if } d_j(i,i') <= c(i,i'), \forall j \\ c(i,i') & \text{otherwise } \prod_{j \in J(i,i')} \frac{1 - d_j(i,i')}{1 - c_j(i,i')} \end{cases} \tag{3.8}$$

3.3.5 Sensitivity Analysis

In considering results from decision analysis, evaluation of the stability of outcomes in the face of uncertainties in scores and weights is important. This typically is done through sensitivity analyses using either a local or global approach (e.g., see*Ganji et al.* (2016); *Hyde et al.* (2003, 2004); *Saltelli* (2002)). We use both approaches. First, we conduct a simple local one-at-a-time sensitivity analysis for each performance score, in which $x_{i,j}$ ranges from the minimum score of 0 to the maximum of 100. Then to test the robustness of our method, we also conduct a generalized sensitivity analysis, which broadens beyond the sensitivity of each individual parameter set. A generalized sensitivity analysis can be used in situations where (1) models contain ill-defined parameters, (2) statistical distributions are used to reflect parametric uncertainty, and (3) results depend on a problem-defining behavioral outcome that can be categorized into a *behavior* and *nonbehavior* (*Hornberger and Spear*, 1981). By categorizing the outcome into a binary behavior (i.e. it either occurs or does not occur for a give scenario and set of parameter), this methodology is a useful technique for identifying inherent uncertainties in the model structure and important parametric relations (*Hornberger and Spear*, 1981).

In this generalized sensitivity analysis, we perform a Monte Carlo simulation of 1000 runs in which all parameters (either all weights $\boldsymbol{W}$ or all scores $\boldsymbol{X}$) are determined from a Gaussian distribution about the given parameter value, where $\bar{X}$ equals the sample mean of x_i or x_j, and s is the sample standard deviation of $\boldsymbol{W}$ or $\boldsymbol{X}$, respectively. Scores are treated as parameters because data sources are imperfect due to limited sample size and function assumptions used to calculate $x_{i,j}$ (Table 3.2 and Table S1). Weights (i.e. stakeholder importances) also are parameterized due to the assumption that the limited stakeholder interviews are only a sample of the entire population of possible responses. The simulations were then separated into two outcome groups, based on the resulting ranking.

For this study, we are specifically interested in what weights and parameters are associated with outcomes where either rainwater harvesting or pond sand filter achieves the highest rankings as they avoid salinity problems associated with tubewells and also technological challenges associated with managed aquifer recharge (MAR). Simulations are classified as achieving the *behavior* if rainwater harvesting and pond sand filter rank as the highest two alternatives. If outcome differs such that alternatives pond, MAR, and/or tubewell rank in the highest two alternatives, then the simulation is classified as a *nonbehavior*. The distributions of each criterion and weight are then determined and compared based on their behavior or nonbehavior classification.

3.4 Data

Data include a variety of physical, social, and economic data collected in southwest Bangladesh. Social data include regional water quality perceptions, perceptions of manage-

Table 3.2: Data sources for MCDA. See Table S1 in supporting information for additional details, including formulas and scoring for each criterion.

Group	Criteria	Source	Interpretation
Technical	Variability in Supply	Average of number of months used	Usage frequency of the source in a given year
	Variability in Quality	Qualitative Interviews	Quality variance due to season or location
	Water Quality	Function of TDS, Salinity, Arsenic, and pathogens	Quality of water sources
	Maintenance Requirements	Qualitative Interviews	Time and effort required for regular maintenance
	Failure Rate	Qualitative Interviews	Frequency of failure
Economic	Construction Cost	Blanchet, 2014	Construction or purchase cost of source
	Potential for NGO or Governmental Help	Qualitative Interviews	Likelihood for economic assistance from entity outside of community
	Maintenance Cost	Blanchet, 2014	Cost of regular maintenance
	Transportation Cost	Qualitative Interviews	Transportation cost from source to household
Social	Sense of Ownership	Qualitative Interviews	Likelihood that source users feel ownership and responsibility of the source
	Discrimination	Qualitative Interviews	Likelihood of discrimination in source usage based on economic status, gender, and relative location to source
	Misinformation	Qualitative Interviews	Likelihood that source users are misinformed about ownership, quality, and function of source
	Persons Served	Average of how many people use the source	Number of users source can serve
	Job Creation	Qualitative Interviews	Likelihood of job creation for local community member due to source
Environmental	Prevalence of Source	Number of each used for drinking water in Khulna District	Number of each source currently used in the area
	Distance to Source	Travel time to source	Time need to travel to source
	Hazard Impact	Qualitative Interviews	Likelihood that source will be negatively impacted by an environmental hazard, such as cyclone, flood, or drought
	Resilience	Qualitative Interviews	Likelihood that source can recover from a negative hazard impact

Figure 3.3: Weights between 1 and 0 of each criterion as determined by stakeholder surveys.

ment/technology success, managed aquifer recharge community surveys, and interviews with non-governmental organizations (NGO) partners and academic experts (Table 3.2). Environmental and technical feasibility factors are determined from regional water quality data and geospatial information. Economic factors are informed from reported cost estimates for the region (*Blanchet*, 2014). Criteria weights come from average responses from a emailed survey given to NGO ($n = 3$) and academic experts ($n = 13$) (see supporting information for survey design) as well as from semi-structured interviews during 17 local stakeholder focus groups ($n \approx 85$) (Fig. 3.3).

3.4.1 Surveys

In the surveys, NGO and academic stakeholders designated criteria from 1 (not at all important) to 5 (extremely important) as a measures of one's perception of the importance of various criteria. The measures of importance were used as weights in subsequent analyses. Stakeholders responses were averaged and divided by the maximum possible weight to obtain the stakeholder group's overall criteria weights (Fig. 3.3). NGO survey respondents included three Bangladeshi not-for-profit NGOs. Academic stakeholders included eight American and two Bangladeshi environmental scientists as well as two American and two Bangladeshi environmental social scientists. The emailed survey required approximately 5-10 minutes and ended with three open-ended response questions, which were assessed to ensure quality responses. In every case, respondents answered all 10 questions.

3.4.2 Focus Groups

Local community member engaged in conversation with the research team in focus groups, ranging from 2 to 30 participants. Participants responded to prompted questions about drinking water source use, success, failure, risks, and user desires. The participants also evaluated drinking water alternatives by providing unprompted criteria and indicators for success. Participants suggested reasons and empirical evidence to support one alternative over another, for example, highlighting problems with implementation design and community values and dynamics. This type of community focus group has been shown to refine decision processes and ensure that communities are fully involved in the final selection of indicators (**?**).

The interviews were led by two Bangladeshi translators and one American from the research team. The translators verbally summarized the responses which were transcribed by the research team member. The conversations lasted 5-15 minutes depending on the participants' interest and engagement. Translators gave their first impressions from the

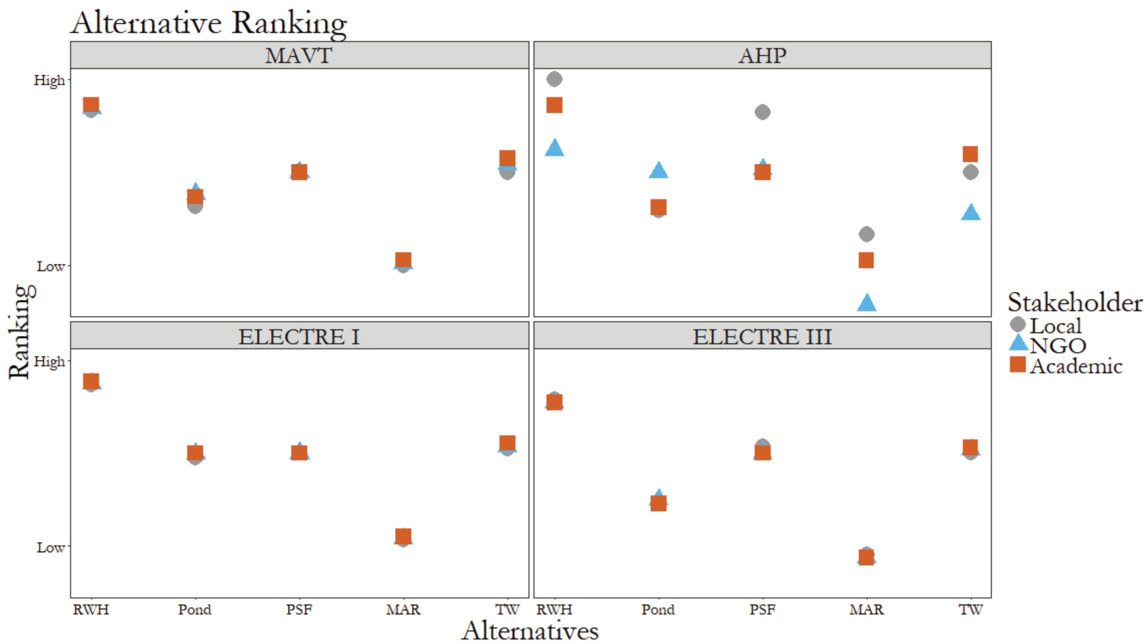

Figure 3.4: The ranking (y-axis) of the five alternatives (x-axis) as it varies among the MCDA methods (subplot) and stakeholder preference (color).

focus groups after each interview, and the researcher's notes were confirmed during these conversations. The notes and summary of each focus group was reviewed by the research members upon return from the field sites. At this point, criteria weights and alternatives scores (designated by "Qualitative Interviews" source in Table 3.2) were determined from trends the combined interviews of all focus groups.

3.5 Results

In all methods, rainwater harvesting is the highest ranked alternative and managed aquifer recharge (MAR) is the lowest (Fig. 3.4). Pond, pond sand filter, and tubewell rank in the middle with tubewell and pond sand filter generally exceeding the ranking of pond. Differences between the MCDA methods explain more variance than stakeholder preferences, except for AHP, as seen by the overlapping markers in each subplot of Fig. 3.4. Even when considering extreme one-at-a-time scenarios, MAR can never outrank rainwater harvesting (Fig. 3.5). Pond, tubewell, and pond sand filter can only surpass rainwater

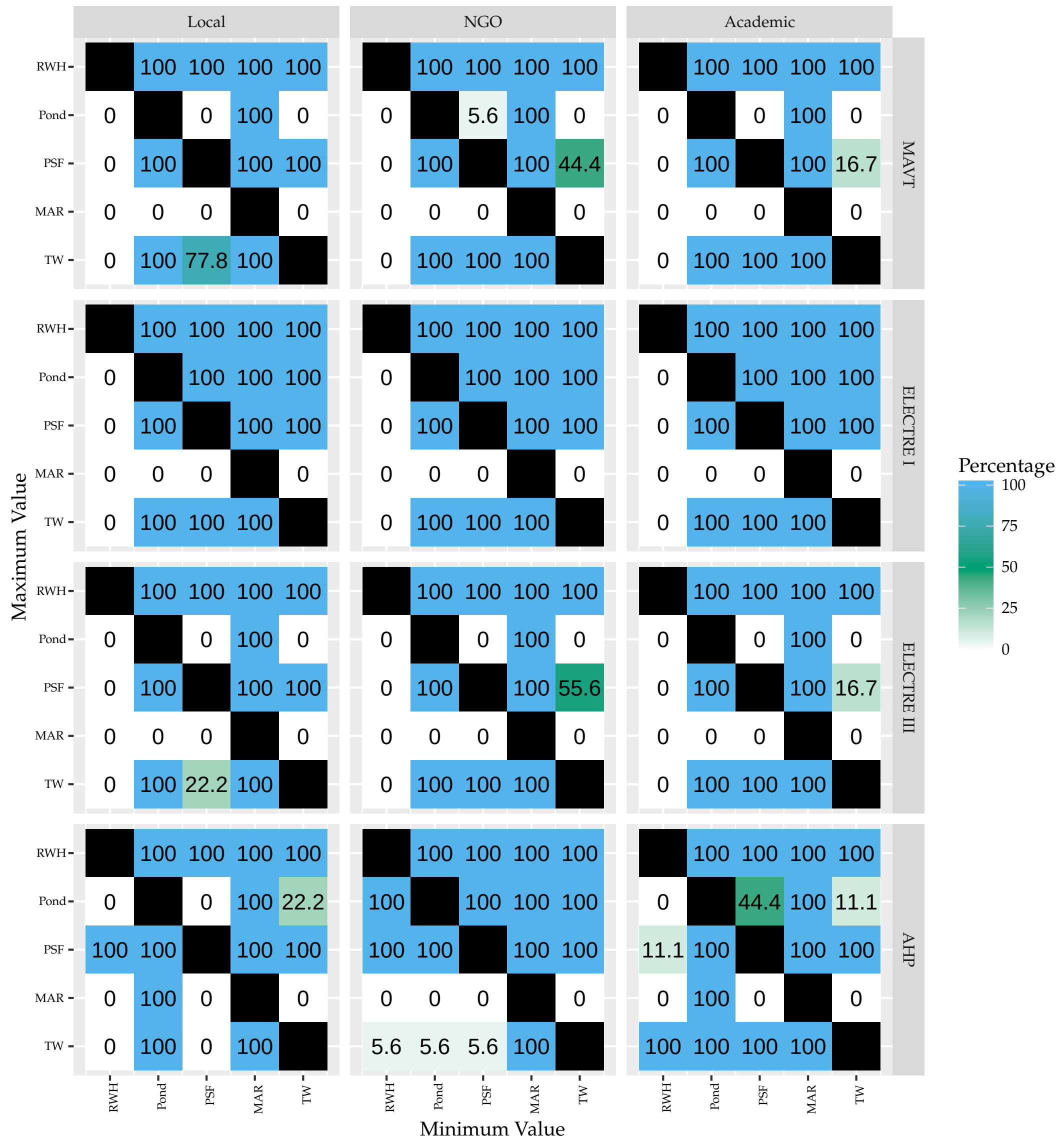

Figure 3.5: Heat map of frequency of exceeding ranking of another alternative in one-at-a-time scenarios. If cell equals 100%, then the maximum of the y-axis alternative exceeds the minimum value of the x-axis alternative in every scenario. If the cell equals 0% then the maximum value of the y-axis alternative never reaches the minimum possible value of the x-axis alternative.

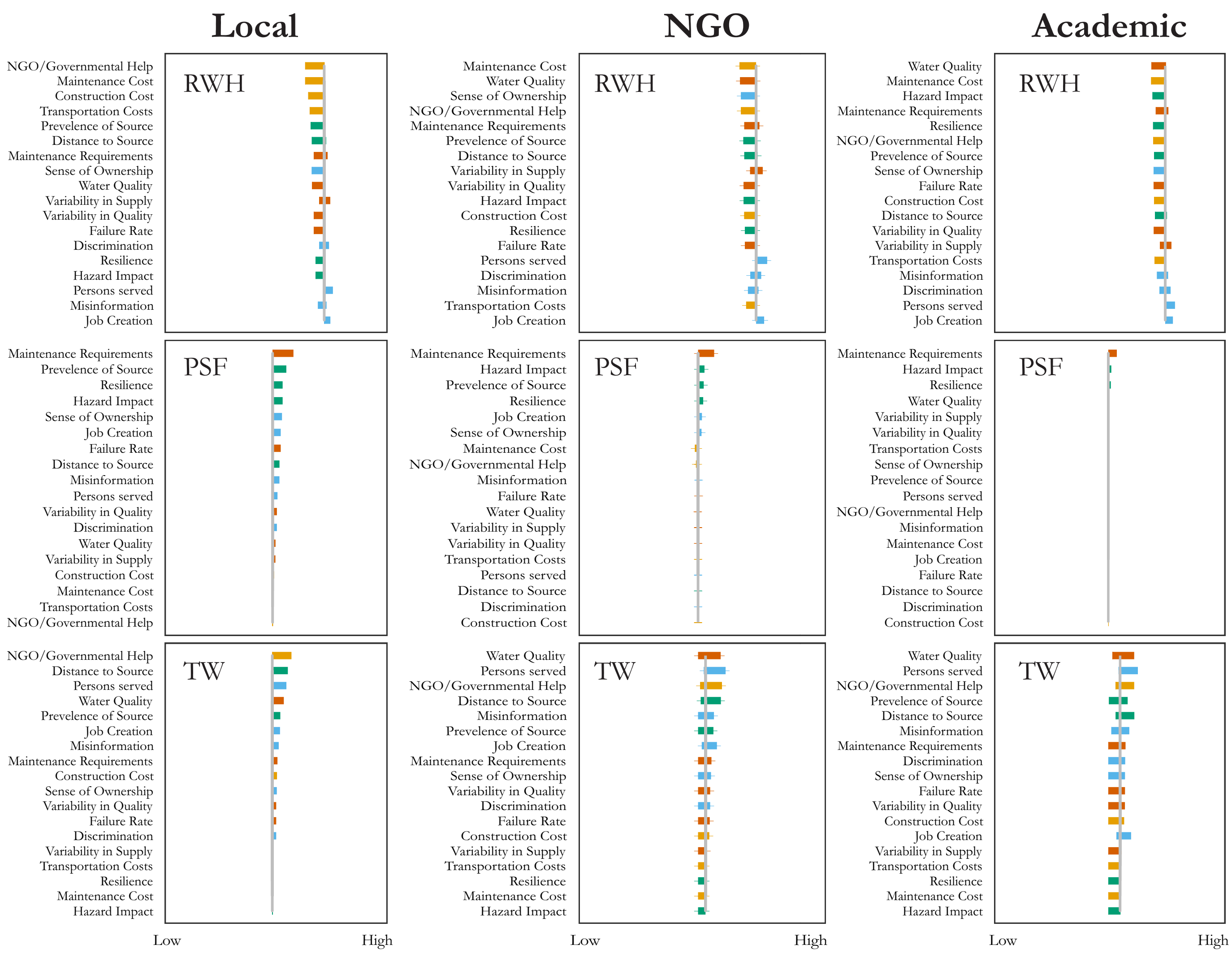

Figure 3.6: Tornado diagrams of criteria sensitivity for the top three ranked alternatives–rainwater harvesting (RWH), pond sand filter (PSF), and tubewell (TW)–in MAVT. See supporting information figures S1-S3 for all other tornado diagrams.

harvesting as the highest ranked alternative in the AHP method (Fig. 3.5). MAR can only exceed the pond ranking if using the AHP method (Fig. 3.5). This robustness of ranking order suggests an insensitivity to extreme values within the scoring matrix $\boldsymbol{X}$. This is further depicted in the narrow range of the possible ranks for each alternative (Fig. 3.6).

The one-at-a-time sensitivity results also suggest that all criteria categories are equally significant in the overall ranking of the alternatives (Table 3.3, and Figs. 3.6 and S1-S3 in supporting information). However, it is possible that weighting of different criteria leads to

Table 3.3: The most significant criteria category for each alternative and method, as determined from the one-at-a-time sensitivity analysis and the tornado diagrams (Fig. 3.6 and Figs. S1-S3 in supporting information).

Alternative	Method			
	MAVT	AHP	ELECTRE I	ELECTRE III
RWH	Economic > Technical > Environmental > Social	Technical > Economic > Social > Environmental	Environmental > Technical > Social > Economic	Economic > Environmental > Social > Technical
Pond	Technical > Economic > Environmental > Social	Technical > Economic > Social > Environmental	Economic > Technical > Social > Environmental	Economic > Environmental > Social > Technical
PSF	Environmental > Technical > Social > Economic	Technical > Economic > Social > Environmental	Economic > Technical > Environmental > Social	Technical > Environmental > Economic = Social
MAR	Technical = Economic > Environmental > Social	Technical > Economic > Social > Environmental	Environmental = Social > Technical > Economic	Social > Economic > Environmental > Technical
TW	Environmental > Technical = Economic = Social	Social > Technical > Economic > Environmental	Environmental > Technical > Economic > Social	Economic > Environmental > Technical > Social

Table 3.4: The most significant criteria category for each alternative and stakeholder, as determined from the one-at-a-time sensitivity analysis and the tornado diagrams ((Fig. 3.6 and Figs. S1-S3 in supporting information).

Alternative	Stakeholder		
	Local	NGO	Academic
RWH	Economic > Technical > Environmental > Social	Environmental = Technical > Economic > Social	Social > Economic > Technical = Environmental
Pond	Economic > Technical = Environmental > Social	Technical > Economic > Environmental > Social	Technical = Economic > Social > Environmental
PSF	Technical > Economic > Environmental > Social	Technical > Economic > Environmental > Social	Technical > Environmental > Economic = Social
MAR	Economic > Technical > Environmental > Social	Technical > Social = Environmental > Economic	Social > Environmental = Technical = Economic
TW	Environmental > Technical = Economic > Social	Technical > Environmental > Economic > Social	Social = Economic > Environmental = Technical

differences in the importance of criteria categories between stakeholders (Table 3.4). Economic criteria are most significant among local stakeholders, whereas technical criteria are most significant with NGO stakeholders (Table 3.4). The social criteria are most significant with academic stakeholders (Table 3.4). Nevertheless, no specific criteria are highlighted as extremely significant to the final outcome.

Similarly, the generalized sensitivity analysis does not show any noticeably significant criteria, suggesting that criteria are equal in importance (Figs. 3.7 and 3.8). The range for most sensitive parameters between behavior and nonbehavior outcomes include weights from all criteria categories–technical, economic, social, and environmental–although the differences in ranges between behavior and nonbehavior outcomes are barely noticeable (Fig. 3.7). Sensitive criterion weights are different in AHP, ELECTRE I, and ELECTRE III as shown in Figs. S28, S30, and S32 in the supporting information.

The scores of alternate/criterion pairs are more sensitive, albeit only slightly, than the weighting schemes when differentiating between behavior and nonbehavior categories (see slight shifts in parameter distributions in Fig. 3.8 as compared to negligible shifts in Fig. 3.7). Across all methods and stakeholder groups, the sensitive $x_{i,j}$ are most often associated with switching of ranking between ponds and tubewells (Figs. S29-S33 in supporting information). Significant $x_{i,j}$ range across all four criteria categories, suggesting method robustness especially since x_j for rainwater harvesting are often insensitive.

Academic and NGO survey results show differences between expected ranking of alternatives and MCDA ranking (Fig. 3.9). Academic stakeholders expected rainwater harvesting and pond sand filter to rank as the best alternatives, but considered pond water to be the least preferred option. Similarly, NGO stakeholders ranked rainwater harvesting as top alternative, but considered tubewell, pond sand filter, and MAR as equally preferred sources (Fig. 3.9).

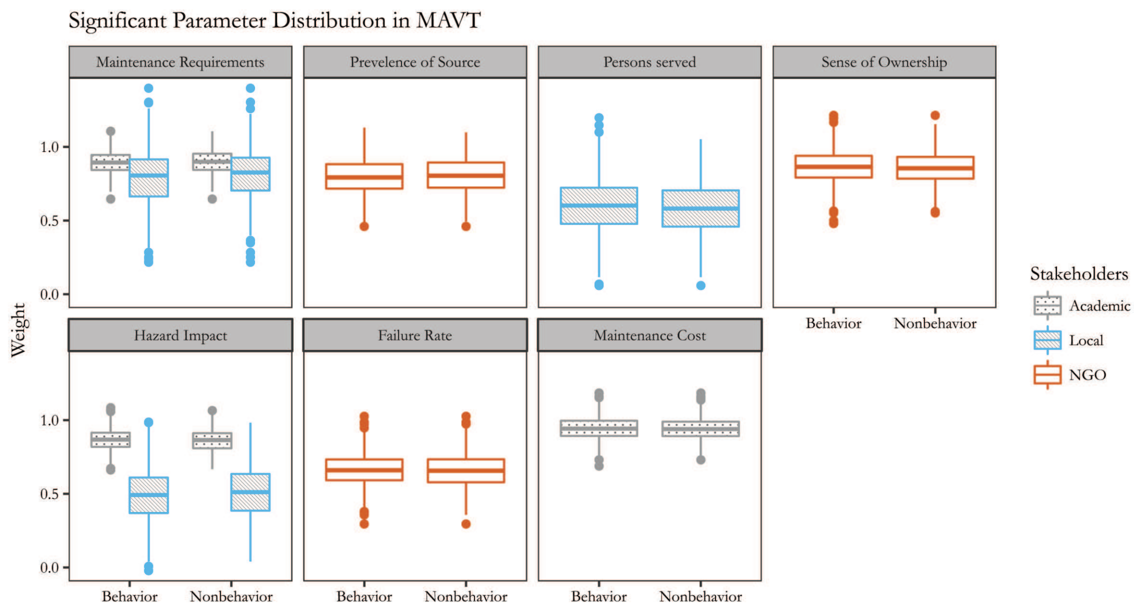

Figure 3.7: Distribution of generalized sensitivity analysis weights w_j for top three most significant criteria (based on weighting) in local, NGO, and academic simulations that result in differences between behavior and nonbehavior outcomes in MAVT.

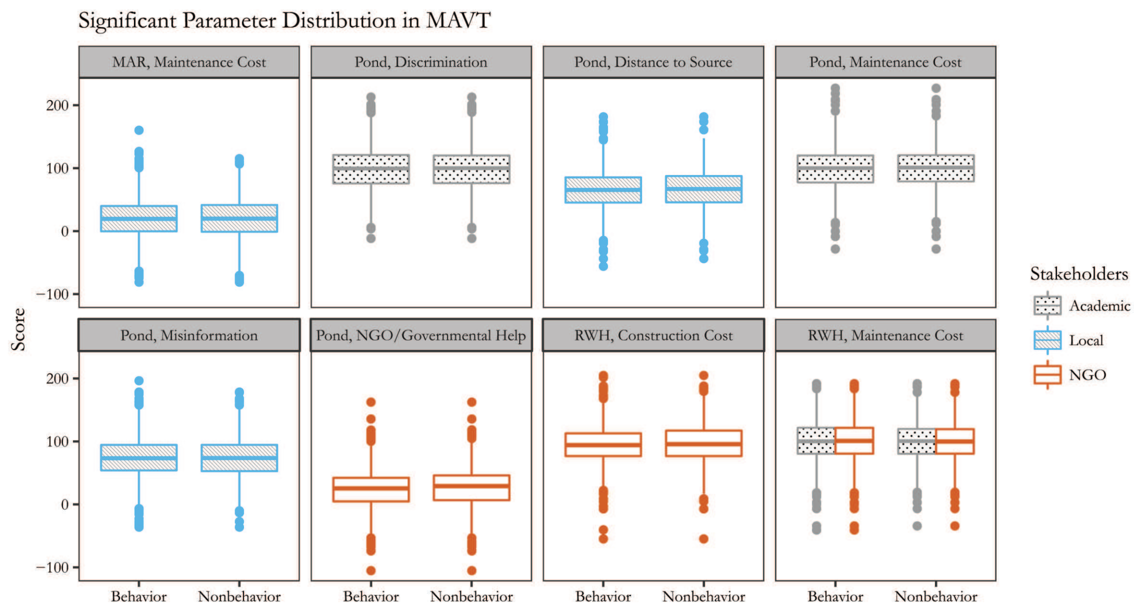

Figure 3.8: Distribution of generalized sensitivity analysis scores $x_{i,j}$ for top three sensitive parameters (based on scores) in local, NGO, and academic simulations that result in differences between behavior and nonbehavior outcomes in MAVT.

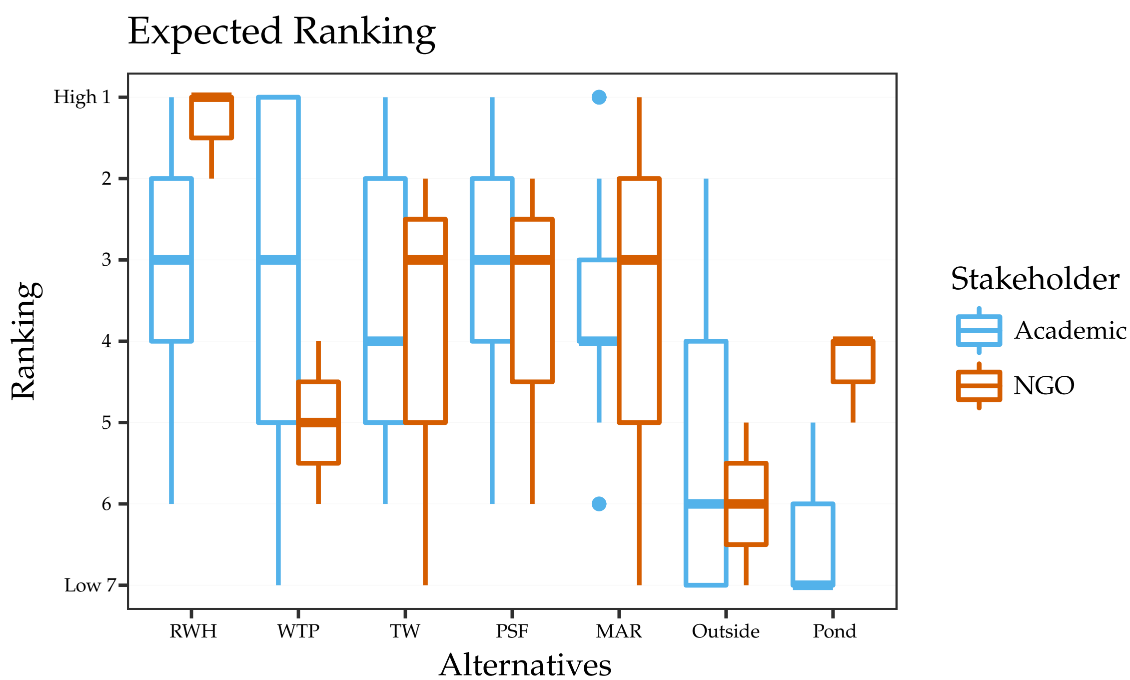

Figure 3.9: Expected ranking of alternatives as determined from academic and NGO survey results. Expected ranking refers to the predicted relative ranking of different sources, where ”RWH” is rainwater harvesting, ”WTP” is water treatment plant, ”TW” is tubewell, ”PSF” is pond sand filter, ”MAR” is managed aquifer recharge, ”outside” is water purchased outside the community, and ”pond” is pond water.

3.6 Discussion

This MCDA allows for a methodical and transparent evaluation of the drinking water alternatives and criteria affecting their success in coastal Bangladesh. After considering multiple MCDA methods and stakeholder preferences, our results robustly suggest rainwater harvesting is the top ranked drinking water source and is, therefore, most likely to succeed. By demonstrating that differing methods achieve similar results, MCDA tools give confidence that resources should be directed toward supporting, promoting, and even improving the rainwater harvesting sources in the study area.

Alternatively, the consistently low ranking of MAR may suggest unlikely future success of the technology. MAR scored poorly across all criteria categories, which especially low performance scores in social criteria. Local community member interviews pointed to significant misunderstanding concerning ownership and responsibility of maintenance of the MAR system. For example, community leaders expressed difficulty in collecting enough money for maintenance. Community users would rather wait for a NGO or governmental organization to pay for the maintenance, resulting in communities sometimes going months or years without a functioning MAR system. These types of social discontentments with MAR have also been seen in other studies (**?***Blanchet*, 2014). Extensive communication with community users, as well as other social dimensions, must be increased to improve use and performance of MAR (*Blanchet*, 2014).

NGO and academic stakeholders ranked MAR as the second (tied with pond sand filter) and fourth best alternative, respectively (Fig. 3.9). It is likely that the stakeholders (1) had limited background knowledge of the MAR technology, (2) felt an affinity toward MAR, or (3) undervalued the importance of the social criteria in MAR success, given that they later gave high importance to the social criteria. This divergence between the stakeholders' initial ranking and MCDA ranking supports the basis for holistic decision analysis methods. MCDA gives potential insights into complex problems that may be misconstrued in a quick assessment. When a decision is based on multiple (often conflicting) weighted criteria, a decision maker may resort to heuristic problem solving and intuition in making the decision. MCDA allows for a more transparent structure the problem and an explicit evaluation of multiple criteria.

In this study, stakeholder preferences, with respect to the importance of different criteria, play little role in the ranking of alternatives. The greater variance between MCDA methods emphasizes the need for appropriate method selection and thorough understanding of method process. Confusion by method choice, especially when different methods do not necessarily recommend the same solution for the same problem, can deter stakeholders and decision-makers from using MCDA methods (**?**). Because some methods are more analytically rigorous (e.g. ELECTRE I and ELECTRE III), it may be best to build tools that group MCDA methods and allow stakeholders to input parameters and run multiple methods instantaneously under different scenarios (**????**).

The lack of sensitivity among weights and criteria shows the robustness of different methods in capturing the performance of alternatives, despite imprecise data and uncertain parameter characterization. While it is likely that attributes within and across criteria categories may be interconnected, no one category appears more important than another. For example, we found that social and economic factors are just as important as environmental and technical aspects of water resource management. This is especially important to consider when engineers and decision-makers lack proper data and metrics to measure social criteria. In problems when social factors may affect the decision outcome, decision-makers should seek advice from appropriate socioeconomic experts to better gather and understand social criteria data.

This study assumes a typically high quality of rainwater harvesting systems, but without proper water quality testing and treatment this may not be an adequate assumption at all sites and scenarios (*Islam et al.*, 2015). Alternative assessment and planning is the first step to reaching sustainable solutions, but water managers must also acknowledge the need for robust research in infrastructure failure as well as water quality and treatment. Positive

MCDA ranking results do not ensure successful water systems implementation and management. Failure to consider unexpected infrastructure or management obstacles could increase risk of hazardous health implications.

Although this study uses MCDA methods to identify a ranking of single alternatives, it does not consider combinations of drinking water sources acting as discrete alternatives (**?**). Currently all residents use multiple sources (*Jakariya*, 2005; *Islam et al.*, 2007, 2015; *Blanchet*, 2014; *Benneyworth et al.*, 2016), so it is likely that a more realistic water management design would lead to the use of more than one source (*McBean et al.*, 2013). Rainwater harvesting is likely to succeed broadly, but other alternatives could be partial, or backup, sources. For example, it would not be unreasonable to promote rainwater harvesting as the primary drinking water source while still maintaining the occasional functioning of community pond sand filters for use in case of drought. On the other hand, rainwater harvesting might be the top single solution, especially if a variety of NGOs or governmental programs promoted and invested in the solution, such that the harvesting storage capacity exceeded the water resource demand (*Islam et al.*, 2007; *Alam et al.*, 2012).

When attempting to factor in local context (*Cai et al.*, 2004; *Starkl et al.*, 2013), decision-makers must acknowledge that communities are not homogeneous in terms of needs and preferences. Environmental, demographic, cultural, and historical variables have all been identified as reasons for variations among communities (*Jakariya*, 2005). In this context, we concede that our analysis is calibrated with data from a very small region of coastal Bangladesh. It is likely at both a smaller, site-specific scale and across a broader region, we would find discrepancies in our results. However, it may be possible to extrapolate our methods and results to other regions, especially by applying our insights to inform future data collection and survey implementation. From our analysis, we know that social acceptance

Another important consideration of decision analysis methods is the complexity of the problem. In every simple method, the decision-maker has to assume the appropriate level of complexity to address the problem. Here, we group alternatives based on technology. Conversely, we could have incorporated a more precise definition of the various alternatives that would have split alternatives into a greater number of options (e.g. privately-owned rainwater harvesting separated from community rainwater harvesting sources) which would have required further data collection. In our analysis, information on the small details about sources that could contribute to their ultimate success is not considered due to the limited quantity and quality of available data. As we categorized qualitative data from the focus group interviews, we reduced subjectivity by limiting the number of categorizations (see the five categories in Table S1 in the supporting information). Decision models rely on a balance between model accuracy and the expense of data collection and implementation of more complex models.

Despite the limitations of academic conjecture and modeling, the residents of Polder 32 and the surrounding regions are still faced with water insecurity and health risks. This research elucidates the multifaceted approach that will be needed to resolve water management problems, spanning the technical, economic, social, and environmental realms. Our findings support the similar studies that generally regard rainwater harvesting as an effective, high quality, improved source of drinking water (*Ansari et al.*, 2010; *Ahmed et al.*, 2011; *Alam et al.*, 2012; *Islam et al.*, 2013; *Abedin et al.*, 2014; *Blanchet*, 2014; *Arku et al.*, 2015; *Neibaur and Anderson*, 2016; *WHO and UNICEF*, 2017), but we demonstrate evidence of this assumption with our holistic evaluation of the water source. Stakeholders can begin to focus their efforts on making rainwater harvesting more sustainable through a better understanding of water quality (*Ahmed et al.*, 2011; *Arku et al.*, 2015; *Islam et al.*, 2015), successful implementation of community rainwater harvesting resources (*Domènech et al.*, 2012; *Opare*, 2012; *Neibaur and Anderson*, 2016), and collaboration of local residents and physical and social scientist (*Cai et al.*, 2004; *Ansari et al.*, 2010; *Starkl et al.*, 2013). The overall capacity community and individual rainwater harvesting will likely need to be assessed and increased, while the site-specific testing of water quality should be encouraged.

Meanwhile, the adaptation and implementation at local and national levels will require coordination between governments, NGOs, and community stakeholders to pragmatically install additional rainwater harvesting systems at homes, schools, and community structures (*Abedin et al.*, 2014). This integrated approach has the most promising outlook for addressing water insecurities and reducing the overall vulnerability of coastal communities (*Hoque et al.*, 2016; *Abedin et al.*, 2014).

3.7 Conclusions

Decision analysis methods highlight the usefulness of thorough data collection and modeling to better understand critical factors in water management. Although decision modeling can be dependent on the particular method process, stakeholder preferences, and imprecise data, method cross checking and sensitivity analysis can ensure for robust results. Often a decision-maker's intuition differs from a thorough model analysis. This likely due to the decision-maker's inability to fully structure the decision into (1) an objective, (2) set of alternatives, and (3) list of weighted criteria. MCDA can serve as a useful first step in addressing complex water management problems, especially in rural regions where an adequate understanding of the local context is key to success.

CHAPTER 4

FARZANA'S JOURNEY: A CHILDREN'S BOOK FOR RESEARCH-BASED, EDUCATIONAL OUTREACH IN REMOTE COMMUNITIES OF BANGLADESH

4.1 Introduction

Academics are encouraged to integrate their research with education and societal outreach. Some U.S. federal funding agencies, such as the National Science Foundation (NSF) are now insisting that scientists describe how their proposed research will have "broader impacts". Researchers must contribute not only to the growing fund of knowledge, but to the more immediate societal good. The *broader impacts* criterion pushes researchers to engage in activities beyond their research, such as sharing data, mentoring graduate students, engaging undergraduates in research, translating research results into instructional materials for classroom use, increasing the participation of groups that because of gender, ethnicity, disability, and/or geographic location are underrepresented in science, enhancing the research and educational infrastructures at their institutions, or working directly with the public (see for example *Mathieu et al.* (2009); *Dyer* (1999); *Magrath* (1999); *Roberts* (2009); *Andrews et al.* (2005)). Too often societal engagement outside academia is overlooked, unsuccessful, or transient at best.

One analysis of broader impacts statements from recent award abstracts reveals that 89% of researchers propose broader impacts for science, 43% discussed potential benefits for society, and 37% proposed dissemination activities beyond the scholarly community (*Roberts*, 2009). Those who discussed potential societal benefits, however, were no more likely to propose dissemination activities than researchers who only discussed broader impacts for science (*Roberts*, 2009). Perhaps the science community has not yet achieved sustainable and efficient methods of science communication and outreach with the non-science community. Alternatively, perhaps barriers to participating in outreach (e.g. lack of time, lack of information about opportunities, and lack of support (*Andrews et al.*, 2005)) inhibit scientists from engaging. Considering the challenges of international and cross-cultural science communication (e.g., travel requirements, language and cultural barriers, funding, etc.), it is obvious why large-scale societal outreach is a challenge.

Nevertheless, if researchers strive to achieve broader impacts, science communication and collaboration will be key. Effective articulation of science is critical to extend the reach of geoscience education into settings and cultures to which access has previously been limited. Cultural and language hurdles can be overcome through mutually beneficial collaboration with partners (*Ray*, 1999). Partners can include both research-related parties (e.g., research institutions, funding organizations, governmental agencies, etc.) as well as community communication facilitators (e.g., community leaders, media, artists, schools, etc.).

Here, we use a children's book to (1) effectively achieve a direct and sustainable STEM educational outreach with impoverished, remote communities in Bangladesh, and (2) build relationships with partners through collaboration during the creation and distribution of the book. Collaboration includes relationships with in-country partners like Dhaka University, Bangladeshi translators and editors, and primary and secondary schools, as well as U.S.-based groups like artists, media, and transdiciplinary institutions across Vanderbilt University. The purpose of the project is to increase local students' understanding of the natural world and environmental change through a two-pronged sustainability effort. The principal vehicle for delivering this goal will be through the presentation and discussion of the book itself. However, the book will be a tangible resource and community tie that persists after the culmination of our research project.

4.2 Background

4.2.1 Study Area

Bangladesh and its deltaic landscape is shaped by a broad range of environmental, economic, and social circumstances that mirror settings across many nations in Southeast Asia. Approximately 160 million Bangladeshis live in an area the size of Iowa, with one-third of the population living below the poverty line (*Yoshino et al.*, 2017). In the coastal environment, Bangladesh is increasingly affected by the longer-term pressures of sea level rise (*Ali*, 1996; *Karim and Mimura*, 2008), land subsidence (*Auerbach et al.*, 2015; *Wilson et al.*, 2017), and access to safe groundwater (*Shumaker*, 2017; *Benneyworth et al.*, 2016; *Benneyworth*, 2016; *Worland et al.*, 2015; *Rahman et al.*, 2011) and their confluence with an increasingly dense coastal population. As a result, Bangladesh is considered one of the most vulnerable countries with respect to climate change (*Huq*, 2001). The increased frequency of cyclones, poldering (i.e. reclaiming and embanking islands), and subsequent flooding add additional stress to this poverty-prone landscape, leading to livelihood changes and population displacement. The nation's environmental instability due to intense urbanization as well as multiple catastrophes–cyclones, floods, salinity, arsenic–has made Bangladesh a country of continuous research and policy innovation.

4.2.2 Research

The Vanderbilt Integrated Social, Environmental and Engineering (ISEE) Bangladesh Project takes a multidisciplinary approach to investigate the coupling and coevolution of the physical and human systems in southwest Bangladesh. The relationship between environmental conditions and human migration is multidimensional, and few studies have addressed exactly how this complex relationship operates and under what conditions the environment affects migration decisions. The complexity of these human-environment interactions in low-lying regions, such as Bangladesh, are especially significant with increased risk of climate change impacts. The overarching goals of the ISEE project are to (1) identify social and environmental factors most important in maintaining stability or for motivating decisions to migrate; (2) determine how these factors differ within and across diverse social and physical landscapes; and (3) assess how these variables are likely to interact under a variety of scenarios for social and environmental change. The ISEE Bangladesh project was funded in part by the Office of Naval Research - Multidisciplinary University Research Initiative Award #N00014-11-1-0683, which granted 5 years of funding between 2011 to 2016. The research team published numerous studies exploring water quality and resources (*Benneyworth et al.*, 2016; *Ayers et al.*, 2016; *Worland et al.*, 2015; *Gunda et al.*, 2015; *Ayers et al.*, 2017), landscape alteration (*Auerbach et al.*, 2015; *Wilson et al.*, 2014), climate change (*Ackerly et al.*, 2015; *Peters et al.*, 2017), and associated social migration (*Ackerly et al.*, 2015; *Donato et al.*, 2016). We had not disseminated broadly, however, our findings and understanding of the coupled human-natural system with the local residents or decision makers until Fall 2017 with this project. Prior to that time, few ties existed between the local communities and our ISEE research.

4.3 Story and Design

This project involves the writing, illustration, and distribution of a place-based children's book title *Farzana's Journey: A Bangladesh story of the water, land, and people* (see Section 4.6). The main storyline follows a young girl, Farzana, who must walk a long distance to fetch her family's water. Her usual journey quickly develops into an adventure as she meets a variety of animal characters, who relay a story about her ever-changing environment and the subsequent human adaptation. More advanced topics including geomorphology, water availability, climate, and traditional livelihoods are further explained through complementary diagrams throughout the narrative. Ultimately Farzana appreciates the uniqueness of her local environment and the adaptations of her ancestors and future generations. She feels a sense of agency in understanding and interacting with the world around her. Prepared in English and translated to Bengali, the book targets young children in our research area, but hopefully impacts teachers, parents, and local community leaders throughout Bangladesh. The book was self published by IngramSparks along with a second English version, now sold on Amazon (https://www.amazon.com/Farzanas-Journey-Bangladesh-Story-People/dp/0999278606). Examples of similar environmental children's books that have been successful include *Alber's And the Tide Comes in: Exploring a Georgia Salt Marsh* (2012) and *Monisha and the Stone Forest* (*Hughes*, 2012; *Hughes et al.*, 2015).

Collaborations with partners were essential, not only to the creation of the book, but also to the overall broader impact of the book. The text was crafted with the help of the Vanderbilt Writing Studio, where writers have the opportunity to meet with trained writing consultants. Non-science consultants assisted with the book narrative and language to better craft a cohesive storyline and describe scientific research without the use of scientific jargon. The Curb Center for Art, Enterprise & Public Policy at Vanderbilt University developed partnerships with creative leaders affiliated with Vanderbilt University. The center offered resources and mentorship in initiating and implementing the children's book project by applying creative and entrepreneurial methodologies to problems. The Center funded a major portion of the project, but also provided training and support through (1) invited structured discussion on topics of cultural differences and assumptions, (2) information on institutional outreach opportunities and limitations, and (3) anecdotal evidence of other successful creative initiatives sparked by academic research. The Curb Center also connected the author to Nashville's public art community by referring illustrators who contributed to the book and through exposure with an exhibition of the project in the Curb Center gallery space.

Perhaps the most meaningful collaboration, however, during the creation of *Farzana's Journey* was the illustration process. Eight artists, who were previously unaffiliated with the research, worked alongside the author to co-produce the storybook graphics. Four of the artists were Vanderbilt University undergraduate art majors, one of which was a double major in Earth and Environmental Sciences. Three artists were personal acquaintances of the author. The final artist was a Nashville, TN local illustrator, who served as the creative director of the entire collaboration. The artists split illustration tasks, including background painting, figure and animal sketching, digital coloring, and scientific diagram creation. With the help of the creative director and graphic designer, these elements were combined and paired with the text to create the book.

These varied partnerships were essential in crafting a cohesive narrative and jargon-free language of the children's book. We were able to overcome a variety of science communication hurdles including (1) writing for multiple audiences (Bangladeshi children, American children, and non-science community), (2) twisting a seemingly bleak story into a story of human adaptability, (3) transitioning between scientific topics while maintaining the storyline, (4) verbally and visually depicting the setting to unfamiliar audiences, (5) fostering cultural and environmental relatability with Bangladeshi readers, and (6) preserving the intent of the story through translation from English to Bengali. Although the success of the book can not be quantified without comprehensive surveying and structured interviews, anecdotal evidence suggest that the narrative and illustrations sufficiently communicated the setting, scientific concepts, and the moral of *Farzana's Journey*.

4.4 Impact

The book was distributed to educational institutions and individual children in southwestern Bangladesh during our October 2017 field visit. We delivered 500 copies, written in Bangla, to 12 primary and secondary schools. Copies were left with each school library as well as handed directly to students. Translators facilitated a short presentation and gifting of the book to the headmaster, teacher, and classroom of each school. In the presentation, the story was introduced to generate interest, discussion, and, potentially, local stories that related to the book narrative. The author and translators discussed the broader motivation and findings of the ISEE project with school administrators and teachers. They shared the intent of the book–to increase local students' understanding of the natural world and environmental change–to ensure that book was received as a gesture of gratitude for the local communities' support in the ISEE research.

In the classroom, the translators discussed the formation of the delta, fluvial geomorphology, tides, water quality, and other main concepts of the book with the students. Children of all ages were encouraged to think deeply about the local environment. Students conversed about *why* the environment is the way that it is and *how* environmental processes shape natural (and anthropogenic) change. Portions of the book were read aloud in each class and students were encouraged to continue their studies outside of the classroom. Although the conversations were brief, several teachers expressed their intention to resume the discussion with students at a later time. Many teachers even requested supplemental books and resources.

In Nashville, the book was exhibited at the Curb Center gallery space and at multiple local bookstores. The book is also available for purchase on Amazon and has sold 25 copies as of January 2018. The book has been highlighted through various media channels at Vanderbilt University and at a conference presentation at the 2017 American Geophysical Union Annual Meeting.

4.5 Discussion

With regard to the initial goals, the *Farzana's Journey* project seems to have been a moderate success. At a minimum, Bangladeshi students were exposed to local natural processes, environmental science concepts, and the history of coupled natural-human systems. The book increased public awareness of the natural environment and human adaptation that is characteristic in coastal Bangladesh with science and non-science communities in both Bangladesh and the U.S. The project also created new academic and societal partnerships with a variety of non-science collaborators during book development. But whether the project leaves long-term impact with the target audience and project collaborators is less clear. It is likely that enduring engagement will be necessary to ensure the sustainability of the conversation, but achieving this will be a challenge given the international communication requirements, the end of the ISEE project, and the impending graduation of the project leader. Nevertheless, book distribution by the university and the author will continue.

4.6 The Book

Images of *Farzana's Journey* are included on the following pages.

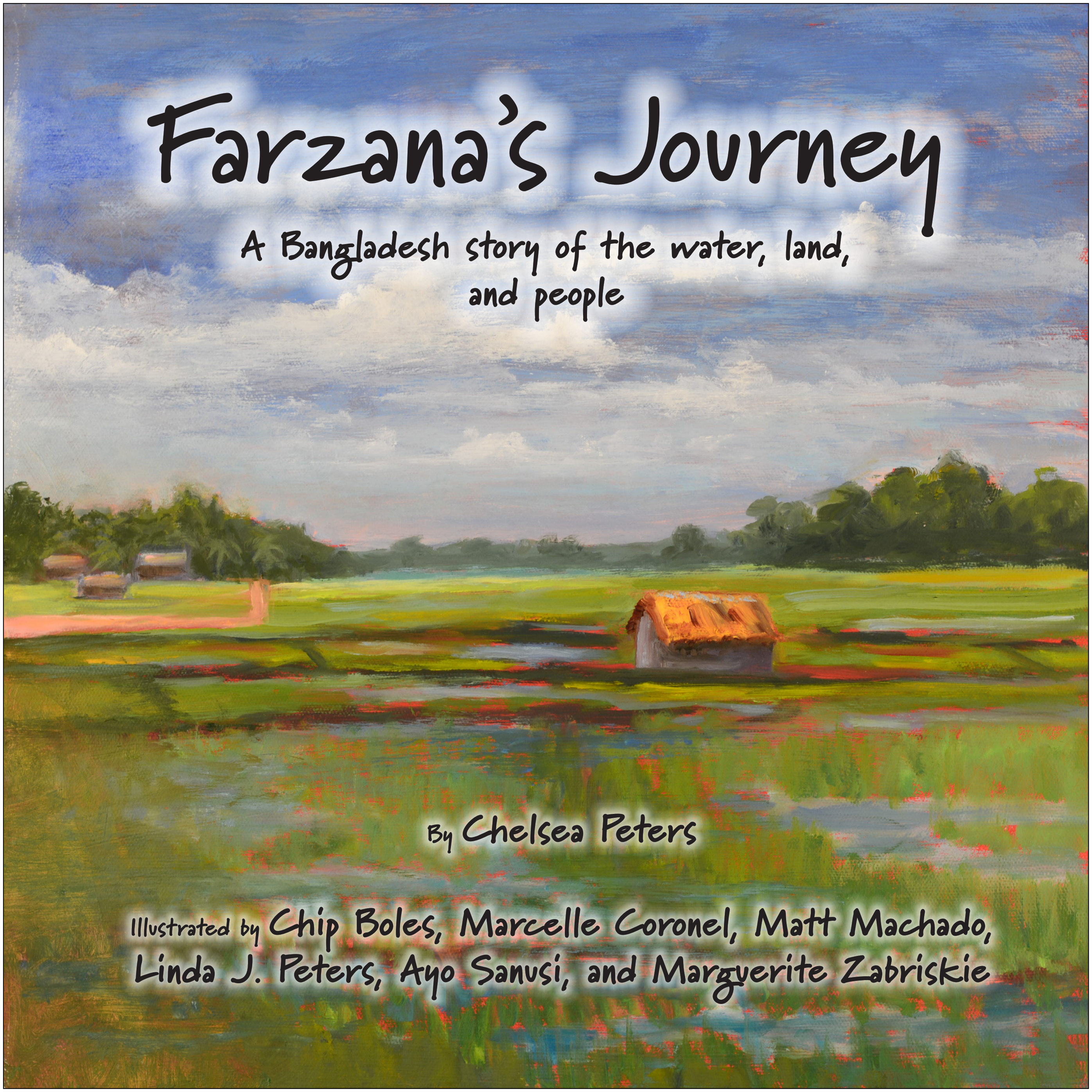
Farzana's Journey
A Bangladesh story of the water, land, and people
By Chelsea Peters
Illustrated by Chip Boles, Marcelle Coronel, Matt Machado, Linda J. Peters, Ayo Sanusi, and Marguerite Zabriskie

We dedicate this book to all the women and girls who have to walk to fetch their water each and every day to provide for their families, and to the polder residents, who show incredible generosity, curiosity, and joy in life.

ISBN: 978-0-9992786-0-4

Illustrations by Chip Boles, Marcelle Coronel, Matthew Machado, Linda J. Peters, Ayo Sanusi, and Marguerite Zabriskie

Layout and design by Lauren Howell Anderson

Published by IngramSpark

This book was prepared through the Bangladesh project of the Vanderbilt Institute for Energy and Environment at the Vanderbilt University. The author, Chelsea Peters, was a graduate student involved in research through the Civil and Environmental Engineering department and Earth and the Environmental Sciences.

Support for the book was provided by the National Science Foundation Graduate Research Fellowship, Office of Naval Research, and Vanderbilt University funding through the Curb Center, the Civil and Environmental Engineering department, and the Earth and Environmental Sciences department.

We would like to acknowledge the hard work and dedication of many Vanderbilt researchers, artists, and reviewers who were instrumental in rewriting, adapting, and illustrating the story. This book includes illustrations contributed by multiple talented artists from Tennessee and Mississippi, who diligently portrayed scientific and cultural accuracy in their artwork. The author and illustrators would like to thank the following organizations, schools, and individuals for participating in the preparation of this book:

Vanderbilt Curb Center for Art, Enterprise & Public Policy
Vanderbilt Institute for Energy and Environment
Vanderbilt Civil and Environmental Engineering
Vanderbilt Earth and Environmental Sciences
Dhaka University
Sanjana Zerin
Saddam Hossain
Ratna Rahima
Rachel Gould
J.T. Winders
Kelly Shaw
Christopher Tasich

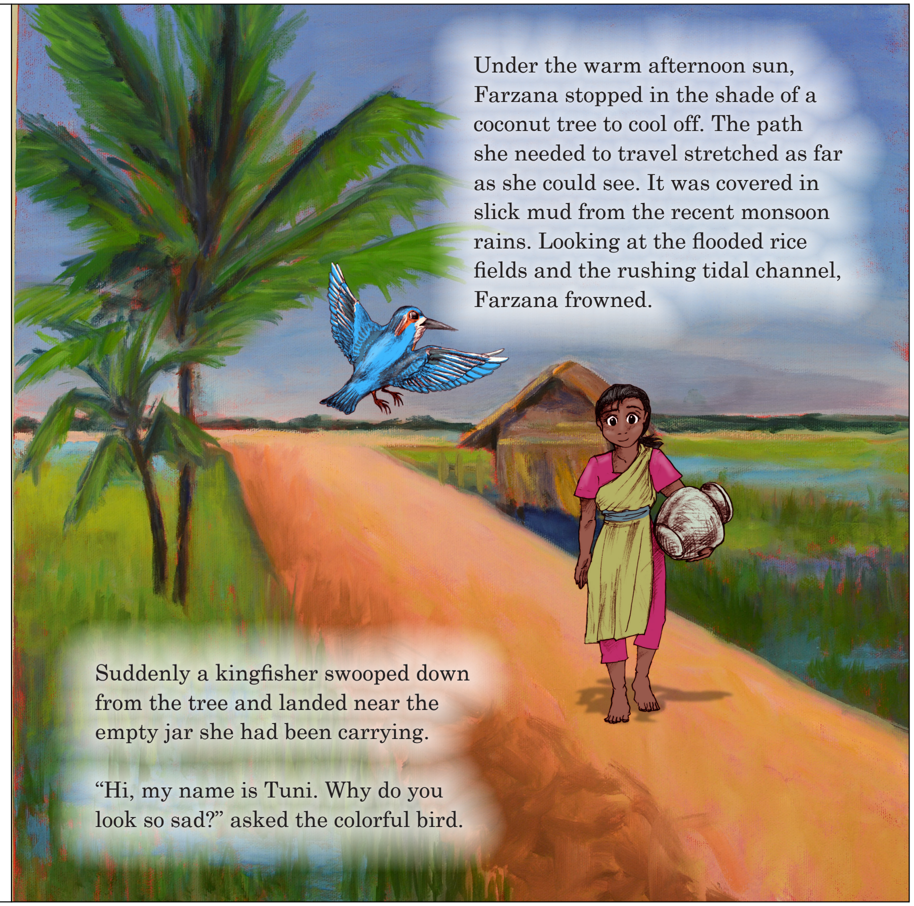

Under the warm afternoon sun, Farzana stopped in the shade of a coconut tree to cool off. The path she needed to travel stretched as far as she could see. It was covered in slick mud from the recent monsoon rains. Looking at the flooded rice fields and the rushing tidal channel, Farzana frowned.

Suddenly a kingfisher swooped down from the tree and landed near the empty jar she had been carrying.

“Hi, my name is Tuni. Why do you look so sad?” asked the colorful bird.

Farzana said, “I’m headed to the pond sand filter in the next village. Each day I make this long walk to fetch water for my family. I don’t understand why I need to walk so far when the world looks like it is covered in water.”

Tuni gave her a thoughtful look. “Can I join you on your walk? I can tell you a story about your people and this land that may answer your question.”

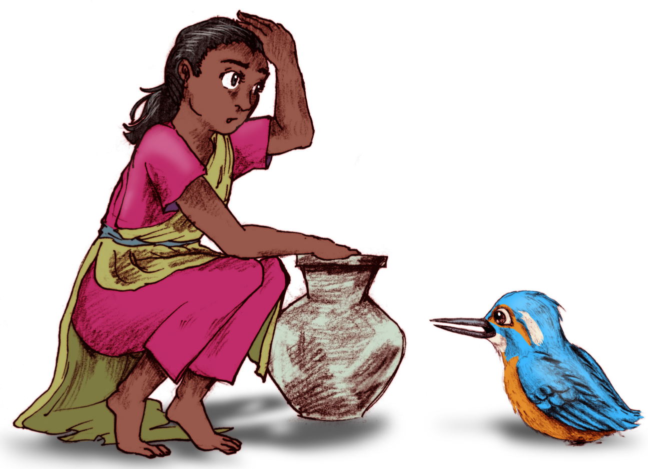

Curious, Farzana picked up her water jar and the two started down the path atop the embankment wall. “It is said,” the wise bird began, “that your ancestors settled here in Bangladesh because it was the most fertile area in all the land! As snow from the Himalayan mountains melted, the water formed huge rivers that flowed south across Bangladesh.”

“We call those the Ganges, Brahmaputra, and Meghna rivers!” exclaimed Farzana.

“Yes!” Tuni grinned at her. “If only you could see the rivers from my point of view!” Tuni took off and soared high above Farzana, shouting down to her, “The rivers are connected, forming the largest delta in the world! Eventually the rivers weave through these tidal channels and empty into the Bay of Bengal.”

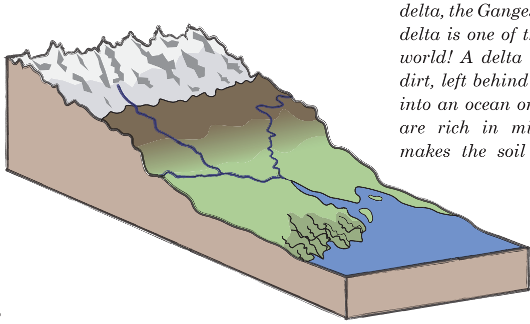

What makes this delta so special? The largest delta, the Ganges, Brahmaputra, and Meghna delta is one of the most fertile regions in the world! A delta is formed from sediment, or dirt, left behind by a river as it slowly enters into an ocean or lake. These delta sediments are rich in minerals and nutrients. This makes the soil excellent for growing food!

Farzana looked at the tidal channel thoughtfully. She had never imagined her home connected to lands so far away. Farzana knew, however, how very important the tidal channel was to her family. “This tidal channel provides the water we use to grow our rice,” said Farzana, looking at the green fields. She would have to help her family harvest the crop in a few weeks.

“Yes,” Tuni agreed. “Like the tidal channels, the rivers were always overflowing and this frequent flooding enabled your ancestors to first grow rice paddy. The massive amounts of water also made life difficult,” continued Tuni. “The same flooding rivers that brought life to the paddy also destroyed homes and villages. So, generations of people learned to depend on and adapt to the changing rivers.”

Seeing Farzana's confused expression, Tuni continued, "The rivers move slowly back and forth across the delta, carving out new channels and washing away old ones." Tuni swept his wing back and forth to show the pattern of the rivers. Skeptical, Farzana interrupted, "I've never seen the rivers moving like a snake!"

"Snake! Where is the snake?!" cried a voice from below. At that moment, a crab popped his head out of the mud and dashed to hide behind Farzana.

Giggling, Farzana scooped up the crab, while Tuni laughed, saying, "Don't worry! We were only talking about the rivers."

With a sigh of relief, the embarrassed crab introduced himself, "I'm Lalu and this bank is my home."

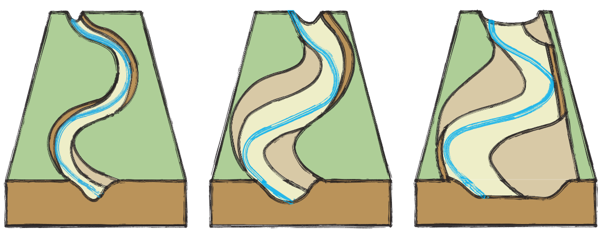

How do rivers move? Over time the river erodes, or cuts away, the bank on one side of the river channel. At the same time, the sediment that has eroded builds up on the opposite bank. These paired patterns create the side-to-side movement of river migration.

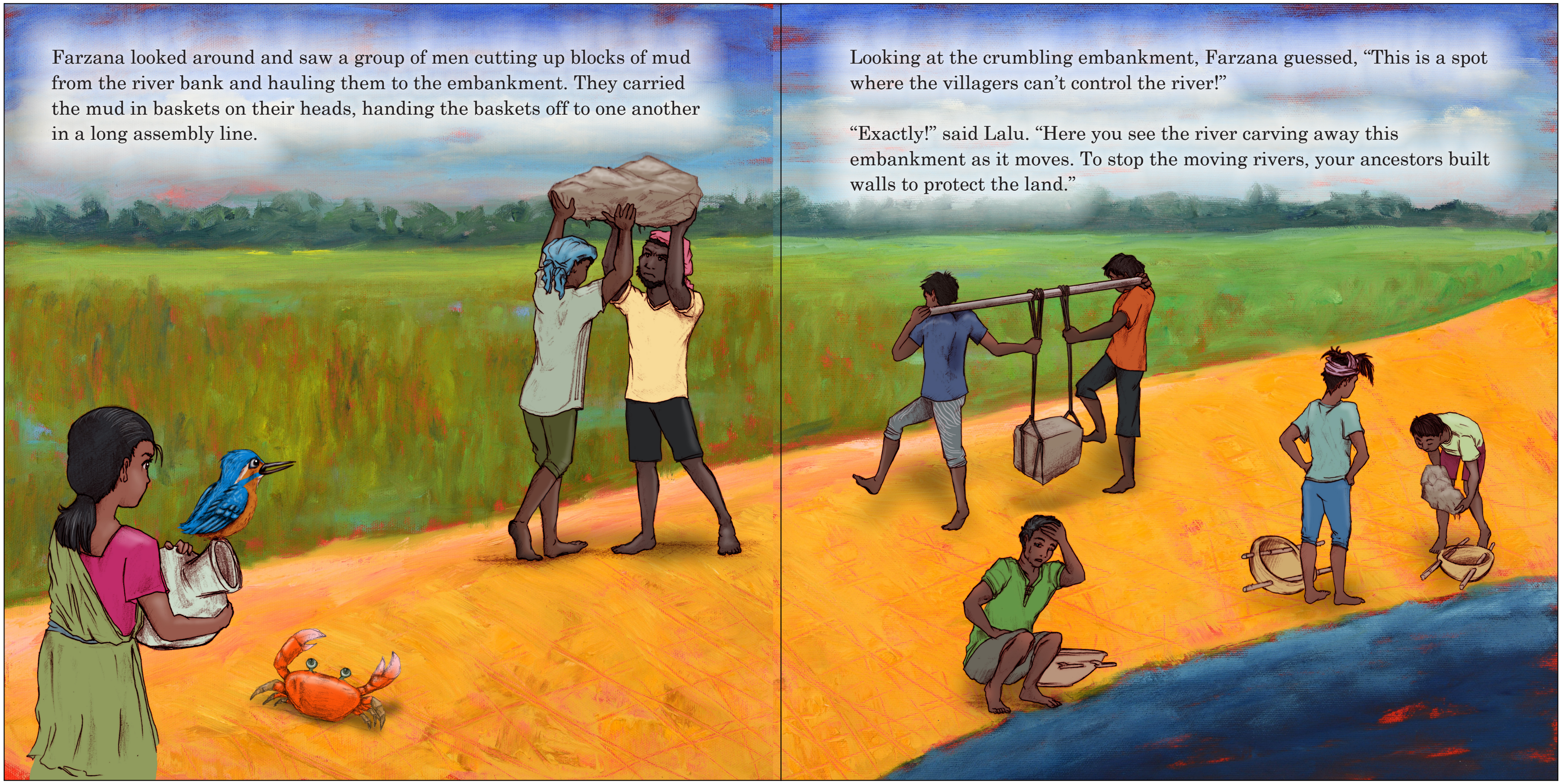

Farzana looked around and saw a group of men cutting up blocks of mud from the river bank and hauling them to the embankment. They carried the mud in baskets on their heads, handing the baskets off to one another in a long assembly line.

Looking at the crumbling embankment, Farzana guessed, “This is a spot where the villagers can’t control the river!”

“Exactly!” said Lalu. “Here you see the river carving away this embankment as it moves. To stop the moving rivers, your ancestors built walls to protect the land.”

Tuni added, “If you look closely you can also see the rivers moving in other ways. See? Rivers change with each tide. The rising tides bring up water from the sea to mix with the river, while the falling tide pulls the water back out to sea. The water is fresh during the rainy season, but it turns salty in the dry season.” Farzana looked over to the tidal channel to see the rising water. The rushing water was chasing small crabs out of their holes and up the steep bank.

“I guess both crabs and humans play in the mud of the embankment!” Farzana laughed, setting Lalu down. After she picked up her water jar and waved at the men, the trio started down the path.

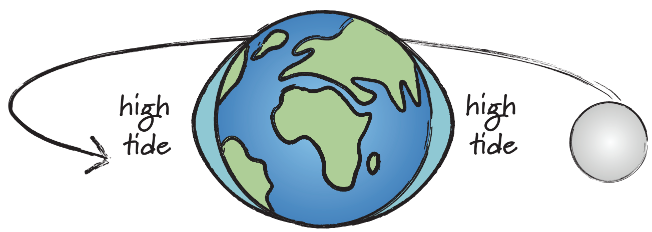

How do tides work? Tides are the rising and falling of sea levels that take place every day. This is caused by the pull of the moon’s gravity on the Earth. The moon tugs on objects closest to itself, causing the oceans on opposite sides of the world to move. This swelling of the ocean water creates the high tide.

Soon the path neared a wooden dock. Farzana noticed a pair of hairy feet sticking out from under a tarp on one of the boats.

Tiptoeing over to the boat, the group peered underneath. The movement shocked a sticky macaque monkey covered in honey. The monkey rubbed her eyes from the bright sun.

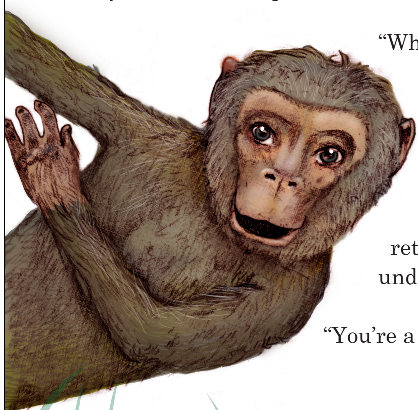

"What are you doing here?" asked Farzana.

With a sneaky grin, the monkey whispered, "Men from the village were collecting honey in the forest this morning, and I snuck on their boat to have a taste. When the men returned, I was trapped! I hid from them under this tarp."

"You're a long way from home!" blurted Farzana.

The monkey scanned the horizon, where rice fields sprawled as far as she could see, and sighed, “I remember when all of this land was forest!”

“What do you mean?” asked Farzana.

The monkey explained, “All of this land was once covered in mangrove trees, but the people now use this land to live and farm. When the people developed the land, they cut down the mangroves, except for a part of the Sundarbans forest.” The monkey pointed toward the mangrove forest across the channel.

Just then, the group heard the men approaching the dock. The friends scattered away from the boat. The monkey waved goodbye, slipping back underneath the tarp.

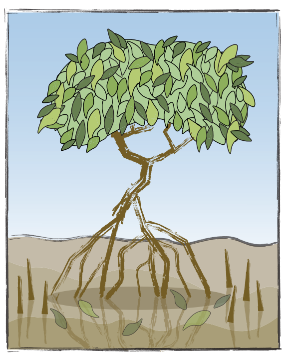

Why are the Sundarbans so important? The Sundarbans are the largest forest of salt water mangroves in the world. Mangrove trees can live in the salt water because their roots filter out the salt, giving the tree fresh water to drink. These mangroves are very important for the wildlife that live in the forest. The forest also protects coastal areas from erosion, especially during large storms.

Farzana watched the boat disappear into the distance. The monkey seemed sad about people living here now, and Farzana felt the ancient connection to the Sundarbans. But Farzana had lived her entire life on the island, so how could she know anything different? The monkey loved the Sundarbans, just as she loved her home! Her embanked island, which the community called a polder, was surrounded by over 50 other similar polders. She felt gratitude for the polders and the embankments that protected them. Although she disliked the long walk along the embankment path, she understood her life would be impossible without the walls protecting her home.

Where are the polders? These islands are located in southwestern Bangladesh, between the larger towns to the north and Sundarbans in the south.

Suddenly, a shrill squeak interrupted Farzana's thoughts. "Hey, look out! You almost stepped on me!" Farzana looked down and saw a mudskipper sitting next to one of her footprints.

Farzana asked the land-crawling fish, "Are you okay, little friend?"

"It happens all the time!" the skipper sobbed. "These embankments make my life difficult!"

Sliding across the mud, the fish propped himself up on the side of a tide pool. The mudskipper complained, “People trample my home and the embankment traffic ruins my peace and quiet. And that’s not all! Ever since the embankment walls were built, water stopped spilling over into the land during the high tide. Now there are fewer tide pools for me to hide in.”

“Wow! People have altered this land even more than I realized,” said Farzana.

“Land and water!” corrected the mudskipper. “The water no longer carries mud to the fields, so the channels are becoming more narrow and shallow as they fill in with sediment.”

As Tuni and Lalu climbed back up the embankment, Farzana paused to say goodbye to the mudskipper. “I hope that in the future we can protect my home, while also protecting yours.”

As the trio approached the next village, a group of feeding cows blocked the path. A cow curiously eyed the bird, crab, and little girl.

“What an odd bunch!” the cow said. “Where are you headed?”

Farzana explained her long walk to the pond sand filter and what she had learned about people’s adaptions to the environment.

She ended, “But I still don’t understand why we are surrounded by water yet have so little to drink.”

The cow agreed, “Drinking water has always been a problem.”

Chewing on the grass, the cow mumbled, “First people dug ponds to catch rainwater, but the water soon became dirtied with....”

“Manure!” cried out Tuni. Farzana turned to see the bird hopping in circles, brushing off his feet from a pile he had just tripped over.

Farzana laughed and told him to watch his step. With an embarrassed cough, the cow said, “The water was dirtied with bacteria from the livestock.”

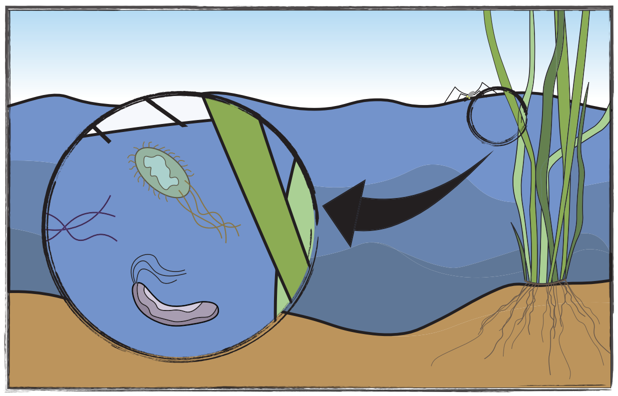

How does water make people sick? It’s not the water that makes people sick, but what is in the water. Sometimes water is polluted with poop from animals or humans. The poop carries germs that can make us sick if we drink the polluted water.

“People hoped that water below the ground would be safer to drink,” continued the cow.

Tuni interrupted, “Do you remember how the river moved and formed the surface of the land? Those same rivers moved grains of sediment that trapped water, called pore water. The pore water is stored underground as new sediment covers the surface, ultimately forming underground reservoirs of water called groundwater.”

Lalu was busy digging a hole next to them. When he reached a certain depth, the hole began to fill with water. Lalu called out to Farzana, “Look! I found the water table, which marks the top of the groundwater!”

How does groundwater form? When it rains, water soaks into the ground and moves down through spaces between the dirt and rocks. This water is called pore water. Eventually the pore water seeps deep into the Earth and there, all the small spaces completely fill with water. The boundary between completely-filled and partially-filled pores is called the water table.

The cow continued, “The people installed wells hoping to find clean water. Unfortunately, they often found water that was too salty to drink or the water was poisoned with natural chemicals like arsenic, making humans sick.”

Tuni explained, “But the people adapted by drinking rainwater and pond water instead. Households used containers to catch rainwater during the rainy season.”

Farzana looked over at a nearby house. Clay jars and barrels surrounded the house to catch the water falling from the roof.

“Meanwhile, villages built pond sand filters that would clean the pond water,” finished Tuni.

“No wonder I have to walk so far to get my water!” exclaimed Farzana.

“The pond sand filter is over there. I’ll get back to my lunch and let you fetch your water,” said the cow.

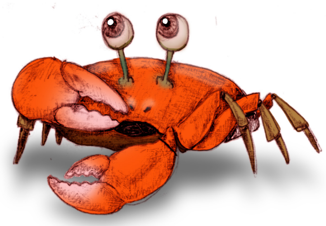

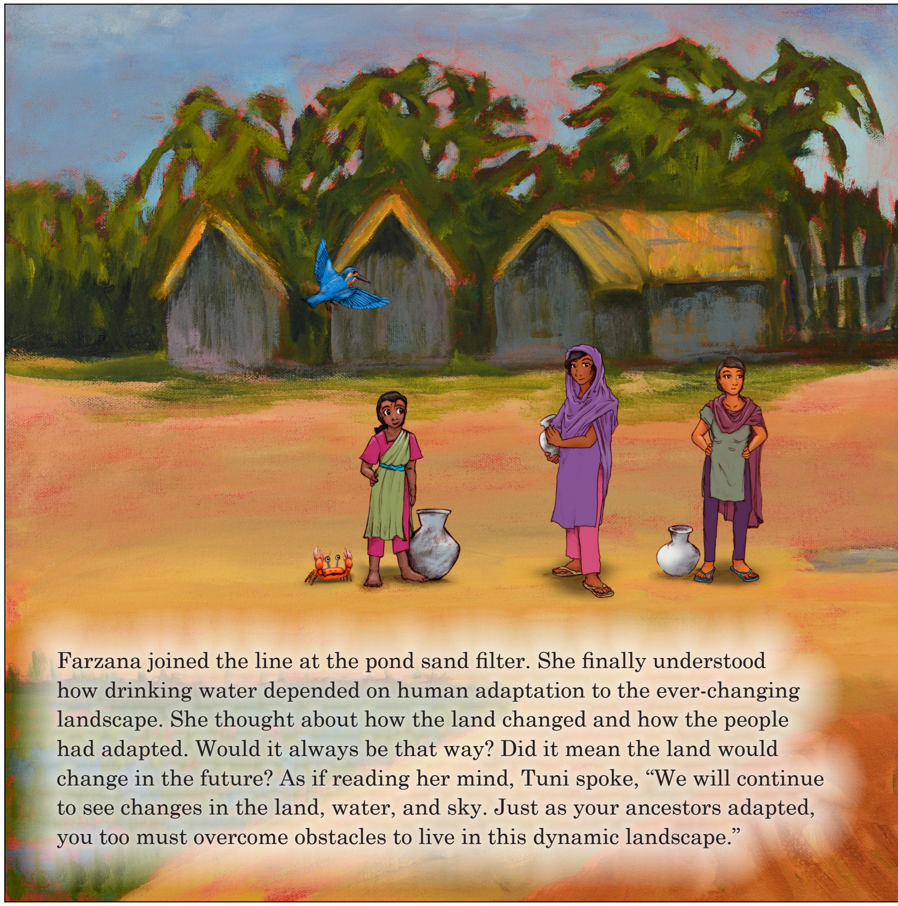

Farzana joined the line at the pond sand filter. She finally understood how drinking water depended on human adaptation to the ever-changing landscape. She thought about how the land changed and how the people had adapted. Would it always be that way? Did it mean the land would change in the future? As if reading her mind, Tuni spoke, “We will continue to see changes in the land, water, and sky. Just as your ancestors adapted, you too must overcome obstacles to live in this dynamic landscape.”

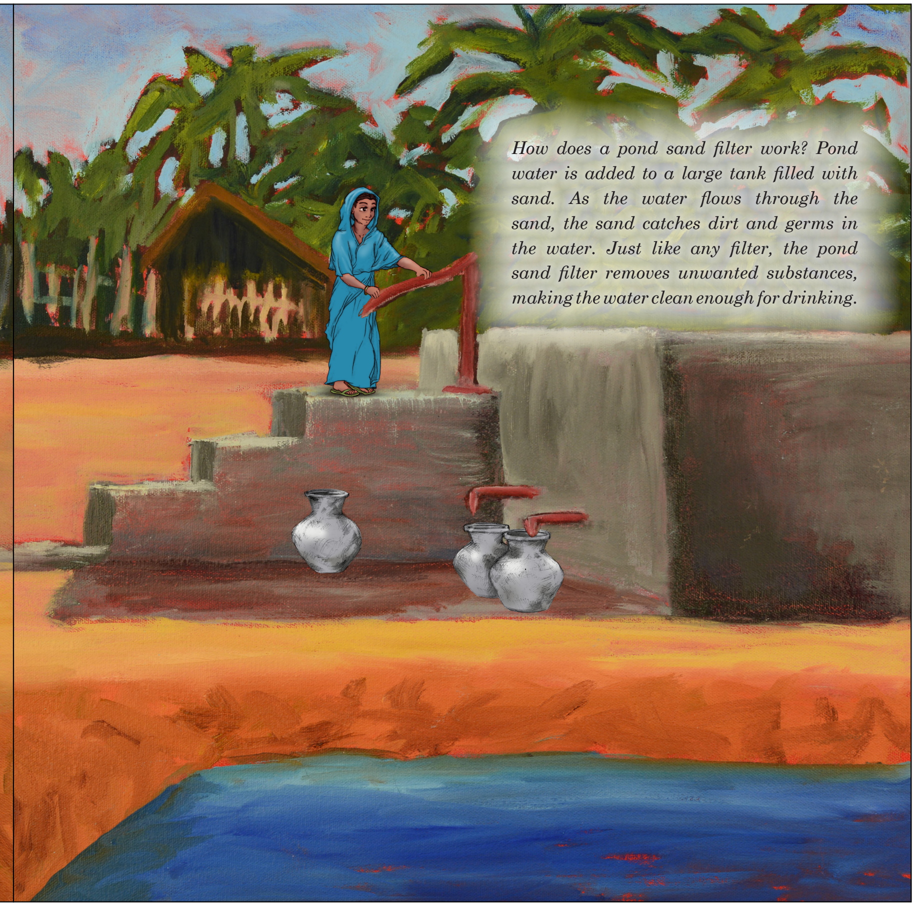

How does a pond sand filter work? Pond water is added to a large tank filled with sand. As the water flows through the sand, the sand catches dirt and germs in the water. Just like any filter, the pond sand filter removes unwanted substances, making the water clean enough for drinking.

Lalu climbed to the top of the tank and nodded. “As people transform the Earth, the climate changes. You may see differences in the monsoon and stronger cyclones.”

“I can help build cyclone shelters and educate my family and friends about these dangers!” Farzana assured him.

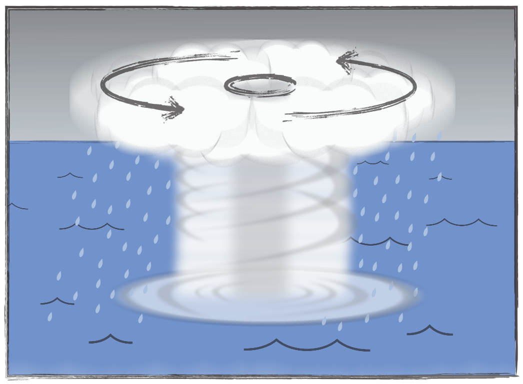

How does a cyclone form? The warm ocean water heats the air above it, causing it to rise and form clouds. Cooler air replaces the warm air, but it will also heat up and rise. As this cycle repeats, huge storm clouds form that begin to spin around a center point, called the eye.

Lalu continued, “Those storms may also flood the polder. Because the embankments prevent new rivers from adding sediment to the inside of the polder, the polder inside the embankment wall is too low and floods easily. This happens because the sediments are compacted, or packed down, over time.”

How can communities prepare for flooding? After cyclones, polders can flood. When this happens, people can temporarily open embankments to allow water to move freely between the inside of the polder and the river channel. The moving water carries the sediment from the river to the polder inside the embankment. This new sediment builds up the height of the polder land. Afterwards, the embankment can be rebuilt and rice paddy can be planted again.

Farzana looked over her shoulder to see the difference between the height of the ground inside and outside the embankment. “I have heard that some communities have opened the embankments to allow water and sediment into the polder. The new sediment has restored the land to the natural height. We can adapt too!”

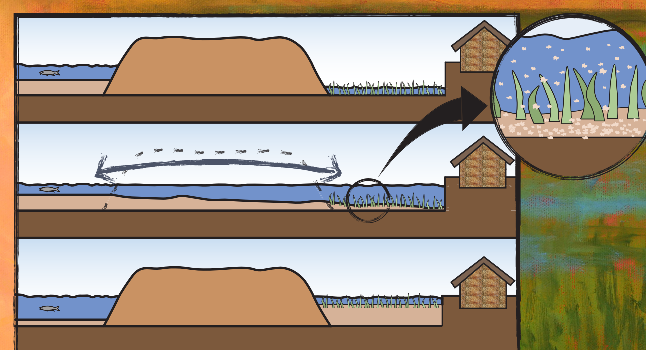

With each pump, the water trickled into her jar. As she finally finished pumping, Farzana reflected on the challenges her community had faced. She knew that she would play a role in helping provide water for her community. She was proud that her ancestors had come such a long way, and she was ready to make a difference in the future.

“Tuni, you are right! My life and this land are connected. Change can be difficult, but this ever-changing land is what makes my home so special.”

Farzana smiled at her new friends and said, “Let’s head back.” The three friends set off down the dirt path toward home.

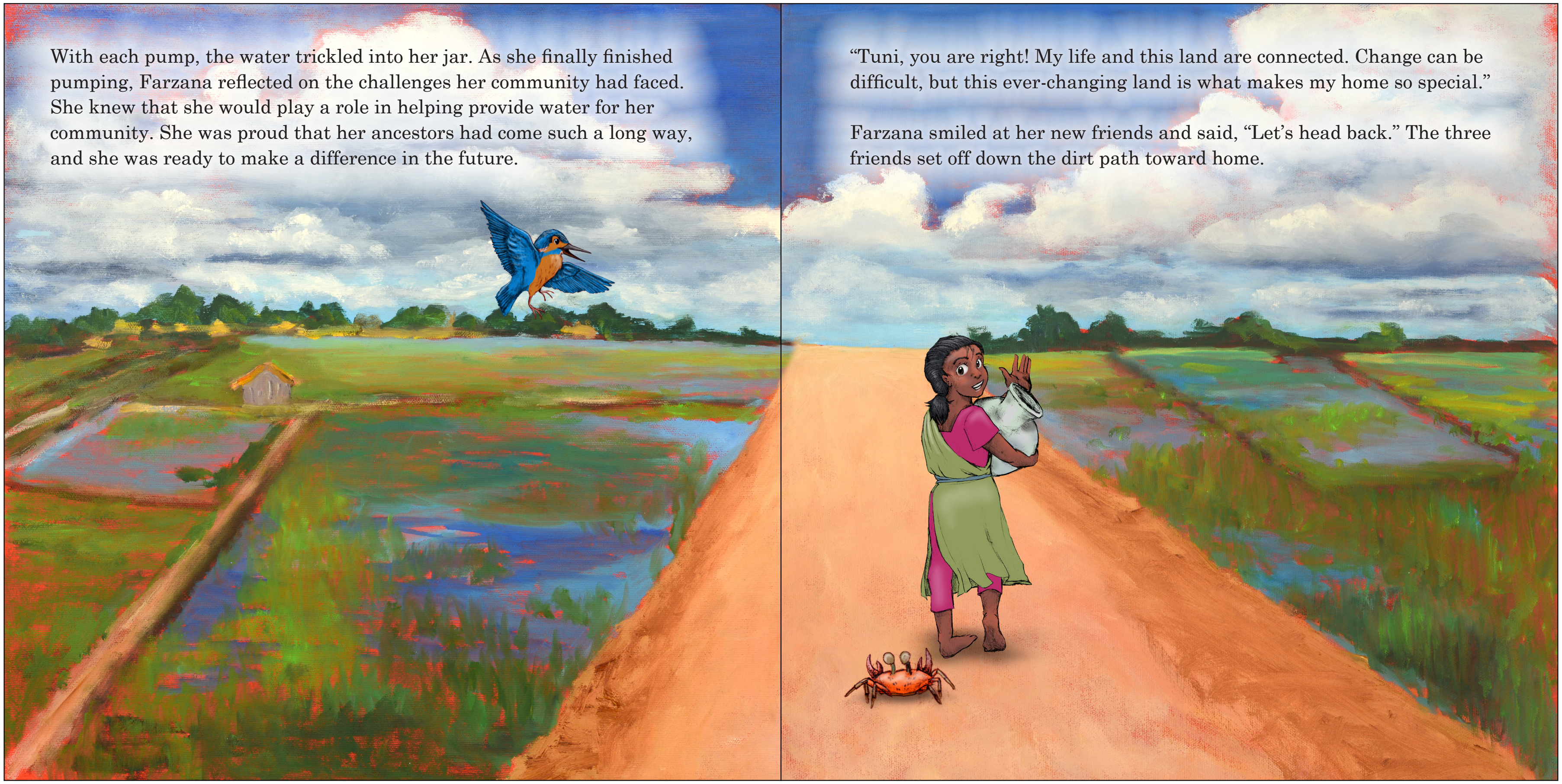

Photo by Saddam Hossain

About the Author...

Chelsea Peters, second from right, is a PhD candidate in Environmental Engineering at Vanderbilt University. She is a hydrologist who has conducted water research in coastal Bangladesh for several years. She has an intense love for environmental sciences, and especially enjoys teaching and community outreach. In her spare time, you can find Chelsea dreaming about travels to exotic destinations or cuddling her cat Abigail.

About the Illustrators...

Serving as art director and finishing artist, Chip Boles is an artist, illustrator, and muralist based in Nashville, TN.

Figure illustrator Marcelle Coronel is a pre-med student at Vanderbilt University, who is double majoring in Art and Medicine, Health, and Society with a minor in Chemistry. Her artworks vary from printmaking to sculptural ceramics, and she focuses on producing pieces that connects art her love for both the visual arts and sciences.

Diagram artist Matthew Machado is a student at Vanderbilt University, who works in several different mediums, including photography and video, that mainly focus on themes of environmentalism.

Landscape artist Linda J. Peters is an oil colorist and plein air painter based in Oxford, MS.

Animal illustrator Ayo Sanusi is an Economics and Art major at Vanderbilt University, who delights in artsy projects and little kids.

Colorist Marguerite Zabriskie is also a student at Vanderbilt University majoring in Art and Medicine, Health, and Society.

About the Research...

This book is motivated by the Vanderbilt Integrated Social, Environmental and Engineering Bangladesh Project (http://www.vanderbilt.edu/ISEEBangladesh/), which takes a multidisciplinary approach to investigate the coupling and coevolution of the physical and human systems in southwest Bangladesh. Studies explore water quality and resources, landscape alteration, climate change, and associated social migration. The purpose of this book is to increase local students' understanding of the natural world and to encourage pride in human adaptation to challenging environments.

VANDERBILT UNIVERSITY®

NSF

Office of Naval Research ONR Science & Technology

Photo by Chelsea Peters

Photo by Saddam Hossain

CHAPTER 5

SYNTHESIS

Freshwater, although absolutely essential to life, can be difficult to find and manage in remote, underdeveloped regions. In coastal Bangladesh, this problem manifests in lengthy water shortages during the dry season, and a variety of quality problems associated with untreated coastal water. Nevertheless, these types of water resource challenges are not unique to Bangladesh.

At the 2012 United Nations Summit, governments committed to a set of sustainable development goals (SDGs) to end poverty, protect the planet, and promote wellbeing (*Arguelles et al.*, 2016). One goal is to achieve universal and equitable access to safe and affordable drinking water for all by 2030. In rural regions across Africa, Asia, and other developing states, societies are far from reaching this goal (*WHO and UNICEF*, 2017). With continued climate change, research also suggests increasing challenges and vulnerability of drinking water systems amongst these already susceptible populations (*Hoque et al.*, 2016; *Wong et al.*, 2014; *Jiménez Cisneros et al.*, 2014; *Hijioka et al.*, 2014; *Streatfield and Karar*, 2008). To overcome these obstacles, research must aim to better understand the local context of water systems–both hydrologically and socially. Only then can we equip the local communities with the knowledge and means to better manage their water resources to achieve the water SDGs. This dissertation was a step toward understanding the water systems that impact coastal Bangladesh.

We focused on a coastal region where freshwater is inadequate for drinking water security. Hopeful for a means of identifying untapped resources, we first sought to understand groundwater-surface water exchanges to better explain the existence of rare, but useful, potable groundwater. Without extensive data collection and alternative means of surveying, we found that our inferences about groundwater-surface water interactions pointed more to the heterogeneity of local landscape than to any one hydrological process that could resolve water insecurities. The complexity of local landscape, as well as small-scale processes (such as recharge, delta formation, tidal dynamics, and sediment permeability), restricted our ability to deduce the exact location of fresh groundwater.

After concluding that groundwater would be unsuitable for drinking on Polder 32, we considered alternative drinking water sources. We broadened our work to include an interdisciplinary assessment of available drinking water resources. Decisions about resources would include a variety of factors that extended beyond environmental sciences, and, therefore, required an interdisciplinary assessment of the human-natural system. We demonstrated how decision modeling and alternative assessment can be the first step to reaching sustainable solutions in complex water management problems. Acknowledging that (1) communities are heterogeneous and that (2) models rely on a balance between model accuracy and expense of implementation, we argued that value of these interdisciplinary decision models lies in increasing participation and transparency in resource management, rather than being the sole predictor of successful solutions.

In addition to these interdisciplinary models, it is also essential that we continue to extend the reach of scientific research into settings and cultures to which access has previously been limited. Understanding of water systems and management decision-making is often inconsequential without science communication and collaboration. Chapter 4 demonstrates dialogue, collaboration, and public outreach by scientists, artists, and students concerned with enhancing environmental educational and social opportunity in rural communities. Through this type of work, we can expand relevant research on coupled human-natural systems in underdeveloped, data-limited, and remote regions, not through academic endeavors alone, but rather through a cascade of communication and outreach.

5.1 Themes and Caveats

Site specific research in remote regions highlight small-scale heterogeneity and data limitations–both of which are especially important when striving to achieve global goals like the SDGs.[1] This dissertation work is extremely relevant to the setting and communities of Polder 32, but is unlikely to capture the discrepancies that we might observe across a broader region. In Chapter 2, for example, we speculate about groundwater-surface water exchange processes on Polder 32, yet we acknowledge that the heterogeneity is a strong control on the process. In order to extrapolate to a broader coastal region, we would need to conduct a regional investigation with additional piezometer monitoring and surveying. Outside of Polder 32, we would also expect to find varying demographic, cultural, and community factors, which all have been identified as controls for drinking water success (*Jakariya*, 2005). Therefore our Chapter 3 findings should be considered in the local context and as a methodology that could be extended to regional trends. The difficulties of heterogeneity (across landscapes, aquifers, communities, etc.) in data sparse regions is common (see *Michael and Khan* (2016) and *Weinman* (2010) for hydrological examples and *Ahmed et al.* (2016) and *Ackerly et al.* (2015) for societal examples), and should not be seen as a hindrance to research. Instead newly-found variations and data limitations can highlight gaps for the focus of future research.

5.2 Outlook

The success and sustainability of global water systems will be difficult to achieve. For this reason, continued efforts to understand water systems, and their complex interactions between human-natural systems, will be essential. Innovation and ambitious research can lead this effort, but it ultimately will be sustained by science communication and relevance

[1] The importance of heterogeneity and sparse data networks is also explored in Appendix A. There is often a tradeoff between (bottom-up) small-scale studies and (top-down) broader, more generalizable investigations. This tradeoff is especially important to consider in multi-scalar processes in data limited regions such as Bangladesh.

to society.

Appendix A

SATELLITE-DERIVED METHANE EMISSIONS FROM INUNDATION IN BANGLADESH

A.1 Introduction

Methane (CH_4) is one of the most important greenhouse gases, produced by a combination of natural and anthropogenic sources. Each molecule of CH_4 has 25 times the direct global warming potential of a molecule of carbon dioxide (*Solomon et al.*, 2007). After a leveling off from 1999 to 2006 (*Dlugokencky et al.*, 1992; *Simpson et al.*, 2006), atmospheric CH_4 concentrations are rising again (*Dlugokencky et al.*, 2009; *Nisbet et al.*, 2014) and have reached 260% the pre-industrial levels ($\sim$700 parts per billion (ppb)) (*WMO*, 2013). Global CH_4 sources are relatively well known, but the strength of each source and sink component and their associated trends are not. This is particularly true in understudied regions with high CH_4 emissions, hence the motivation for this case study of inundation-caused CH_4 emissions in Bangladesh.

Most natural sources of methane emissions are a result of methanogenesis (a microbial decomposition process), as seen in wetlands and animal digestion. Wetlands are considered to be the largest single source of CH_4, contributing approximately 20–40% of global emissions (*Walter et al.*, 2001; *EPA*, 2010). CH_4 concentrations vary considerably, temporally and spatially, to the extent that fluctuations in wetland emissions are thought to be the dominant contribution to interannual variability in surface emissions, explaining 50–90% of the global emission anomalies (*Morrissey and Livingston*, 1992; *Walter et al.*, 2001; *Frankenberg et al.*, 2005a; *Bousquet et al.*, 2006; *Pison et al.*, 2013). With warm weather and water-logged soil, rice paddies act like wetlands, producing 20–100 Tg CH_4 each year (approximately 15–20% of anthropogenic emissions) (*Sass et al.*, 1999). Due to these variations and flux measurement limitations, the source strength of wetlands, and similarly inundated rice cultivation areas, is particularly uncertain, and has been estimated as the highest of all CH_4 sources (*IPCC*, 1994; *Lelieveld et al.*, 1998; *Denier Van Der Gon et al.*, 2000). A better understanding of CH_4 distribution and emissions is indispensable for a correct assessment of its impact on global climate change (*Houghton, J. et al.*, 2001; *Frankenberg et al.*, 2005a).

The number of studies investigating ground-based fluxes of CH_4 have increased with awareness of climate change, but networks are still sparse and limitedly representative of larger regions (*Bartlett et al.*, 1993; *Aulakh et al.*, 2001; *Xiong et al.*, 2008). Ground-based measurements are directly related with the local sources, making extrapolation nearly impossible (*Bruhwiler et al.*, 2014; *Denier Van Der Gon et al.*, 2000, *and references therein*). Meanwhile satellite observations overcome these limitations with global coverage and large sampling volumes, particularly in regions that are poorly sampled by ground-based networks (*Chazette et al.*, 1998; *Clerbaux et al.*, 2003; *Frankenberg et al.*, 2005a). Satellite instruments measure gas concentration in the vertical column of air, which can be used to estimate in situ emission rates with proper compensation for transport and chemical conversion. Because CH_4 is a well-mixed greenhouse gas, with a lifetime of approximately 10 years, total column measurements must have high precision to detect variability in concentrations (*Meirink et al.*, 2006). The accuracy of satellite observations is debated due to systematic biases from errors in vertical profiles, uncertainties in the presence of clouds, inadequate night observations, and potential regional effects (*Frankenberg et al.*, 2005a,b; *Gloudemans et al.*, 2005; *Meirink et al.*, 2006, 2008; *Bergamaschi et al.*, 2007; *Xiong et al.*, 2008; *Parker et al.*, 2011).

Often studies extrapolate satellite observations of dry-air column-averaged mole fraction of CH_4 (XCH_4) or high-spatial ground-based measurements to the opposing temporal or spatial scales (i.e. small-scale, seasonal rice paddy emissions are upscaled to regional yearly emissions and vice versa) (*Denier Van Der Gon et al.*, 2000). Some studies attempt to inform inverse models with either ground-based in situ measurements or atmospheric observations (*Chen and Prinn*, 2006; *Bergamaschi et al.*, 2007; *Streets et al.*, 2013; *Turner et al.*, 2016, *and references therein*), but few evaluate the degree of consistency between both surface and satellite observations (*Bergamaschi et al.*, 2009). Direct comparison of both measurements is challenging due to (1) limited number of samples from sparse ground-based networks and few valid satellite measurements (cloud-free observations), (2) probing of different air masses (*Bergamaschi et al.*, 2009), and (3) limited precision and accuracy (*Meirink et al.*, 2006). Additionally, areas of intermediate size fall in the gap between large- and small-scale datasets with inadequate sample sizes from solely ground or satellite measurements (*Denier Van Der Gon et al.*, 2000). Studies that have compared inverse climate models with surface and satellite observations, suggest that a compilation of datasets may be able to constrain model emission estimates, especially over areas in Southeast Asia, where timing of summer rice emissions can be difficult to properly calibrate (*Chen and Prinn*, 2006; *Bergamaschi et al.*, 2009).

Initiatives to estimate country-specific contributions to the global CH_4 emissions from paddy fields and wetlands have been undertaken in numerous Asian countries, including China, India, Indonesia, Thailand, and the Philippines (*Neue and Sass*, 1998). Depending on the methods, calculated country emission rates can vary widely. The most common methods include (1) IPCC methodologies based on general or country-specific emission factors, (2) model-based approaches that incorporate complex transport and regional parameters, and (3) techniques using satellite-derived observations. Both emission factor and modeling methods can be difficult in understudied regions due to insufficient calibration from ground-based data and considerable seasonal differences. Alternatively, a satellite-based study could give insight on large-scale regional emissions and temporal patterns.

Bangladesh, which comprises most of the Ganges-Brahmaputra-Meghna (GBM) delta, is a region of particular interest for studying spatio-temporal variations of CH_4 emissions. It is the sixth largest producer of rice in the world (third in Southeast Asia) and experiences seasonal flooding and atmospheric convection during the monsoon (*Xiao et al.*, 2006; *Mosleh and Hassan*, 2014). Agriculture accounts for approximately 63% of the total area, with most being rice paddy (*Mosleh and Hassan*, 2014). Current rice production in Bangladesh is around 34.2 million tons (*Bangladesh Bureau of Statistics*, 2009), and the need is expected to increase by 50-60% to meet the 2050 population of 233 million (*Ali et al.*, 2014). Furthermore, 80% of the total land area is floodplain and has a significant likelihood of at least temporary inundation (*Hasan and Mulamoottil*, 1994). Consequently rice cultivation and wetlands are main contributers to Bangladesh CH_4 emissions (*Bergamaschi et al.*, 2009; *Kavitha and Nair*, 2016). The country is one of the most densely-populated countries in the world, having approximately 160 million people with a total area of 143,998 km^2 (*FAO*, 2014). Few studies, however, have focused on Bangladesh, making CH_4 emission data is extremely limited. Bangladesh and its deltaic landscape exhibit a broad range of environmental, economic, and social circumstances that are relevant to many nations in South and Southeast Asia.

The aim of this chapter is to explore the seasonal enhancement of atmospheric CH_4 in Bangladesh correlated with rice cultivation and inundation using satellite observations. We derive atmospheric CH_4 concentrations from three space-based passive spectrometer CH_4 products and then incorporate space-based passive microwave land-water fractions as a proxy for emission source area. These products are then converted to surface fluxes and annual emissions using a simple inverse model. We consider the uncertainties associated with extrapolation of our satellite-derived emissions and compare these emission estimates to inventories of ground-based surface CH_4 fluxes and annual Bangladesh emissions.

A.2 Study Area

Bangladesh experiences a tropical humid climate with wide seasonal variations in rainfall, warm temperatures, and high humidity (*Rashid*, 1977; *Chowdhury*, 2010; *Shahid*, 2010). Four climatic seasons are recognized: (i) dry winter (December-February), (ii) premonsoon (March-May), (iii) monsoon (June-September), and (iv) post monsoon (October-November) (Fig. A.1) (*Alamgir et al.*, 2015). Rainfall is uneven throughout the country, with the northwest part of the country receiving only 1400 mm, compared to 4400 mm in the northeast.

The rice crop-growing period in Bangladesh is divided into three main seasons: (i) aman (June to December) that depends on monsoon rains, until irrigated in mid-September; (ii) aus (March to August) that is typically unirrigated and only fed by rains; and (iii) boro (January to June) that relies on groundwater irrigation (Fig. A.1) (*Mosleh and Hassan*, 2014). A large number of the irrigation wells are active in northwestern Bangladesh, resulting in over 4,800,000 ha of irrigated boro rice (*Shahid*, 2011; *Mosleh and Hassan*, 2014; *Alamgir et al.*, 2015). Nearly 50% of the cropland is double cropped and 13% is triple cropped (*Maclean et al.*, 2002).

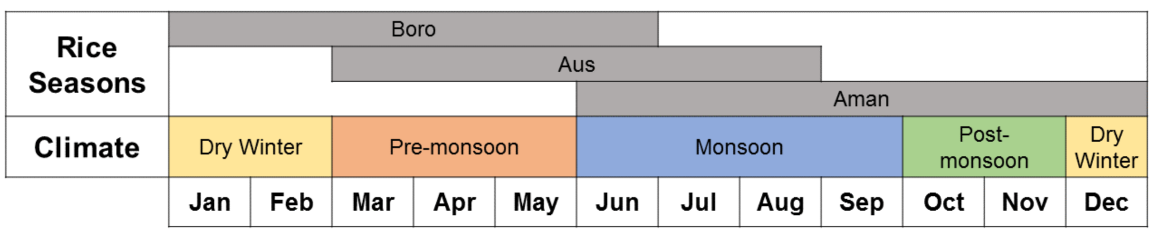

Figure A.1: Climate and rice cropping seasons in Bangladesh.

There are no recent inventories of Bangladesh greenhouse gas sources. However farmers do raise livestock, leading to high densities of poultry and cattle (*Lerner and Matthews*, 1988; *FAO*, 2005). Emission estimates from livestock were reported as 0.9 Tg CH_4 yr^{-1} in 1995 and 2000 (*Yamaji et al.*, 2003) and 0.6 Tg CH_4 yr^{-1} for 2008/2009 (*Jahan and Azad*, 2013). Bangladesh does have several natural wetland environments, including the Sundarban mangrove forest that covers 6,017 km^2 of the coastal zone. Other major forests include the semi-evergreen forest in the eastern hills and the deciduous sal forest on the central and northwestern terraces. Additionally, fresh water swamp forests occupy low-lying areas of Sylhet and depressions within the semi-evergreen forest (*Hossain*, 2001). Ocean waters of the Bay of Bengal also can be regarded as a minor source due to bacterial methanogene-

Table A.1: Data sources and details.

Data	Source/Instrument	Measurement	Dates	Resolution
TRMM-TMI	TRMM-TMI v7.1	% Area Inundated	Jan 2002-Dec 2015	1° x 1° grid
AIRS	330 hPa, V6 L3 product, NASA EOS/Aqua	XCH_4	Jan 2003-Dec 2014	1° x 1° grid
SCIAMACHY	IMAP-DOAS product, ESA ENVISAT	XCH_4	Mar 2002-Dec 2011	2° x 2° grid
GOSAT	SRFP ESA GHG-CCI product, JAXA GOSAT TANSO	XCH_4	Jun 2009-Dec 2014	1° x 1° grid
CarbonTracker	NOAA ESRL Global Greenhouse Gas Reference Network	CH_4 Surface Flux	Jan 2000-Dec 2010	1° x 1° grid
Surface Water Gauges	Bangladesh Water Development Board	Anomaly water height	Dec 2002-Jan 2008	281 locations

sis and bacterial oxidation in surface water on the shelf close to the Ganges/Brahmaputra mouth (*Berner et al.*, 2003).

A.3 Datasets

A.3.1 Atmospheric Infrared Sounder (AIRS)

AIRS was launched from the NASA EOS/Aqua platform in May 2002 as a nadir cross-track scanning infrared spectrometer (*Pagano et al.*, 2003). This instrument captures infrared energy from the Earth and separates it into 2378 wavelength channels that cover 69-1136, 1217-1613, and 2169-2674 cm^{-1}. It has a spatial resolution of 13.5 km at nadir and the satellite crosses the equator at approximately 1:30 A.M. and 1:30 P.M. local time, resulting in near global coverage twice a day. We used the AIRS Version 6 Level 3 (L3) product that has been averaged to 1° by 1° grid cells (Table A.1). These L3 products are separated into an ascending and descending portion of the orbit, based on the direction of movement of the satellite. These two parts of the orbit were averaged for our study. Monthly product means for each grid box were aggregated. Due to AIRS' higher sensitivity in the middle to upper troposphere, we only use the AIRS CH_4 concentrations at 300 hPa by converting to XCH_4 using AIRS surface pressure and water vapor observations. Monthly averages for the Bangladesh region (22°-26°N and 88°-93°E) were analyzed from January 2003 to December 2014. We use 0.5-1.6% for AIRS XCH_4 profiles as reported in *Xiong et al.* (2008).

A.3.2 SCanning Imaging Absorption spectroMeter for Atmospheric CHartographY (SCIAMACHY)

SCIAMACHY was on board the European Space Agency's environmental satellite ENVISAT, receiving data from March 2002 to April 2012 (*Bovensmann et al.*, 1999). ENVISAT flew in a sun-synchronous polar low Earth orbit crossing the equator at 10:00 A.M. local time, achieving complete global coverage every 6 days. SCIAMACHY measured spectra of solar radiation in the spectral region of 240 – 2400 nm in nadir, limb, and solar and lunar occultation viewing modes. The SCIAMACHY near-infrared nadir spectra contain information about atmospheric trace gases, including CH_4, CO_2, CO, and N_2O (*Frankenberg et al.*, 2006). In this study we use 2° by 2° grid cell, monthly CH_4 averages derived from an IMAP-DOAS XCH_4 product. The product was retrieved from SCIAMACHY SWIR spectra (channel 6) using the IMAP-DOAS algorithm developed at University of Heidelberg and SRON (*SCRON*, 2007). The derivation of XCH_4 has been extensively described in *Frankenberg et al.* (2005a,b, 2006, 2008a,b, 2011) and *Butz et al.* (2010). The typical ground pixel size of SCIAMACHY is 30 km (along-track) times 60 to 120 km (across-track) (*Scheepmaker and Frankenberg*, 2007). Retrieval quality deteriorated after November 2005 due to high noise in detector pixels, but retrievals are still use for our analysis (*SCRON*, 2007; *Frankenberg et al.*, 2011). Similar to the AIRS time series, monthly averages were calculated across Bangladesh from January 2003 to December 2011. Over ocean retrievals in SCIAMACHY are only possible with low clouds and, therefore, ignored in this study. We use a 1.5-2% precision for SCIAMACHY XCH_4 (*Frankenberg et al.*, 2005a,b; *Gloudemans et al.*, 2005; *Meirink et al.*, 2006; *Bergamaschi et al.*, 2009).

A.3.3 Greenhouse Gases Observing Satellite (GOSAT)

The Thermal And Near infrared Sensor for carbon Observation (TANSO) - Fourier Transform Spectrometer (FTS), on board the satellite GOSAT (launched by JAXA in January 2009) also provides XCH_4. The satellite moves in a sun-synchronous low orbit and uses a short-wave infrared spectral analysis of sunlight backscattered by the Earth's surface and atmosphere at 90-280 km intervals. GOSAT observations are spatially sparse, but temporally dense since the satellite revisits sampling locations every three days (*Kuze et al.*, 2009). We used the XCH_4 product (ESA GHG-CCI Initiative) from the SRFP algorithm provided by SRON/KIT. The retrieval method has been described in detail by (*Butz et al.*, 2009, 2010, 2011). Similar to SCIAMACHY, ocean retrievals were ignored in this study. Valid data was only partially available between June 2009 and December 2014 at the native resolution of GOSAT. We assume a GOSAT error of 0.4-0.8% with estimated biases between -17 and 2 ppb (*Parker et al.*, 2011).

A.3.4 Tropical Rainfall Measuring Mission Microwave Imager (TRMM-TMI)

The CH_4 emission source area was calculated from land-water fraction as a proxy for inundation area. Land-water fraction was retrieved from the Tropical Rainfall Measuring Mission (TRMM) Microwave Imager (TMI). The TRMM satellite was launched in November 1997 with the TMI instrument, a dual-polarization passive microwave conical scanning radiometer with an incidence angel of 52.8°, which operates at 10.65, 19.4, 21.3, and 85.5 GHz (*Gao et al.*, 2006). The TRMM orbit and sensor swath result in spatial coverage between ±38° latitudes. The product used in this analysis is 1° by 1° between 22°-26°N and 88°-93°E, excluding pixels over the Bay of Bengal, and averaged on a monthly timescale between January 2002 to December 2015. The method we used to calculate inundation area has been presented in previous studies that demonstrated the capabilities of satellite observations to recover wetland extents and dynamics (*Purvaja and Ramesh*, 2001; *Prigent*

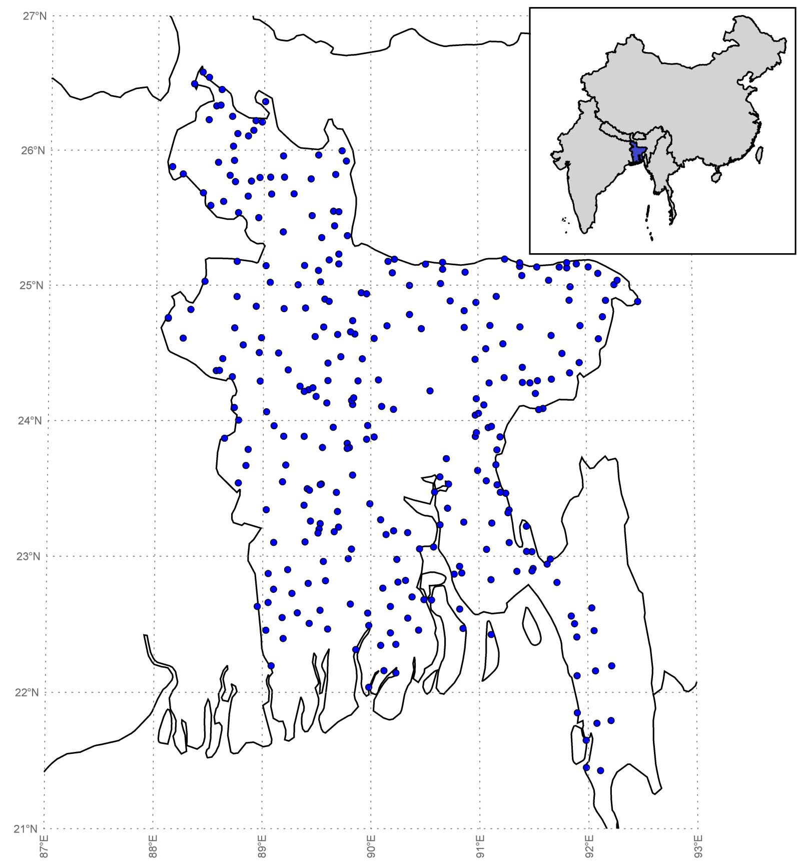

Figure A.2: Bangladesh and the location of the surface water gauges (blue circles).

et al., 2007; *Papa et al.*, 2010). *Papa et al.* (2006) successfully captured inundation and rice cultivation over the Indian subcontinent using a similar passive microwave land-surface emissivity detection.

A.3.5 Surface Water Gauges

Surface water levels were obtained for 281 locations, consisting of 773,526 records, from the Bangladesh Water Development Board (Fig. A.2). Water level measurements were recorded daily at each location from time intervals between 30 December 2002 and 3 January 2008. The average time series length is approximately 4.5 years with a maximum of 5 years and a minimum of 1 month. All water levels were referenced to mean sea level and sites include both tidal and non-tidal rivers. An average time series was calculated from the anomaly of all gauges to serve as a proxy for country-wide change in inundation and as validation for seasonal fluctuations in TRMM-TMI.

A.3.6 CarbonTracker

The CarbonTracker-CH_4 monthly average CH_4 surface flux product was used to validate our model flux estimates. The National Oceanic and Atmospheric Administration (NOAA) Earth System Research Laboratory data was downloaded from the NOAA ESRL Global Greenhouse Gas Reference Network website (*NOAA ESRL*, 2017; *Peters et al.*, 2007). The time variation of the CarbonTracker CH_4 flux was found between 22°-26°N and 88°-93°E from January 2000 to December 2010.

A.3.7 Inventory of CH_4 Emissions in South East Asia

An inventory of ground-based surface flux measurements was established from a review of 32 studies from rice paddies and natural wetlands in South Asia (Table A.2). These estimates spanned from 1988 to 2010 and typically used chamber methods for collecting point measurements of surface fluxes. We document the minimum and maximum fluxes measured in each of the studies to better understand the range of possible surface emissions (Table A.2). The inventory includes flux measurements from a variety of rice paddies, differing in season, irrigation scheme, rice species, fertilizer, etc. The natural environments include a wetland, marsh, mangrove, estuary, and bay.

An additional inventory of reported annual emissions from Bangladesh was also compiled. The emissions include 28 upscaled estimates of annual rice emissions derived from variations of IPCC guidelines or complex emission models between 1990 and 2015. The disparity among estimation techniques, emission rate factors, and modeling tools has led to large discrepancies on the country-wide scale. We compare this inventory to both the ground-based surface flux inventory and our satellite-derived flux estimates to evaluate consistency between methodologies and discuss carbon modeling uncertainties.

Table A.2: Methane emissions (mg CH_4 m^{-2} h^{-1}) from rice paddy and wetlands in South Asia.

Location	Natural		Anthropogenic		Season	Environment	Years	Reference
	min	max	min	max				
Bangladesh			5.0	66			2005-2006	*Frei et al.* 2007
			20.0	37				
			1.0	25	dry		2010-2012	*Ali et al.* 2014
China			7.4	47	full year		1989-1991	*Wassmann et al.* 1993
			0.9	6			1994	*Cai et al.* 1997
			1.5	100			1988-1994	*Khalil et al.* 1998
			1.1	5			2000-2002	*Zou et al.* 2005
	0	55				freshwater marsh	2001-2002	*Ding et al.* 2004
	0	20				plateau wetland	2002	*Hirota et al.* 2004
			0.5	17			2009-2010	*Hou et al.* 2012
India			4	17			1994	*Adhya et al.* 1994
			2.1	7	wet		1993	*Singh et al.* 1996
			1.1	14	dry		1997	*Adhya et al.* 2000
			0.9	16	wet			
	0	9			full year	bay		
	2	14			full year	mangrove		*Purvaja and Ramesh* 2001
	2	46			full year	esuary		
			0.1	4			1999	*Ghosh et al.* 2003
			0.0	2	wet		2006	*Das and Baruah* 2008
			0.0	33	dry			*Datta et al.* 2013
	2.28	386			full year	mangrove	2003	*Biswas et al.* 2007
			1.0	48	wet			
Indonesia			18	27	wet		1992-1993	*Ghani Nugroho et al.* 1997
			7	33			1994	*Ghani Nugroho et al.* 1994
			0	4			1995	*Makarim et al.* 1995
Japan			1.0	140			1991, 1993	*Yagi et al.* 1996
			1.0	80			1997	*Inubushi et al.* 2001
			0.2	55	wet		2004	*Naser et al.* 2007
			15.0	75			2007-2008	*Kato et al.* 2012
Philippines			0.2	187	wet		1991-1992	*Denier van der Gon* 1994
			0.2	4	dry		1992	*Denier van der Gon and Neue* 1995
			0.0	260	dry, post harvest		1992	*Denier van der Gon et al.* 1996
			0.0	250	wet, post harvest			
			0.3	18	dry		1994-1998	*Corton et al.* 2000
			7.4	40	wet			
Taiwan			2.5	3	dry		1999	*Liou et al.* 2003
			8.7	9	wet			
Thailand			0.6	59				*Jermsawatdipong et al.* 1994
			0	47	dry			*Yagi et al.* 1994
			0	56	wet			*Yagi et al.* 1994
Southeast Asia	**0**	**55**	**0**	**260**				
All of Bangladesh			**1**	**66**				

A.4 Methods

A.4.1 Satellite-derived CH_4 Concentrations

To determine country-wide XCH_4 increases due to Bangladesh emissions, we remove the regional baseline XCH_4. The baseline XCH_4 (hereafter called the background signal) refers to the ambient XCH_4 associated with emissions outside of Bangladesh. To determine this background signal, we considered atmospheric advection in and out of Bangladesh.

A.4.1.1 HYSPLIT Trajectories

Air mass origin was calculated using the Hybrid Single-Particle Lagrangian Integrated Trajectory model (HYSPLIT4) provided by NOAA's Air Resource Laboratory (*Draxler and Hess*, 1997, 1998; *Draxler*, 1999; *Stein et al.*, 2015; *Rolph*, 2017). Forward and back-trajectories were calculated starting on the sides of a rectangular grid surrounding Bangladesh. Trajectories that did not cross over Bangladesh were rejected. The remaining trajectories were evaluated in terms of their residence time over Bangladesh as well as their position 96, 72, 48, 24 hours before and after they entered Bangladesh for the first time (see Appendix B). Trajectories were started for 18 positions on the rectangle surrounding Bangladesh, for each day of each month, four times a day, and for three different heights above the surface (500, 1500, and 2500 m), so that in total around 6500 trajectories were calculated for each month. Monthly density maps of air mass origin were generated from the trajectory data.

A.4.1.2 Residence Time

The mean residence time represents the mean time a mass plume resided within country boundaries. The mean monthly residence time was calculated from the residence time of each individual back-trajectory over Bangladesh and subsequent averaging over the month.

A.4.1.3 Plume Trajectories

The monthly XCH_4 increase ($XCH_{4increase}$) due to emissions from Bangladesh was calculated from regression of XCH_4 by the HYSPLIT density (ρ) weighting such that

$$XCH_{4increase} = \frac{\sum \rho_{f24} XCH_4 - \sum \rho_{b24} XCH_4}{48}, \tag{A.1}$$

where $XCH_{4increase}$ is in ppb, ρ_{f24} is the 24 h forward-trajectory HYSPLIT density, ρ_{b24} is the 24 h backward trajectory HYSPLIT density, XCH_4 is the spatial monthly mixing ratio of each satellite (ppb), and denominator represents the time between the forward and backward trajectories (h). We use ± 24 h because of the short residence time calculated in Section A.4.1.2.

XCH_4 uncertainties are determined from reported values of AIRS, SCIAMACHY, and GOSAT error. A three-month moving average smoothing window was applied to the calculated XCH_4 increases to remove noise from satellite XCH_4 uncertainties.

A.4.2 Advection-Inundation Methane Emissions (AIME) Model

To compute the emissions responsible for the XCH_4 increases, we use a simple inverse model that incorporates the emission source area and CH_4 advection.

Monthly source area is determined from the inundation area using TRMM-TMI land-water fraction. The land-water fraction variations are compared to relative changes in surface water levels to validate this inundation area proxy. Due to the timescale of anerobic microbiology of flooded areas, CH_4 production reaches a steady state after the soil stays anoxic for several weeks (*Conrad*, 2002). Therefore, we delay the inundation area to find the best cross correlation with satellite fluctuations. Atmospheric advection is determined from the CH_4 residence time, as calculated by HYSPLIT in Section A.4.1.2.

The Advection-Inundation Methane Emissions (AIME) model is based on the following equation, which is solved for the surface flux F,

$$f(t) = cF\chi(t+d)\frac{R(t)}{m}\frac{M_{air}}{M_{CH_4}} - \alpha, \tag{A.2}$$

where $f(t)$ is the atmospheric CH_4 concentration (ppb) due to Bangladesh emissions through time t, F is the flux (mg CH_4 m^{-2} h^{-1}), $\chi(t+d)$ is the monthly land-water fraction shifted by lag d (days), $R(t)$ is the monthly residence time (h), m is the atmospheric mass (approximately 10,000 kg m^{-2} at sea level), M_{air} is the molar mass of air (kg mol^{-1}), M_{CH_4} is the molar mass of CH_4 (kg mol^{-1}), c is a conversion constant equal to 1000 (ppb ppm^{-1}), and

α is concentration (ppb) of CH_4 due to other sources. We match the average seasonal amplitude of the XCH_4 increases to the calculated concentrations $f(t)$. We vary F and choose the value that produced a curve with the highest correlation with the XCH_4 increase. Unrelated emissions sources are accounted for through a vertical shift α equivalent to

$$\alpha = f(t) - g(t), \tag{A.3}$$

where $g(t)$ is the XCH_4 increase calculated from satellite observations. This vertical shift is necessary due to (1) probing of different air masses (AIRS vs. full column measurements of SCIAMACHY and GOSAT), (2) inability to account for CH_4 sinks, and (3) additional CH_4 sources, such as livestock and natural gas. The uncertainty associated with $f(t)$ is determined from an assumed flux error of 10 mg CH_4 m^{-2} h^{-1}, the standard deviation of the residence time, an inundation area uncertainty of 5%, an atmospheric column mass uncertainty of 100 kg m^2, and a vertical offset error of 10 ppb. See Appendix B for error propagation details.

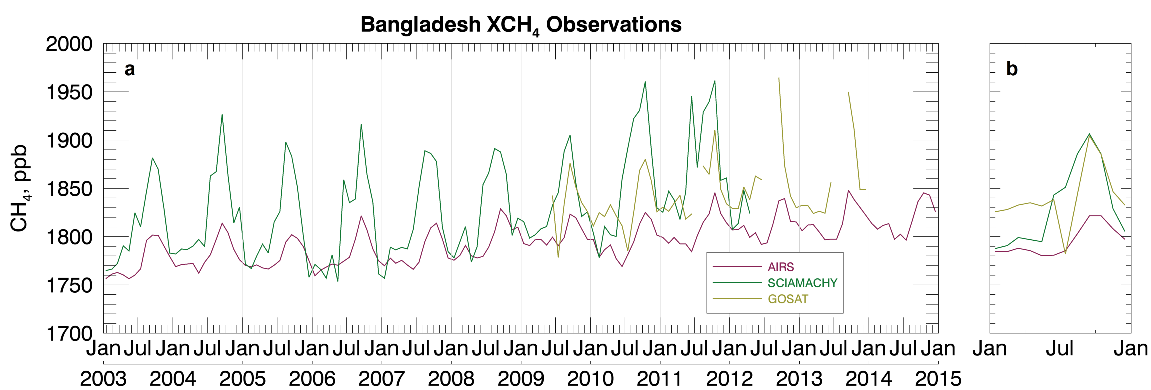

Figure A.3: Bangladesh XCH_4 from AIRS, SCIAMACHY, and GOSAT satellites (a) between 2003 and 2015. Average annual cycle is show on right (b).

A.4.3 Comparison to Other Estimates

We compared our AIME models estimates to (1) emissions inventories of South Asia surface fluxes, (2) reported Bangladesh annual emissions, and (3) CarbonTracker surface fluxes in Bangladesh. The AIME model annual flux was compared directly to the reported fluxes in Table A.2. To upscale the AIME average annual fluxes to we used the following equation

$$E = cF\overline{\chi(t+d)}A, \tag{A.4}$$

where E is the average annual flux (Tg yr^{-1}) between 2003 and 2015 from Bangladesh, F is the AIME flux (mg CH_4 m^{-2} h^{-1}) calculated in Equation 2, $\overline{\chi(t+d)}$ is the average monthly land-water fraction shifted by lag d (days) through time t, A is the area of Bangladesh equal to $1.4757x10^{11}$ m^2 (*Islam*, 2010), and c is a conversion coefficient equal to $8.76x10^{-12}$ hr Tg mg^{-1} yr^{-1}. These country-wide annual fluxes were compared to a variety of model calculated emissions from previous studies. The CarbonTracker fluxes were compared to the average total surface flux across Bangladesh equal to F scaled by $\chi(t+d)$.

A.5 Results

A.5.1 Satellite-derived CH_4 Concentrations

A.5.1.1 General Observations

Between 2003 and 2015, AIRS observations range from 1756 to 1848 ppb in Bangladesh (Fig. A.3.a). Seasonal highs frequently occur in September and October, while lows appear in May and July. SCIAMACHY Bangladesh observations range from 1754 to 1962 ppb, with the lowest concentrations occurring later in the year (February to June) (Fig. A.3.a). Valid SCIAMACHY data in Bangladesh is limited after 2009, due to deterioration of retrieval quality (*Frankenberg et al.*, 2011). Although valid data is confined to 2009-2013, GOSAT observations show similar seasonal patterns, with concentrations ranging from 1778 to 1964 ppb (Fig. A.3.a). On average, AIRS observations are 35 and 50 ppb less than SCIAMACHY and GOSAT, respectively. The mean uncertainty in XCH_4 is 29 ppb (1.6%), 37 ppb (2%), and 15 ppb (0.8%) in AIRS, SCIAMACHY, and GOSAT, respectively (see Fig. B.2 in Appendix B).

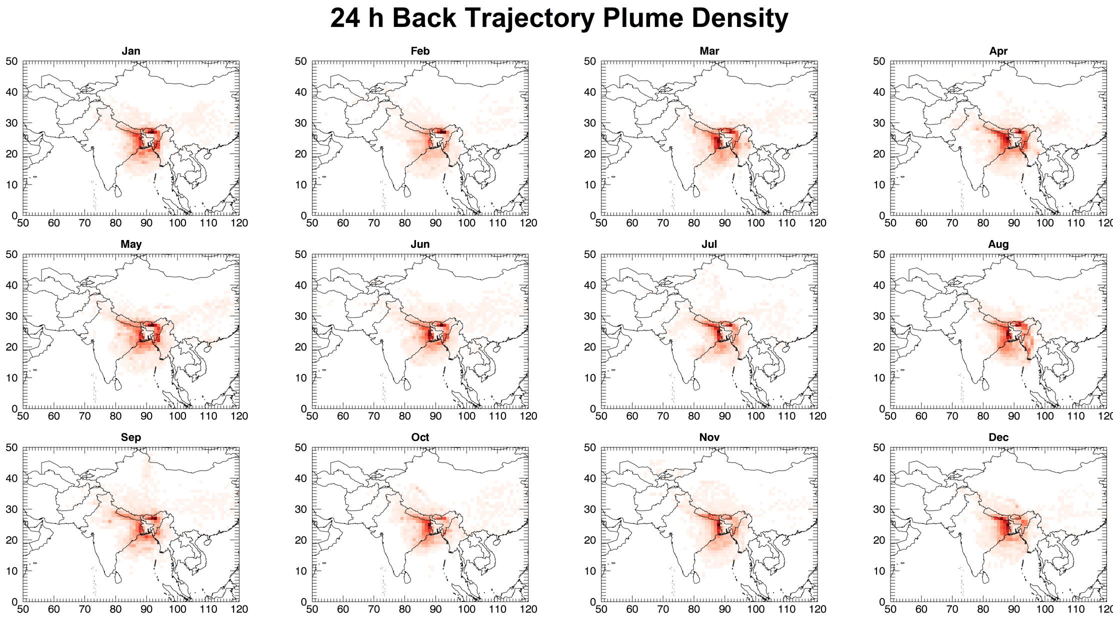

Figure A.4: HYSPLIT Back Trajectory density at 24h prior to entering Bangladesh.

A.5.1.2 HYSPLIT Trajectories

Our back-trajectory analysis indicate that trajectories most often originate east of Bangladesh between northern India and the middle of the Bay of Bengal (Fig. A.4). Longer back trajectories (48-96 h) show that the trajectories swing from a northeastern origin during the dry months to a southeastern origin during the raining season (see Appendix B). Seasonal effects are accentuated by the strong latitudinal gradients in CH_4 concentrations, as well as strong nearby sources of emissions (e.g. in India and Southeast Asia).

A.5.1.3 Calculated CH_4 Concentrations

Differences between Bangladesh and background observations result in concentrations between -0.5 to 7.8 ppb, -7.1 to 20 ppb, and 0.8 to 31.2 ppb for the three satellites (Fig. A.5.a). The average seasonal fluctuations show seasonal differences of approximately 3 ± 1, 7 ± 2, and 12 ± 4 ppb for AIRS, SCIAMACHY, and GOSAT, respectively (Fig. A.5.b). See Appendix B for non-smoothed XCH_4 increases.

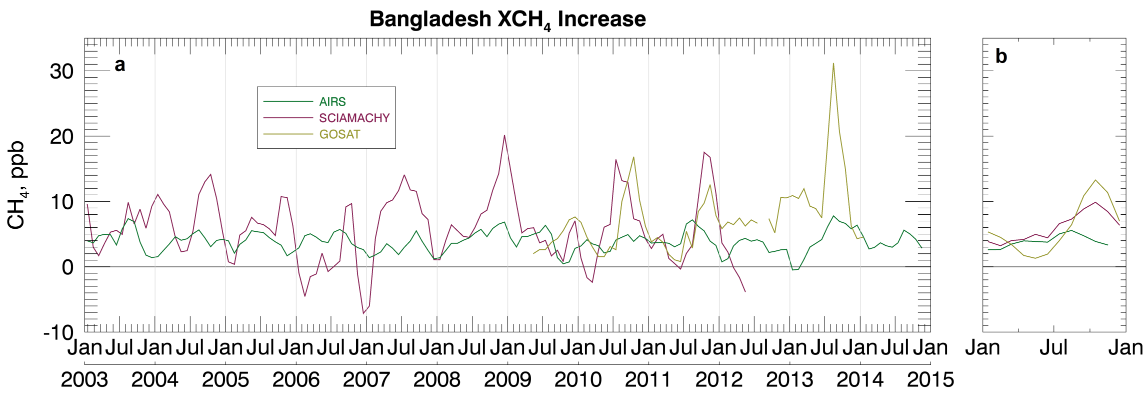

Figure A.5: Smoothed XCH_4 increases from Bangladesh, calculated from Equation 2 and filtered with a three-month moving average. Average monthly variations are shown on the right (b).

A.5.2 AIME Model

A.5.2.1 Emission Source Area

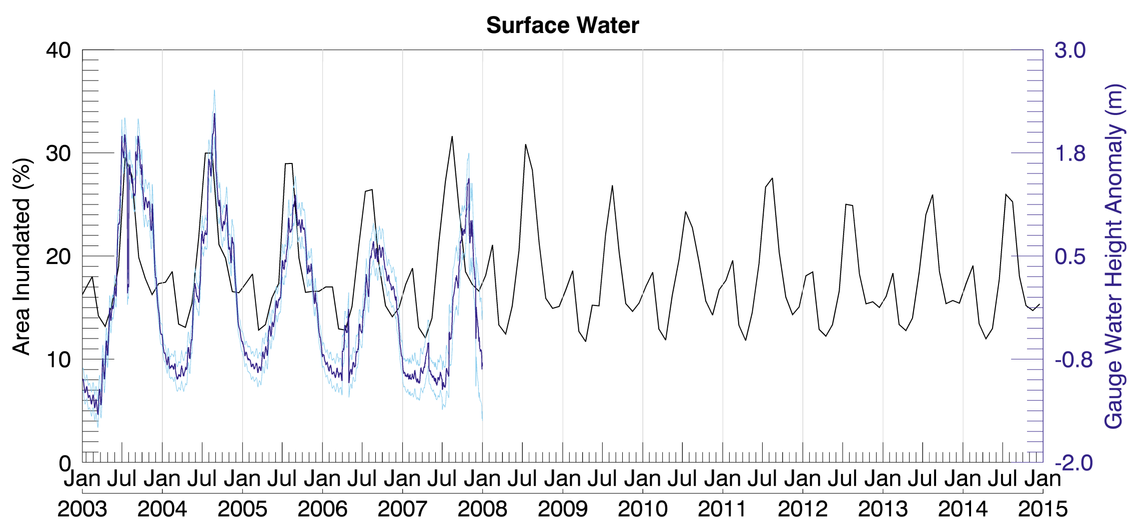

Figure A.6: Average anomaly of surface water, as measured from gauges (blue), and average monthly water fraction from TRMM-TMI (black). Light blue band defines the 95% confidence interval. Peak water levels occur in early September. Bangladesh inundation ranges from 11-31% of total area.

TRMM-TMI shows seasonal fluctuations in inundation between 10.9 to 31.8% of the total country (Fig. A.6). The annual peak occurs between July and August with a secondary peak in February. Seasonal lows occur in March. The years 2007-2008 show the greatest range in percent inundated. Peak gauge water levels often occur in August and show variations in timing (Fig. A.6). Gauges suggest an average seasonal variation of 2 m in surface waters that parallel interannual discrepancies in TRMM-TMI. The gauge standard deviation ranges between 0.76 m in winter months and 2.0 m during mean peak water levels, suggesting regional differences in summer flooding. Gauge levels lag behind TRMM-TMI observations and do not capture the peak in February.

A.5.2.2 Emission Advection

As determined by our HYSPLIT trajectory analysis, the mean residence time of emitted CH_4 within Bangladesh boarders is 22.0 ± 5.5 h (Fig. A.7). The residence time decreases significantly during the wet season.

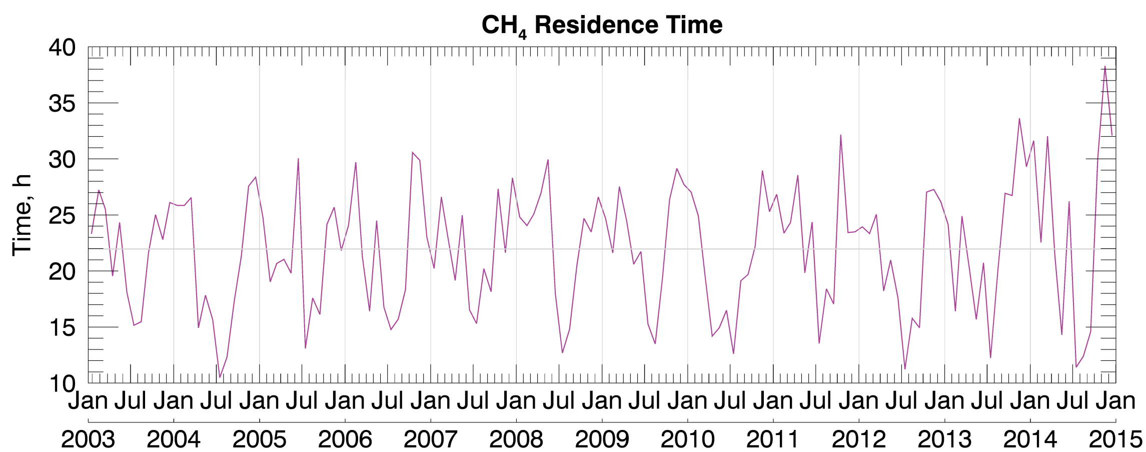

Figure A.7: Monthly average residence time for CH_4 to reside within Bangladesh country boarders. Mean residence time is 22 ± 5.5 h.

A.5.2.3 AIME Model Calculation

The correlation coefficient between maximum XCH_4 and maximum inundation was calculated for various time lags between the two signals. The maximum correlation occurred at lags from 20 to 65 days for the three satellites (Table A.3). Although this appears to be a large range, the delay could be set to any number of days within the 4 to 10

Table A.3: Calculated fluxes (mg CH_4 m^{-2} h^{-1}) required to match seasonal amplitude of satellite-derived XCH_4 increases from Bangladesh emissions.

	AIRS	**SCIAMACHY**	**GOSAT**
TRMM delay (days)	10	65	60
Correlation Coefficient	0.42	0.37	0.40
α (ppb)	0	1	7
Inundation Flux (mg CH_4 m^{-2} h^{-1})	**4**	**9**	**19**

week period without a significant impact on the correlation (see Fig. B.6 in Appendix B). AIRS XCH_4 increases are coincident with average annual fluxes under 4 mg CH_4 m^{-2} h^{-1}, SCIAMACHY XCH_4 increases suggest 9 mg CH_4 m^{-2} h^{-1}, and GOSAT suggests 19 mg CH_4 m^{-2} h^{-1} (Fig. A.8).

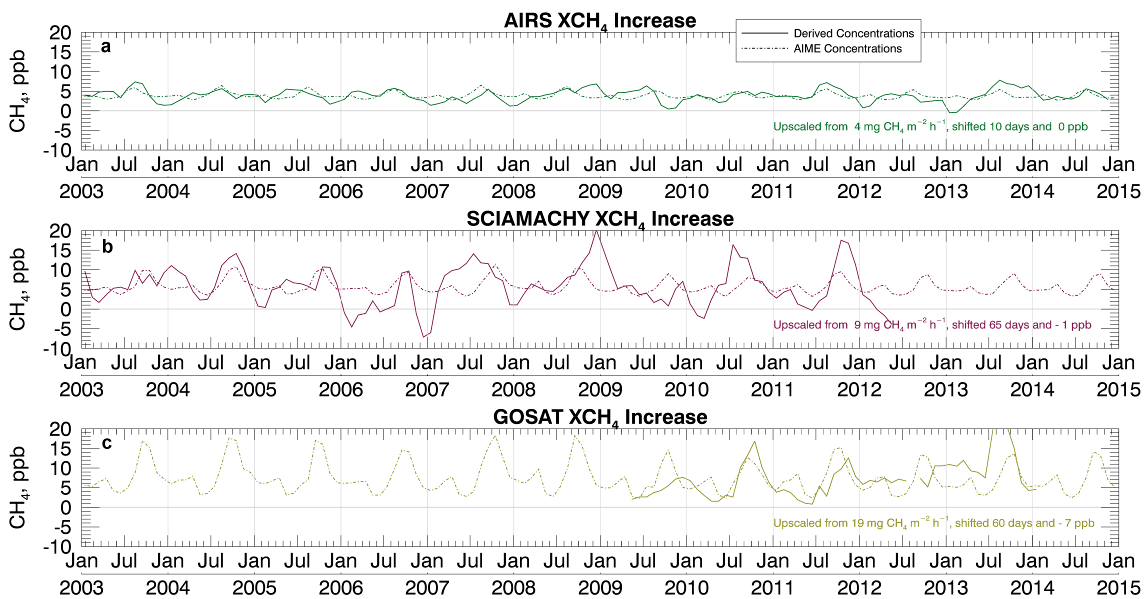

Figure A.8: Comparison of satellite-derived emissions after removal of the background signal (solid line) to AIME model concentrations (dashed line). The AIME concentrations are determined using average yearly fluxes (Equation 1).

For example, we determine the average annual flux to be 4 $\pm$ 10 mg CH_4 m^{-2} h^{-1} with a delay time of 10 days using AIRS XCH_4 increase. The contribution of this emission accounts for the entire source of the the overall XCH_4 increase because of the need for a 0 ppb vertical shift (Table A.3). Both SCIAMACHY and GOSAT require a larger lag, as well as a vertical shift to account for the non-inundation effects (Table A.3). After these appropriate adjustments, the AIME models show agreement with the SCIAMACHY and GOSAT, respectively (Fig. A.8). See Fig. B.6 for AIME model error for each of the satellites.

A.5.3 Other CH_4 Models

CarbonTracker surface fluxes show a similar annual cycle to the AIME total surface fluxes in Fig. A.9. The magnitude of the seasonal fluctuation of CarbonTracker most closely aligns with GOSAT, although the flux peak occurs between 1-2 months prior to the AIME estimates and the magnitude of the flux is generally higher than our estimates.

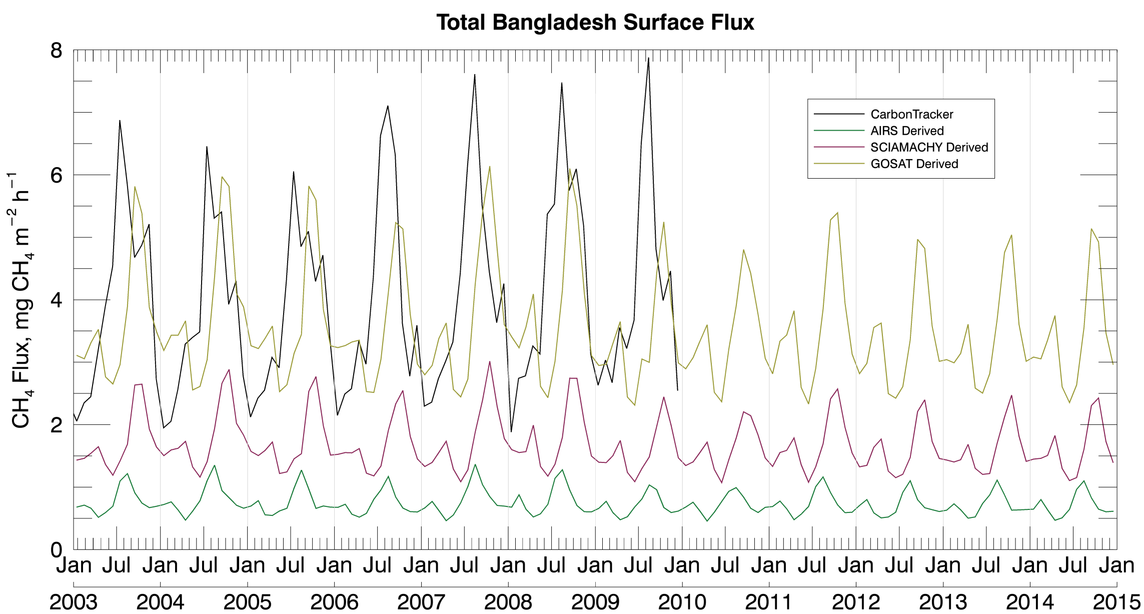

Figure A.9: Total surface CH_4 flux from Bangladesh as derived from the AIME average annual flux from AIRS (4 mg CH_4 m^{-2} h^{-1}), SCIAMACHY (9 mg CH_4 m^{-2} h^{-1}), and GOSAT (19 mg CH_4 m^{-2} h^{-1}). CarbonTracker posterier fluxes are also shown until 2010.

A.5.4 Reported Fluxes and Annual Emissions

Our modeling results are compared to the emissions inventories of both South Asia surface fluxes and Bangladesh annual emissions. Our inventory highlights a large range

(0 to 260 mg CH_4 m^{-2} h^{-1}) of measured ground-based fluxes across South Asia (Table A.2). Both reported rice and wetland fluxes span three orders of magnitude and share substantially overlapping spatiotemporal characteristics. The highest fluxes were reported from a 1992 chamber study in the Philippines from fertilized rice paddy (*Denier van der Gon and Neue*, 1995). Negligible fluxes, approaching 0 mg CH_4 m^{-2} h^{-1}, were reported in multiple studies under a variety of field environments and conditions.

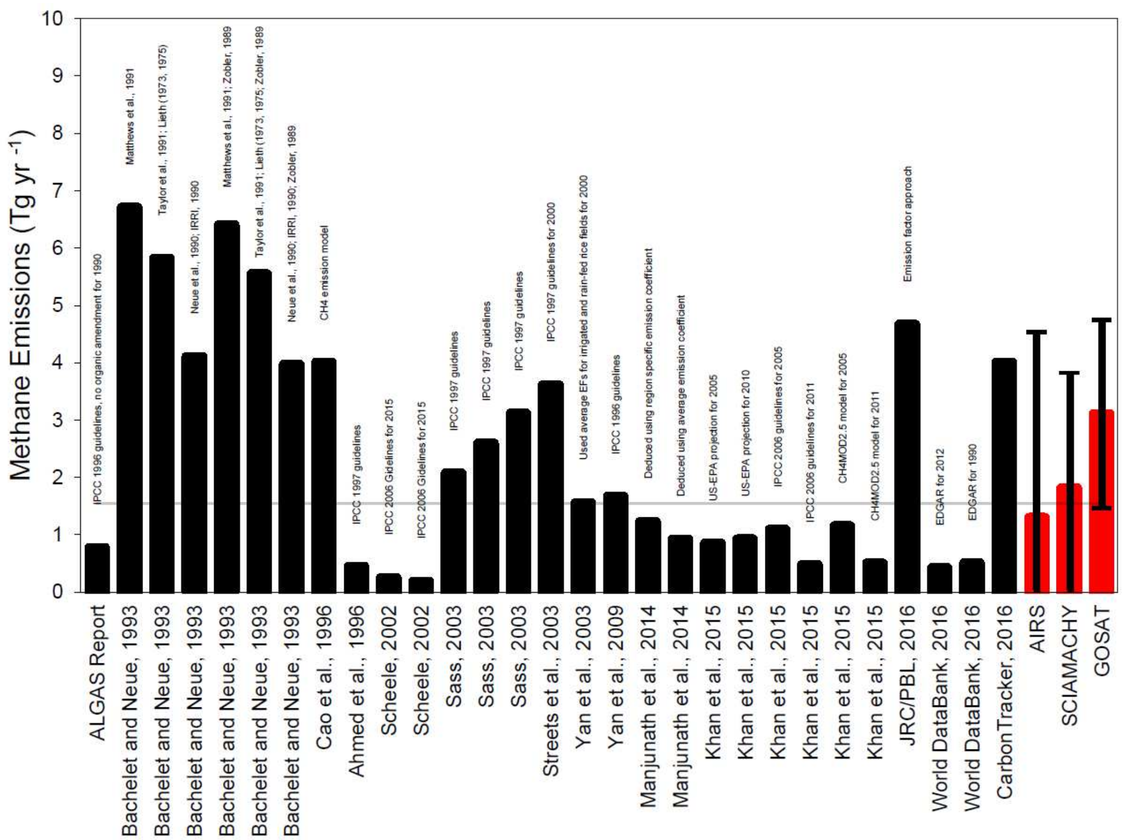

Figure A.10: Graphical summary of 32 calculated estimates of the annual methane emission from Bangladesh. Estimates range from 0.18 Tg CH_4 yr^{-1} to 6.70 Tg CH_4 yr^{-1} with a median value of 1.55 Tg CH_4 yr^{-1}. The red bars show the upscaled annual emissions calculated from the AIME models in this study (See Table A.3).

Reported annual emissions from rice cultivation in Bangladesh range from early estimates of approximately 7 Tg CH_4 yr^{-1} to more recent studies suggesting 0.18 Tg CH_4 yr^{-1} (Fig. A.10). Methods to determine these values typically follow the IPCC guidelines, using emission factors and activity coefficients. Our calculated average surface fluxes from

AIME were upscaled to annual emissions equaling 1.3±3.2, 1.8±2.0, 3.1±1.6 for AIRS, SCIAMACHY, and GOSAT, respectively.

A.6 Discussion

Extrapolation from top-down and bottom-up CH_4 datasets is highly uncertain in intermediate-sized, data-sparse regions with significant spatio-temporal variability. Here we explore the seasonal variations of country-wide CH_4 emissions in Bangladesh using remotely-sensed products of CH_4 and inundation. As expected, we found that XCH_4 retrievals suggest higher concentrations in Bangladesh compared to global and background regions. Even after removal of the regional ambient XCH_4, we see a significant enhancement of atmospheric CH_4 in Bangladesh during the monsoon season. This anomalously strong seasonal fluctuation has also been observed in larger regions across South Asia (*Patra et al.*, 2009; *Xiong et al.*, 2009; *Kavitha and Nair*, 2016), and is attributed to high emission intensity from extensive inundation, rice cultivation, and the vertical atmospheric transport during the summer monsoon (*Xiao et al.*, 2006; *Xiong et al.*, 2009). Recent isotopic evidence suggests that global CH_4 rises since 2007 were dominated by significant increases in biogenic methane emissions, particularly from expansion of tropical wetlands and agricultural sources (*Nisbet et al.*, 2016). We do not see an increase in the extent of inundation or in CH_4 emissions in the region since that time.

A.6.1 Method Uncertainty

By using three independent satellites, we highlight disparities between XCH_4 products. SCIAMACHY observations exceed variations seen in AIRS and GOSAT as well as adjacent regions of India (*Kavitha and Nair*, 2016). Studies use SCIAMACHY XCH_4 with varying degrees of success making evaluation of the impact of the detector pixel degradation after 2005 difficult (*Frankenberg et al.*, 2011). *Meirink et al.* (2008) report that some areas, particularly in subtropical regions that are poorly constrained by surface networks, may be affected by regional systematic errors. The bias correction applied to SCIAMACHY does not consider these regional errors that potentially lead to shifts in the overall distribution of emission estimates. With large discrepancies between our satellites, we suggest that the fixed uncertainty of 2.0% is insufficient for Bangladesh because SCIAMACHY is likely improperly calibrated for this region. The lesser concentrations observed by AIRS, however, may be an underestimation due to AIRS' vertical weighting. As discussed early, AIRS observations are most sensitive to middle to upper troposphere CH_4 concentration. Nevertheless, *Xiong et al.* (2009) argue that this region's intensive convection allows for sufficient mixing to justify the use of AIRS XCH_4.

The inconsistent spatiotemporal distribution of valid SCIAMACHY and GOSAT observations is also a concern. Temporal differences arise during the monsoon season, when monthly averages are comprised of only a few observations across Bangladesh. Unfortunately cloud interference reduces valid retrievals during the peak of both aus and aman cultivation and seasonal inundation. The overlap of these critical periods limits our certainty in the timing and extent of inundation-caused emissions. GOSAT is especially limited during this period as seen from the missing data between June to October.

Due to the number of HYSPLIT trajectory simulations, we have high confidence in atmospheric advection pathways around Bangladesh. The residence time of CH_4 over Bangladesh fluctuates significantly due to the monsoonal season but still falls within the $\pm$ 24 h HYSPLIT densities for the majority of the simulations. A more conservative method of regressing over $\pm$ 48 h would decrease our estimates of the XCH_4 increase over Bangladesh (see Fig. B.9 in Appendix B).

Previous studies differentiate between rice and wetland emissions (*Chen and Prinn*, 2006). Our study, however, demonstrates that similarities in ground-based flux measurements and general source strength uncertainty encourages the consolidation of source area and emission patterns in Bangladesh. Observed inundation patterns show good agreement with wetland dynamics from the larger Indian Subcontinent and previous Bangladesh inundation studies (*Mirza and Monirul Qader Mirza*, 2002; *Papa et al.*, 2006; *Islam et al.*, 2010). Similarly, the spike in inundation early in the year, associated with groundwater irrigation of boro rice, agrees with spatial distribution of the rice cropping extent presented in *Gumma et al.* (2014) and *Mosleh and Hassan* (2014). It is unnecessary to distinguish short term flooding patterns when using monthly resolution XCH_4 and inundation datasets. To validate this claim, we use the high resolution gauge network to check our monthly inundations observations. The only discrepancy between the satellite and gauge data is likely caused by river gauge inability to detect changes in groundwater irrigation schemes. Although studies demonstrate CH_4 emission differences caused by changes in various short term rice cropping practices, our spatiotemporal scale balances these effects over the entire country. For example, continuous flooding through intensification of rice cultivation stimulates additional CH_4 emissions (*Ali et al.*, 2014). Alternatively, midseason drainage oxygenates the soil and significantly reduces emissions (*Yagi et al.*, 1996; *Corton et al.*, 2000). In the tidal zones of Bangladesh, fluctuating tidal inundation also can provide periods of oxygen supply in natural wetlands and mangroves (*Purvaja and Ramesh*, 2001). Our study does not address these scenarios but rather estimates the overall contribution of all inundated areas.

It is important to note, however, that previous CH_4 modeling efforts have demonstrated extensive disagreement in simulations of wetland areal extent and associated CH_4 emissions (*Ringeval et al.*, 2011, 2010, 2012; *Wania et al.*, 2013; *Melton et al.*, 2013, *and references therein*). Often large variability exists between models that use inundation dataset information and those that independently determine wetland area (*Melton et al.*, 2013). Nearly a three-fold difference between published estimates of global wetland extent highlights the scope of the discrepancy (*Wania et al.*, 2013; *Melton et al.*, 2013). The vast seasonal fluctuations in inundation dynamics of the GBM delta will only magnify these uncertainties. Previous studies suggest that approximately 50% (75,000 km^2) of Bangladesh is covered in wetlands, including rivers, estuaries, mangrove swamps, marsh, oxbow lake and beels, water storage reservoirs, fish ponds, and other lands that are seasonal inundated (*Gopal and Wetzel*, 1995; *Islam et al.*, 2010). Meanwhile, rice cultivation takes approximately 30% for boro, 7% for aus, and 39% for aman (*Gumma et al.*, 2014; *Mosleh and Hassan*, 2014). Our study suggests differences in inundation timing of each of these areas result in only 11-31% of the total area to be flooded at one time.

It is possible that the time required to develop anoxic conditions for methanogenesis causes a delay in the fluctuations in XCH_4. According to (*Conrad*, 2002), CH_4 production only reaches a steady state after soil stays anoxic for several weeks. Although some of the reductive processes may occur simultaneously, researchers have described the reduction process in inundated paddy fields as two sequential steps (*Takai and Kamura*, 1966; *Kimura*, 2000). First, aerobic and facultative anaerobic microorganisms decrease Eh by consuming O_2 and NO_3^-, reducing ferric oxides/oxyhydroxides, and producing NH_4^+ and CO_2 (*Kimura*, 2000; *Conrad*, 2002). The second stage includes metabolism by SO_4^{-2}-reducers and methanogens, which produce the CH_4 byproduct. Furthermore, CH_4 produced after inundation may remain in the soil for sometime before escaping to the atmosphere (*Minoda et al.*, 1996; *Kimura*, 2000). *Ali et al.* (2014) report significant increases in CH_4 fluxes 35-49 days after inundation, while both *Adhya et al.* (2000) and *Datta et al.* (2013) report peak fluxes approximately 60-65 days after transplanting. The timing of this lag between initial inundation and water-air exchange of CH_4 may explain the TRMM-TMI delay we use in our AIME models. The use of monthly averaged observations makes the lag even harder to detect. Slowly varying changes in the background cannot be separated from higher frequency variations caused by emissions. Additionally the poorly constrained signal is even more ambiguous with the three-month smoothing of the XCH_4 increase over Bangladesh.

One assumption we make is that the inundated area accounts for all seasonal variations in CH_4, which describes between 50 to 100% (depending on the satellite) of all emissions from Bangladesh. By matching the AIME model to the satellite-derived concentrations based on amplitude, we assume all seasonal fluctuations correlate to changes in the source area extent. We ignore sources that potentially fluctuate in response to temperature or other unforeseen cyclical events. The vertical shift in Equation 2, however, is representative of the atmospheric concentration due to constant, non-seasonal emissions, such as livestock, natural gas, landfills, etc. After converting these concentrations (α in Table A.3) to fluxes, we find that constant, non-seasonal emissions contribute 0.0, 0.3, and 2.3 Tg CH_4 yr^{-1} using background signals of AIRS, SCIAMACHY, and GOSAT, respectively. Previous studies in Bangladesh have estimated livestock emissions up to 0.6 Tg CH_4 yr^{-1} (*Jahan and Azad*, 2013). But India's livestock population emitted 11.8 Tg CH_4 yr^{-1} in 2003, including emissions from enteric fermentation (10.7 Tg CH_4 yr^{-1}) and manure management (1.1 Tg CH_4 yr^{-1}) (*Chhabra et al.*, 2013; *Ciais et al.*, 2013). Our estimates suggest values closer to *Jahan and Azad* (2013) but are possible even for the smaller size of Bangladesh, especially considering that α encompasses all constant emissions, not only livestock sources.

A.6.2 Comparison to Other Estimates

When compiling our South Asia CH_4 flux inventory, we found that many of the independent estimates of CH_4 fluxes differed significantly in magnitude. Our average annual surface flux falls within this range, and upscales to annual emissions near the median value of previous country-wide estimates for Bangladesh. We demonstrate an alternative methodology for analyzing country-wide CH_4 trends in understudied regions, where satellite-based datasets may be the most reliable.

The tropics are not currently well resolved by CarbonTracker-CH4 due to sparse observational coverage and a rapid convection that limits the discrimination of small scale variability (*Bruhwiler et al.*, 2014). The ground-based observational network may never be adequate in tropical regions, such as Bangladesh, so it seems that remote sensing observations may be the only way to constrain the CarbonTracker model. Therefore, the comparison of CarbonTracker and our surface flux estimates may not validate one another, but rather serve as constraints for future regional estimates. Currently, CarbonTracker CH_4 surface fluxes suggest greater overall emissions from the region with seasonal fluctuation that peak earlier than XCH_4 and TRMM-TMI observations.

Bangladesh produces 50.6 million ton/year of rice, which is 6.8% of the global total of 738.1 million ton/year (*FAO*, 2014). If all rice growing regions had similar emissions per ton of rice produced, the global methane emissions from rice production would be 19.1-45.6 Tg/yr, which falls within the large range of possible rice emissions (*IPCC*, 1994; *Lelieveld et al.*, 1998; *Denier Van Der Gon et al.*, 2000; *Sass et al.*, 1999). This satellite-derived AIME model may provide a method to better estimate country-wide CH_4 emissions from inundation.

Appendix B

SUPPORTING INFORMATION FOR APPENDIX A

B.1 AIME Calculations

The AIME model is based on the following equation, which is solved for F,

$$f(t) = cF\chi(t+d)\frac{R(t)}{m}\frac{M_{air}}{M_{CH_4}} - \alpha, \tag{B.1}$$

where the variables equal

$$\begin{aligned}
f(t) &= \text{atmospheric concentration } ppb\, CH_4 \text{ due to Bangladesh emissions through time } t \\
F &= \text{flux } mg\, CH_4\, m^{-2}\, h^{-1} \\
\chi(t+d) &= \text{monthly land-water fraction } m^2 \text{ shifted by lag } d\ days \\
R(t) &= \text{monthly residence time } h \text{ of plume} \\
m &= 10,000\, kg\, m^{-2} \\
M_{air} &= 0.02897\, kg\, mol^{-1} \\
M_{CH_4} &= 0.01604\, kg\, mol^{-1} \\
c &= 1000\, m^{-2} \\
\alpha &= ppv\, CH_4 \text{ due to other sources.}
\end{aligned}$$

We matched the average seasonal amplitude of the satellite-derived concentration to the calculated emissions $f(t)$. We varied F and chose the value that produced a curve with the highest correlation with the satellite-derived concentrations. Unrelated emissions sources are accounted for through a vertical shift α equivalent to

$$\alpha = f(t) - g(t), \tag{B.2}$$

where $g(t)$ is the satellite-derived mixing ratio increase calculated in Section A.4.1.

The error associated with the AIME model was determined by the following equation

$$\delta f(x) = \sqrt{\left(f(x)\sqrt{\left(\frac{\delta F}{F}\right)^2 + \left(\frac{\delta \chi(t+d)}{\chi(t+d)}\right)^2 + \left(\frac{\delta R(t)}{R(t)}\right)^2 + \left(\frac{\delta m}{m}\right)^2}\right)^2 + \sqrt{(\delta\alpha)^2}}, \tag{B.3}$$

where the parameters are equal to

$$\begin{aligned}
\delta F &= 10\, mg\, CH_4\, m^{-2}\, h^{-1} \\
\delta \chi(t+d) &= 0.05\, \chi(t+d)\, m^2 \\
\delta R(t) &= std(R(t)) = 5.5\, h \\
\delta m &= 100\, kg\, m^2 \\
\delta \alpha &= 10\, ppb.
\end{aligned}$$

After determining the surface flux F, we upscaled the emissions to annual Bangladesh emissions E (Tg yr^{-1}) using

$$E = cF\overline{\chi(t+d)}A, \tag{B.4}$$

where the conversion factor c is equal to 8.76e-12 and A is the area of Bangladesh equal to $1.4757x10^{11}$ m^2. The uncertainty for E is determined by

$$\delta E = E\sqrt{\left(\frac{\delta F}{F}\right)^2 + \left(\frac{\delta \chi(t+d)}{\chi(t+d)}\right)^2}. \tag{B.5}$$

B.2 Additional Figures

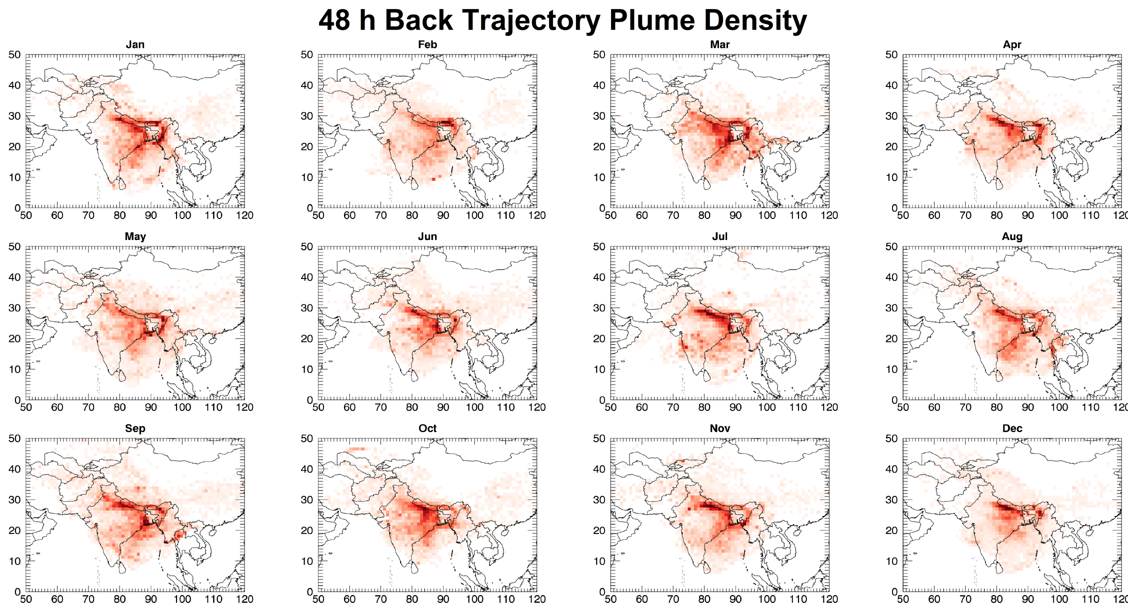

Figure B.1: HYSPLIT back trajectory density at 48h prior to entering Bangladesh.

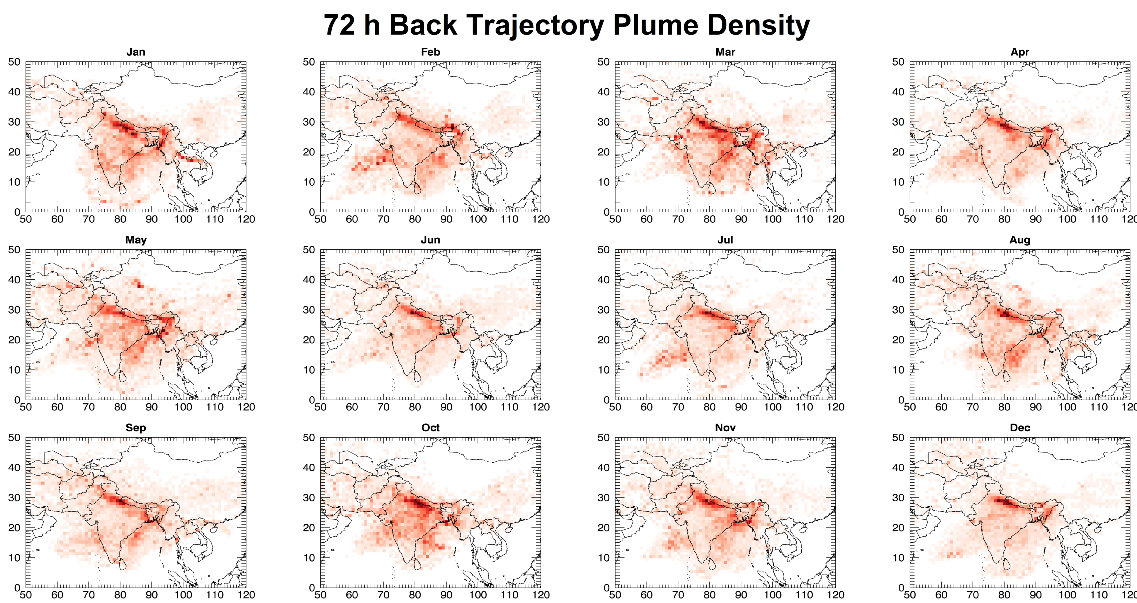

Figure B.2: HYSPLIT back trajectory density at 72h prior to entering Bangladesh.

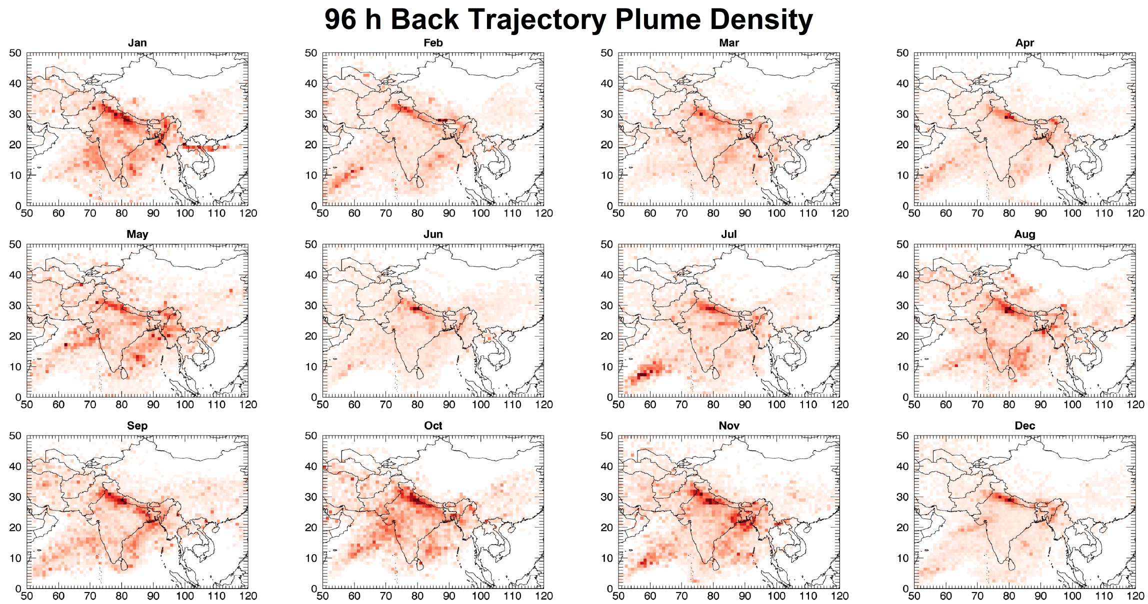

Figure B.3: HYSPLIT back trajectory density at 96h prior to entering Bangladesh.

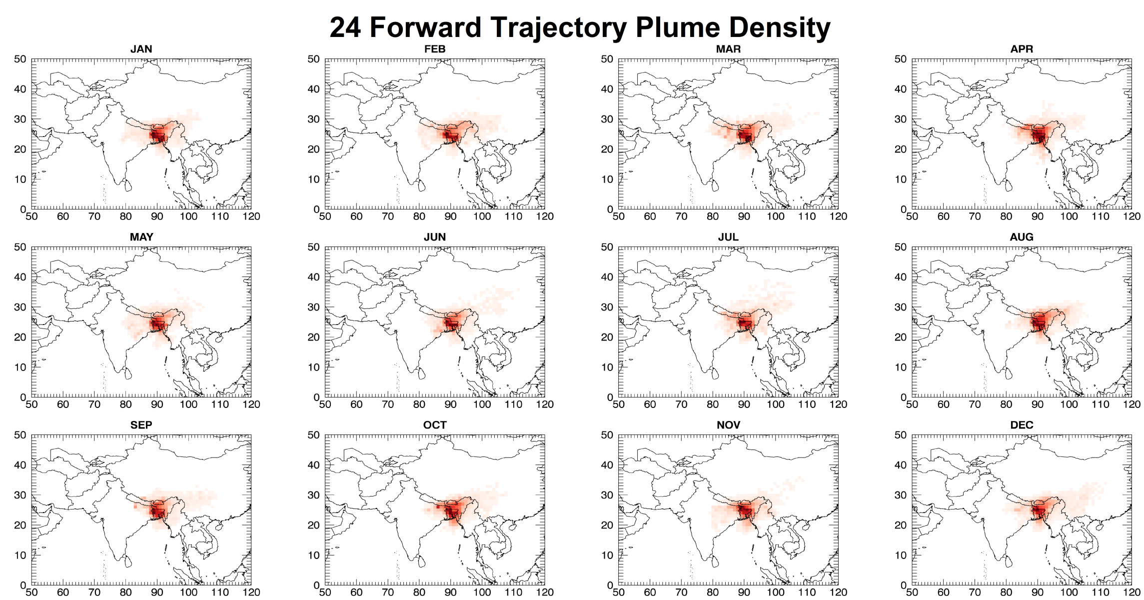

Figure B.4: HYSPLIT forward trajectory density at 24h after entering Bangladesh.

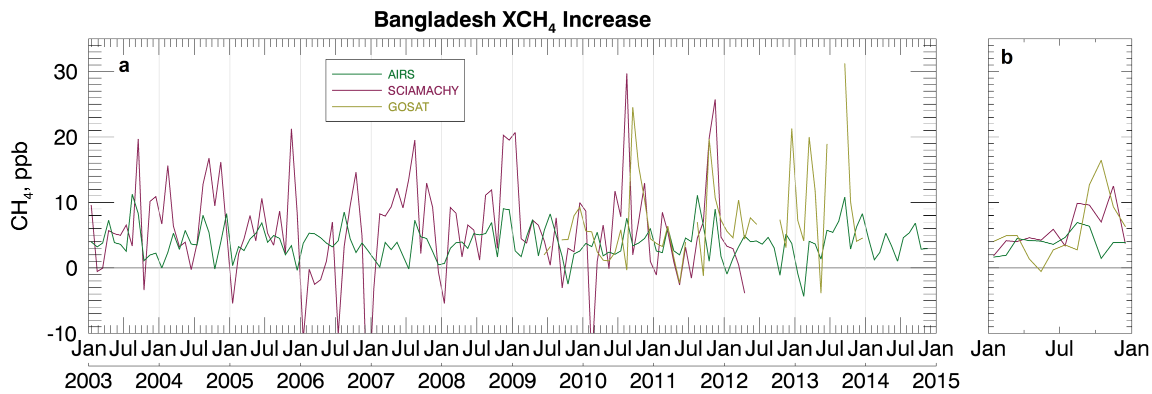

Figure B.5: XCH_4 increases from Bangladesh, calculated by taking the regression of the XCH_4 satellite observations weighted by +/- 24 h trajectory HYSPLIT density plots. Average monthly variations are shown on the right (b).

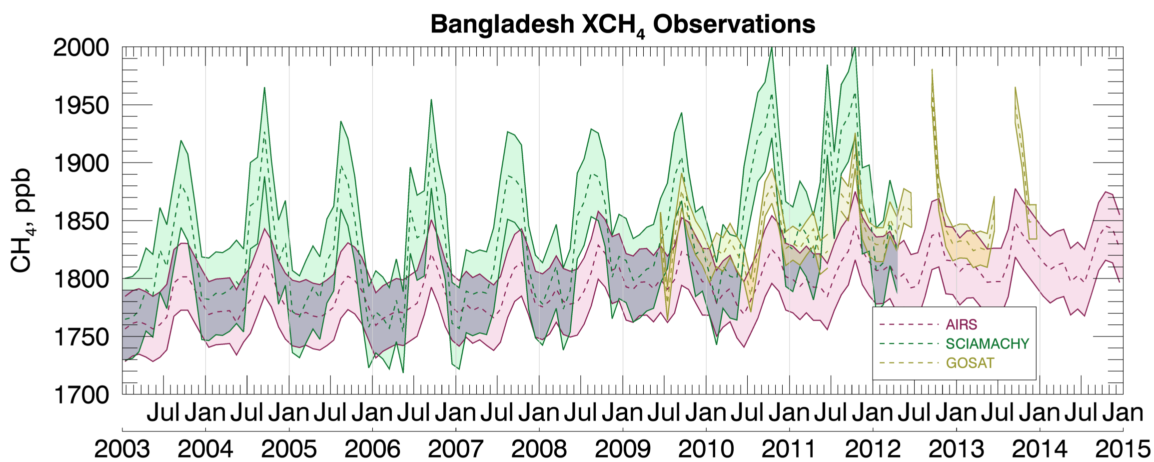

Figure B.6: AIRS, SCIAMACHY, and GOSAT XCH_4 retrievals over Bangladesh with their associated error.

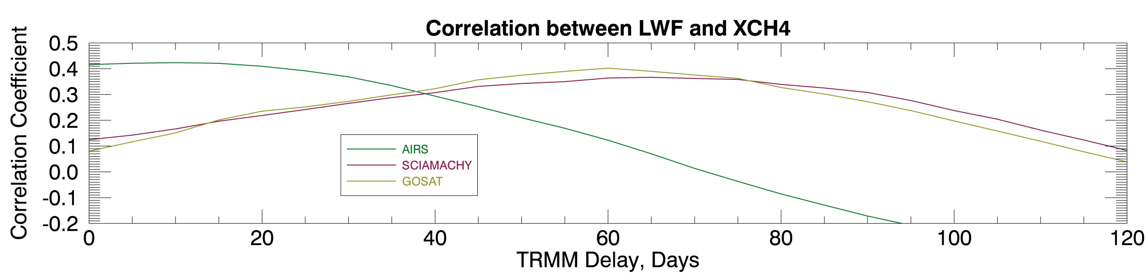

Figure B.7: Correlation coefficients between satellite emissions and land-water fraction shifted by 1 day increments.

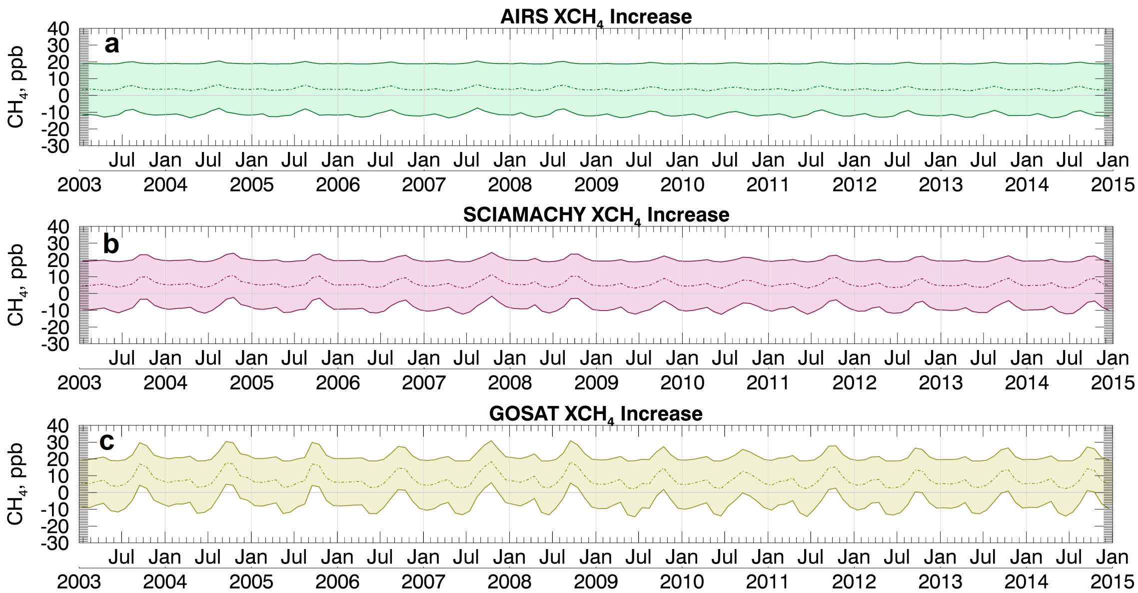

Figure B.8: AIME estimates from each satellite with calculated error as determined from Equation 3.

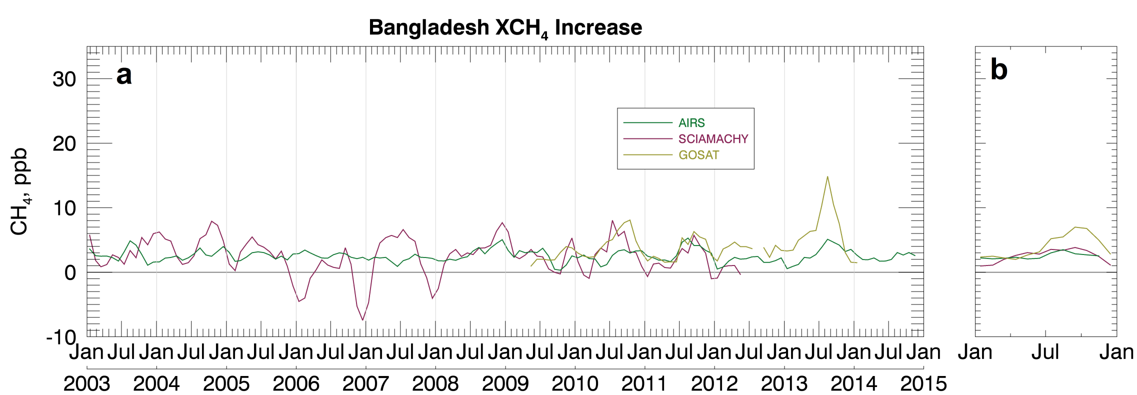

Figure B.9: Three-month moving averaged smoothed XCH_4 increases from Bangladesh, calculated by taking the regression of the XCH_4 satellite observations weighted by +/- 48 h trajectory HYSPLIT density plots. Average monthly variations are shown on the right (b).

Appendix C

MCDA DETAILS AND FIGURES

C.1 Introduction

This supporting information document contains the survey used for stakeholder perceptions, details on datasets, and several figures associated with the MCDA model results.

C.2 Survey

This survey will be used to inform a multicriteria decision model on freshwater drinking water sources and technologies in the poldered region of southwest Bangladesh. The model intends to evaluate the success of different drinking water sources by a ranking of different physical and social criteria.

1. What is your first name? (This will be confidential and will not be shared with unauthorized individuals.)

2. Rank the following drinking water sources/technology. A score of 1 is for the **best option** for polder inhabitants.

_______________ Pond (unfiltered)

_______________ Managed Aquifer Recharge

_______________ Rainwater harvesting

_______________ Pond sand filter

_______________ Tubewell

_______________ Water Treatment Plant

_______________ Purchased water from outside of community

____

3. When choosing the best drinking water source/technology, what is the importance of each of these criteria?

	Extremely Important	Very Important	Moderately Important	Slightly Important	Not at all Important
Cost	○	○	○	○	○
Technical Success	○	○	○	○	○
Social Acceptance	○	○	○	○	○
Environmental Feasibility	○	○	○	○	○

4. How important are these **technical aspects** to the success of the source/technology?

	Extremely Important	Very Important	Moderately Important	Slightly Important	Not at all Important
Temporal variability in water SUPPLY (seasonal/yearly changes in availability	○	○	○	○	○
Temporal vraiability in water QUALITY (seasonal/yearly changes in quality)	○	○	○	○	○
Failure Rate	○	○	○	○	○
Maintenance requirements	○	○	○	○	○
Quality of water	○	○	○	○	○

5. How important are these **social aspects** to the success of the water source/technology?

	Extremely Important	Very Important	Moderately Important	Slightly Important	Not at all Important
Sense of ownership	○	○	○	○	○
Discriminate affection source use	○	○	○	○	○
Misinformation about source	○	○	○	○	○
Job creation related to source	○	○	○	○	○
Number of people served	○	○	○	○	○

6. How important are these **environmental aspects** to the success of the water source/technology?

	Extremely Important	Very Important	Moderately Important	Slightly Important	Not at all Important
Prevalence of source	○	○	○	○	○
Distance to source	○	○	○	○	○
Potential hazard impact (cyclone, inundation)	○	○	○	○	○
Resilience of source	○	○	○	○	○

7. How important are these **economic aspects** to the success of the water source/technology?

	Extremely Important	Very Important	Moderately Important	Slightly Important	Not at all Important
Construction cost	○	○	○	○	○
Maintenance cost	○	○	○	○	○
Transportation cost	○	○	○	○	○
Financial assistance from NGO/government	○	○	○	○	○

8. What **other aspects** should be considered when making decisions about polder water sources?

9. Which source/technology will be **most successful** at providing drinking water to polder residence in the future? Why?

10. Do you believe the answers to the previous questions depend on which **stakeholder** (e.g. local community member, ngo, academic) is answering the question? Why?

C.3 Table and Figures

Table C.1: Data sources and formulas used to calculate scores.

Group	Criteria	Source	Data Used	Formula	Value		Interpretation
Technical	Variability in Supply	Average of number of months used	BEMS, pilot, HH; BEMS; MAR	Average (# of months used)	RWH	5.26	Usage frequency of the source in a given year
					Pond	8.80	
					PSF	10.42	
					MAR	5.00	
					TW	11.37	
	Variability in Quality	Qualitative Interviews	----	----	RWH	5.00	Quality variance due to season or location
					Pond	2.00	
					PSF	4.00	
					MAR	4.00	
					TW	4.00	
	Water Quality	Function of TDS, Salinity, Arsenic, and pathogens	BEMS, pilot, HH; BEMS; MAR	- Sal/Max Sal - TDS/Max TDS - 0.5 (for Arsenic if TW) - 0.5 (for Pathogens if SW) - 0.5 (if perceived as salty); (if no salinity or TDS data is available, use the average value for TW)	RWH	-0.03	Quality of water sources
					Pond	-0.60	
					PSF	-0.14	
					MAR	-0.36	
					TW	-0.64	
	Maintenance Requirements	Qualitative Interviews	----	----	RWH	4.00	Time and effort required for regular maintenance
					Pond	5.00	
					PSF	1.00	
					MAR	1.00	
					TW	4.00	
	Failure Rate	Qualitative Interviews	----	----	RWH	5.00	Frequency of failure
					Pond	4.00	
					PSF	3.00	
					MAR	3.00	
					TW	4.00	
Economic	Construction Cost	*Blanchet*, 2014		Average	RWH	42500	Construction or purchase cost of source
					Pond	410000	
					PSF	50000	
					MAR	600000	
					TW	205000	
	Potential for NGO or Governmental Help	Qualitative Interviews	----	----	RWH	5.00	Likelihood for economic assistance from entity outside of community
					Pond	2.00	
					PSF	5.00	
					MAR	5.00	
					TW	2.00	
	Maintenance Cost	*Blanchet*, 2014		Average	RWH	0.00	Cost of regular maintenance
					Pond	0.00	
					PSF	100.00	
					MAR	3250.00	
					TW	0.00	
	Transportation Cost	Qualitative Interviews	----	----	RWH	0.00	Transportation cost from source to household
					Pond	10.00	
					PSF	0.00	
					MAR	0.00	
					TW	0.00	
Social	Sense of Ownership	Qualitative Interviews	----	----	RWH	5.00	Likelihood that source users feel ownership and responsibility of the source
					Pond	4.00	
					PSF	3.00	
					MAR	2.00	
					TW	4.00	
	Discrimination	Qualitative Interviews	----	----	RWH	3.00	Likelihood of discrimination in source usage based on economic status, gender, and relative location to source
					Pond	5.00	
					PSF	4.00	
					MAR	3.00	
					TW	4.00	
	Misinformation	Qualitative Interviews	----	----	RWH	4.00	Likelihood that source users are misinformed about ownership, quality, and function of source
					Pond	4.00	
					PSF	3.00	
					MAR	1.00	
					TW	3.00	
	Persons Served	Average of how many people use the source	Data = range of number of people using the source	Sum (Mean (Range of people using the source))/Total number of each source	RWH	6.00	Number of users source can serve
					Pond	708.00	
					PSF	712.00	
					MAR	300.00	
					TW	83.00	
	Job Creation	Qualitative Interviews	----	----	RWH	1.00	Likelihood of job creation for local community member due to source
					Pond	2.00	
					PSF	2.00	
					MAR	2.00	
					TW	2.00	
Environmental	Prevalence of Source	Number of each used for drinking water in Khulna District	MAR, BEMS; MAR-salinity; BEMS pilot, HH, Amanda	Number of each source used for drinking water in Khulna district	RWH	187.00	Number of each source currently used in the area
					Pond	110.00	
					PSF	70.00	
					MAR	7.00	
					TW	122.00	
	Distance to Source	Travel time to source	BEMS, pilot, HH	Average travel time to source (minutes)	RWH	1.91	Time need to travel to source
					Pond	5.02	
					PSF	4.72	
					MAR	15.00	
					TW	11.39	
	Hazard Impact	Qualitative Interviews	----	----	RWH	5.00	Likelihood that source will be negatively impacted by an environmental hazard, such as cyclone, flood, or drought
					Pond	1.00	
					PSF	2.00	
					MAR	3.00	
					TW	5.00	
	Resilience	Qualitative Interviews	----	----	RWH	5.00	Likelihood that source can recover from a negative hazard impact
					Pond	2.00	
					PSF	2.00	
					MAR	3.00	
					TW	5.00	

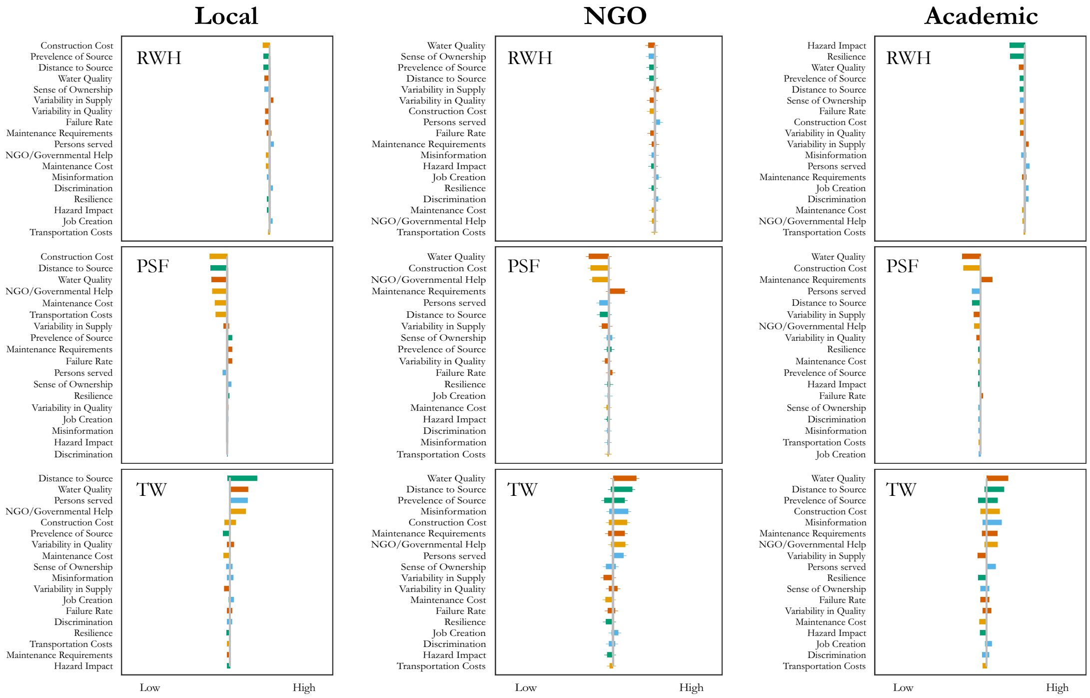

Figure C.1: Tornado diagrams for ELECTRE I OAT simulations for the three stakeholders (Local, NGO, and Academic). The width of the bar represents the possible range (x-axis) of final ranking of the given alternative if that one criteria (y-axis) is varied from its highest and lowest possible values. The color of the bar corresponds to the category of the criteria. The bars are arranged in each subplot from most significant criteria (largest bar) at the top to least significant criteria at the bottom (smallest bar). Note that the significant criteria vary between subplots.

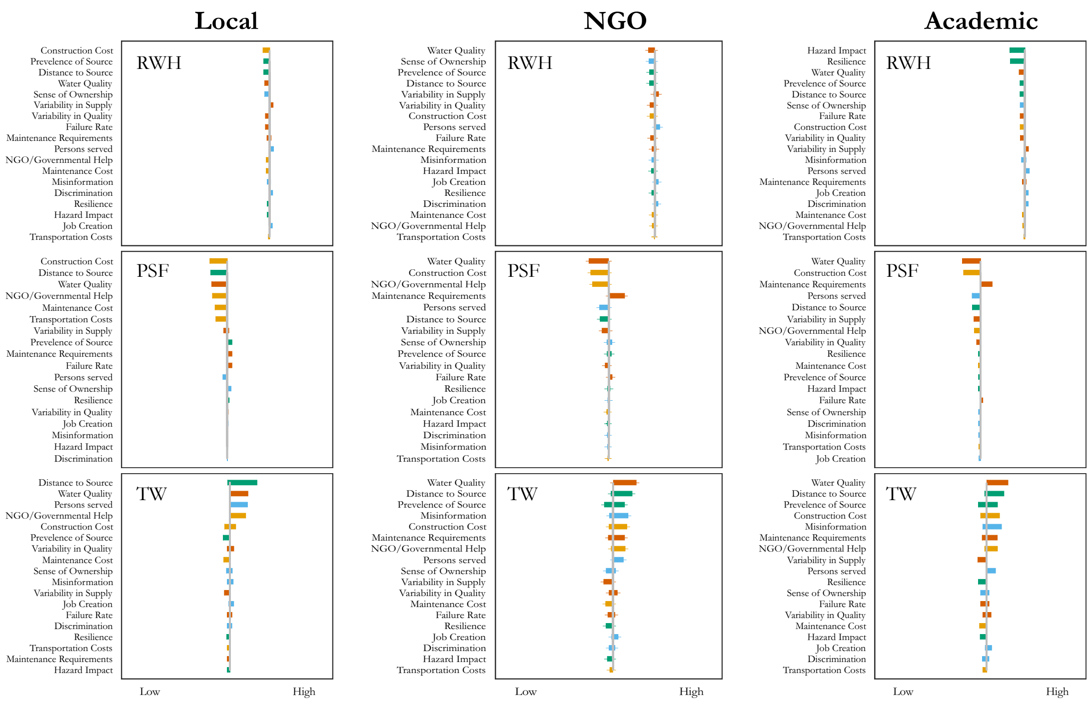

Figure C.2: Tornado diagrams for ELECTRE III OAT simulations for the three stakeholders (Local, NGO, and Academic). The width of the bar represents the possible range (x-axis) of final ranking of the given alternative if that one criteria (y-axis) is varied from its highest and lowest possible values. The color of the bar corresponds to the category of the criteria. The bars are arranged in each subplot from most significant criteria (largest bar) at the top to least significant criteria at the bottom (smallest bar). Note that the significant criteria vary between subplots.

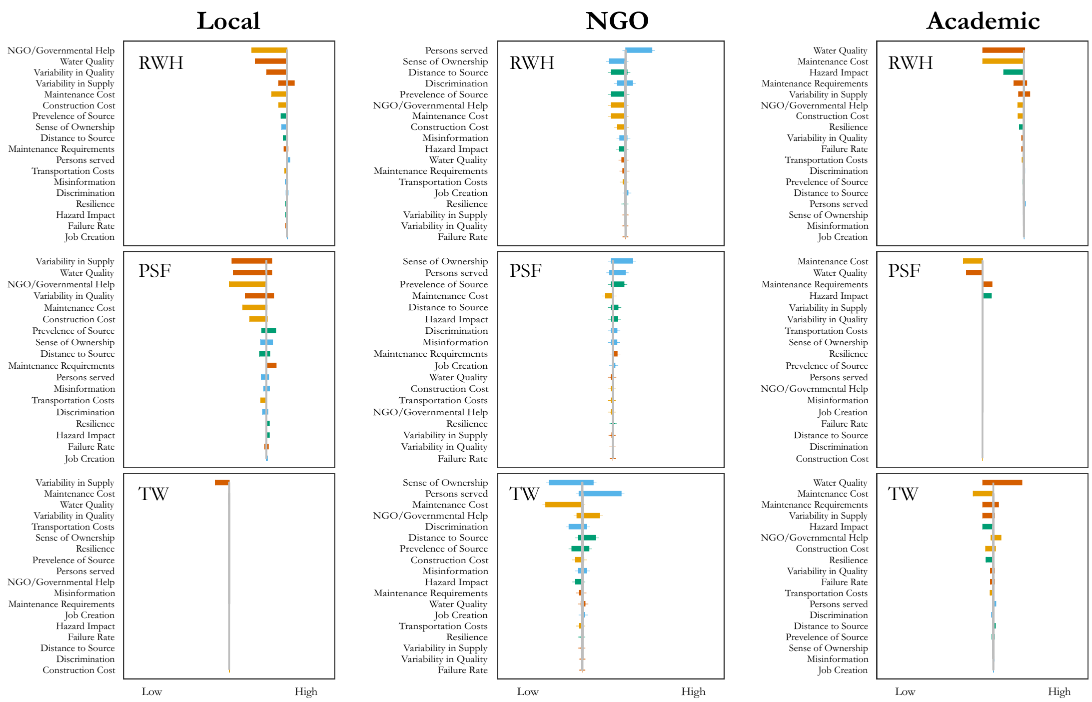

Figure C.3: Tornado diagrams for AHP OAT simulations for the three stakeholders (Local, NGO, and Academic). The width of the bar represents the possible range (x-axis) of final ranking of the given alternative if that one criteria (y-axis) is varied from its highest and lowest possible values. The color of the bar corresponds to the category of the criteria. The bars are arranged in each subplot from most significant criteria (largest bar) at the top to least significant criteria at the bottom (smallest bar). Note that the significant criteria vary between subplots.

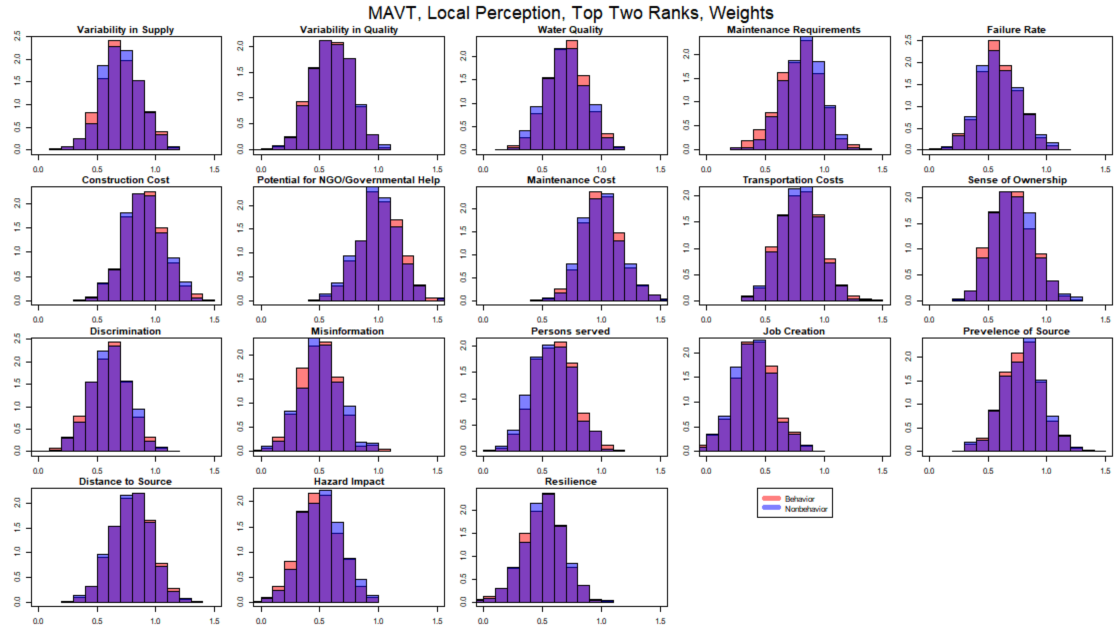

Figure C.4: Distributions of behavior (RWH and PSF are top two ranking alternatives) and nonbehavior (RWH and PSF are not top two ranking alternatives) for **MAVT Local** simulations. The Monte Carlo simulations change the weighting of each criteria by the standard deviation of the **stakeholder weights**.

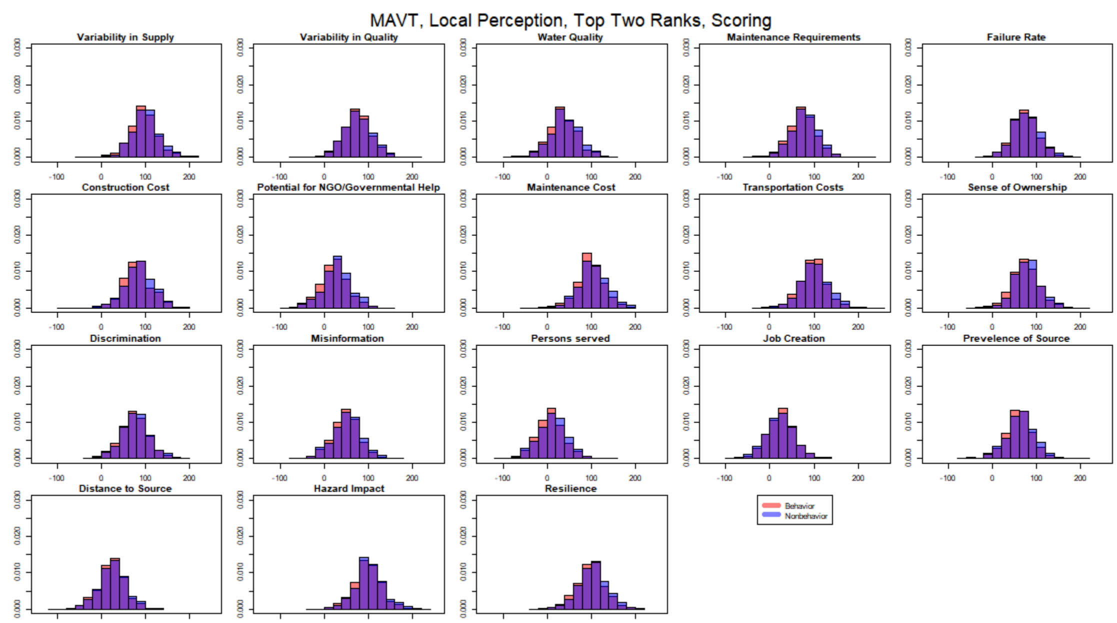

Figure C.5: Distributions of behavior (RWH and PSF are top two ranking alternatives) and nonbehavior (RWH and PSF are not top two ranking alternatives) for **MAVT Local**. The Monte Carlo simulations change the scoring of each criteria by the standard deviation of that **criteria score**.

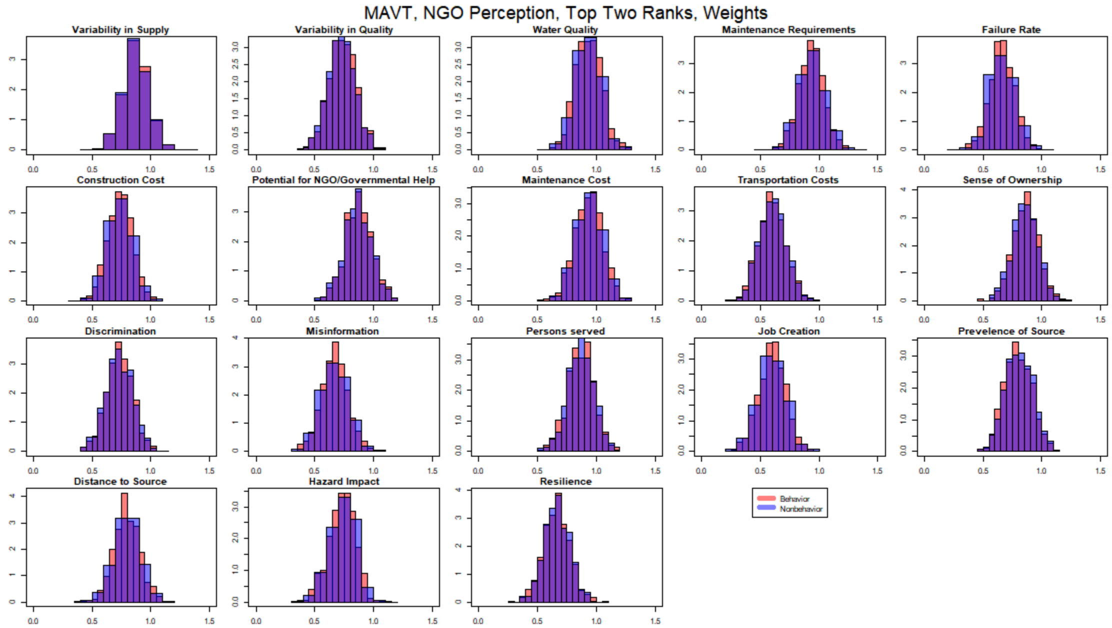

Figure C.6: Distributions of behavior (RWH and PSF are top two ranking alternatives) and nonbehavior (RWH and PSF are not top two ranking alternatives) for **MAVT NGO** simulations. The Monte Carlo simulations change the weighting of each criteria by the standard deviation of the **stakeholder weights**.

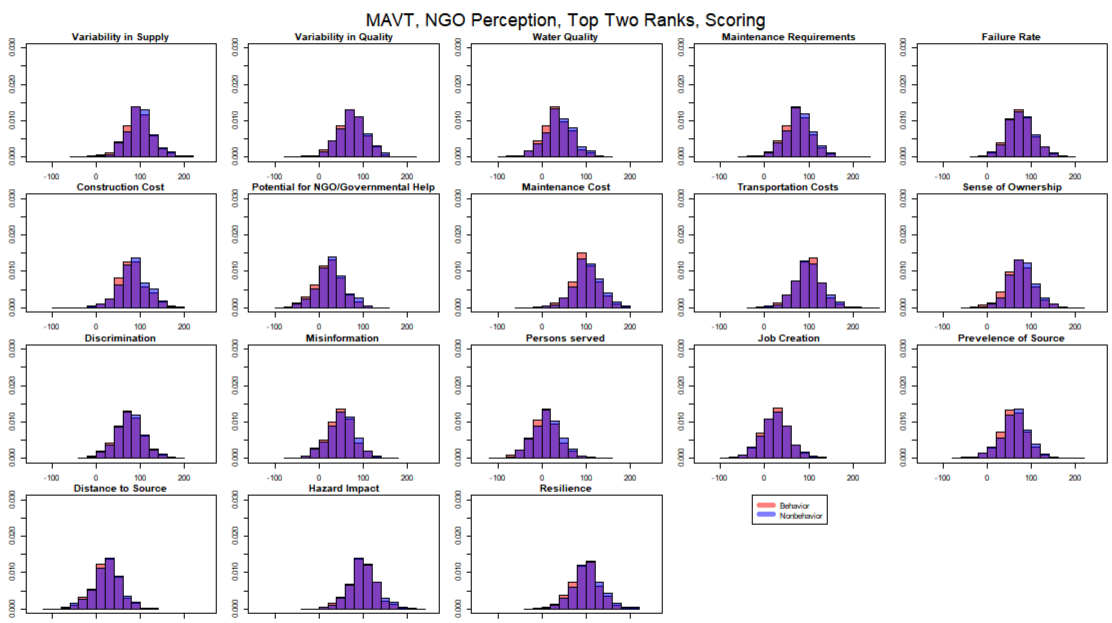

Figure C.7: Distributions of behavior (RWH and PSF are top two ranking alternatives) and nonbehavior (RWH and PSF are not top two ranking alternatives) for **MAVT NGO**. The Monte Carlo simulations change the scoring of each criteria by the standard deviation of that **criteria score**.

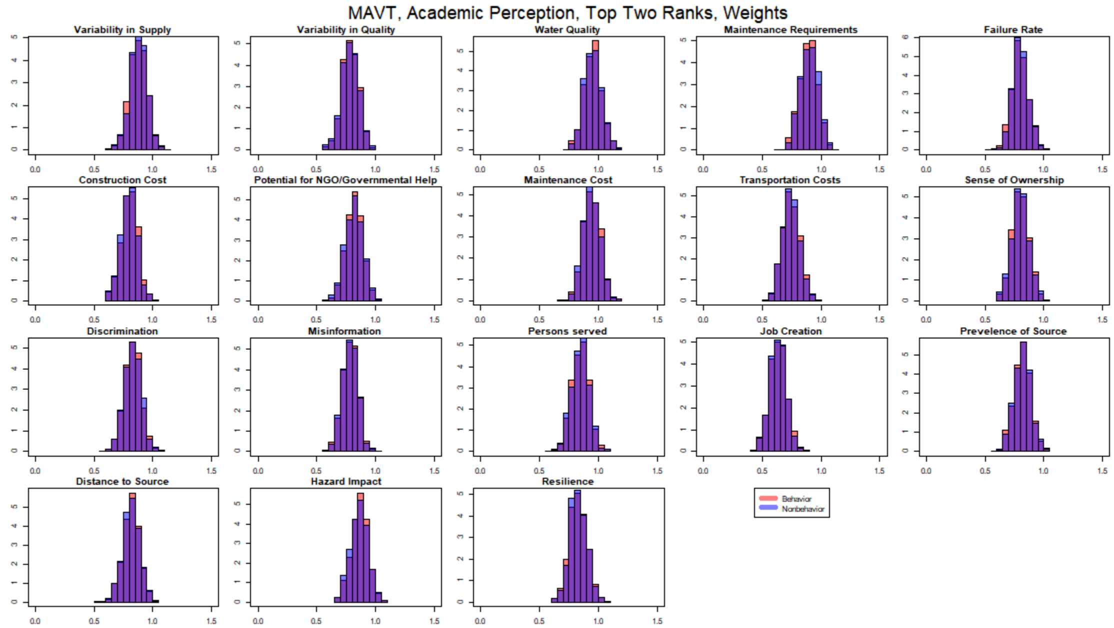

Figure C.8: Distributions of behavior (RWH and PSF are top two ranking alternatives) and nonbehavior (RWH and PSF are not top two ranking alternatives) for **MAVT Academic** simulations. The Monte Carlo simulations change the weighting of each criteria by the standard deviation of the **stakeholder weights**.

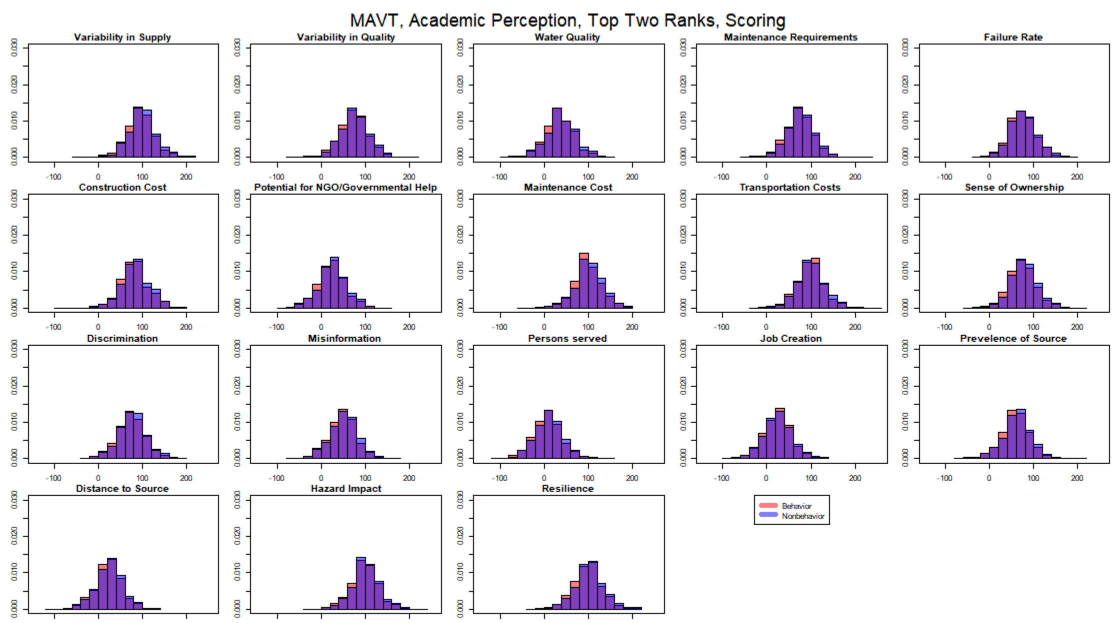

Figure C.9: Distributions of behavior (RWH and PSF are top two ranking alternatives) and nonbehavior (RWH and PSF are not top two ranking alternatives) for **MAVT Academic**. The Monte Carlo simulations change the scoring of each criteria by the standard deviation of that **criteria score**.

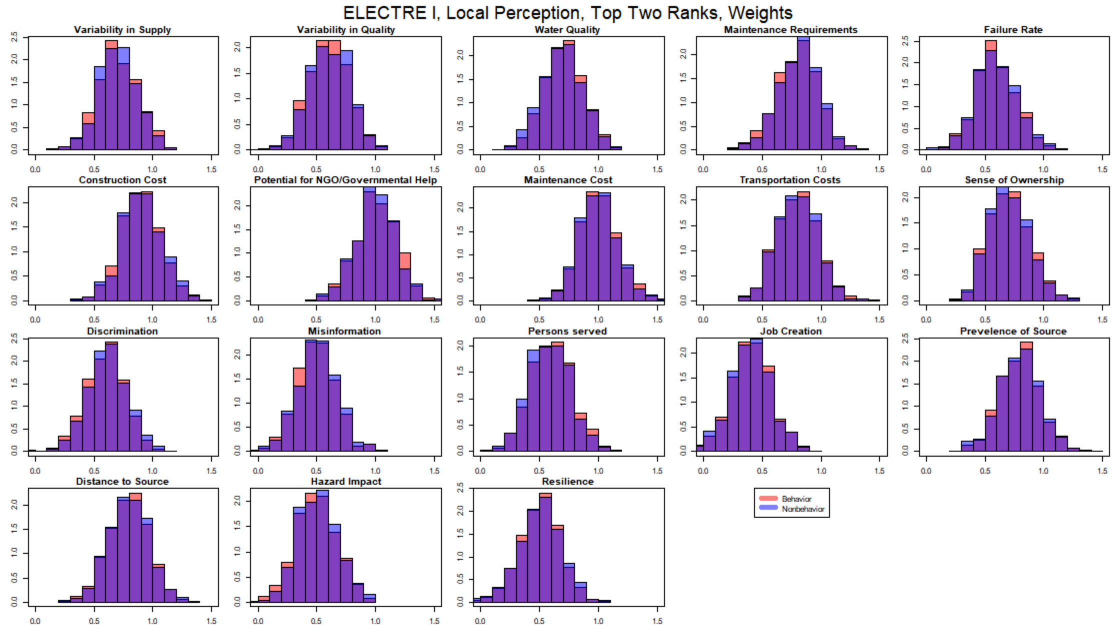

Figure C.10: Distributions of behavior (RWH and PSF are top two ranking alternatives) and nonbehavior (RWH and PSF are not top two ranking alternatives) for **ELECTRE I Local** simulations. The Monte Carlo simulations change the weighting of each criteria by the standard deviation of the **stakeholder weights**.

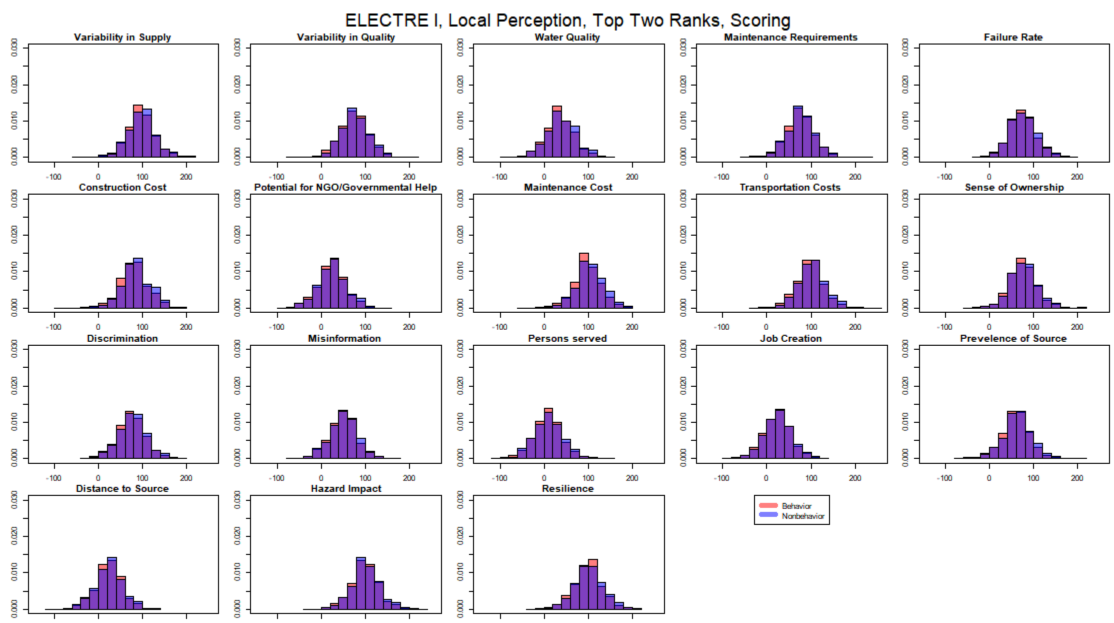

Figure C.11: Distributions of behavior (RWH and PSF are top two ranking alternatives) and nonbehavior (RWH and PSF are not top two ranking alternatives) for **ELECTRE I Local**. The Monte Carlo simulations change the scoring of each criteria by the standard deviation of that **criteria score**.

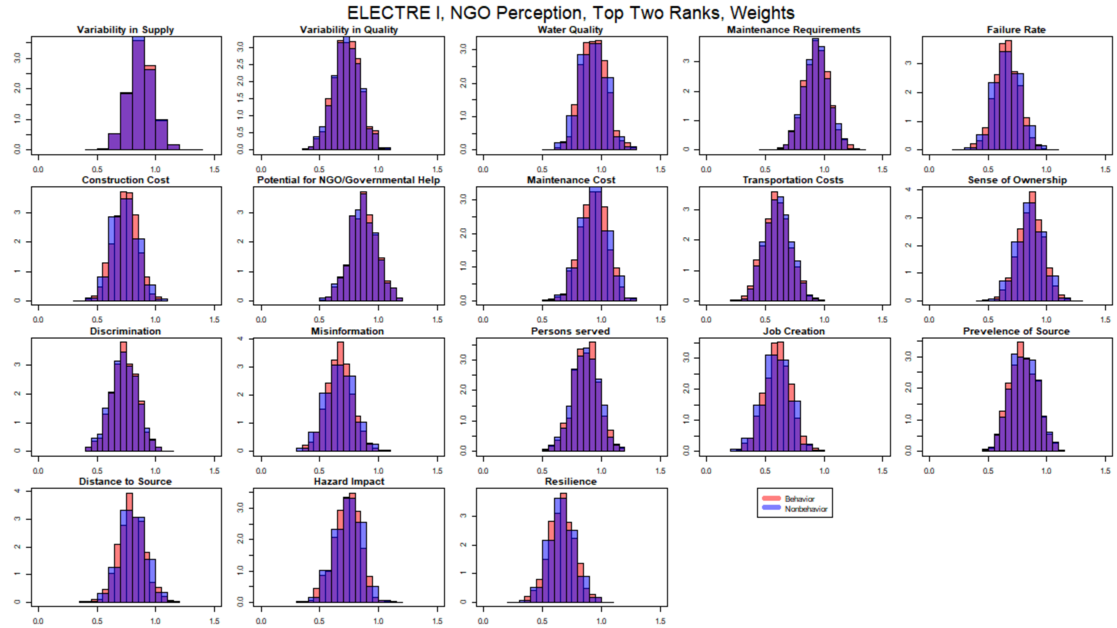

Figure C.12: Distributions of behavior (RWH and PSF are top two ranking alternatives) and nonbehavior (RWH and PSF are not top two ranking alternatives) for **ELECTRE I NGO**. The Monte Carlo simulations change the weighting of each criteria by the standard deviation of the **stakeholder weights**.

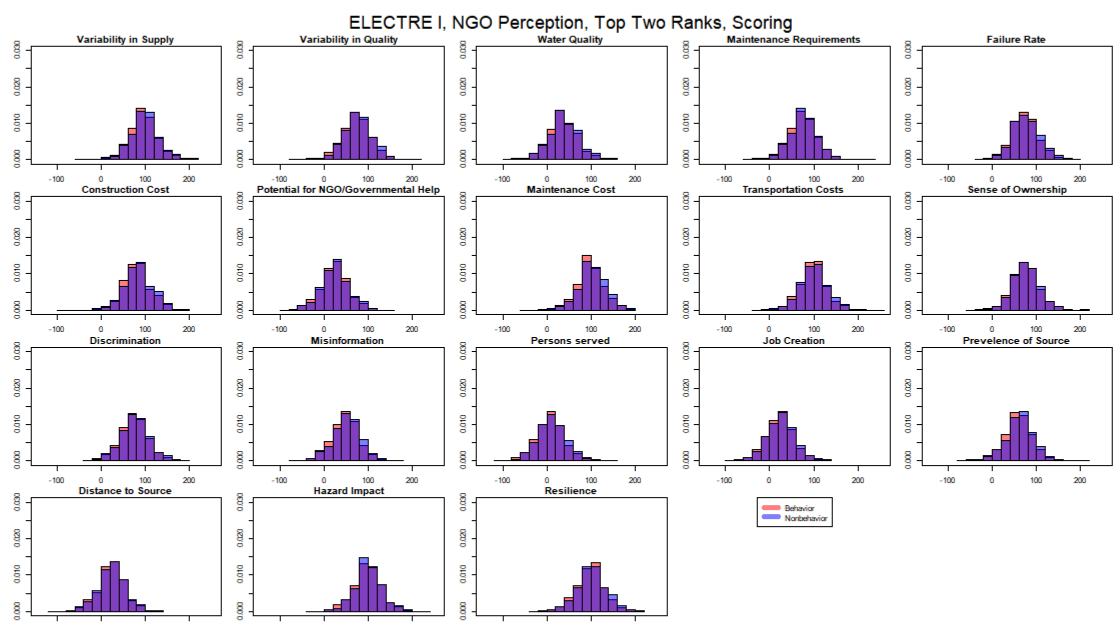

Figure C.13: Distributions of behavior (RWH and PSF are top two ranking alternatives) and nonbehavior (RWH and PSF are not top two ranking alternatives) for **ELECTRE I NGO**. The Monte Carlo simulations change the scoring of each criteria by the standard deviation of that **criteria score**.

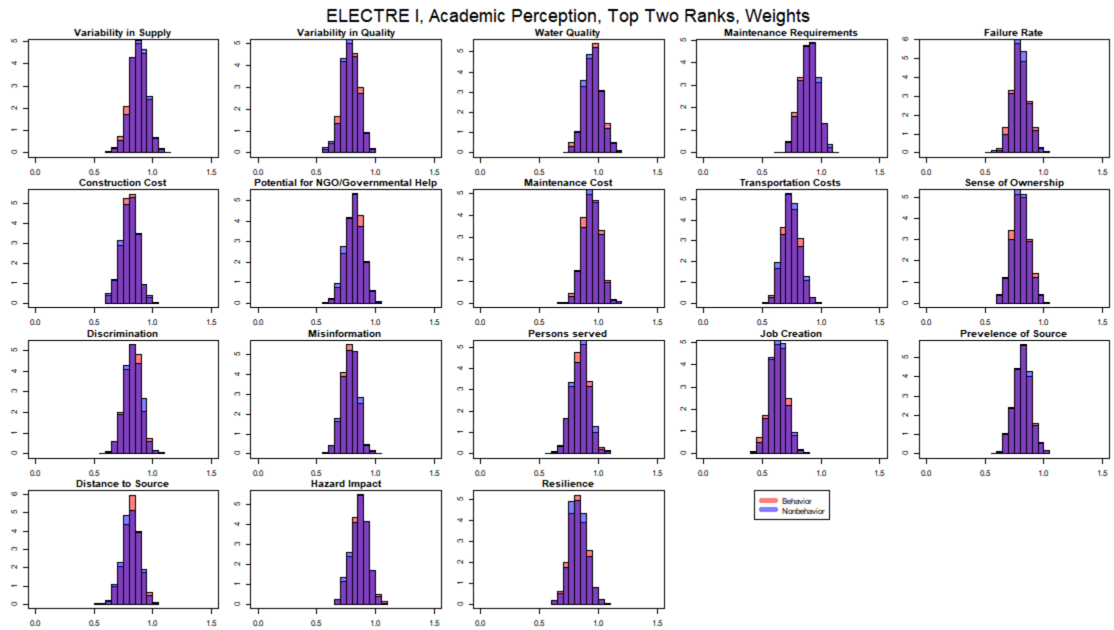

Figure C.14: Distributions of behavior (RWH and PSF are top two ranking alternatives) and nonbehavior (RWH and PSF are not top two ranking alternatives) for **ELECTRE I Academic**. The Monte Carlo simulations change the weighting of each criteria by the standard deviation of the **stakeholder weights**.

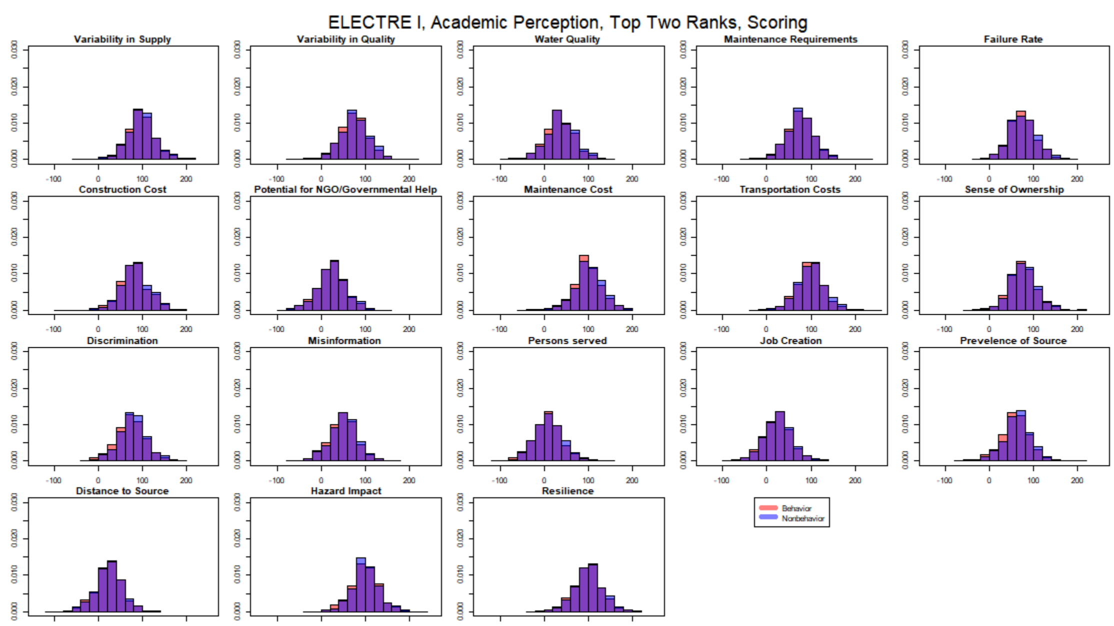

Figure C.15: Distributions of behavior (RWH and PSF are top two ranking alternatives) and nonbehavior (RWH and PSF are not top two ranking alternatives) for **ELECTRE I Academic**. The Monte Carlo simulations change the scoring of each criteria by the standard deviation of that **criteria score**.

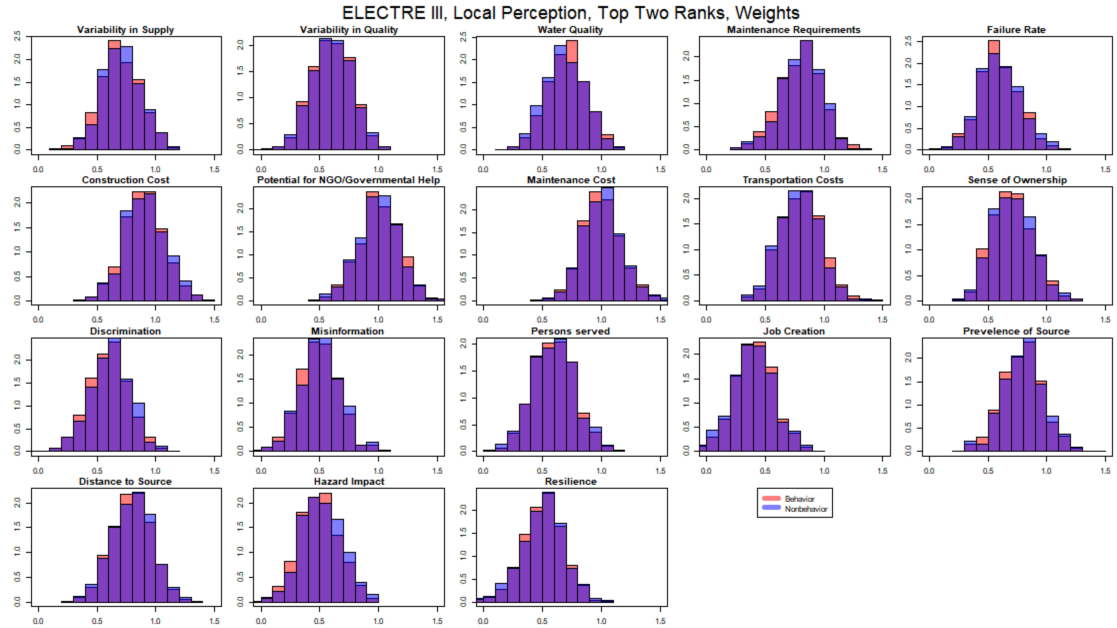

Figure C.16: Distributions of behavior (RWH and PSF are top two ranking alternatives) and nonbehavior (RWH and PSF are not top two ranking alternatives) for **ELECTRE III Local**. The Monte Carlo simulations change the weighting of each criteria by the standard deviation of the **stakeholder weights**.

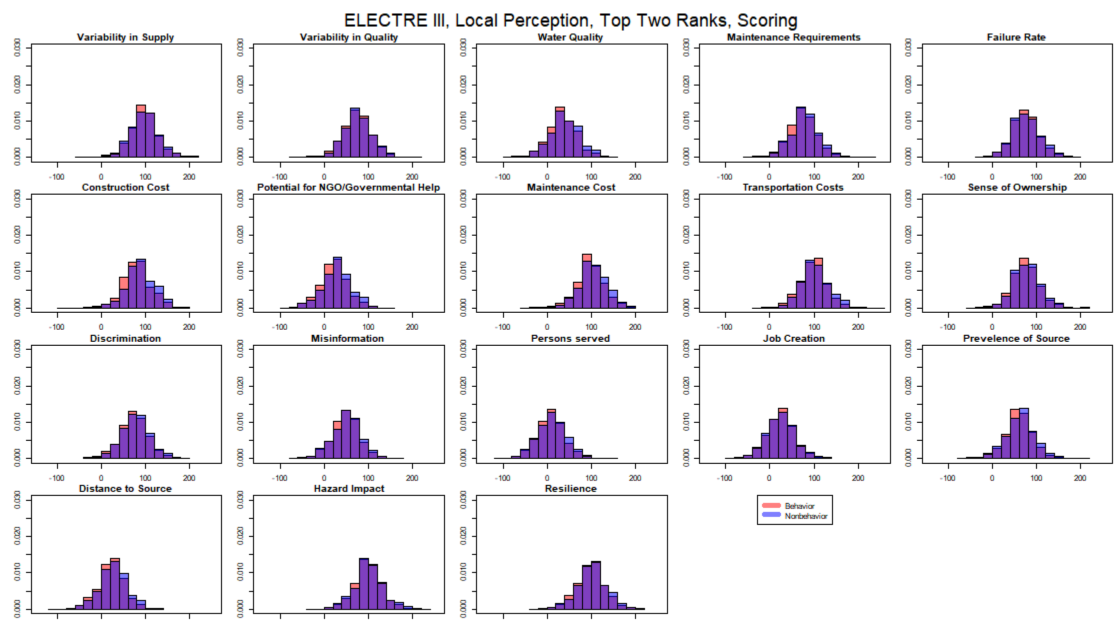

Figure C.17: Distributions of behavior (RWH and PSF are top two ranking alternatives) and nonbehavior (RWH and PSF are not top two ranking alternatives) for **ELECTRE III Local**. The Monte Carlo simulations change the scoring of each criteria by the standard deviation of that **criteria score**.

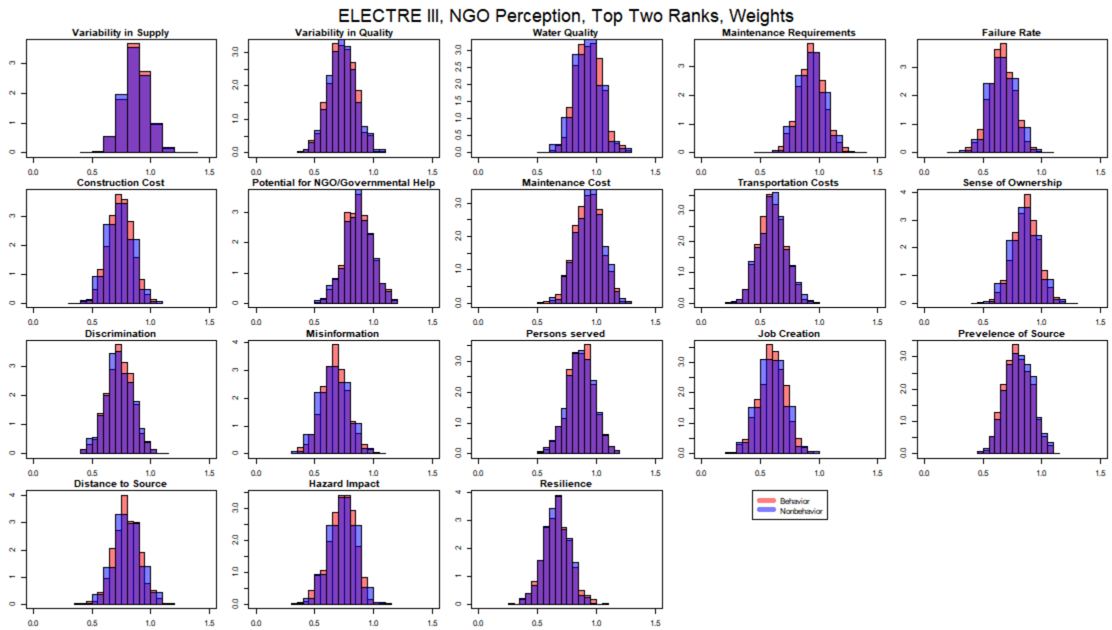

Figure C.18: Distributions of behavior (RWH and PSF are top two ranking alternatives) and nonbehavior (RWH and PSF are not top two ranking alternatives) for **ELECTRE III NGO**. The Monte Carlo simulations change the weighting of each criteria by the standard deviation of the **stakeholder weights**.

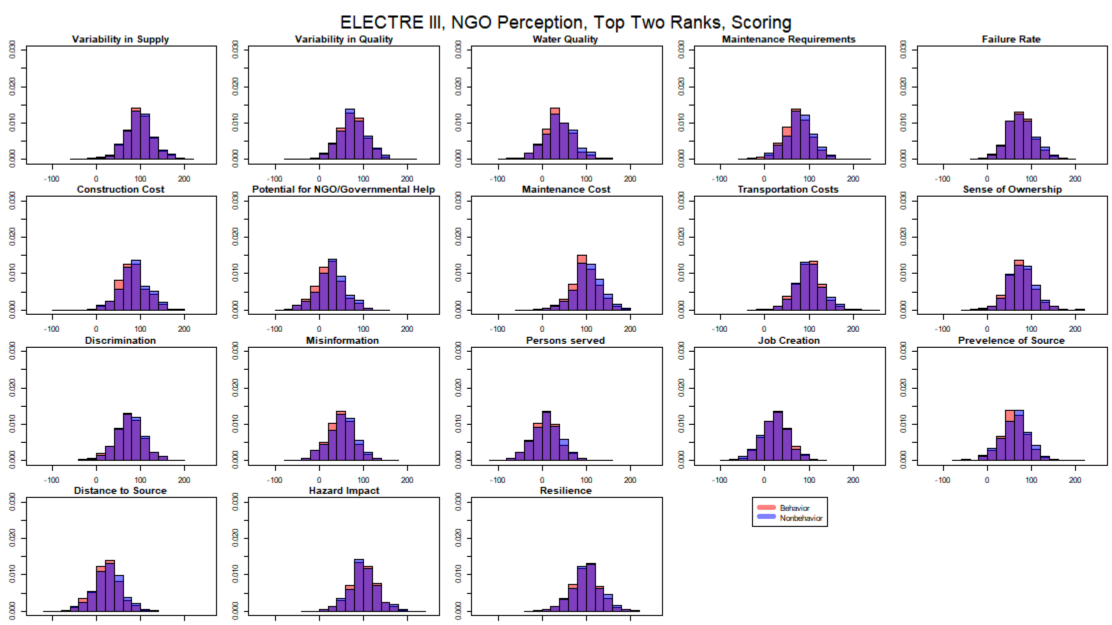

Figure C.19: Distributions of behavior (RWH and PSF are top two ranking alternatives) and nonbehavior (RWH and PSF are not top two ranking alternatives) for **ELECTRE III NGO**. The Monte Carlo simulations change the scoring of each criteria by the standard deviation of that **criteria score**.

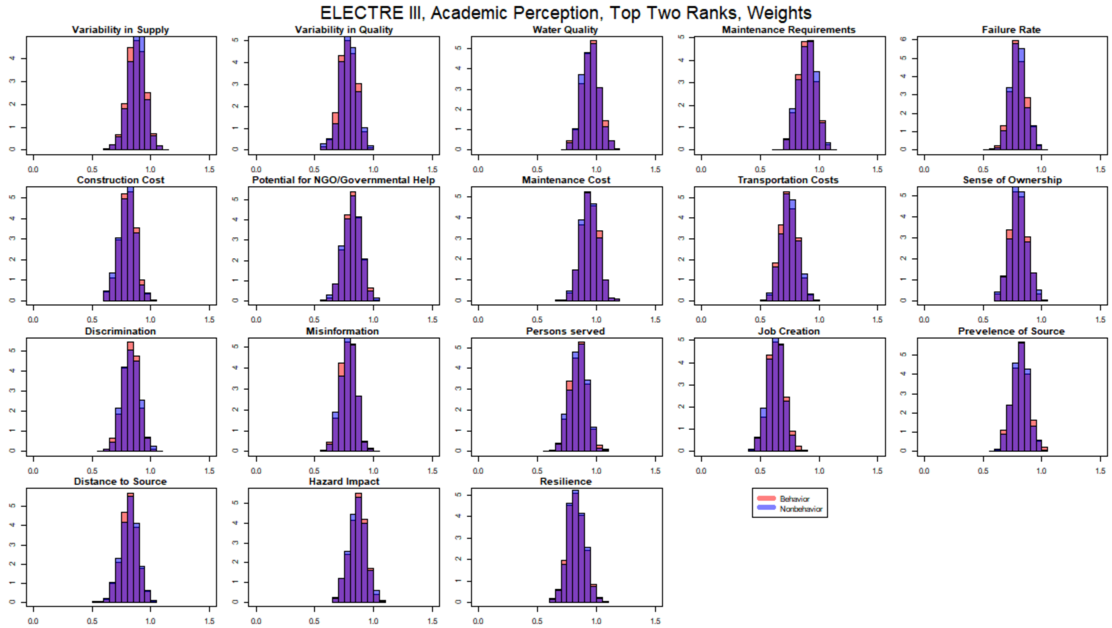

Figure C.20: Distributions of behavior (RWH and PSF are top two ranking alternatives) and nonbehavior (RWH and PSF are not top two ranking alternatives) for **ELECTRE III Academic**. The Monte Carlo simulations change the weighting of each criteria by the standard deviation of the **stakeholder weights**.

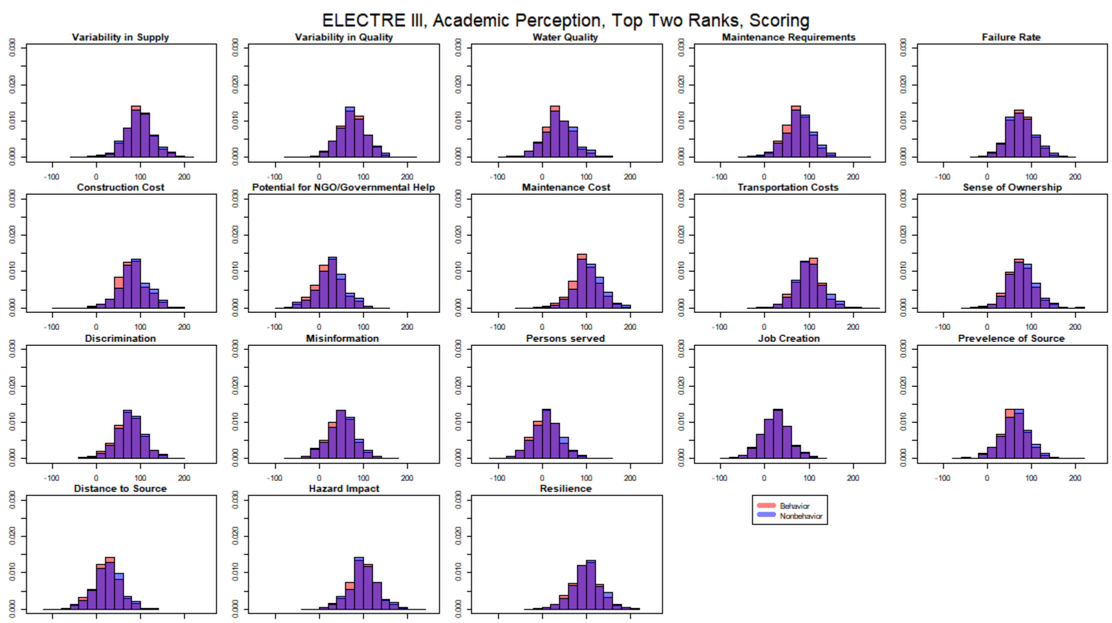

Figure C.21: Distributions of behavior (RWH and PSF are top two ranking alternatives) and nonbehavior (RWH and PSF are not top two ranking alternatives) for **ELECTRE III Academic**. The Monte Carlo simulations change the scoring of each criteria by the standard deviation of that **criteria score**.

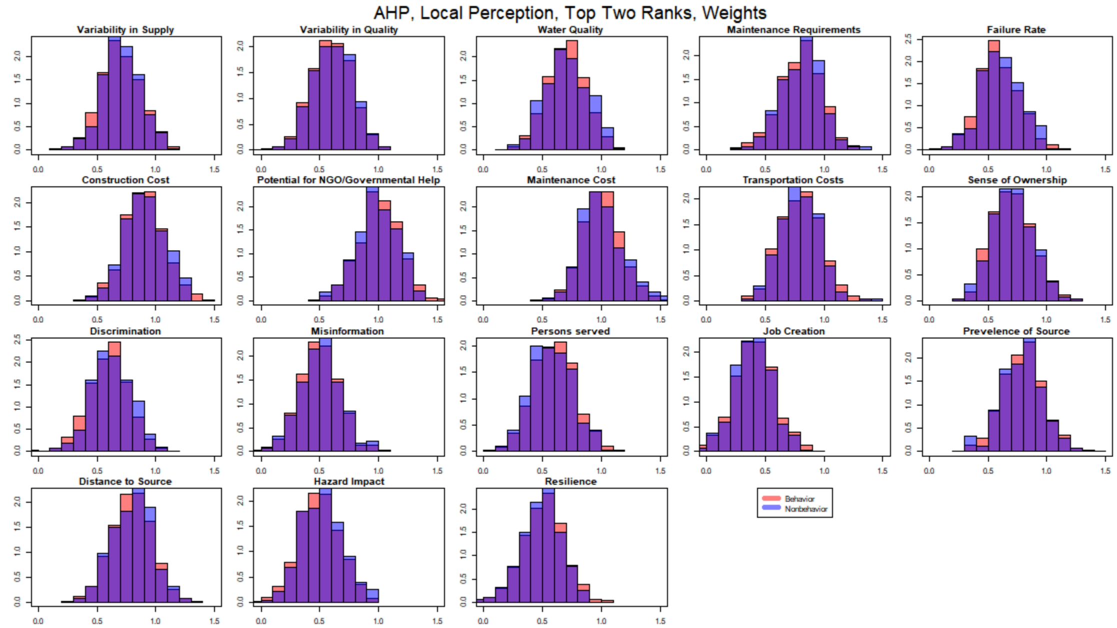

Figure C.22: Distributions of behavior (RWH and PSF are top two ranking alternatives) and nonbehavior (RWH and PSF are not top two ranking alternatives) for **AHP Local** simulations. The Monte Carlo simulations change the weighting of each criteria by the standard deviation of the **stakeholder weights**.

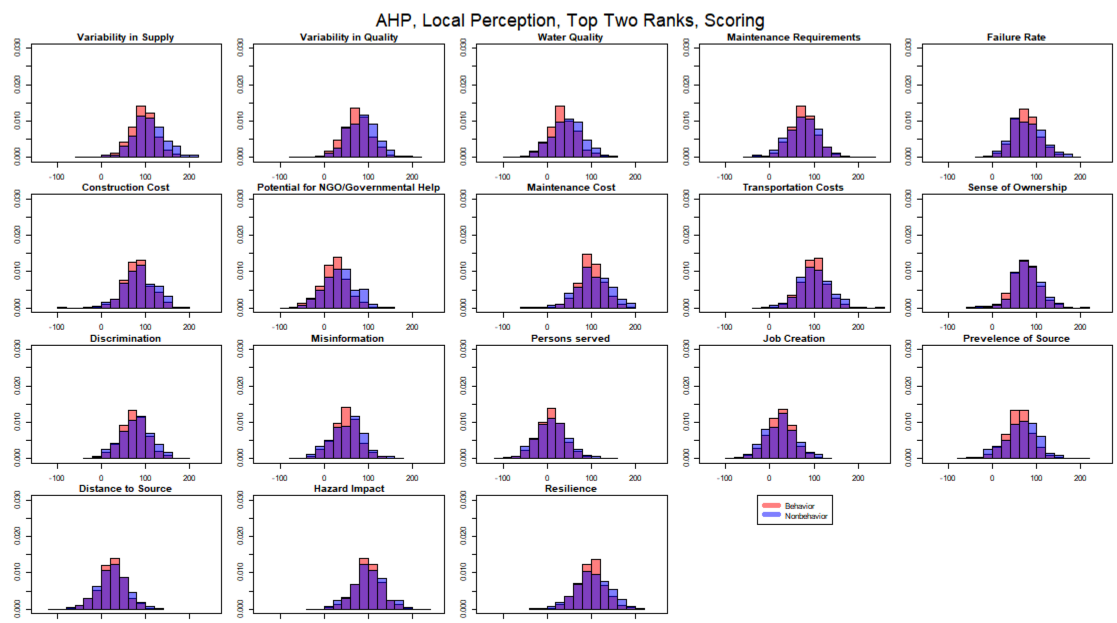

Figure C.23: Distributions of behavior (RWH and PSF are top two ranking alternatives) and nonbehavior (RWH and PSF are not top two ranking alternatives) for **AHP Local**. The Monte Carlo simulations change the scoring of each criteria by the standard deviation of that **criteria score**.

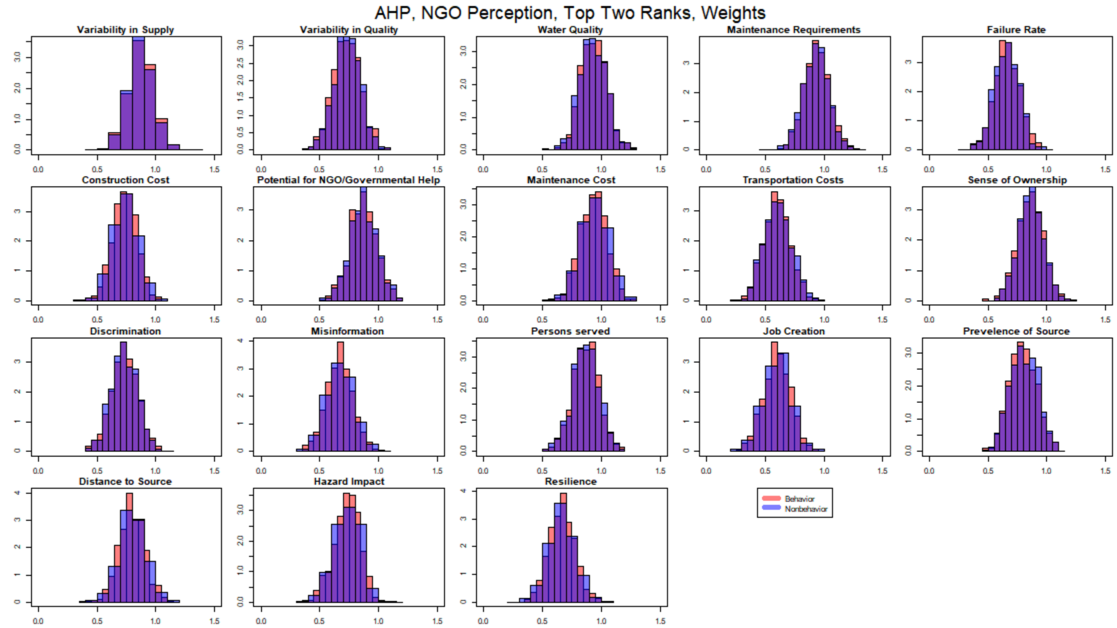

Figure C.24: Distributions of behavior (RWH and PSF are top two ranking alternatives) and nonbehavior (RWH and PSF are not top two ranking alternatives) for **AHP NGO** simulations. The Monte Carlo simulations change the weighting of each criteria by the standard deviation of the **stakeholder weights**.

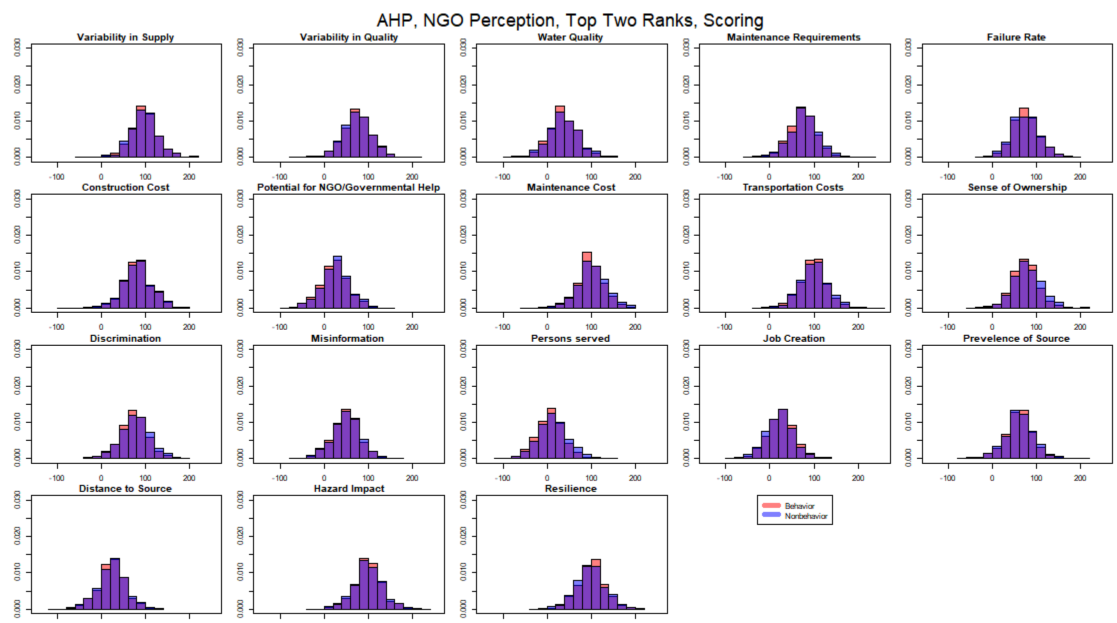

Figure C.25: Distributions of behavior (RWH and PSF are top two ranking alternatives) and nonbehavior (RWH and PSF are not top two ranking alternatives) for **AHP NGO**. The Monte Carlo simulations change the scoring of each criteria by the standard deviation of that **criteria score**.

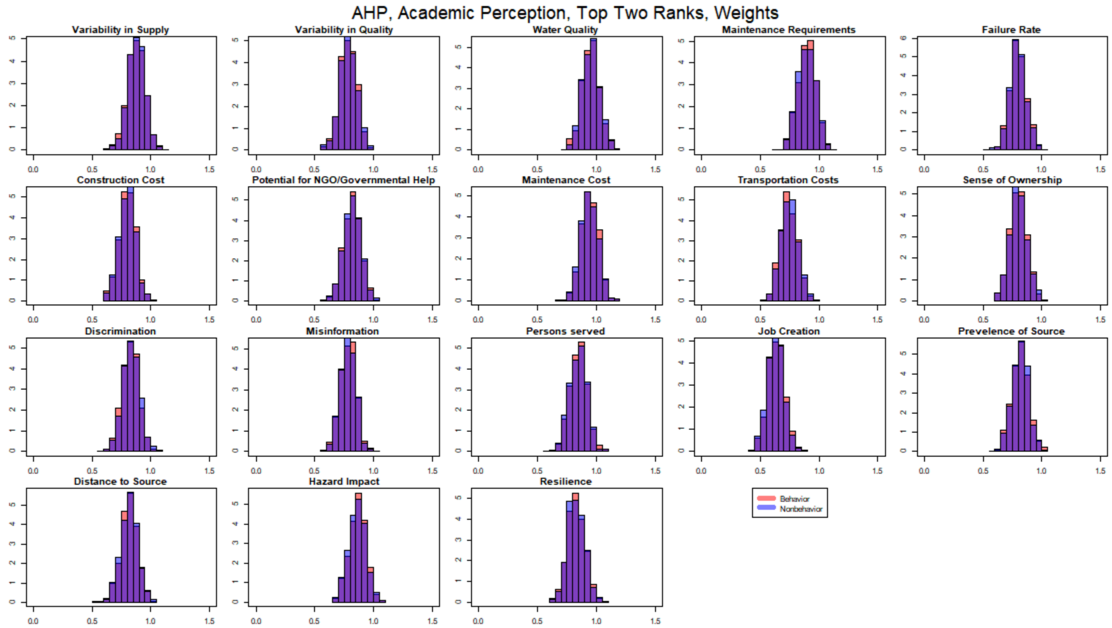

Figure C.26: Distributions of behavior (RWH and PSF are top two ranking alternatives) and nonbehavior (RWH and PSF are not top two ranking alternatives) for **AHP Academic** simulations. The Monte Carlo simulations change the weighting of each criteria by the standard deviation of the **stakeholder weights**.

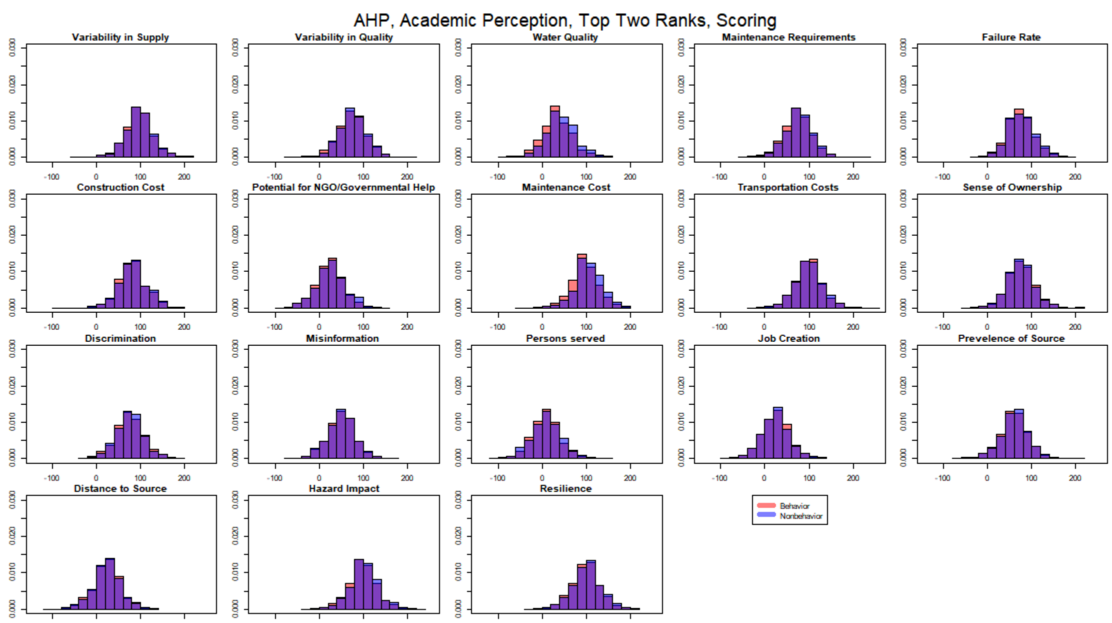

Figure C.27: Distributions of behavior (RWH and PSF are top two ranking alternatives) and nonbehavior (RWH and PSF are not top two ranking alternatives) for **AHP Academic**. The Monte Carlo simulations change the scoring of each criteria by the standard deviation of that **criteria score**.

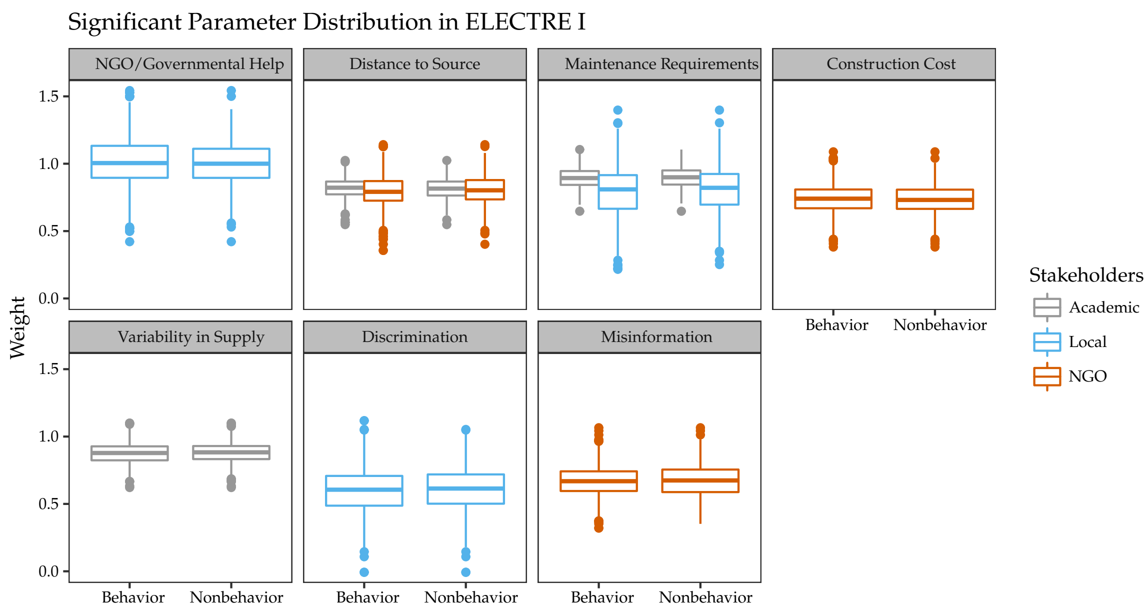

Figure C.28: Distribution of GSA weights w_j for top three most significant criteria (based on **weighting**) in local, NGO, and academic simulations that result in differences between behavior and nonbehavior outcomes in **ELECTRE I**.

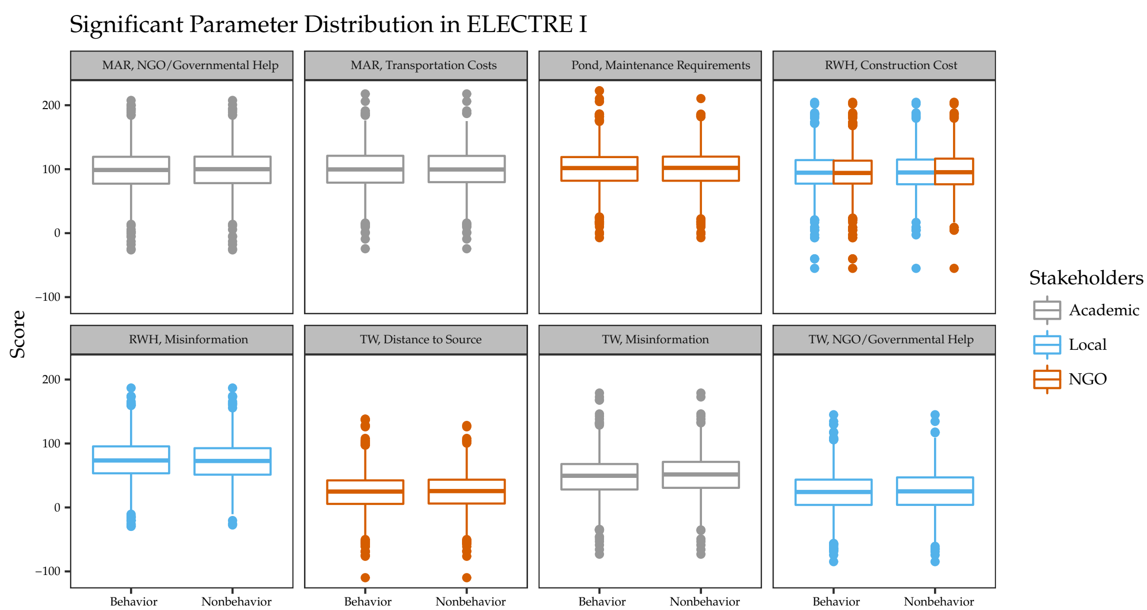

Figure C.29: Distribution of GSA scores $x_{i,j}$ for top three sensitive parameters (based on **scores**) in local, NGO, and academic simulations that result in differences between behavior and nonbehavior outcomes in **ELECTRE I**.

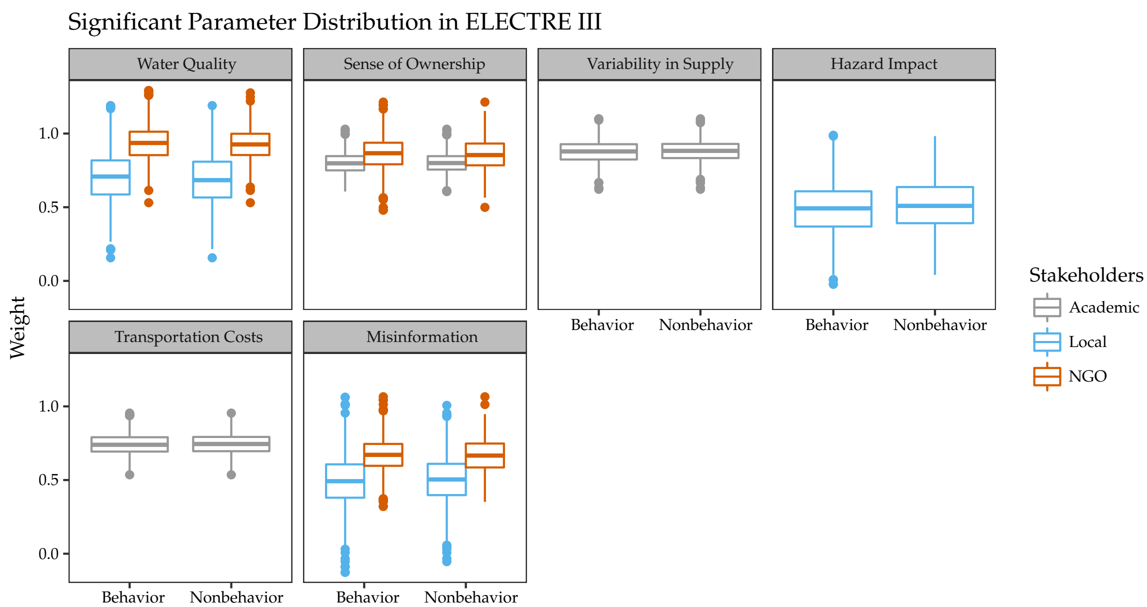

Figure C.30: Distribution of GSA weights w_j for top three most significant criteria (based on weighting) in local, NGO, and academic simulations that result in differences between behavior and nonbehavior outcomes in **ELECTRE III**.

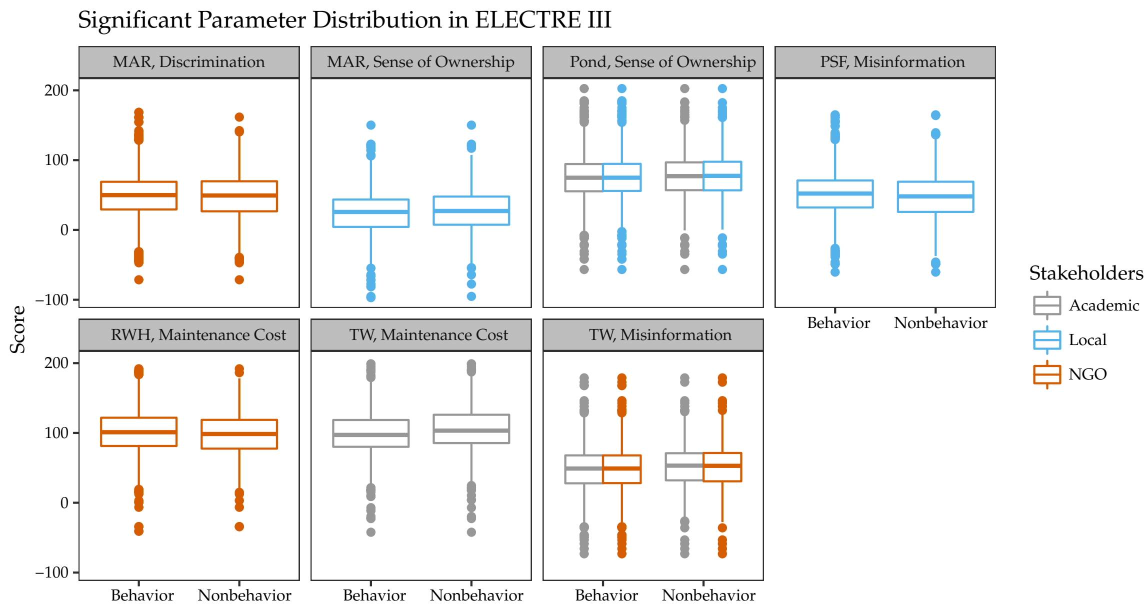

Figure C.31: Distribution of GSA scores $x_{i,j}$ for top three sensitive parameters (based on **scores**) in local, NGO, and academic simulations that result in differences between behavior and nonbehavior outcomes in **ELECTRE III**.

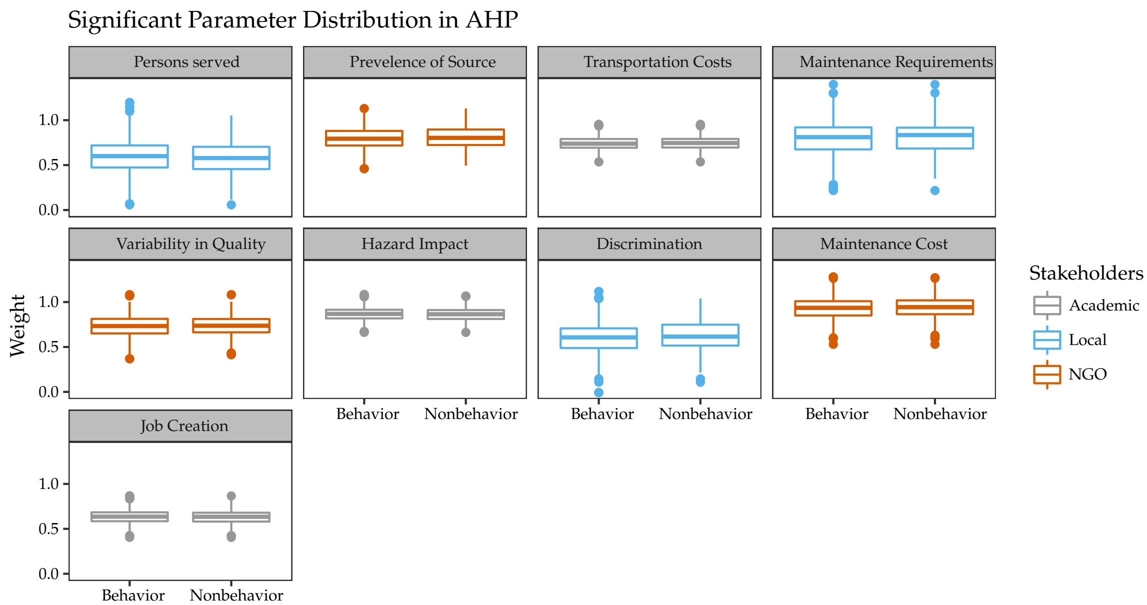

Figure C.32: Distribution of GSA weights w_j for top three most significant criteria in (based on **weighting**) local, NGO, and academic simulations that result in differences between behavior and nonbehavior outcomes in **AHP**.

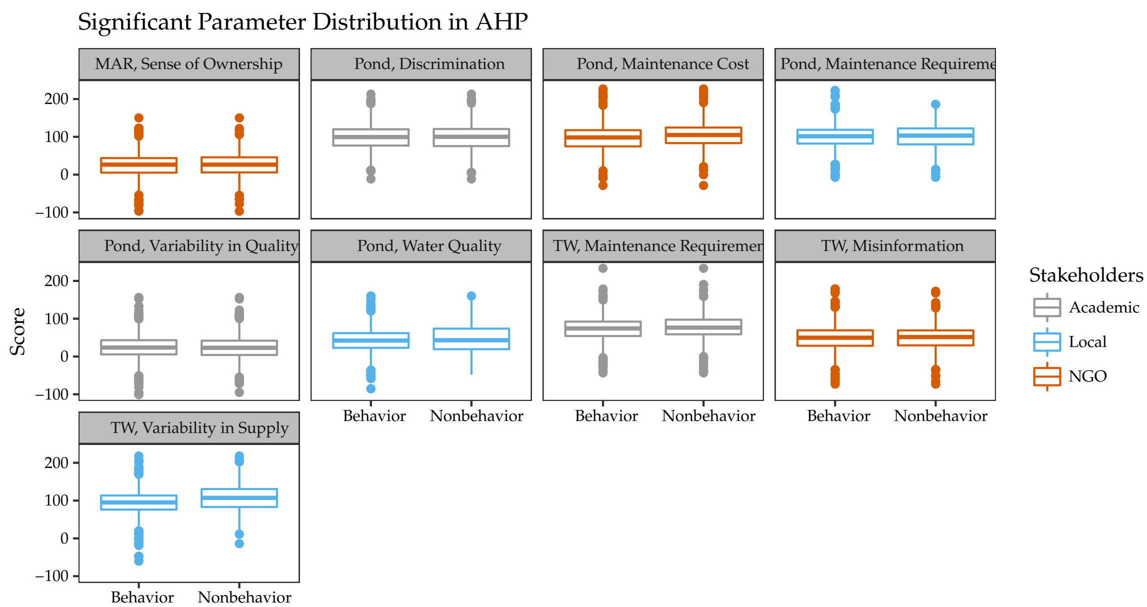

Figure C.33: Distribution of GSA scores $x_{i,j}$ for top three sensitive parameters (based on **scores**) in local, NGO, and academic simulations that result in differences between behavior and nonbehavior outcomes in **AHP**.

Abedin, M. A., U. Habiba, and R. Shaw (2014), Community Perception and Adaptation to Safe Drinking Water Scarcity: Salinity, Arsenic, and Drought Risks in Coastal Bangladesh, *Int. J. Disaster Risk Sci.*, *5*, 110–124, doi:10.1007/s13753-014-0021-6.

Ackerly, B. A., M. M. Anam, and J. Gilligan (2015), Environment, political economies and livelihood change — QUT ePrints, in *Environ. Migr. Adapt. Evid. Polit. Clim. Chang. Bangladesh*, edited by B. Mallick and B. Etzold, AH Development Publishing House (AHDPH), Dhaka, Bangladesh.

Adhya, T. K., K. A. Rath, P. K. Gupta, V. R. Rao, S. N. Das, K. M. Parida, D. C. Parashar, and N. Sethunathan (1994), Methane emission from flooded rice fields under irrigated conditions, *Biol. Fertil. Soils*, *18*, 245–248.

Adhya, T. K., S. R. Mishra, a. K. Rath, K. Bharati, S. R. Mohanty, B. Ramakrishnan, V. R. Rao, and N. Sethunathan (2000), Methane efflux from rice-based cropping systems under humid tropical conditions of eastern India, *Agric. Ecosyst. Environ.*, *79*(1), 85–90, doi:10.1016/S0167-8809(99)00144-9.

Ahmed, M. F., S. Ahuja, M. Alauddin, S. J. Hug, J. R. Lloyd, A. Pfaff, T. Pichler, C. Saltikov, M. Stute, and A. van Geen (2016), Ensuring Safe Drinking Water in Bangladesh, *Science (80-.).*, pp. 1687–1688.

Ahmed, W., T. Gardner, and S. Toze (2011), Microbiological Quality of Roof-Harvested Rainwater and Health Risks: A Review, *J. Enviromental Qual.*, *40*, 1–9, doi:10.2134/jeq2010.0345.

Alam, M., M. Sultana, G. B. Nair, R. B. Sack, D. A. Sack, A. K. Siddique, A. Ali, A. Huq, and R. R. Colwell (2006), Toxigenic Vibrio cholerae in the aquatic environment of Mathbaria, Bangladesh, *Appl. Environ. Microbiol.*, *72*(4), 2849–2855, doi:10.1128/AEM.72.4.2849-2855.2006.

Alam, R., G. Munna, M. A. I. Chowdhury, M. S. K. A. Sarkar, M. Ahmed, M. T. Rahman, F. Jesmin, and M. A. Toimoor (2012), Feasibility study of rainwater harvesting system in Sylhet City, *Environ. Monit. Assess.*, *184*, 573–580, doi:10.1007/s10661-011-1989-7.

Alamgir, M., S. Shahid, M. K. Hazarika, S. Nashrrullah, S. B. Harun, and S. Shamsudin (2015), Analysis of Meteorological Drought Pattern During Different Climatic and Cropping Seasons in Bangladesh, *JAWRA J. Am. Water Resour. Assoc.*, *51*(3), 794–806, doi:10.1111/jawr.12276.

Alber, M. (2012), *And the Tide Comes In...: Exploring a Georgia Salt Marsh (Long Term Ecological Research)*, Taylor Trade Publishing, Lanham, Maryland.

Ali, A. (1996), Vulnerability of Bangladesh to Climate Change and Sea Level Rise through Tropical Cyclones and Storm Surges, in *Clim. Chang. Vulnerability Adapt. Asia Pacific*, pp. 171–179, Springer, Dordrecht, Dordrecht, doi:10.1007/978-94-017-1053-4-16.

Ali, M. A., M. a. Sattar, M. N. Islam, and K. Inubushi (2014), Integrated effects of organic, inorganic and biological amendments on methane emission, soil quality and rice productivity in irrigated paddy ecosystem of Bangladesh: Field study of two consecutive rice growing seasons, *Plant Soil*, *378*(1-2), 239–252, doi:10.1007/s11104-014-2023-y.

Andrews, E., A. Weaver, D. Hanley, J. Shamatha, and G. Melton (2005), Scientists and Public Outreach: Participation, Motivations, and Impediments, *J. Geosci. Educ.*, *53*(3), 281–293.

Ansari, M. S., H. M. N. Islam, and K. Roy (2010), *Functionality and Social Acceptance of Safe Water Technology-Pond Sand Filter and Rainwater Harvesting System in South-West Coastal Region of Bangladesh*, VDM Verlag, Saarbrucken, Germany.

Appleyard, S. (1995), The Impact Of Urban Development On Recharge And Groundwater Quality In A Coastal Aquifer Near Perth, Western Australia, *Hydrogeol. J.*, *3*(2), 65–75, doi:10.1007/s100400050072.

Arguelles, M., N. Bennet, C. Daniels, J. Mee, E. Samper, and S. Ullrich (2016), 2015 Annual Performance Report: UNDP Global Environmental Finance Unit, *Tech. Rep. 2015*, United Nations Development Programme, New York.

Arku, F., S. Omari, B. Adu-Okoree, and A. Abduramane (2015), Harvested rainwater: quality, adequacy, and proximity in Ghanaian rural communities, *Dev. Pract.*, *25*(8), 1160–1169, doi:10.1080/09614524.2015.1081676.

Auerbach, L. W., S. L. Goodbred Jr, D. R. Mondal, C. A. Wilson, K. R. Ahmed, K. Roy, M. S. Steckler, C. Small, J. M. Gilligan, and B. A. Ackerly (2015), Flood risk of natural and embanked landscapes on the GangesBrahmaputra tidal delta plain, *Nat. Clim. Chang.*, *5*(2), 153–157, doi:10.1038/nclimate2472.

Aulakh, M. S., R. Wassmann, and H. Rennenberg (2001), Methane emissions from rice fields- quantification, mechanisms, role of management, and mitigation options, *Adv. Agron.*, *70*, 193–260, doi:10.1016/S0065-2113(01)70006-5.

Ayers, J. C., S. Goodbred, G. George, D. Fry, L. Benneyworth, G. Hornberger, K. Roy, M. R. Karim, and F. Akter (2016), Sources of salinity and arsenic in groundwater in southwest Bangladesh, *Geochem. Trans.*, *17*(4), 1–22, doi:10.1186/s12932-016-0036-6.

Ayers, J. C., G. George, D. Fry, L. Benneyworth, C. Wilson, L. Auerbach, K. Roy, M. R. Karim, F. Akter, and S. Goodbred (2017), Salinization and arsenic contamination of surface water in southwest Bangladesh, *Geochem. Trans.*, *18*(1), 4, doi:10.1186/s12932-017-0042-3.

Bahar, M. M., and M. S. Reza (2010), Hydrochemical characteristics and quality assessment of shallow groundwater in a coastal area of southwest Bangladesh, *Environ. Earth Sci.*, *61*(5), 1065–1073, doi:10.1007/s12665-009-0427-4.

Bangladesh Bureau of Statistics (2009), The yearbook of Agriculture Statistics, Bangladesh Bureau of Statistics, Ministry of planning Govt. People's Repub. of Bangladesh, *Tech. rep.*, Bangladesh Bureau of Statistics, Dhaka, Bangladesh.

Bangladesh Bureau of Statistics (2012), Census population and housing census 2011: socio-economic and demographic report, national series, *Tech. rep.*, Bangladesh Bureau of Statistics, Dhaka, Bangladesh.

Bangladesh Bureau of Statistics (2014), Census population and housing census 2011: national report, union statistics, volume 2, *Tech. rep.*, Bangladesh Bureau of Statistics, Dhaka, Bangladesh.

Bangladesh Bureau of Statistics (2015a), Disaster-related Statistics 2015: Climate Change and Natural Disaster Perspectives, *Tech. rep.*, Bangladesh Bureau of Statistics, Khulna, Bangladesh.

Bangladesh Bureau of Statistics (2015b), Census population and housing census 2011: community report. Zila: Khulna., *Tech. rep.*, Bangldesh Bureau of Statistics, Khulna, Bangladesh.

Bartlett, K. B., R. C. Harriss, Karen B. Bartlett, and Robert C. Harriss (1993), Review and assessment of methane emissions from wetlands, *Chemosphere*, *26*(1-4), 261–320, doi:10.1016/0045-6535(93)90427-7.

Belton, V., and T. J. T. Stewart (2002), *Multiple Criteria Decision Analysis*, Springer US, Boston, MA, doi:10.1007/978-1-4615-1495-4.

Benayoun, R., B. Roy, and B. Sussman (1966), ELECTRE: Une méthode pour guider le choix en présence de points de vue multiples, *Note Trav.*, *96*.

Benneyworth, L., J. Gilligan, J. C. Ayers, S. Goodbred, G. George, A. Carrico, M. Rezaul Karim, F. Akter, D. Fry, K. Donato, and B. Piya (2016), Drinking water insecurity: water quality and access in coastal south-western Bangladesh, *Int. J. Environ. Health Res.*, pp. 1–17, doi:10.1080/09603123.2016.1194383.

Benneyworth, L. M. (2016), Factors Affecting Drinking Water Security in South-Western Bangladesh, Ph.D. thesis, Vanderbilt University, Nashville, Tennessee.

Bergamaschi, P., C. Frankenberg, J. F. Meirink, M. Krol, F. Dentener, T. Wagner, U. Platt, J. O. Kaplan, S. Körner, M. Heinmann, E. J. Dlugokencky, and A. Goede (2007), Satellite charactography of atmospheric methane from SCIAMACHY on board ENVISAT: 2. Evaluation based on inverse model simulations, *J. Geophys. Res. Atmos.*, *112*(2), 1–26, doi:10.1029/2006JD007268.

Bergamaschi, P., C. Frankenberg, J. F. Meirink, M. Krol, M. G. Villani, S. Houweling, F. Dentener, E. J. Dlugokencky, J. B. Miller, L. V. Gatti, A. Engel, and I. Levin (2009), Inverse modeling of global and regional CH4 emissions using SCIAMACHY satellite retrievals, *J. Geophys. Res. Atmos.*, *114*, doi:10.1029/2009JD012287.

Berner, U., J. Poggenburg, E. Faber, D. Quadfasel, and A. Frische (2003), Methane in ocean waters of the Bay of Bengal: Its sources and exchange with the atmosphere, *Deep. Res. Part II Top. Stud. Oceanogr.*, *50*(5), 925–950, doi:10.1016/S0967-0645(02)00613-6.

Bilskie, M., S. Hagen, S. Medeiros, and D. Passeri (2014), Dynamics of sea level rise and coastal flooding on a changing landscape, *Geophys. Reserach Lett.*, *41*(3), 927–934.

Biswas, A. K. (2008), Management of Ganges-Brahmaputra-Meghna System: Way Forward, in *Manag. Transbound. rivers lakes*, chap. 6, pp. 143–164, Springer-Verlag.

Biswas, H., S. K. Mukhopadhyay, S. Sen, and T. K. Jana (2007), Spatial and temporal patterns of methane dynamics in the tropical mangrove dominated estuary, NE coast of Bay of Bengal, India, *J. Mar. Syst.*, *68*(1-2), 55–64, doi:10.1016/j.jmarsys.2006.11.001.

Blanchet, T. (2014), Up-scaling MAR for Providing Community Water Supplies in Saline Areas: Anthropological Study Report, *Tech. rep.*, Drishti Research Center, Dhaka, Bangladesh.

Bousquet, P., P. Ciais, J. B. Miller, E. J. Dlugokencky, D. A. Hauglustaine, C. Prigent, G. R. Van der Werf, P. Peylin, E.-G. Brunke, C. Carouge, R. L. Langenfelds, J. Lathière, F. Papa, M. Ramonet, M. Schmidt, L. P. Steele, S. C. Tyler, and J. White (2006), Contribution of anthropogenic and natural sources to atmospheric methane variability, *Nature*, *443*(7110), 439–443, doi:10.1038/nature05132.

Bouwer, H. (2002), Artificial recharge of groundwater: hydrogeology and engineering, *Hydrogeol. J.*, *10*, 121–142, doi:10.1007/s10040-001-0182-4.

Bouwer, H., and R. C. Rice (1976), A slug test for determining hydraulic conductivity of unconfined aquifers with completely or partially penetrating wells, *Water Resour. Res.*, *12*(3), 423–428, doi:10.1029/WR012i003p00423.

Bovensmann, H., J. P. Burrows, M. Buchwitz, J. Frerik, S. Noel, V. V. Rozanov, K. V. Chance, and A. Goede (1999), SCIAMACHY - Mission objectives and measurement modes, *J. Atmos. Sci.*, *56*, 127–150.

Brouwer, R., S. Akter, L. Brander, and E. Haque (2007), Socioeconomic Vulnerability and Adaptation to Environmental Risk: A Case Study of Climate Change and Flooding in Bangladesh, *Risk Anal.*, *27*(2), doi:10.1111/j.1539-6924.2007.00884.x.

Bruhwiler, L., E. Dlugokencky, K. Masarie, M. Ishizawa, A. Andrews, J. Miller, C. Sweeney, P. Tans, and D. Worthy (2014), CarbonTracker-CH4: An assimilation system for estimating emissions of atmospheric methane, *Atmos. Chem. Phys.*, *14*(16), 8269–8293, doi:10.5194/acp-14-8269-2014.

Bui, D. D., A. Kawamura, T. N. Tong, H. Amaguchi, and N. Nakagawa (2012), Spatio-temporal analysis of recent groundwater-level trends in the Red River Delta, Vietnam, *Hydrogeol. J.*, *20*(8), 1635–1650, doi:10.1007/s10040-012-0889-4.

Burgess, W. G., M. A. Hoque, H. A. Michael, C. I. Voss, G. N. Breit, and K. M. Ahmed (2010), Vulnerability of deep groundwater in the Bengal Aquifer System to contamination by arsenic, *Nat. Geosci.*, *3*(2), 83–87, doi:10.1038/ngeo750.

Butz, A., O. P. Hasekamp, C. Frankenberg, and I. Aben (2009), Retrievals of atmospheric CO2 from simulated space-borne measurements of backscattered near-infrared sunlight: Accounting for aerosol effects, *Appl. Opt.*, *48*, 3322, doi:10.1364/AO.48.003322.

Butz, A., O. P. Hasekamp, C. Frankenberg, J. Vidot, and I. Aben (2010), CH4 retrievals from space-based solar backscatter measurements: Performance evaluation against simulated aerosol and cirrus loaded scenes, *J. Geophys. Res. Atmos.*, *115*(24), doi:10.1029/2010JD014514.

Butz, A., S. Guerlet, O. Hasekamp, D. Schepers, A. Galli, I. Aben, C. Frankenberg, J.-M. Hartmann, H. Tran, A. Kuze, G. Keppel-Aleks, G. Toon, D. Wunch, P. Wennberg, N. Deutscher, D. Griffith, R. Macatangay, J. Messerschmidt, J. Notholt, and T. Warneke (2011), Toward accurate CO2 and CH4 observations from GOSAT, *Geophys. Res. Lett.*, *38*(14), doi:10.1029/2011GL047888.

Cai, X., L. Lasdon, and A. M. Michelsen (2004), Group Decision Making in Water Resources Planning Using Multiple Objective Analysis, *J. Water Resour. Plan. Manag.*, *130*(1), 4–14, doi:10.1061/(ASCE)0733-9496(2004)130:1(4).

Cai, Z., G. Xing, X. Yan, H. Xu, H. Tsuruta, K. Yagi, and K. Minami (1997), Methane and nitrous oxide emissions from rice paddy fields as affected by nitrogen fertilisers and water management, *Plant Soil*, *196*(1), 7–14, doi:10.1023/A:1004263405020.

Calizaya, A., O. Meixner, L. Bengtsson, and R. Berndtsson (2010), Multi-criteria Decision Analysis (MCDA) for Integrated Water Resources Management (IWRM) in the Lake Poopo Basin, Bolivia, *Water Resour. Manag.*, *24*(10), 2267–2289, doi:10.1007/s11269-009-9551-x.

Carslaw, H. S., and J. C. Jaeger (1959), *Conduction of Heat in Solids*, Oxford University Press, London, UK.

Carson, M., A. Köhl, D. Stammer, A. B. A. Slangen, C. A. Katsman, R. S. W. van de Wal, J. Church, and N. White (2016), Coastal sea level changes, observed and projected during the 20th and 21st century, *Clim. Change*, *134*(1-2), 269–281, doi:10.1007/s10584-015-1520-1.

Chazette, P., C. Clerbaux, and G. Mégie (1998), Direct estimate of methane radiative forcing by use of nadir spectral radiances., *Appl. Opt.*, *37*(15), 3113–3120, doi:10.1364/AO.37.003113.

Chen, Y.-H., and R. G. Prinn (2006), Estimation of atmospheric methane emissions between 1996 and 2001 using a three-dimensional global chemical transport model, *J. Geophys. Res*, *111*, doi:10.1029/2005JD006058.

Chesnaux, R., R. P. Chapuis, and J. W. Molson (2006), A New Method to Characterize Hydraulic Short-Circuits in Defective Borehole Seals, *Ground Water*, *44*(5), 676–681, doi:10.1111/j.1745-6584.2006.00208.x.

Chhabra, A., K. R. Manjunath, S. Panigrahy, and J. S. Parihar (2013), Greenhouse gas emissions from Indian livestock, *Clim. Chang.*, *117*, 329–344, doi:10.1007/s10584-012-0556-8.

Chowdhury, M. R., and N. Ward (2004a), Hydro-meteorological variability in the greater Ganges-Brahmaputra-Meghna basins, *Int. J. Climatol.*, *24*(12), 1495–1508, doi:10.1002/joc.1076.

Chowdhury, M. R., and N. Ward (2004b), Hydro-meteorological variability in the greater Ganges-Brahmaputra-Meghna basins, *Int. J. Climatol.*, *24*(12), 1495–1508, doi:10.1002/joc.1076.

Chowdhury, N. T. (2010), Water management in Bangladesh: an analytical review, *Water Policy*, *12*(1), 32, doi:10.2166/wp.2009.112.

Chowdhury, R. K., and R. Rahman (2008), Multicriteria decision analysis in water resources management: the malnichara channel improvement, *Int. J. Sci. Technol.*, *5*(2), 195–204, doi:10.1007/s11269-009-9551-x.

Ciais, P., C. Sabine, G. Bala, L. Bopp, V. Brovkin, J. Canadell, A. Chhabra, R. DeFries, J. Galloway, M. Heimann, C. Jones, C. Le Quéré, R. B. Myneni, S. Piao, and P. Thornton (2013), Carbon and Other Biogeochemical Cycles. In: Climate Change 2013: The Physical Science Basis. Contribution of Working Group I to the Fifth Assessment Report of the Intergovernmental Panel on Climate Change, *Tech. rep.*, Intergovernmental Panel on Climate Change, Cambridge, doi:10.1017/CBO9781107415324.

Cinelli, M., S. R. Coles, and K. Kirwan (2014), Analysis of the potentials of multi criteria decision analysis methods to conduct sustainability assessment, *Ecol. Indic.*, *46*, 138–148, doi:10.1016/J.ECOLIND.2014.06.011.

Clerbaux, C., J. Hadji-Lazaro, S. Turquety, G. Mégie, and P.-F. Coheur (2003), Trace gas measurements from infrared satellite for chemistry and climate applications, *Atmos. Chem. Phys. Discuss.*, *3*(2), 1495–1508, doi:10.5194/acpd-3-2027-2003.

Conrad, R. (2002), Control of microbial methane production in wetland rice fields, *Nutr. Cycl. Agroecosystems*, *64*(1-2), 59–69, doi:10.1023/A:1021178713988.

Cook, P. G., G. R. Walker, G. Buselli, I. Potts, and A. R. Dodds (1992), The application of electromagnetic techniques to groundwater recharge investigations, *J. Hydrol.*, *130*, 201–229.

Corton, T. M., J. B. Bajita, F. S. Grospe, R. R. Pamplona, J. a. Assis, R. Wassmann, R. S. Lantin, and L. V. Buendia (2000), Methane emission from irrigated and intensively managed rice fields in Central Luzon (Philippines), *Nutr. Cycl. Agroecosystems*, *58*(1-3), 37–53, doi:10.1023/A:1009826131741.

Das, K., and K. K. Baruah (2008), A comparison of growth and photosynthetic characteristics of two improved rice cultivars on methane emission from rainfed agroecosystem of northeast India, *Agric. Ecosyst. Environ.*, *124*(1-2), 105–113, doi:10.1016/j.agee.2007.09.007.

Datta, A., J. B. Yeluripati, D. Nayak, K. Mahata, S. Santra, and T. Adhya (2013), Seasonal variation of methane flux from coastal saline rice field with the application of different organic manures, *Atmos. Environ.*, *66*, 114–122, doi:10.1016/j.atmosenv.2012.06.008.

Davidson, N. C. (2014), How much wetland has the world lost? Long-term and recent trends in global wetland area, *Mar. Freshw. Res.*, *65*, 934–941, doi:10.1071/MF14173.

Davis, K. M. (2007), Using Apparent Electrical Conductivity (ECa) via Electromagnetic Induction (EMI) to Characterize Soils and the Stratigraphy for Wetland Restoration, Ph.D. thesis, North Carolina State University.

Denier van der Gon, H. A. C. (1994), Impact of gypsum application on the methane emission from a wetland rice field, *Global Biogeochem. Cycles*, *8*(June), 127–134.

Denier van der Gon, H. A. C., and H. U. Neue (1995), Methane emission from a wetland rice field as affected by salinity, *Plant Soil*, *170*(2), 307–313, doi:10.1007/BF00010483.

Denier van der Gon, H. A. C., N. van Breemen, H.-U. Neue, R. S. Lantin, J. B. Aduna, M. C. R. Alberto, and R. Wassmann (1996), Release of entrapped methane from wetland rice fields upon soil drying, *Global Biogeochem. Cycles*, *10*(1), 1–7, doi:10.1029/95GB03460.

Denier Van Der Gon, H. A. C., P. M. van Bodegom, S. Houweling, P. H. Verburg, N. Van Breemen, H. a. C. D. van der Gon, P. M. van Bodegom, S. Houweling, P. H. Verburg, and N. Van Breemen (2000), Combining upscaling and downscaling of methane emissions from rice fields: Methodologies and preliminary results, *Nutr. Cycl. Agroecosystems*, *58*(1-3), 285–301, doi:10.1023/A:1009863107151.

Ding, W., Z. Cai, and D. Wang (2004), Preliminary budget of methane emissions from natural wetlands in China, *Atmos. Environ.*, *38*, 751–759, doi:10.1016/j.atmosenv.2003.10.016.

Dlugokencky, E. J., S. Houweling, L. Bruhwiler, K. A. Masarie, P. M. Lang, J. B. Miller, and P. P. Tans (1992), Atmospheric methane levels off: Temporary pause or a new steady-state?, *Geophys. Res. Lett.*, *30*(19), doi:10.1029/2003GL018126.

Dlugokencky, E. J., L. Bruhwiler, J. W. C. White, L. K. Emmons, P. C. Novelli, S. A. Montzka, K. A. Masarie, P. M. Lang, A. M. Crotwell, J. B. Miller, and L. V. Gatti (2009), Observational constraints on recent increases in the atmospheric CH ₄ burden, *Geophys. Res. Lett.*, *36*(18), L18,803, doi:10.1029/2009GL039780.

Domènech, L., H. Heijnen, and D. Saurí (2012), Rainwater harvesting for human consumption and livelihood improvement in rural Nepal: benefits and risks, *Water Environ. J.*, *26*(4), 465–472, doi:10.1111/j.1747-6593.2011.00305.x.

Donato, K. M., A. R. Carrico, B. Sisk, and B. Piya (2016), Different but the Same, *Ann. Am. Acad. Pol. Soc. Sci.*, *666*(1), 203–218, doi:10.1177/0002716216650843.

Doolittle, J., M. Petersen, and T. Wheeler (2001), Comparison of two electromagnetic induction tools in salinity appraisals, *J. Soil Water Conserv.*, *56*(3), 257–262.

Draxler, R. (1999), HYSPLIT4 user's guide–NOAA Tech. Memo. ERL ARL-230, *Tech. rep.*, NOAA Air Resources Laboratory, Silver Spring, MD.

Draxler, R., and G. D. Hess (1997), Description of the HYSPLIT4 modeling system, *Tech. rep.*, NOAA Air Resources Laboratory, Silver Spring, MD.

Draxler, R., and G. D. Hess (1998), An overview of the HYSPLIT4 modeling system of trajectories, dispersion, and deposition, *Aust. Meterol. Mag.*, *47*, 295–308.

Dyer, T. G. (1999), Retrospect and Prospect: Understanding the American Outreach University, *J. High. Educ. Outreach Engagem.*, *4*(1), 52–64.

EPA (2010), Methane and Nitrous Oxide Emissions from Natural Sources, *Tech. rep.*, U.S. Enviromental Protection Agency, Washington, D.C.

Erban, L. E., S. M. Gorelick, and H. A. Zebker (2014), Groundwater extraction, land subsidence, and sea-level rise in the Mekong Delta, Vietnam, *Environ. Res. Lett.*, *9*(8), 084,010, doi:10.1088/1748-9326/9/8/084010.

FAO (2005), Livestock Sector Brief: Bangladesh.

FAO (2014), FAO Statistical Yearbook.

Ferguson, G., and T. Gleeson (2012), Vulnerability of coastal aquifers to groundwater use and climate change, *Nat. Clim. Chang.*, *2*(5), 342–345, doi:10.1038/nclimate1413.

Fetter, C. W. (2001), *Applied Hydrogeology*, 4 ed., Pearson Education, Upper Saddle River, New Jersey.

Figueira, J., S. Greco, B. Roy, and R. Slowinski (2013), An Overview of ELECTRE Methods and their Recent Extensions, *J. MultiCriteria Decis. Anal.*, *20*, 61–85, doi:10.1002/mcda.1482.

Frankenberg, C., J. F. Meirink, M. van Weele, U. Platt, and T. Wagner (2005a), Assessing Methane Emissions from Global Space-Borne Observations, *Science (80-.).*, *308*, 1010–1014, doi:10.1126/science.1106644.

Frankenberg, C., U. Platt, and T. Wagner (2005b), Iterative maximum a posteriori (IMAP)-DOAS for retrieval of strongly absorbing trace gases: Model studies for CH 4 and CO 2 retrieval from near infrared spectra of SCIAMACHY onboard ENVISAT, *Atmos. Chem. Phys*, *5*, 9–22.

Frankenberg, C., J. F. Meirink, P. Bergamaschi, A. P. H. Goede, M. Heimann, S. Körner, U. Platt, M. van Weele, and T. Wagner (2006), Satellite chartography of atmospheric methane from SCIAMACHY on board ENVISAT: Analysis of the years 2003 and 2004, *J. Geophys. Res.*, *111*(D7), D07,303, doi:10.1029/2005JD006235.

Frankenberg, C., P. Bergamaschi, A. Butz, S. Houweling, J. F. Meirink, J. Notholt, A. K. Petersen, H. Schrijver, T. Warneke, and I. Aben (2008a), Tropical methane emissions: A revised view from SCIAMACHY onboard ENVISAT, *Geophys. Res. Lett.*, *35*(15), L15,811, doi:10.1029/2008GL034300.

Frankenberg, C., T. Warneke, A. Butz, I. Aben, F. Hase, P. Spietz, and L. R. Brown (2008b), Pressure broadening in the 2ν 3 band of methane and its implication on atmospheric retrievals, *Atmos. Chem. Phys. Atmos. Chem. Phys.*, *8*(17), 5061–5075.

Frankenberg, C., I. Aben, P. Bergamaschi, E. J. Dlugokencky, R. Van Hees, S. Houweling, P. Van Der Meer, R. Snel, and P. Tol (2011), Global column-averaged methane mixing ratios from 2003 to 2009 as derived from SCIAMACHY: Trends and variability, *J. Geophys. Res. Atmos.*, *116*(4), 1–12, doi:10.1029/2010JD014849.

Frei, M., M. Razzak, M. Hossain, M. Oehme, S. Dewan, and K. Becker (2007), Methane emissions and related physicochemical soil and water parameters in ricefish systems in Bangladesh, *Agric. Ecosyst. Environ.*, *120*(2-4), 391–398, doi:10.1016/j.agee.2006.10.013.

Furbish, D. J. (1991), The response of water level in a well to a time series of atmospheric loading under confined conditions, *Water Resour. Res.*, *27*(4), 557–568.

Gain, A., and C. Giupponi (2014), Impact of the Farakka Dam on Thresholds of the Hydrologic Flow Regime in the Lower Ganges River Basin (Bangladesh), *Water*, *6*(8), 2501–2518, doi:10.3390/w6082501.

Gain, A. K., C. Giupponi, and F. G. Renaud (2012), Climate Change Adaptation and Vulnerability Assessment of Water Resources Systems in Developing Countries: A Generalized Framework and a Feasibility Study in Bangladesh, *Water*, *4*, 345–366, doi: 10.3390/w4020345.

Gain, A. K., Y. Wada, A. K. Gain, and Y. Wada (2014), Assessment of Future Water Scarcity at Different Spatial and Temporal Scales of the Brahmaputra River Basin, *Water Resour. Manag.*, *28*, 999–1012, doi:10.1007/s11269-014-0530-5.

Ganji, A., H. R. Maier, and G. C. Dandy (2016), A modified Sobol' sensitivity analysis method for decision-making in environmental problems, *Enviromental Model. Softw.*, *75*, 15–27, doi:10.1016/j.envsoft.2015.10.001.

Gao, H., E. F. Wood, T. J. Jackson, M. Drusch, and R. Bindlish (2006), Using TRMM/TMI to Retrieve Surface Soil Moisture over the Southern United States from 1998 to 2002, *J. Hydrometeorol.*, *7*(1), 23–38, doi:10.1175/JHM473.1.

Ghani Nugroho, S., J. Lumbanraja, H. Suprapto, W. Sabe Ardjasa, H. Haraguchi, M. Kimura, S. Ghani Nugraha, L. Lumbanraja, H. Suprapta, and M. Kimura (1994), Methane emission from an indonesian paddy field subjected to several fertilizer treatments, *Soil Sci. Plant Nutr*, *40*(2), 275–281, doi:10.1080/00380768.1994.10413301.

Ghani Nugroho, S., J. Lumbanraja, H. Suprapto, W. Sabe Ardjasa, M. Kimura, and L. Lumbanraja (1997), Effect of rice variety on methane emission from an Indonesian paddy field, *Soil Sci. Plant Nutr. Soil Sci. Plant Nutr*, *43*(4), 799–809, doi:10.1080/00380768.1997.10414646.

Ghosh, S., D. Majumdar, and M. C. Jain (2003), Methane and nitrous oxide emissions from an irrigated rice of North India, *Chemosphere*, *51*(3), 181–195, doi:10.1016/S0045-6535(02)00822-6.

Gloudemans, A. M. S., H. Schrijver, Q. Kleipool, M. M. P. Van Den Broek, A. G. Straume, G. Lichtenberg, R. M. Van Hees, I. Aben, and J. F. Meirink (2005), The impact of SCIAMACHY near-infrared instrument calibration on CH 4 and CO total columns, *Atmos. Chem. Phys*, *5*, 2369–2383.

Gopal, B., and R. G. Wetzel (1995), Limnology in Developing Countries, *New Delhi Inter. Assoc. Limn.*, *1*, 1–230.

Greenwood, W. J., S. Kruse, and P. Swarzenski (2006), Extending electromagnetic methods to map coastal pore water salinities, *Ground Water*, *44*(2), 292–299, doi:10.1111/j.1745-6584.2005.00137.x.

Gregg, D. O. (1966), An Analysis of Ground-Water Fluctuations Caused by Ocean Tides in Glynn County, Georgia, *Groundwater*, *4*(3), 24–32.

Gumma, M. K., P. S. Thenkabail, A. Maunahan, S. Islam, and A. Nelson (2014), Mapping seasonal rice cropland extent and area in the high cropping intensity environment of Bangladesh using MODIS 500m data for the year 2010, *ISPRS J. Photogramm. Remote Sens.*, *91*, 98–113, doi:10.1016/j.isprsjprs.2014.02.007.

Gunda, T., L. Benneyworth, and E. Burchfield (2015), Exploring water indices and associated parameters: a case study approach, *Water Policy*, *17*(1), 98, doi:10.2166/wp.2014.022.

Hajkowicz, S., and K. Collins (2007), A Review of Multiple Criteria Analysis for Water Resource Planning and Management, *Water Resour. Manag.*, *21*, 1553–1566, doi:10.1007/s11269-006-9112-5.

Halford, K. J., and E. L. Kuniansky (2002), Documentation of spreadsheets for the analysis of aquifer-test and slug-test data, *Tech. rep.*, USGS.

Hasan, S., and G. Mulamoottil (1994), Natural resource management in Bangladesh, *Ambio*, *23*(2), 141–145.

Hertel, T. W., M. B. Burke, and D. B. Lobell (2010), The poverty implications of climate-induced crop yield changes by 2030, *Glob. Environ. Chang.*, *20*(4), 577–585, doi:10.1016/J.GLOENVCHA.2010.07.001.

Hijioka, Y., E. Lin, J. J. Pereira, R. T. Corlett, X. Cui, G. E. Insarov, R. D. Lasco, E. Lindgren, and A. Surjan (2014), Asia, in *Clim. Chang. 2014 Impacts, Adapt. Vulnerability. Part B Reg. Asp. Contrib. Work. Gr. II to Fifth Assess. Rep. Intergov. Panel Clim. Chang.*, edited by V. Barros, C. Field, D. Dokken, M. Mastrandrea, K. Mach, T. Bilir, M. Chatterjee, K. Ebi, Y. Estrada, R. Genova, B. Girma, E. Kissel, A. Levy, S. MacCracken, P. Mastrandrea, and L. White, pp. 1327–1370, University Press, Cambridge, United Kingdom and New York, NY, USA.

Hirota, M., Y. Tang, Q. Hu, S. Hirata, T. Kato, W. Mo, G. Cao, and S. Mariko (2004), Methane emissions from different vegetation zones in a Qinghai-Tibetan Plateau wetland, *Soil Biol. Biochem.*, *36*(5), 737–748, doi:10.1016/j.soilbio.2003.12.009.

Hoefel, F. G., and R. L. Evans (2001), Impact of low salinity porewater on seafloor electromagnetic data: A means of detecting submarine groundwater discharge?, *Estuar. Coast. Shelf Sci.*, *52*(2), 179–189, doi:10.1006/ecss.2000.0718.

Holländer, H. M., R. Mull, and S. N. Panda (2009), A concept for managed aquifer recharge using ASR - wells for sustainable use of groundwater resources in an alluvial coastal aquifer in Eastern India, *Phys. Chem. Earth Parts*, *34*, 270–278, doi:10.1016/j.pce.2008.05.001.

Hoque, M. A., P. F. D. Scheelbeek, P. Vineis, A. E. Khan, K. M. Ahmed, and A. P. Butler (2016), Drinking water vulnerability to climate change and alternatives for adaptation in coastal South and South East Asia, *Clim. Change*, *136*(2), 247–263, doi:10.1007/s10584-016-1617-1.

Hornberger, G. M., and R. C. Spear (1981), An Approach to the Preliminary Analysis of Environmental Systems, *J. Environ. Manage.*, *12*, 7–18.

Horneman, A., A. Van Geen, D. V. Kent, P. E. Mathe, Y. Zheng, R. K. Dhar, S. O'connell, M. A. Hoque, Z. Aziz, M. Shamsudduha, A. A. Seddique, and K. M. Ahmed (2004), Decoupling of As and Fe release to Bangladesh groundwater under reducing conditions. Part I: Evidence from sediment profiles, *Geochim. Cosmochim. Acta*, *68*(17), 3459–3473, doi:10.1016/j.gca.2004.01.026.

Hossain, M. K. (2001), Overview of the forest biodiversity in Bangladesh, in *Assessment, Conserv. Sustain. Use For. Biodivers.*, chap. 6, pp. 33–35, SCBD, Montreal.

Hou, H., S. Peng, J. Xu, S. Yang, and Z. Mao (2012), Seasonal variations of CH4 and N2O emissions in response to water management of paddy fields located in Southeast China, *Chemosphere*, *89*(7), 884–892, doi:10.1016/j.chemosphere.2012.04.066.

Houghton, J., Y., D. J. G. Ding, D. J. Griggs, M. Noguer, P. J. van der Linden, X. Dai, K. Maskell, and C. A. Johnson (2001), Climate Change 2001: The Scientific Basis. Contribution of Working Group I to the Third Assessment Report of the Intergovernmental Panel on Climate Change, *Tech. rep.*, Intergovernmental Panel on Climate Change, Cambridge, United Kingdom and New York, NY, USA.

Huang, H., and I. J. Won (2000), Conductivity and Susceptibility Mapping Using Broadband Electromagnetic Sensors, *J. Environ. Eng. Geophys.*, *5*(4), 31–41, doi:10.4133/JEEG5.4.31.

Hughes, N. (2012), *Monish and the Stone Forest*, Geological Society of Inda, Gavipuram, Bangalore.

Hughes, N. C., P. Ghosh, and D. Bhattacharya (2015), The monishar pathorer bon (Monisha and the Stone Forest) Book Project: Novel Educational Outreach to Children in Rural Communities, Eastern Indian Subcontinent, *J. Geosci. Educ.*, *63*, 18–28, doi:1089-9995/2015/63(1)/18/11.

Huq, S. (2001), Climate change and Bangladesh, *Science (80-.).*, *294*(5547), 1617, doi:10.1126/science.294.5547.1617.

Hussain, M. D., and A. Ziauddin (1989), Rainwater use in Bangladesh - A case study in Dacope Upozilla, in *Proc. Int. Conf. Rainwater Cist. Syst.*, Manila, Philippines.

Hyde, K., H. R. Maier, and C. Colby (2003), Incorporating Uncertainty in the PROMETHEE MCDA Method, *J. Multi-Criteria Decis. Anal.*, *12*(4-5), 245–259, doi:10.1002/mcda.361.

Hyde, K. M., H. R. Maier, and C. B. Colby (2004), Reliability-Based Approach to Multicriteria Decision Analysis for Water Resources, *J. Water Resour. Plan. Manag.*, *130*(6), 429–438, doi:10.1061/(ASCE)0733-9496(2004)130:6(429).

Immerzeel, W. (2008), Ocean circulation: Thermohaline circulation, *Int. J. Climatol.*, *28*, 243–254, doi:10.1002/joc.

Immerzeel, W. W., P. Droogers, S. M. de Jong, and M. F. P. Bierkens (2009), Large-scale monitoring of snow cover and runoff simulation in Himalayan river basins using remote sensing, *Remote Sens. Environ.*, *113*(1), 40–49, doi:10.1016/j.rse.2008.08.010.

Ingersoll, L., O. J. Zobel, and A. C. Ingersoll (1954), Heat Conduction: With Engineering Geological And Other Applications.

Inubushi, K., H. Sugii, S. Nishino, and E. Nishino (2001), Effect of aquatic weeds on methane emission from submerged paddy soil, *Am. J. Bot.*, *88*(6), 975–979, doi:10.2307/2657078.

IPCC (1994), Climate Change. Radiative forcing of climate change and an evaluation of the IPCC IS92 emission scenarios, *Tech. rep.*, Intergovernmental Panel on Climate Change, Cambridge, United Kingdom and New York, NY, USA.

Islam, A. S., S. K. Bala, and M. A. Haque (2010), Flood inundation map of Bangladesh using MODIS time-series images, *J. Flood Risk Manag.*, *3*(3), 210–222, doi:10.1111/j.1753-318X.2010.01074.x.

Islam, M. A., H. Sakakibara, M. R. Karim, and M. Sekine (2013), Potable water scarcity: options and issues in the coastal areas of Bangladesh, *J. Water Health*, *11*(3), 532–542, doi:10.2166/wh.2013.215.

Islam, M. A., A. K. Azad, M. A. Akber, M. Rahman, and I. Sadhu (2015), Effectiveness of solar disinfection (SODIS) in rural coastal Bangladesh, *J. Water Health*, *13*(4), 1113–1122, doi:10.2166/wh.2015.186.

Islam, M. M., M. Kabir, and F. N.-F. Chou (2007), Feasibility study of rainwater harvesting techniques in Bangladesh, *Rainwater Urban Des.*, pp. 726–733.

Islam, S. N. (2010), Threatened wetlands and ecologically sensitive ecosystems management in Bangladesh, *Front. Earth Sci. China*, *4*(4), 438–448, doi:10.1007/s11707-010-0127-0.

Jacob, C. E. (1940), On the flow of water in an elastic artesian aquifer, *Eos, Trans. Am. Geophys. Union*, *21*(2), 574–586.

Jahan, S., and A. K. Azad (2013), Estimation of Greenhouse Gas Emission from the Livestock Sector of Bangladesh, *Int. J. Sci. Res.*, *4*(1), 1148–1155.

Jahangir Alam, M., I. Ara Begum, J. Buysse, and G. Van Huylenbroeck (2012), Energy consumption, carbon emissions and economic growth nexus in Bangladesh: Cointegration and dynamic causality analysis, *Energy Policy*, *45*, 217–225, doi:10.1016/J.ENPOL.2012.02.022.

Jakariya, M. (2005), Sustainable safe water options in Bangladesh: experiences from the Arsenic Project at Matlab (AsMat), *Nat. Arsen. Groundw. Occur. Remediat. Manag.*, pp. 319–330.

Jelgersma, S. (1996), Land subsidence in coastal lowlands, in *Sea-Level Rise Coast. Subsid.*, edited by J. Milliman and B. Haq, pp. 47–62, Kluwer Academic Publishers.

Jermsawatdipong, P., J. Murase, P. Prabuddham, Y. Hasathon, N. Khomthong, K. Naklang, A. Watanabe, H. Haraguchi, and M. Kimura (1994), Methane emission from plots with differences in fertilizer application in thai paddy fields, *Soil Sci. Plant Nutr.*, *40*(1), 63–71, doi:10.1080/00380768.1994.10414279.

Jha, M. K., V. M. Chowdary, Y. Kulkarni, and B. C. Mal (2014), Rainwater harvesting planning using geospatial techniques and multicriteria decision analysis, *Resour. Conserv. Recycl.*, *83*, 96–111, doi:10.1016/J.RESCONREC.2013.12.003.

Jiménez Cisneros, B., T. Oki, N. W. Arnell, G. Benito, J. G. Cogley, P. Döll, T. Jiang, and S. S. Mwakalila (2014), Freshwater resources. In: Climate Change 2014: Impacts, Adaptation, and Vulnerability. Part A: Global and Sectoral Aspects. Contribution of Working

Group II to the Fifth Assessment Report of the Intergovernmental Panel on Climate Change, *Tech. rep.*, Intergovernmental Panel on Climate Change, Cambridge, United Kingdom and New York, NY, USA.

Johnston, M. A., J. H. Meyer, M. J. Savage, and R. Van Antwerpen (1994), Electromagnetic induction as a technique for diagnosing and mapping soil salinity, *Proc. South African Sugar Technol. Assoc.*, pp. 65–69.

Jongman, B., P. Ward, and J. Aerts (2012), Global exposure to river and coastal flooding: long term trends and changes, *Glob. Environ. Chang. Hum. Policy Dimens.*, *22*(4), 823–835, doi:10.1016/j.gloenvcha.2012.07.004.

Karim, M. F., and N. Mimura (2008), Impacts of climate change and sea-level rise on cyclonic storm surge floods in Bangladesh, *Glob. Environ. Chang.*, *18*(3), 490–500, doi:10.1016/J.GLOENVCHA.2008.05.002.

Kato, F., N. Inoue, S. Kasuga, A. Yoshikawa, T. Hayakawa, H. Murata, and S. Kasajima (2012), Estimation of methane emission rates from a rice paddy field using a naturally ventilated tunnel, *Grassl. Sci.*, *58*(2), 59–65, doi:10.1111/j.1744-697X.2012.00249.x.

Kavitha, M., and P. R. Nair (2016), Region-dependent seasonal pattern of methane over Indian region as observed by SCIAMACHY, *Atmos. Environ.*, *131*(2016), 316–325, doi:10.1016/j.atmosenv.2016.02.008.

Khalil, M. a. K., R. a. Rasmussen, M. J. Shearer, R. W. Dalluge, L. X. Ren, and C.-L. Duan (1998), Measurements of methane emissions from rice fields in China, *J. Geophys. Res.*, *103*(D19), 25,181, doi:10.1029/97JD02611.

Khublaryan, M. G., A. P. Frolov, and I. O. Yushmanov (2008), Seawater intrusion into coastal aquifers, *Water Resour.*, *35*(3), 274–286, doi:10.1134/S0097807808030032.

Kimura, M. (2000), Anaerobic microbiology in waterlogged rice fields Kimura - Google Scholar, in *Soil Biochem.*, edited by J. Bollag and G. Stotzky, chap. 10, pp. 35–138, Marcel Dekker, New York.

Kirkwood, C. W. (1997), *Stategic Decision Making: Multiobjective Decision Analysis with Spreadsheets*, Brooks/Cole, Cengage Learning.

Klassen, J., and D. Allen (2017), Assessing the risk of saltwater intrusion in coastal aquifers, *J. Hydrol.*, *551*, 730–745, doi:10.1016/J.JHYDROL.2017.02.044.

Kuze, A., H. Suto, M. Nakajima, and T. Hamazaki (2009), Thermal and near infrared sensor for carbon observation Fourier-transform spectrometer on the Greenhouse Gases Observing Satellite for greenhouse gases monitoring, *Appl. Opt.*, *48*(35), 6716–6733, doi:10.1364/AO.48.006716.

Lambrakis, N., and G. Kallergis (2001), Reaction of subsurface coastal aquifers to climate and land use changes in Greece: modelling of groundwater refreshening patterns under natural recharge conditions, *J. Hydrol.*, *245*(1-4), 19–31, doi:10.1016/S0022-1694(01)00334-1.

Lelieveld, J., P. J. Crutzen, and F. J. Dentener (1998), Changing concentration, lifetime and climate forcing of atmospheric methane, *Tellus B Chem. Phys. Meteorol.*, *50*(2), 128–150, doi:10.3402/tellusb.v50i2.16030.

Lerner, J., and E. Matthews (1988), Methane Emissions from Animals: A Global High-Resolution Data Base, *Global Biogeochem. Cycles*, *2*(2), 139–156.

Li, H., G. Li, J. Cheng, and M. C. Boufadel (2007), Tide-induced head fluctuations in a confined aquifer with sediment covering its outlet at the sea floor, *Water Resour. Res.*, *43*(3), 1–12, doi:10.1029/2005WR004724.

Liou, R. M., S. N. Huang, and C. W. Lin (2003), Methane emission from fields with differences in nitrogen fertilizers and rice varieties in Taiwan paddy soils, *Chemosphere*, *50*(2), 237–246, doi:10.1016/S0045-6535(02)00158-3.

Liu, J., T. Dietz, S. R. Carpenter, M. Alberti, C. Folke, E. Moran, A. N. Pell, P. Deadman, T. Kratz, J. Lubchenco, E. Ostrom, Z. Ouyang, W. Provencher, C. L. Redman, S. H. Schneider, and W. W. Taylor (2007), Complexity of Coupled Human and Natural Systems, *Science (80-.).*, *317*(5844), 1513–1516, doi:10.1126/science.1144004.

Maas, C., and W. J. De Lange (1987), On the negative phase shift of groundwater tides near shallow tidal rivers - The Gouderak anomaly, *J. Hydrol.*, *92*(3-4), 333–349, doi:10.1016/0022-1694(87)90022-9.

Maclean, J., D. C. Dawe, B. Hardy, and G. P. Hettel (2002), *Rice almanac: Source book for the most important economic activity on earth*, 3rd ed., CABI Publishing.

Magrath, C. P. (1999), Engagement and the Twenty-First Century University, *J. Public Serv. Outreach*, *4*(1), 3–7.

Makarim, A. K., A. Bey, R. Boer, and P. Setyanto (1995), Methane gas from lowland rice fields in Indonesia: Development and research directions, *Tech. rep.*, Central Research Institute for Food Crops, Bogor, Indonesia.

Mallick, B., and J. Vogt (2014), Population displacement after cyclone and its consequences: empirical evidence from coastal Bangladesh, *Nat. Hazards*, *73*(2), 191–212, doi:10.1007/s11069-013-0803-y.

Manheim, F. T., D. E. Krantz, and J. F. Bratton (2004), Studying ground water under delmarva coastal bays using electrical resistivity, *Ground Water*, *42*(7), 1052–1068, doi:10.1111/j.1745-6584.2004.tb02643.x.

Mathieu, R. D., C. Pfund, and D. Gillian-Daniel (2009), Leveraging the NSF Broader-Impacts Criterion for Change in STEM Education, *Chang. Mag. High. Learn. Leveraging NSF Broader-Impacts Criterion Chang. STEM Educ.*, *40*(3), 50–55, doi:10.3200/CHNG.41.3.50-55.

McBean, E. A., M. A. Rajib, and M. M. Rahman (2013), Improved sustainability of water supply options in areas with arsenic-impacted groundwater, *Water*, *5*, 1941–1951, doi:10.3390/w5041941.

McGranahan, G., D. Balk, and B. Anderson (2007), The rising tide: assessing the risks of climate change and human settlements in low elevation coastal zones, *Environ. Urban.*, *19*, 17–37, doi:10.1177/0956247807076960.

McNeill, J. (1980), Electrical conductivity of soils and rocks, *Tech. rep.*, Geonics Limited.

Mehedi, H., A. K. Nag, and S. Farhana (2010), *Climate Induced DisplacementCase Study of Cyclone Aila in the Southwest Coastal Region of Bangladesh*, Humanitywatch, Khulna, Bangladesh.

Meirink, J. F., H. J. Eskes, and A. P. H. Goede (2006), Sensitivity analysis of methane emissions derived from SCIAMACHY observations through inverse modelling, *Atmos. Chem. Phys. Atmos. Chem. Phys.*, *6*, 1275–1292.

Meirink, J. F., P. Bergamaschi, C. Frankenberg, M. T. S. D'Amelio, E. J. Dlugokencky, L. V. Gatti, S. Houweling, J. B. Miller, T. Röckmann, M. G. Villani, and M. C. Krol (2008), Four-dimensional variational data assimilation for inverse modeling of atmospheric methane emissions: Analysis of SCIAMACHY observations, *J. Geophys. Res.*, *113*(D17), 1–20, doi:10.1029/2007JD009740.

Melton, J. R., R. Wania, E. L. Hodson, B. Poulter, B. Ringeval, R. Spahni, T. Bohn, C. A. Avis, D. J. Berling, G. Chen, A. V. Eliseev, S. N. Denisov, P. O. Hopcroft, D. P. Lettenmaier, W. J. Riley, J. S. Singarayer, Z. M. Subin, H. Tian, S. Zurcher, V. Brovkin, P. M. van Bodegom, T. Kleinen, Z. C. Yu, and J. O. Kaplan (2013), Present state of global wetland extent and wetland methane modelling: conclusions from a model inter-comparison project (WETCHIMP), *Biogeosciences*, *10*, 753–788.

Michael, H. A., and M. R. Khan (2016), Impacts of physical and chemical aquifer heterogeneity on basin-scale solute transport: Vulnerability of deep groundwater to arsenic contamination in Bangladesh, *Adv. Water Resour.*, *98*, 147–158, doi:10.1016/j.advwatres.2016.10.010.

Michael, H. A., and C. I. Voss (2009), Controls on groundwater flow in the Bengal Basin of India and Bangladesh: regional modeling analysis, *Hydrogeol. J.*, *17*, 1561–1577.

Minoda, T., M. Kimura, and E. Wada (1996), Photosynthates as dominant source of CH4 and CO2 in soil water and CH4 emitted to the atmosphere from paddy fields, *J. Geophys. Res. Atmos.*, *101*(D15), 21,091–21,097, doi:10.1029/96JD01710.

Mirza, M. M. Q., and M. Monirul Qader Mirza (2002), Global warming and changes in the probability of occurrence of floods in Bangladesh and implications, *Glob. Environ. Chang.*, *12*(2), 127–138, doi:10.1016/S0959-3780(02)00002-X.

Mirza, M. Q., R. A. Warrick, N. J. Ericksen, and G. J. Kenny (1998), Trends and persistence in precipitation in the Ganges, Brahmaputra and Meghna river basins, *Hydrol. Sci. J.*, *43*(6), 845–858, doi:10.1080/02626669809492182.

Mondal, M. S., J. U. Chowdhury, and M. R. Ferdous (2010), Risk-Based Evaluation for Meeting Future Water Demand of the Brahmaputra Floodplain Within Bangladesh, *Water Resour. Manag.*, *24*(5), 853–869, doi:10.1007/s11269-009-9475-5.

Morgan, J. P., and W. G. McIntire (1959), Quantenary Geology of the Bengal Basin, East Pakistan and India, *Bull. Geol. Soc. Am.*, *70*, 319–342.

Morrissey, L. A., and G. P. Livingston (1992), Methane emissions from Alaska Arctic tundra: An assessment of local spatial variability, *J. Geophys. Res.*, *97*(D15), 16,661–16,670, doi:10.1029/92JD00063.

Mosleh, M. K., and Q. K. Hassan (2014), Development of a remote sensing-based ”boro” rice mapping system, *Remote Sens.*, *6*(3), 1938–1953, doi:10.3390/rs6031938.

MPO (1987), Groundwater resources of Bangladesh. Technical Report Nr 5, Master Plan Organisation, Dhaka, *Tech. rep.*, Harza Engineering, USA, Mott MacDonald Ltd, UK, Meta Consultants, USA and EPC Ltd, Bangladesh, Dhaka, Bangladesh.

Mulligan, A. E., R. L. Evans, and D. Lizarralde (2007), The role of paleochannels in groundwater/seawater exchange, *J. Hydrol.*, *335*(3-4), 313–329.

Mutikanga, H. E., S. K. Sharma, and K. Vairavamoorthy (2011), Multi-criteria Decision Analysis: A Strategic Planning Tool for Water Loss Management, *Water Resour. Manag.*, *25*(14), 3947–3969, doi:10.1007/s11269-011-9896-9.

Naser, H. M., O. Nagata, S. Tamura, and R. Hatano (2007), Methane emissions from five paddy fields with different amounts of rice straw application in central Hokkaido, Japan, *Soil Sci. Plant Nutr.*, *53*(1), 95–101, doi:10.1111/j.1747-0765.2007.00105.x.

Neibaur, E. E., and E. P. Anderson (2016), An examination of factors affecting sustainability of domestic rainwater harvesting systems in a rural, semi-arid region of Mexico, *Water Sci. Technol. Water Supply*, *16*(5), 1388–1397, doi:10.2166/ws.2016.066.

Neue, H. U., and R. L. Sass (1998), The budget of methane from rice fields, *IG Act. Newsl.*, *12*, 3–11.

Neumann, B., A. T. Vafeidis, J. Zimmermann, and R. J. Nicholls (2015a), Future Coastal Population Growth and Exposure to Sea-Level Rise and Coastal Flooding - A Global Assessment, *PLoS One*, *10*(3), e0118,571, doi:10.1371/journal.pone.0118571.

Neumann, J., K. Emanuel, S. Ravela, L. Ludwig, and C. Verly (2015b), Risks of Coastal Storm Surge and the Effect of Sea Level Rise in the Red River Delta, Vietnam, *Sustainability*, *7*(6), 6553–6572, doi:10.3390/su7066553.

Nicholls, R. J. (2004), Coastal flooding and wetland loss in the 21st century: changes under the SRES climate and socio-economic scenarios, *Glob. Environ. Chang.*, *14*, 69–86, doi:10.1016/j.gloenvcha.2003.10.007.

Nicholls, R. J., and A. Cazenave (2010), Sea-level rise and its impact on coastal zones., *Science*, *328*(5985), 1517–20, doi:10.1126/science.1185782.

Nisbet, E. G., E. J. Dlugokencky, and P. Bousquet (2014), Methane on the rise–again., *Science (80-.).*, *343*(6170), 493–495, doi:10.1126/science.1247828.

Nisbet, E. G., E. J. Dlugokencky, M. R. Manning, D. Lowry, R. E. Fisher, J. L. France, S. E. Michel, J. B. Miller, B. Vaughn, P. Bousquet, J. A. Pyle, M. Cain, R. Brownlow, G. Zazzeri, A. C. Manning, C. Labuschagne, E. W. Wolff, R. Holloway, A. Administration, A. Sciences, L. Road, and C. Sciences (2016), Rising atmospheric methane: 2007-2014 growth and isotopic shift, *Global Biogeochem. Cycles*, *30*(9), 1356–1370, doi:10.1002/2016GB005406.

NOAA ESRL (2017), CarbonTracker-CH4.

Nobi, N., and A. D. Gupta (1997), Simulation of Regional Flow and Salinity Intrusion in an Integrated Stream-Aquifer System in Coastal Region: Southwest Region of Bangladesh, *Groundwater*, *35*(5), 786–796, doi:10.1111/j.1745-6584.1997.tb00147.x.

Opare, S. (2012), Rainwater harvesting: an option for sustainable rural water supply in Ghana, *GeoJournal*, *77*(5), 695–705, doi:10.2307/23324853.

Oude Essink, G. H. P., E. S. Van Baaren, and P. G. B. De Louw (2010), Effects of climate change on coastal groundwater systems: A modeling study in the Netherlands, *Water Resour. Res.*, *46*(10), 1–16, doi:10.1029/2009WR008719.

Paerl, H. W., N. S. Hall, B. L. Peierls, and K. L. Rossignol (2014), Evolving Paradigms and Challenges in Estuarine and Coastal Eutrophication Dynamics in a Culturally and Climatically Stressed World, *Estuaries and Coasts*, *37*(2), 243–258, doi:10.1007/s12237-014-9773-x.

Pagano, T. S., H. H. Aumann, D. E. Hagan, and K. Overoye (2003), Prelaunch and In-flight Radiometric Calibration of the Atmospheric Infrared Sounder (AIRS), *Tech. rep.*, IEEE Trans. Geosci. Remote Sens.

Papa, F., C. Prigent, F. Durand, and W. B. Rossow (2006), Wetland dynamics using a suite of satellite observations: A case study of application and evaluation for the Indian Subcontinent, *Geophys. Res. Lett.*, *33*(8), 2–5, doi:10.1029/2006GL025767.

Papa, F., C. Prigent, F. Aires, C. Jimenez, W. B. Rossow, and E. Matthews (2010), Interannual variability of surface water extent at the global scale, 19932004, *J. Geophys. Res.*, *115*(D12), D12,111, doi:10.1029/2009JD012674.

Parker, R., H. Boesch, A. Cogan, A. Fraser, L. Feng, P. I. Palmer, J. Messerschmidt, N. Deutscher, D. W. T. Griffith, J. Notholt, P. O. Wennberg, and D. Wunch (2011), Methane observations from the Greenhouse Gases Observing SATellite: Comparison to ground-based TCCON data and model calculations, *Geophys. Res. Lett.*, *38*, L15,807, doi:10.1029/2011GL047871.

Patra, P. K., N. N. Star, C. Springs, and D. Worthy (2009), Validation of CH4 surface emission using forward chemistry-transport model, in *18th Int. Emiss. Invent. Conf.*, pp. 1–11.

Peters, C. N., R. Bennartz, and G. M. Hornberger (2017), Satellite-derived methane emissions from inundation in Bangladesh, *J. Geophys. Res. Biogeosciences*, *122*(5), 1137–1155, doi:10.1002/2016JG003740.

Peters, W., A. R. Jacobson, C. Sweeney, A. E. Andrews, T. J. Conway, K. Masarie, J. B. Miller, L. M. P. Bruhwiler, G. Pétron, A. I. Hirsch, D. E. J. Worthy, G. R. van der Werf, J. T. Randerson, P. O. Wennberg, M. C. Krol, and P. P. Tans (2007), An atmospheric perspective on North American carbon dioxide exchange: CarbonTracker, *Proc. Natl. Acad. Sci. U. S. A.*, *104*(48), 18,925–30, doi:10.1073/pnas.0708986104.

Pison, I., B. Ringeval, P. Bousquet, C. Prigent, and F. Papa (2013), Stable atmospheric methane in the 2000s: key-role of emissions from natural wetlands, *Atmos. Chem. Phys*, *13*, 11,609–11,623, doi:10.5194/acp-13-11609-2013.

Post, V. E. A. (2005), Fresh and saline groundwater interaction in coastal aquifers: Is our technology ready for the problems ahead?, *Hydrogeol. J.*, *13*(1), 120–123, doi:10.1007/s10040-004-0417-2.

Prigent, C., F. Papa, F. Aires, W. B. Rossow, and E. Matthews (2007), Global inundation dynamics inferred from multiple satellite observations, 19932000, *J. Geophys. Res.*, *112*(D12), D12,107, doi:10.1029/2006JD007847.

Priyantha Ranjan, S., S. Kazama, and M. Sawamoto (2006), Effects of climate and land use changes on groundwater resources in coastal aquifers, *J. Environ. Manage.*, *80*(1), 25–35, doi:10.1016/J.JENVMAN.2005.08.008.

Purvaja, R., and R. Ramesh (2001), Natural and and anthropogenic methane emission from coastal wetlands of South India, *Environ. Manage.*, *27*(4), 547–557, doi: 10.1007/s002670010169.

Rahman, M. A. T., R. K. Majumder, S. H. Rahman, and M. A. Halim (2011), Sources of deep groundwater salinity in the southwestern zone of Bangladesh, *Environ. Earth Sci.*, *63*(2), 363–373.

Rahman, R., and M. Salehin (2013), Disaster Risk Reduction. Approaches Bangladesh, in *Disaster Risk Reduction. Approaches Bangladesh*, edited by R. Shaw, F. Mallick, and A. Islam, pp. 65–90, Springer.

Rashid, H. E. (1977), *Geography of Bangladesh*, Westview Press.

Ravenscroft, P. (2003), Overview of the hydrogeology of Bangladesh, in *Groundw. Resour. Dev. Bangladesh Backgr. to Arsen. Cris. Agric. potential, Environ.*, edited by A. Rahman and P. Ravenscrot, chap. 3, pp. 43–86, Dhaka University Press, Dhaka, Bangladesh.

Ravenscroft, P., W. G. Burgess, K. M. Ahmed, M. Burren, and J. Perrin (2005), Arsenic in groundwater of the Bengal Basin, Bangladesh: Distribution, field relations, and hydrogeological setting, *Hydrogeol. J.*, *13*, 727–751, doi:10.1007/s10040-003-0314-0.

Ray, E. J. (1999), Outreach, engagement will keep academia relevant to twenty-first century societies, *J. Public Serv. Outreach*, *4*, 21–27.

Rhoades, J. D., and F. Chanduvi (1999), *Soil salinity assessment: Methods and interpretation of electrical conductivity measurements*, vol. 57, Food & Agriculture Org.

Richter, B. D., J. V. Baumgartner, D. P. Braun, and J. Powell (1998), A spatial assessment of hydrologic alteration within a river network, *Regul. Rivers Res. Manag.*, *14*, 329–340.

Ringeval, B., N. de Noblet-Ducoudré, P. Ciais, P. Bousquet, C. Prigent, F. Papa, and W. B. Rossow (2010), An attempt to quantify the impact of changes in wetland extent on methane emissions on the seasonal and interannual time scales, *Global Biogeochem. Cycles*, *24*(a), 1–12, doi:10.1029/2008GB003354.

Ringeval, B., P. Friedlingstein, C. Koven, P. Ciais, N. De Noblet-Ducoudré, B. Decharme, and P. Cadule (2011), Climate-CH 4 feedback from wetlands and its interaction with the climate-CO 2 feedback, *Biogeosciences*, *8*, 2137–2157, doi:10.5194/bg-8-2137-2011.

Ringeval, B., B. Decharme, S. L. Piao, P. Ciais, F. Papa, N. De Noblet-Ducoudré, C. Prigent, P. Friedlingstein, I. Gouttevin, C. Koven, and A. Ducharne (2012), Modelling sub-grid wetland in the ORCHIDEE global land surface model: evaluation against river discharges and remotely sensed data, *Geosci. Model Dev*, *5*, 941–962, doi:10.5194/gmd-5-941-2012.

Roberts, M. R. (2009), Realizing Societal Benefit from Academic Research: Analysis of the National Science Foundation's Broader Impacts Criterion, *Soc. Epistemol.*, *23*(3-4), 199–219, doi:10.1080/02691720903364035.

Rogers, M., and M. Bruen (1998), Choosing realistic values of indifference, preference and veto thresholds for use with environmental criteria within ELECTRE, *Eur. J. Oper. Res.*, *107*(3), 542–551, doi:10.1016/S0377-2217(97)00175-6.

Rojstaczer, S. (1988), Determination of fluid flow properties from the response of water levels in wells to atmospheric loading, *Water Resour. Res.*, *24*(11), 1927–1938.

Rolph, G. D. (2017), Real-time Environmental Applications and Display sYstem (READY) Website, *Tech. rep.*, NOAA Air Resources Laboratory, College Park, MD.

Roy, B. (1991), The outranking foundations aproach and the methods, *Theory Decis.*, *31*, 49–73, doi:10.1007/BF00134132.

Roy, B., M. Present, and D. Silhol (1986), A programming method for determining which Paris metro stations should be renovated, *Eur. J. Oper. Res.*, *24*(2), 318–334, doi:10.1016/0377-2217(86)90054-8.

Sá, F., C. Sanders, and S. Patchineelam (2015), Arsenic fractionation in estuarine sediments: Does coastal eutrophication influence As behavior?, *Mar. Pollut. Bull.*, *96*(1), 496–501.

Saaty, T. L. (2008), Decision making with the analytic hierarchy process, *Int. J. Serv. Sci.*, *1*(1), 83–98.

Saltelli, A. (2002), Sensitivity Analysis for Importance Assessment, *Risk Anal.*, *22*(3), 579–590, doi:10.1111/0272-4332.00040.

Sass, R. L., F. M. Fisher, A. Ding, and Y. Huang (1999), Exchange of methane from rice fields: National, regional, and global budgets, *J. Geophys. Res.*, *104*(D21), 26,943–26,951, doi:10.1029/1999JD900081.

Scheepmaker, R., and C. Frankenberg (2007), SRON/JPL SCIAMACHY IMAP-DOAS v6.0 XCH4: Product Specification Document, *Tech. rep.*, SRON Netherlands Institute for Space Research.

Schmidt, C. W. (2015), Delta Subsidence: An Imminent Threat to Coastal Populations., *Environ. Health Perspect.*, *123*(8), A204–9, doi:10.1289/ehp.123-A204.

Scholten, L., N. Schuwirth, P. Reichert, and J. Lienert (2015), Tackling uncertainty in multi-criteria decision analysis An application to water supply infrastructure planning, *Eur. J. Oper. Res.*, *242*(1), 243–260, doi:10.1016/j.ejor.2014.09.044.

SCRON (2007), SCRON.

Seitzinger, S. P., and L. Phillips (2017), Nitrogen stewardship in the Anthropocene., *Science*, *357*(6349), 350–351, doi:10.1126/science.aao0812.

Shahid, S. (2010), Recent trends in the climate of Bangladesh, *Clim. Res.*, *42*(3), 185–193, doi:10.3354/cr00889.

Shahid, S. (2011), Impact of climate change on irrigation water demand of dry season Boro rice in northwest Bangladesh, *Clim. Change*, *105*, 433–453, doi:10.1007/s10584-010-9895-5.

Shamsudduha, M., R. G. Taylor, K. M. Ahmed, and A. Zahid (2011), The impact of intensive groundwater abstraction on recharge to a shallow regional aquifer system: evidence from Bangladesh, *Hydrogeol. J.*, *19*(4), 901–916, doi:10.1007/s10040-011-0723-4.

Shofade, O. (2011), Considering hierarchical structure of criteria in ELECTRE decision aiding methods, Ph.D. thesis, Universitat Rovira i Virgili Escola, Tarragona.

Shuai, P., P. S. K. Knappett, S. Hossain, A. Hosain, K. Rhodes, K. M. Ahmed, and M. B. Cardenas (2017), The Impact of the Degree of Aquifer Confinement and Anisotropy on Tidal Pulse Propagation, *Groundwater*, doi:10.1111/gwat.12509.

Shumaker, R. (2017), Perceptions of Drinking Water Quality in Southwestern Bangladesh, Ph.D. thesis, Vanderbilt University, Nashville, Tennessee.

Simpson, I., F. S. Rowland, S. Meinardi, and D. R. Blake (2006), Influence of biomass burning during recent fluctuations in the slow growth of global tropospheric methane, *Geophys. Res. Lett.*, *33*, doi:10.1029/2006GL027330.

Singh, J. S., S. Singh, A. S. Raghubanshi, S. Singh, and A. K. Kashyap (1996), Methane flux from rice/wheat agroecosystem as affected by crop phenology, fertilization and water level, *Plant Soil*, *183*, 323–327.

Small, C., and R. J. Nicholls (2003), A Global Analysis of Human Settlement in Coastal Zones, *J. Coast. Reserach*, *19*(3), 584–599.

Solomon, S., D. Qin, M. Manning, Z. Chen, M. Marquis, K. B. Averyt, M. Tignor, and H. L. Miller (2007), Climate Change 2007: The Physical Science Basis. Contribution of Working Group I to the Fourth Assessment Report of the Intergovernmental Panel on Climate Change, *Tech. rep.*, Intergovernmental Panel on Climate Change, Cambridge, United Kingdom and New York, NY, USA.

Starkl, M., N. Brunner, and T.-A. Stenström (2013), Why Do Water and Sanitation Systems for the Poor Still Fail? Policy Analysis in Economically Advanced Developing Countries, *Environ. Sci. Technol.*, *47*(12), 6102–6110, doi:10.1021/es3048416.

Stein, A. F., R. R. Draxler, G. D. Rolph, B. J. B. Stunder, M. D. Cohen, F. Ngan, A. F. Stein, R. R. Draxler, G. D. Rolph, B. J. B. Stunder, M. D. Cohen, and F. Ngan (2015), NOAA's HYSPLIT Atmospheric Transport and Dispersion Modeling System, *Bull. Am. Meteorol. Soc.*, *96*(12), 2059–2077, doi:10.1175/BAMS-D-14-00110.1.

Stewart, T. J., and L. Scott (1995), A Scenario-Based Framework for Multicriteria Decision Analysis in Water Resources Planning, *Water Resour. Res.*, *31*(11), 2835–2843, doi: 10.1029/95WR01901.

Streatfield, P. K., and Z. A. Karar (2008), Population challenges for Bangladesh in the coming decades., *J. Health. Popul. Nutr.*, *26*(3), 261–72.

Streets, D. G., T. Canty, G. R. Carmichael, B. de Foy, R. R. Dickerson, B. N. Duncan, D. P. Edwards, J. A. Haynes, D. K. Henze, M. R. Houyoux, D. J. Jacob, N. A. Krotkov, L. N. Lamsal, Y. Liu, Z. Lu, R. V. Martin, G. G. Pfister, R. W. Pinder, R. J. Salawitch, and K. J. Wecht (2013), Emissions estimation from satellite retrievals: A review of current capability, *Atmos. Environ.*, *77*, 1011–1042, doi:10.1016/j.atmosenv.2013.05.051.

Takai, Y., and T. Kamura (1966), The Mechanism of Reduction in Waterlogged Paddy Soil, *Folia Microbiol.*, *11*, 304–313.

Tasich, C. M. (2013), Groundwater-Surface Water Interactions in the Tidally-Dominated Coastal Region of the Bengal Basin: A One-Dimensional Numerical Analysis of Tidal and Surface Water Controls on Local Aquifer Systems, Ph.D. thesis, Vanderbilt University, Nashville, Tennessee.

Topp, G. C., W. D. Reynolds, and R. E. Green (1993), Advances in measurement of soil physical properties: Bringing theory into practice., *Soil Sci.*, *156*(6), 429–432.

Tran, L. T., F. Larsen, N. Q. Pham, A. V. Christiansen, N. Tran, H. V. Vu, L. V. Tran, H. V. Hoang, and K. Hinsby (2012), Origin and extent of fresh groundwater, salty paleowaters and recent saltwater intrusions in Red River flood plain aquifers, Vietnam, *Hydrogeol. J.*, *20*(7), doi:10.1007/s10040-012-0874-y.

Trefry, M. G., and C. D. Johnston (1998), Pumping test analysis for a tidally forced aquifer, *Groundwaterater*, *36*(3), 427–433, doi:10.1111/j.1745-6584.1998.tb02813.x.

Turner, A. G., and H. Annamalai (2012), Climate change and the South Asian summer monsoon, *Nat. Clim. Chang.*, *2*(8), 587–595, doi:10.1038/nclimate1495.

Turner, A. J., D. J. Jacob, J. Benmergui, S. C. Wofsy, J. D. Maasakkers, A. Butz, O. Hasekamp, S. C. Biraud, and E. Dlugokencky (2016), A large increase in US methane emissions over the past decade inferred from satellite data and surface observations, *Geophys. Res. Lett.*, *43*, doi:10.1002/2016GL067987.

UN Economic and Social Council (2016), Progress towards the Sustainable Devlopment Goals, *Tech. Rep. July*, United Nations Economic and Social Council, doi:10.1017/S0020818300011322.

Vandenbohede, A., E. Van Houtte, and L. Lebbe (2009), Sustainable groundwater extraction in coastal areas: a Belgian example, *Environ. Geol.*, *57*(4), 735–747, doi:10.1007/s00254-008-1351-8.

Walter, B. P., M. Heimann, and E. Matthews (2001), Modeling Modern Methane Emissions from Natural Wetlands 2. Interannual Variations 1982:1993, *J. Geophys. Res.*, *106*(D24), 34,207–34,219.

Wang, H., T. J. Wright, Y. Yu, H. Lin, L. Jiang, C. Li, and G. Qiu (2012), InSAR reveals coastal subsidence in the Pearl River Delta, China, *Geophys. J. Int.*, *191*(1), 1119–1128, doi:10.1111/j.1365-246X.2012.05687.x.

Wania, R., J. R. Melton, E. L. Hodson, B. Poulter, B. Ringeval, R. Spahni, T. Bohn, C. A. Avis, G. Chen, A. V. Eliseev, P. O. Hopcroft, W. J. Riley, Z. M. Subin, H. Tian, P. M. Van Bodegom, T. Kleinen, Z. C. Yu, J. S. Singarayer, S. Urcher, D. P. Lettenmaier, D. J. Beerling, and J. O. Kaplan (2013), Present state of global wetland extent and wetland methane modelling: methodology of a model inter-comparison project (WETCHIMP), *Geosci. Model Dev*, *6*, 617–641, doi:10.5194/gmd-6-617-2013.

Warrick, R. A., Q. K. Ahmad, N. J. Ericksen, and M. Q. Mirza (1996), The Implications of Climate Change for Bangladesh: A Synthesis, in *Implic. Clim. SeaLevel Chang. Bangladesh*, pp. 1–34, Springer Netherlands, Dordrecht, doi:10.1007/978-94-009-0241-1-1.

Wassmann, R., M. X. Wang, X. J. Shangguan, X. L. Xie, R. X. Shen, Y. S. Wang, H. Papen, H. Rennenberg, and W. Seiler (1993), First records of a field experiment on fertilizer effects on methane emission from rice fields in Hunan-Province (PR China), *Geophys. Res. Lett.*, *20*(19), 2071–2074, doi:10.1029/93GL01915.

Wassmann, R., N. X. Hien, C. T. Hoanh, and T. P. Tuong (2004), Sea Level Rise Affecting the Vietnamese Mekong Delta: Water Elevation in the Flood Season and Implications for Rice Production, *Clim. Change*, *66*(1), 89–107, doi:10.1023/B:CLIM.0000043144.69736.b7.

Weinman, B. (2010), The evolution of aquifers and arsenic in Asia: A study of the fluvio-deltaic processes leading to aquifer formation and arsenic cycling and heterofeneity in Bangladesh, Vietnam, and Nepal, Ph.D. thesis, Vanderbilt University, Nashville, Tennessee.

Werner, A. D., and C. T. Simmons (2009), Impact of Sea-Level Rise on Sea Water Intrusion in Coastal Aquifers, *Groundwater*, *47*(2), 197–204, doi:10.1111/j.1745-6584.2008.00535.x.

WHO, and UNICEF (2017), Progress on drinking water, sanitation and hygiene: 2017 update and SDG baselines, *Tech. rep.*, WHO and UNICEF, Geneva.

Wilson, C., S. Goodbred, C. Small, J. Gilligan, S. Sams, B. Mallick, and R. Hale (2017), Widespread infilling of tidal channels and navigable waterways in human-modified tidal deltaplain of southwest Bangladesh, *Elem. Sci. Anthr.*, *5*(0), 78, doi:10.1525/elementa.263.

Wilson, C. A., S. L. Goodbred Jr, S. L. Goodbred, and S. L. Goodbred Jr (2014), Construction and Maintenance of the Ganges-Brahmaputra-Meghna Delta: Linking Process, Morphology, and Stratigraphy., *Ann. Rev. Mar. Sci.*, *7*(December), 67–88, doi:10.1146/annurev-marine-010213-135032.

WMO (2013), WMO greenhouse gas bulletin: The State of Greenhouse Gases in the Atmosphere Based on Global Observations through 2012, *Tech. rep.*, World Meteorological Organization, Geneva.

Wong, P., I. J. Losada, Gattuso J. -P., J. Hinkel, A. Khattabi, K. L. McInnes, Y. Saito, and A. Sallenger (2014), Coastal systems and low-lying areas. In: Climate Change 2014: Impacts, Adaptation, and Vulnerability. Part A: Global and Sectoral Aspects. Contribution of Working Group II to the Fifth Assessment Report of the Intergovernmental Panel on Climate Change, *Tech. rep.*, Intergovernmental Panel on Climate Change, Cambridge, United Kingdom and New York, NY, USA.

Worland, S. C., G. M. Hornberger, and S. L. Goodbred (2015), Source, transport, and evolution of saline groundwater in a shallow Holocene aquifer on the tidal deltaplain of southwest Bangladesh, *Water Resour. Res.*, *51*(7), 5791–5805, doi:10.1002/2014WR016262.

World Bank (2011), The Cost of Adapting to Extreme Weather Events in a Changing Climate. Bangladesh Development Series Paper No. 67845, *Tech. rep.*, The World Bank, Dhaka, Bangladesh and Washington DC, USA.

World Health Organization (2011), *Guidelines for drinking-water quality*, 4 ed., WHO Press, Geneva.

Wyncoll, D., I. Haigh, B. Gouldby, and D. Hames (2016), Spatial analysis and simulation of extreme coastal flooding scenarios for national-scale emergency planning, *E3S Web Conf.*, *7*, 01,001.

Xia, Y., H. Li, M. C. Boufadel, Q. Guo, and G. Li (2007), Tidal wave propagation in a coastal aquifer: Effects of leakages through its submarine outlet-capping and offshore roof, *J. Hydrol.*, *337*(3-4), 249–257, doi:10.1016/j.jhydrol.2007.01.036.

Xia, Y., H. Li, Y. Yang, and W. Huang (2012), The enhancing effect on tidal signals of a submarine spring connected to a semi-infinite confined aquifer, *Hydrol. Sci. J.*, *57*(6), 1231–1248, doi:10.1080/02626667.2012.701304.

Xiao, X., S. Boles, S. Frolking, C. Li, J. Y. Babu, W. Salas, and B. Moore (2006), Mapping paddy rice agriculture in South and Southeast Asia using multi-temporal MODIS images, *Remote Sens. Environ.*, *100*(1), 95–113, doi:10.1016/j.rse.2005.10.004.

Xiong, X., C. Barnet, E. Maddy, C. Sweeney, X. Liu, L. Zhou, and M. Goldberg (2008), Characterization and validation of methane products from the Atmospheric Infrared Sounder (AIRS), *J. Geophys. Res. Biogeosciences*, *113*(3), 1–14, doi:10.1029/2007JG000500.

Xiong, X., S. Houweling, J. Wei, E. Maddy, F. Sun, and C. Barnet (2009), Methane plume over south Asia during the monsoon season: satellite observation and model simulation, *Atmos. Chem. Phys.*, *9*, 783–794.

Yagi, K., P. Chairoj, H. Tsuruta, W. Cholitkul, and K. Minami (1994), Methane emission from rice paddy fields in the central plain of Thailand, *Soil Sci. Plant Nutr*, *40*(1), 29–37, doi:10.1080/00380768.1994.10414275.

Yagi, K., H. Tsuruta, K. Kanda, and K. Minami (1996), Effect of water management on methane emission from a Japanese rice paddy field: Automated methane monitoring, *Global Biogeochem. Cycles*, *10*(2), 255, doi:10.1029/96GB00517.

Yamaji, K., T. Ohara, and H. Akimoto (2003), A country-specific, high-resolution emission inventory for methane from livestock in Asia in 2000, *Atmos. Environ.*, *37*(31), 4393–4406, doi:10.1016/S1352-2310(03)00586-7.

Yoshino, N., F. Taghizadeh-Hesary, and M. Otsuka (2017), International Remittances and Poverty Reduction: Evidence from Asian Developing Countries. ADBI Working Paper 759, *Tech. rep.*, Asian Development Bank Institute, Tokyo.

Zheng, Y., A. Van Geen, M. Stute, R. Dhar, Z. Mo, Z. Cheng, A. Horneman, I. Gavrieli, H. J. Simpson, R. Versteeg, M. Steckler, A. Grazioli-Venier, S. Goodbred, M. Shahnewaz, M. Shamsudduha, M. A. Hoque, and K. M. Ahmed (2005), Geochemical and hydrogeological contrasts between shallow and deeper aquifers in two villages of Araihazar, Bangladesh: Implications for deeper aquifers as drinking water sources, *Geochim. Cosmochim. Acta*, *69*(22), 5203–5218, doi:10.1016/j.gca.2005.06.001.

Zou, J., Y. Huang, J. Jiang, X. Zheng, and R. L. Sass (2005), A 3-year field measurement of methane and nitrous oxide emissions from rice paddies in China: Effects of water regime, crop residue, and fertilizer application, *Global Biogeochem. Cycles*, *19*(2), 1–9, doi:10.1029/2004GB002401.